IMPERIAL

REGULATORY B CELLS IN ALLERGIC RHINITIS AND ALLERGEN IMMUNOTHERAPY

A thesis submitted to Imperial College London in candidature for the degree of

Doctor of Philosophy (PhD)

Elizabeth Palmer

2024

Immunomodulation Tolerance Group

Allergy and Clinical Immunology

National Heart and Lung Institute, Faculty of Medicine

Imperial College London

ORIGINALITY AND COPYRIGHT DECLARATION

I confirm that the contents of this thesis are my own work, under the supervision of Professor Shamji, Professor Durham, and Dr Kappen, except where references are made. The rational, hypotheses and experimental designs presented in this thesis are my own. Clinical and diagnostic procedures, such as symptom scores, presented in Chapter 3, Chapter 4, Chapter 5, Chapter 6, and Chapter 7 were obtained from Professor Durham, who was the principal investigator for those studies at the Allergy and Clinical Immunology Clinic at the Royal Brompton Hospital. Clinical samples collected as part of the multicentre, double-blind placebo-controlled Phase III PQGrass clinical trial, and study compounds for use in the preclinical virus-like-particle study, both presented in Chapter 6, were obtained from Allergy Therapeutics^{PLC}. Study compounds for use in the preclinical plant-derived bioparticle study, presented in Chapter 6, were obtained from ANGANY Inc.. Nasal fluid extraction, ELISA and ImmunoCAP analysis conducted as part of the Phase III PQGrass 27600 SU was performed in collaboration with other immunomodulation tolerance group laboratory members. All statistical analysis, evaluation and interpretation are my own. This work has not been submitted in application for any other higher degree, and was written independently, with advice and suggestions from my supervisors. The copyright of this thesis rests with the author. Unless otherwise indicated, its contents are licensed under a Creative Commons Attribution-Non-Commercial 4.0 International License (CC BY-NC). Under this license, you may copy and redistribute the material in any medium or format. You may also create and distribute modified versions of the work. This is on the condition that: you credit the author and do not use it, or any derivative works, for a commercial purpose. When reusing or sharing this work, ensure you make the license terms clear to others by naming the license and linking to the license text. Where a work has been adapted, you should indicate that the work has been changed and describe those changes. Please seek permission from the copyright holder for uses of this work that are not included in this license or permitted under UK Copyright Law.

ABSTRACT

Regulatory B cells (Breg) are a subset of B cells with enhanced propensity for IL-10 production that play essential roles in maintaining peripheral tolerance. Allergic diseases (AD), such as allergic rhinitis (AR), arise due to loss of tolerance to sensitising allergen in predisposed atopic individuals, resulting in induction of IgE^+ B cells and T helper 2 (T_H2) and allergen specific T_H2A cellular responses. Allergen immunotherapy (AIT) remains the only disease-curative treatment for AD, however, the exact role of IL-10^+ Breg cells in AR pathophysiology and AIT, remains unclear. This thesis aims to evaluate IL-10^+ Breg cellular subsets in AR, non-atopic controls (NAC), and AIT-treated patients, and assess the capability of IL-10^+ Breg cells to modulate allergen-driven T_H2, T_H2A and regulatory T cell (Treg) responses.

Frequency and IL-10 propensity of heterogenous peripheral IL-10^+ Breg cell subsets were significantly dysregulated in AR compared to NAC. Enumeration of IL-10^+ Breg cells in a cross-sectional study demonstrated the ability of AIT to significantly restore IL-10^+ Breg frequencies in GPA. Moreover, preclinical studies revealed novel AIT approaches utilising allergen-carrier systems demonstrated significant immunogenicity through the induction of IL-10^+ Breg cells. Alternative short-term AIT regimens substantially induced systemic and local blocking IgA and IgG antibody responses during a Phase III clinical study, indirectly evidencing AIT-mediated induction of B cell isotype switch towards protective antibodies. Additionally, functional co-culture systems revealed IL-10^+ Breg cells suppressed allergen-driven T_H2/T_H2A cells in parallel to promotion of Treg cellular responses, partially mediated by IL-10.

Collectively, these findings demonstrate attenuation of IL-10^+ Breg cells contribute towards AR disease pathophysiology and highlight this dearth may result in loss of regulation of T_H2/T_H2A-orchestrated allergic inflammation. Allergen-carrier systems and short-term AIT regimens demonstrate capability to induce IL-10^+ B cells and protective antibody production, giving prominence to their potential therapeutic use for the treatment of AD.

TABLE OF CONTENTS

ORIGINALITY AND COPYRIGHT DECLARATION ____ *2*

ABSTRACT ____ *3*

LIST OF FIGURES ____ *8*

LIST OF TABLES ____ *11*

LIST OF ABBREVIATIONS ____ *14*

PUBLICATIONS AND ABSTRACTS PERTAINING TO THESIS ____ *18*

Peer-Reviewed Publication ____ **18**

Peer-Reviewed Abstracts ____ **18**

ACKNOWLEDGEMENTS ____ *20*

CHAPTER 1. INTRODUCTION ____ *21*

1.1 Allergic Disease ____ **21**

1.2 Allergic Rhinitis ____ **22**

1.2.1 Allergic Rhinitis Clinical Manifestation, Epidemiology and Aetiology ____ 22

1.2.2 Common UK Allergic Rhinitis Causative Allergens ____ 23

1.2.3 Clinical Diagnosis of Allergic Rhinitis ____ 24

1.2.4 Allergic Rhinitis Pathophysiology ____ 25

1.2.5 Allergic Rhinitis Treatment and Management ____ 30

1.3 Allergen Immunotherapy ____ **31**

1.3.1 Allergen Immunotherapy for Allergic Rhinitis ____ 32

1.3.2 Allergen Immunotherapy for Peanut Allergy ____ 34

1.3.3 Immunological Basis of Allergen Immunotherapy Treatment ____ 35

1.3.4 Allergen Immunotherapy Challenges and Alternative Approaches ____ 41

1.4 B Cells ____ **42**

1.4.1 B Cell Ontology, Development and Central Tolerance ____ 42

1.4.2 B Cell Germinal Centre Reactions ____ 44

1.4.3 B Cells in Allergic Inflammation ____ 45

1.4.4 B Cells following Allergen Immunotherapy ____ 46

1.5 Regulatory B Cells ____ **48**

1.5.1 Discovery of Regulatory B Cells ____ 48

1.5.2 Regulatory B Cells Origins, Activation and Phenotypes ____ 49

1.5.3 Immunomodulatory Mechanisms of Regulatory B Cells ____ 54

1.5.4 Regulatory B Cells in Immune Homeostasis and Disease ____ 59

1.5.5 Regulatory B Cells in Allergy ____ 61

1.5.6 Regulatory B Cells in Allergen Immunotherapy ____ 62

1.6 Thesis Hypotheses and Aims ____ **66**

1.6.1 Hypotheses ____ 66

1.6.2 Aims and Objectives in relation to Hypotheses 67

CHAPTER 2. METHODOLOGY 70

2.1 Ethical Statement 70

2.2 Patient Recruitment 70

2.2.1 Clinical Symptom Questionnaires 71

2.3 Peripheral Blood Cell Isolation and Cryopreservation 71

2.4 B Cell and T Cell Enrichment 72

2.5 B Cell Stimulation and Culture 73

2.6 T Cell Stimulation and Culture 73

2.6.1 Cell Trace Violet Cellular Proliferation Staining Kit 73

2.6.2 T cell Stimulants and Proliferation Assay 74

2.7 B and T Cell Co-Cultures 74

2.7.1 IL-10^{+} B Cell Enrichment 74

2.7.2 B and T Cell Co-Culture Set-Up 76

2.8 Flow Cytometry 76

2.8.1 Flow-Cytometry Compensation 76

2.8.2 Flow-Cytometry Cell Staining 77

2.9 Nasal Fluid Extraction 78

2.10 ImmunoCAP100 Antibody Quantification 79

2.11 Enzyme-linked immunosorbent assay (ELISA) 79

2.11.1 Cell Culture Supernatant Cytokine Measurements 79

2.11.2 Antibody Measurements - IgA, IgA2 and IgG ELISA 80

2.12 Unbiased Visualisation Machine Learning Algorithms 81

2.12.1 viSNE 82

2.12.2 FlowSOM 82

2.12.3 SPADE 83

2.13 Statistical Analysis 85

CHAPTER 3. DEEP IMMUNOPHENOTYPING OF IL-10^{+} REGULATORY B CELLS 86

3.1 Introduction 86

3.1.1 Hypothesis and Aims 87

3.2 Results 88

3.2.1 Identification of IL-10^{+} Breg cells in human peripheral blood 88

3.2.2 Ex vivo CpG and CD40L stimulation induces significant IL-10^{+} Breg cell frequencies from human peripheral blood in a dose-dependent manner 90

3.2.3 Combined CpG and CD40L stimulation induces greater IL-10^{+} Breg cell frequencies than singular stimulation 95

3.2.4 CpG and CD40L stimulate IL-10^{+} Breg cells in a time-dependent manner 100

3.2.5 Validation of IL-10^{+} Breg Culture Model Conditions 104

3.2.6 Co-expression of suppressive molecules on IL-10^{+} Breg Cells 111

3.3 Summary 118

CHAPTER 4. DYSREGULATION OF IL-10$^+$ BREG CELLS IN SEASONAL AND PERENNIAL ALLERGIC RHINITIS ____ *119*

4.1 Introduction ____ **119**

4.1.1 Hypotheses and Aims ____ 120

4.2 Results ____ **122**

4.2.1 IL-10$^+$ Regulatory B Cells in AR Patients and NAC ____ 122

4.2.2 Evaluation of IL-10$^+$ Breg cell subsets in SAR and PAR ____ 125

4.2.3 Evaluation of TIM-1$^+$ Breg Cell Subsets in SAR and PAR ____ 132

4.2.4 Evaluation of IgA$^+$ and IgG4$^+$ Breg Cell Subsets in SAR and PAR ____ 135

4.2.5 Computational algorithms confirm dysregulation of TIM-1$^+$ and IL-10$^+$ Breg Cell Subsets in SAR and PAR ____ 139

4.2.6 Correlation between IL-10$^+$ Breg Cells, Clinical Symptom Severity, Age and Gender ____ 142

4.2.7 SAR IL-10$^+$ Breg cell demonstrate reduced sensitivity to CpG stimulation and IL-35$^+$IL-10$^+$TGFβ1$^+$ Breg cell frequencies compared to NAC. ____ 144

4.3 Summary ____ **151**

CHAPTER 5. ALLERGEN IMMUNOTHERAPY RESTORES IL-10$^+$ BREG CELLS IN GPA SAR PATIENTS ____ *152*

5.1 Introduction ____ **152**

5.1.1 Hypotheses and Aims ____ 153

5.2 Results ____ **155**

5.2.1 Dysregulation of IL-10$^+$ Breg cells in SAR are restored following GP-SCIT treatment ____ 155

5.2.2 Evaluation of the effect of SCIT-treatment on TIM-1$^+$ B cells and TIM-1$^+$IL-10$^+$ Breg cell frequencies in GPA ____ 161

5.2.3 GP-SCIT treatment significantly induces serum grass pollen-specific IgG_4 levels compared to GPA and NAC ____ 163

5.2.4 Unbiased machine learning algorithms reveal GP-SCIT upregulates TIM-1 and IL-10 expression on B cell subsets compared to GPA ____ 166

5.2.5 Correlation between IL-10$^+$ Breg Cells, Serum Antibody Levels, Symptom Severity and Treatment Length 170

5.3 Summary ____ **174**

CHAPTER 6. NOVEL APPROACHES OF ALLERGEN IMMUNOTHERAPY, TARGETING IL-10$^+$ BREG CELLS TO INDUCE TOLERANCE ____ *175*

6.1 Introduction ____ **175**

6.1.1 Hypothesis and Aims ____ 176

6.2 Results ____ **177**

6.2.1 Exploratory *ex vivo* study of the immunomodulatory potential of plant-derived *Fel d* 1 eBP to generate IL-10$^+$ Breg cells in CA ____ 177

6.2.2 Exploratory *ex vivo* study to evaluate the immunogenicity of VLP Peanut, with and without MCT, to generate IL-10$^+$ Breg cells from PA ____ 181

6.2.3 RDBPC exploratory study of short-course PQ Grass 27600 SU AIT for the treatment of seasonal allergic rhinoconjuctivitis ____ 187

6.3 Summary ____ **193**

CHAPTER 7. IL-10$^+$ B CELLS SUPPRESS ALLERGEN-STIMULATED T_H2/T_H2A CELLS AND PROMOTE IL-10$^+$ iTREG CELLULAR RESPONSES IN SAR ____ *194*

7.1 Introduction ____ **194**

7.1.1 Hypothesis and Aims ____ 195

7.2 Results ____ **196**

7.2.1 Characterisation of T_H2, T_H2A and iTreg cells in human peripheral blood ____ 196

7.2.2 *Phl p* stimulated T_H2 and T_H2A cell proliferation and cytokine production are suppressed by IL-10 206

7.2.3 T cell co-culture system with CpG and CD40L stimulated 'primed' B cells ____ 209

7.2.4 T cell co-culture system with enriched IL-10$^+$ Breg cells ____ 210

7.3 Summary ____ **215**

CHAPTER 8. DISCUSSION ____ *216*

8.1 Heterogenous IL-10$^+$ Breg cell populations in human peripheral blood are expanded by CpG and CD40L stimulation ____ **216**

8.2 IL-10$^+$ and TIM-1$^+$ Breg cells are significantly dysregulated in SAR and PAR ____ **220**

8.2.1 IL-10$^+$IL-35$^+$TGF-β^+ Breg cells are dysregulated in SAR patients compared to NAC ____ 224

8.3 SCIT restores IL-10$^+$ Breg cell frequencies in SAR to similar levels observed in NAC outside the pollen season ____ **226**

8.4 Novel AIT Approaches modulate IL-10$^+$ Breg cell subsets and enhance levels of protective local and systemic antibodies ____ **229**

8.4.1 *Fel d 1* expressing-eBP stimulates greater frequencies of IL-10$^+$ Breg cell subsets compared to *Fel d 1* alone ____ 229

8.4.2 VLP-Peanut, with and without MCT, is competent at generating IL-10$^+$ Breg cells in children with peanut allergy. ____ 230

8.4.3 PQGrass 27600 SU AIT induces local and systemic levels of grass pollen $sIgG_4$, $sIgA_1$ and $sIgA_2$ blocking antibodies ____ 231

8.5 IL-10$^+$ Breg cells suppress T_H2/T_H2A cellular responses through attenuating proliferative capacity ____ **232**

8.6 IL-10$^+$ Breg cells are dysregulated in AR, restored by AIT and suppress allergen-specific T_H2A cellular responses ____ **235**

CHAPTER 9. SUMMARY AND CONCLUDING REMARKS ____ *238*

CHAPTER 10. STUDY LIMITATIONS ____ *242*

CHAPTER 11. FUTURE STUDIES ____ *244*

CHAPTER 12. BIBLIOGRAPHY ____ *246*

CHAPTER 13. APPENDIX ____ *294*

13.1.1 Appendix Figures ____ 294

LIST OF FIGURES

Figure 1.2.4.1 Temporal Phases of Allergic Rhinitis Pathogenesis. 29
Figure 1.3.3.1 Allergen Immunotherapy Immunological Mechanism. 40
Figure 1.5.2.1 Regulatory B cell Phenotypes throughout the B cell development and maturation process. 53
Figure 1.5.6.1 Proposed Breg-mediated Suppression during Allergen Immunotherapy. 65
Figure 2.7.1.1 Enrichment of IL-10^{+} B cells from human PBMCs. 76
Figure 2.12.3.1 viSNE, FlowSOM and SPADE. 84
Figure 3.2.1.1 Flow cytometry gating strategy to identify IL-10^{+} Breg cells from PBMCs 89
Figure 3.2.2.1 CD40L and CpG stimulation induces IL-10^{+} Breg cells. 91
Figure 3.2.3.1 Combination of CpG and CD40L stimulation induces greater IL-10^{+} Breg cell frequencies compared to singular stimulation. 96
Figure 3.2.3.2 viSNE and FlowSOM confirm induction of IL-10^{+} Breg cells in response to CpG and CD40L stimulation. 98
Figure 3.2.4.1 IL-10^{+} B cells are induced by CpG and CD40L stimulation in a time-dependent manner. 101
Figure 3.2.4.2 viSNE and FlowSOM confirm IL-10^{+} Breg cells are induced by CpG and CD40L stimulation in a time-dependent manner. 102
Figure 3.2.5.1 Comparison of IL-10^{+} Breg Subsets in autologous PBMC and enriched CD19^{+} B cells 106
Figure 3.2.6.1 CpG and CD40L stimulation induces PD-L1, PD-1, CD80, CD86 and TIM-1 expression on B cells. 112
Figure 3.2.6.2 TGF-β1 and IL-35 expression is induced on B cells by CpG and CD40L and co-expressed with IL-10. 114
Figure 4.2.1.1 AR patients demonstrate reduced peripheral IL-10^{+} Breg Cell subsets compared to NAC. 123
Figure 4.2.2.1 SAR and PAR demonstrate significantly reduced IL-10^{+} Breg cell frequencies and IL-10 provision compared to NAC. 128
Figure 4.2.2.2 Cell Surface Marker Expression in IL-10^{-} and IL-10^{+} B cells in NAC, GPA, HDMA and CA. 129
Figure 4.2.3.1 TIM-1^{+} B cells and IL-10^{+}TIM-1^{+} Breg cells are significantly reduced in CA compared to HDMA. 133
Figure 4.2.4.1 IgG_4, but not IgA, expression is significantly enhanced on IL-10^{+} Breg cells compared to IL-10^{-} B cells. 136

Figure 4.2.4.2 Correlation between IL-10$^+$IgA$^+$ and IL-10$^+$IgG$_4^+$ Breg cells and serum sIgE in GPA, HDMA and CA. 137
Figure 4.2.5.1 viSNE Analysis of CD19$^+$ B cells reveals IL-10 and Tim-1 are dysregulated between GPA, CA, HDMA and NAC. 140
Figure 4.2.5.2 FlowSOM Analysis reveals IL-10$^+$ and Tim-1$^+$ Breg cells are dysregulated between GPA, CA, HDMA and NAC. 141
Figure 4.2.6.1 Correlation between IL-10$^+$ B cells and AR patient demographics. 143
Figure 4.2.7.1 GPA demonstrate significantly reduced capability to induce IL-10$^+$ Breg cells in response to CD40L and CpG stimulation compared to NAC. 145
Figure 4.2.7.2 IL-35$^+$ B cells and IL-35$^+$IL-10$^+$TGFβ1$^+$ Breg cell B cells are reduced in GPA compared to NAC. 149
Figure 5.2.1.1 Clinical symptom scores from patients enrolled for cross-sectional study of IL-10$^+$ B cell culture stimulation in GP-SCIT-treated subjects. 156
Figure 5.2.1.2 SCIT-treated GPA demonstrate significantly increased IL-10$^+$ Breg cell frequencies compared to GPA outside of the grass pollen season. 158
Figure 5.2.2.1 TIM-1$^+$ B Cells and TIM-1$^+$IL-10$^+$ Breg cell frequencies in NAC, GPA and GP-SCIT treated patients. 161
Figure 5.2.3.1 Systemic GP-sIgG$_4$ levels were significantly enhanced in SCIT treated subjects compared to GPA 164
Figure 5.2.4.1 viSNE analysis reveals distinct IL-10$^+$ and IL-10$^+$Tim-1$^+$ Breg subsets dysregulated in GPA are restored during SCIT-treatment. 168
Figure 5.2.4.2 FlowSOM analysis reveals IL-10$^+$ and Tim-1$^+$ CD19$^+$ B cells are enhanced following SCIT-treatment. 169
Figure 5.2.5.1 Correlation between SCIT IL-10$^+$ B cell subsets and serum TG-sIgE, TG-sIgG$_4$ and tIgE levels 171
Figure 5.2.5.2 Correlation between SCIT IL-10$^+$ B cell subsets, clinical symptom severity and treatment length 172
Figure 5.2.5.3 Correlation between systemic TG-sIgE, TG-sIgG$_4$ and tIgE levels, clinical symptom severity and treatment length 173
Figure 6.2.1.1 Biosynthetic Allergen eBioparticle expressing Fel d 1 upon its lipid ultrastructure. 178
Figure 6.2.1.2 Plant-derived Fel d 1 eBP generate enhanced IL-10$^+$ B cell frequencies in CA individuals compared to natural Fel d 1. 179
Figure 6.2.2.1 VLP derived from cucumber mosaic virus including tetanus toxin epitopes (CuMV$_{TT}$) genetically fused with Ara h 2 for peanut allergy treatment 182
Figure 6.2.2.2 VLP Peanut significantly induces IL-10$^+$ B cells compared to Ara h 2 and WPE. 184

Figure 6.2.2.3 Unbiased clustering analysis reveals VLP Peanut targets four specific metaclusters corresponding to IL-10^+ B cells.....185
Figure 6.2.3.1 PQGrass 27600 SU Phase III study design and evaluation of GP sIgG, sIgG_4, sIgA1 and sIgA2 levels in NF and serum.....190
Figure 7.2.1.1 Flow cytometry gating strategy to investigate T_H2, T_H2A and iTreg cells subsets in human peripheral blood. 197
Figure 7.2.1.2 Polyclonal Stimulation induces proliferating T_H2 and T_H2A cells in a time-dependent manner.....199
Figure 7.2.1.3 Phl p induces IL-10^+ Breg cells, $CD4^+$ T cells, T_H2, T_H2A and iTreg Subsets in NAC and GPA.....203
Figure 7.2.2.1 IL-10 significantly suppresses T_H2 and T_H2A cell subset proliferation.....207
Figure 7.2.4.1 IL-10^+ Breg cells demonstrate trends of suppressing $CD4^+$ and T_H2A cell proliferation compared to IL-10^- B cells.....211
Figure 13.1.1.1 ELISA optimisation for analysis of Phl p 5 sIgG, sIgA_1 and sIgA_2 levels in nasal fluid and serum. 294
Figure 13.1.1.2 Correlation between IL-10^+ Breg cell subsets and GPA SAR patient demographics. 295
Figure 13.1.1.3 Correlation between IL-10^+ Breg cell subsets and HDMA PAR patient demographics. 296
Figure 13.1.1.4 Correlation between IL-10^+ Breg cell subsets and CA PAR patient demographics. 297
Figure 13.1.1.5 CpG/CD40L primed B cells enhance $CD4^+$ T_H and T_H2 cell proliferation in response to polyclonal and allergen stimulation. 298
Figure 13.1.1.6 CpG/CD40L primed B cell culture supernatant significantly enhances Phl p stimulated T_H2 and T_H2A proliferation and IL-10^+ iTreg cells.....299

LIST OF TABLES

Table 1.3.1.1 Seminal Allergen Immunotherapy clinical studies 33
Table 1.5.1.1 Seminal regulatory B cell studies.....49
Table 2.8.2.1 Antibodies used for cell staining by flow cytometry 78
Table 2.11.2.1 Sandwich ELISA assay conditions for assessment of serum Phl p 5 specific IgA_1, IgA2 and IgG. 81
Table 3.2.1.1 Patient Demographics of NAC used in IL-10^+ Breg culture optimisation experiments 88
Table 3.2.2.1 IL-10^+ Breg Cell Subset Expression Following Stimulation with increasing dosages of CD40L 92
Table 3.2.2.2 IL-10^+ Breg Cell Subset Expression Following Stimulation with increasing dosages of CpG alongside CD40L. 93
Table 3.2.2.3 IL-10^+ Breg Cell Subset Expression Following Stimulation with increasing dosages of CpG alongside CD40L. 94
Table 3.2.3.1 Comparison of CpG and CD40L stimulation of IL-10^+ Breg cells. 99
Table 3.2.4.1 IL-10^+ Breg Subsets are induced by CpG and CD40L stimulation in a time-dependent manner.....103
Table 3.2.5.1 Comparison of IL-10^+ Breg Subsets in autologous PBMC and enriched $CD19^+$ B cell samples.....108
Table 3.2.6.1 PD-L1, PD-1, CD80, CD86 and TIM-1 expression on B cells induced by CpG and CD40L stimulation. 115
Table 3.2.6.2 TGFβ1 and IL-35 expression on B cells is induced by CpG and CD40L stimulation.....117
Table 4.2.1.1 IL-10^+ Breg cell subset frequencies in NAC and AR Patients.....124
Table 4.2.2.1 Patient Demographics of NAC, SAR and PAR patients enrolled for a cross-sectional study of IL-10^+ B cells. 126
Table 4.2.2.2 IL-10^+ Breg Cell subset frequencies in GPA, HDMA, CA and NAC.....130
Table 4.2.2.3 Surface Marker Expression on IL-$10^{+/-}$ B Cells in NAC, GPA, CA and HDMA 131
Table 4.2.3.1 TIM-1^+ B cells and TIM-1^+IL-10^+ Breg cells in NAC, GPA, HDMA and CA.....134
Table 4.2.4.1 IgG_4 expression is significantly enhanced on IL-10^+ Breg cells 138
Table 4.2.7.1 Patient Demographics of subjects enrolled for B cell culture stimulation experiments in NAC and SAR. 146

Table 4.2.7.2 IL-10$^+$ Breg Cell Subsets in SAR and NAC Following stimulation with increasing dosages of CpG alongside CD40L 146
Table 4.2.7.3 Comparison of CpG and CD40L stimulation of IL-10$^+$ Breg cells in SAR and NAC 147
Table 4.2.7.4. IL-35$^+$ B cells are significantly reduced in SAR compared to NAC. 150
Table 5.2.1.1 Patient Demographics and clinical characteristics of subjects enrolled for cross-sectional study of IL-10$^+$ B cell culture stimulation in GP-SCIT-treated subjects. 156
Table 5.2.1.2 IL-10$^+$ Breg Cell subsets in IS and OS NAC, GPA and SCIT-treated patients. 159
Table 5.2.2.1 TIM-1$^+$ B Cells and TIM-1$^+$IL-10$^+$ B cell frequencies in NAC, GPA and GP-SCIT treated patients. 162
Table 5.2.3.1 Systemic GP-sIgG$_4$ levels were significantly enhanced in SCIT treated subjects compared to GPA 165
Table 6.2.1.1 Patient Demographics of subjects enrolled for IL-10$^+$ Breg culture atopic stimulation experiments with plant-derived Fel d 1 eBP and natural purified Fel d 1. 177
Table 6.2.1.2 IL-10$^+$ Breg Cell Subset Expression in CA and NAC following stimulation with Fel d 1 eBP or natural Fel d 1. 180
Table 6.2.2.1 Patient Demographics of subjects recruited for an exploratory ex vivo study to evaluate the reactogenic/hypo-allergic properties of VLP Peanut 182
Table 6.2.2.2 IL-10$^+$ Breg Cell Subset Expression Following stimulation with VLP Peanut, with and without MCT, Ara h 2 and WPE. 186
Table 6.2.3.1 ELISA and ImmunoCAP analysis of grass pollen specific IgG, IgG$_4$, IgA1 and IgA2 levels in nasal fluid and serum 191
Table 7.2.1.1 Patient Demographics and clinical characteristics of NAC and GPA subjects enrolled for T cell experiments. 196
Table 7.2.1.2 Polyclonal Stimulation induces T_H2 and T_H2A in a time-dependent manner .200
Table 7.2.1.3 Polyclonal stimulation induces IL-5 and IL-13 production from PBMCs in a time-dependent manner 201
Table 7.2.1.4 Phl p induces IL-10$^+$ Breg cells and proliferating CD4$^+$ T cells, T_H2, T_H2A and iTreg subsets in NAC and GPA samples. 204
Table 7.2.2.1 Recombinant IL-10 suppresses Phl p-activated CD4$^+$ T cells, T_H2 and T_H2A cell proliferation 208
Table 7.2.4.1 Enriched IL-10$^+$ Breg cells and IL-10$^-$ B cells effects on Phl p-stimulated T_H2/T_H2A and iTreg cell subsets. 214
Table 7.2.4.2 IL-10$^+$ B cells partly mediate suppression of Phlp-stimulated T cell proliferation through IL-10 and IL-35. 214

Table 13.1.1.1 Primed B cell culture supernatant enhances Phl p-stimulated T_H2, T_H2A proliferation and IL-10^+ iTreg cells. 300

LIST OF ABBREVIATIONS

AIT – Allergen Immunotherapy

AID – Activation-induced Cytidine Deaminase

AD – Allergic Disease

APC – Antigen Presenting Cells

AR – Allergic Rhinitis

BP - Bioparticle

Breg – Regulatory B Cell

BM – Bone Marrow

BCR – B Cell Receptor

CA – Cat Allergic

cTF_{FH} – Circulating T Follicular Helper Cell

CD40L – CD40L ligand

CSR – Class Switch Recombination

DC – Dendritic Cell

DCreg – Regulatory Dendritic Cell

DC2 – Type 2 Dendritic Cell

EAE – Experimental Autoimmune Encephalitis

eBP – Enveloped Bioparticle

EPIT – Epicutaneous Immunotherapy

EPR – Early Phase Response

FasL – Fas Ligand

FCεRI – High-Affinity IgE Receptor

FCεRII – Low-Affinity IgE Receptor

FOB – Follicular B Cell

GC – Germinal Centre

GCP – Good Clinical Practice

GE – Global Evaluation Score

GLP – Good Laboratory Practice

GP – Grass Pollen

GPA – Grass Pollen Allergic

HC – Heavy Chain

HDM – House Dust Mite

HDMA – House Dust Mite Allergic

ILC2 – Group 2 Innate Lymphoid Cell

ILIT – Intralymphatic Immunotherapy

ITG – Immune Tolerance Group

LC – Light Chain

LPR – Late Phase Response

LN – Lymph Node

MC - Metacluster

MHC – Major Histocompatibility Complex

MZ – Marginal Zone B Cell

NAC – Non-Atopic Control

PA – Peanut Allergic

Phl p - Phleum pratense

PBMC – Peripheral Blood Mononuclear Cell

QoL – Quality of Life

RA – Rheumatoid Arthritis

RT – Room Temperature

SCIT – Subcutaneous Immunotherapy

SHM – Somatic Hypermutation

SLIT – Sublingual Immunotherapy

SOM – Self Organising Map

SPT – Skin Prick Test

TC – Topical Corticosteroid

TCM – Tissue Culture Media

TG – Timothy Grass

T_H0 – Naive T cell

T_H2 – Type-2 Helper T cell

T_H2A – Allergen-specific T Helper 2 cell

TIM-1 – T cell immunoglobulin and mucin domain 1

T_{FH} – Follicular Helper T cell

T_{FR} – Regulatory Follicular Helper T cell

iTreg – Inducible regulatory T cell

nTreg – Natural regulatory T cell

iTr35 – IL-35^+ inducible regulatory T cell

TLR – Toll-like Receptor

TSLP – Thymic Stromal Lymphopoietin

TNSS – Total Nasal Symptom Score

VAS – Visual Analogue Scale

VLP – Virus-Like Particle

PUBLICATIONS AND ABSTRACTS PERTAINING TO THESIS

Peer-Reviewed Publication

1. **Palmer E,** Layhadi J and Shamji MH. The role of regulatory B cells in allergy and following allergen immunotherapy (*in preparation)*
2. **Palmer E,** Layhadi J, Oleksandra F**,** Durham SR, Shamji MH. IL-10^{+} and IL-35^{+} regulatory B cells are significantly attenuated in allergic rhinitis patients and suppress allergen-driven T_H2/T_H2A immune responses. (*in preparation)*

Peer-Reviewed Abstracts

1. **Palmer E,** Layhadi JA, Turner PJ, Patel N, Oluwayi K, Rusyn O, Skinner MA, Heath MD, de Kam PJ, Shamji MH. Ara h 2-expressing virus-like-particles (VLP) induces IL-10-producing B regulatory cells in peanut-allergic individuals: Novel therapeutic candidate for peanut allergy. EAACI Hybrid Congress 2022. Abstract 400
2. **Palmer E,** Layhadi JA, Oleksandra F, Kappen J, Durham S Shamji MH. IL-10^{+} regulatory B cells are dysregulated in patients with seasonal and perennial allergy. The Journal of Allergy and Clinical Immunology. 2022;149(2)AB59
3. **Palmer E,** Layhadi J, Oleksandra F**,** Durham SR, Shamji MS. Induction of IL-10^{+} B Regulatory Cells leads to immunotolerance recovery with grass-pollen subcutaneous immunotherapy. Poster Presentation, presented at the British Society of Immunology, Tissue Immunology conference. London, July 2023.
4. **Palmer E,** Layhadi J, Oleksandra F**,** Durham SR, Shamji MS. The induction of IL-10 producing B regulatory cells leads to immunotolerance recovery with grass pollen subcutaneous immunotherapy. Oral presentation, presented at EAACI Hybrid Congress 2023. Hamburg, June 2023.

5. Layhadi J, **Palmer E,** Drazdauskaite G, Filipaviciute P, Devine A, Wu L, Turner P, Patel N, Oluwayi K, Rusyn O, Skinner M, Heath M, de Kam P-J, Shamji M. Modulation of T and B cell Responses by Virus-like particle (VLP) Expressing Peanut Allergen Ara h 2: A Novel Vaccine Candidate for Peanut Allergy. The Journal of Allergy and Clinical Immunology, 2022;149(2):AB320

ACKNOWLEDGEMENTS

First and foremost, I would like to offer my most sincere gratitude to my primary supervisor, Professor Mohamed Shamji, for his continuous guidance, support, and advice throughout my doctoral training, equipping me with the invaluable knowledge and skills required to my complete my project. I am also extremely grateful to my supervisors, Dr Jasper Kappen, and Professor Stephen Durham, for their advice and guidance throughout my studies. Thank you to the NHLI Foundation at Imperial College London for granting me the scholarship to pursue my PhD, and for providing me with a supportive research network in which to undertake my doctoral training. I had the opportunity to present internationally with additional funding provided by the NHLI Dean's Award, for which I am also very grateful.

I would like to offer my special thanks to the ITG lab members, past and present, for their kind words, support, training, and many laughs throughout my PhD. In particular I would like to extend my deepest appreciation to Dr Janice Layhadi for answering all of my questions (whatever time of night or day!), teaching me most of my techniques, and as such, being an invaluable support to me throughout my studies. I would also like to extend my thanks to the clinical team, including Olesksandra Fedina, for their support with patient recruitment and the clinical aspects of this project, as well as to the donors for their essential contribution towards my doctoral research.

Finally, to my family, Dad, Mum, Sarah, Dave, Charlotte, and Simon, thank you for continually supporting me to follow my interests, believing in me, and, most importantly, patiently waiting for me to finish. To my best friends, GR, EN, HA, FB, RD, and CA, thank you for putting up with years of me yapping on about cells, missing out on social plans to sit in the lab, and for all your encouragement. Finally, to Charles, thank you for your kindness, understanding, and for never complaining whilst listening to me speak about my PhD project for hours on end. Without you, the completion of this thesis would have been so much harder.

CHAPTER 1. INTRODUCTION

1.1 Allergic Disease

Allergic reactions arise due to inappropriate type I hypersensitive immune reactions to exogenous substances, termed allergens, that are innocuous and inert to most of the population. The global prevalence of AD is approximately 10-30%, with distinct allergies demonstrating geographic variability contingent to local environmental allergen levels and lifestyles (1). AD prevalence within industrialised countries is rising, currently affecting ~30% of the UK population, presenting as a significant socioeconomic and healthcare burden to the NHS, costing over £1 billion annually (2). AD aetiology remains somewhat elusive, with studies reporting predisposition to allergy development involves complicated interplay of genetic, psychosocial, and environmental factors (3). There is also growing traction behind the 'hygiene hypothesis' of AD development, suggesting increasing global sanitisation levels prevent early exposure to environmental allergens which may have inferred a protective effect against disease development, thereby contributing towards the rise in AD prevalence (4, 5). AD clinical symptoms manifest as a continuum, ranging from mild reactions to anaphylaxis which can result in systemic organ failure, causing 20-30 deaths annually in the UK. As such, AD burden can range from being a nuisance to severely implicating individual quality of life (QoL). Extensive research to deepen understanding of immunological pathways underlying AD to enable novel disease curative therapeutic strategies thus remains an area of need to combat the rise in allergy epidemics.

Allergic diseases manifest as hypersensitive immune reactions within affected organs, such as the skin, lung, gastrointestinal tract, or nose, in response to allergen. Allergic disorders of the skin include atopic dermatitis, a chronic inflammatory dermatosis arising due to hypersensitivity reactions to food or environmental allergens that come into contact with the

skin barrier, resulting in cardinal symptoms such as eczema-like eruptions and persistent itching (6). Allergic asthma is an allergic disease of the lung, occurring in response to inhaled allergens, such as dust mites, animal danders, and mold, driving airway hypersensitivity reactions, such as bronchoconstriction, resulting in asthma-related symptoms such as wheezing, cough and sputum production (7). Hypersensitive reactions within the gastrointestinal tract in response to ingested food proteins, such as those found within nuts and milk, result in food allergic disease, characterized by gastrointestinal symptoms, such as nausea and abdominal cramps (8). Allergic disease within the nose is termed AR and is described in-depth in section 1.2.

1.2 Allergic Rhinitis

1.2.1 Allergic Rhinitis Clinical Manifestation, Epidemiology and Aetiology

AR is a chronic inflammatory AD of the nasal mucosa orchestrated through IgE-mediated T_H2-cellular immunity in response to inhaled sensitising aeroallergen (9). AR is manifested by episodic cardinal nasal symptoms including congestion, rhinorrhea, nasal pruritus, and paroxysmal sneezing, and non-nasal symptoms, such as allergic conjunctivitis (9). Moreover, AR is associated with significant physical sequalae, such as chronic rhinosinusitis which can be associated with nasal polyp development, and concomitant asthma in 10-40% of patients, hallmarked by bronchial hyperresponsiveness and airway oedema (10, 11). AR is classified based on patient symptom burden, as mild or moderate-severe, as outlined by the world health organization initiative, Allergic Rhinitis and its Impact on Asthma (ARIA) (12). AR aetiology can also be subclassified as seasonal AR (SAR) or perennial AR (PAR), dependent on temporal symptom patterns and allergen availability. SAR occurs in response to seasonal aeroallergens, such as grass-pollen (GP), whereas PAR occurs in response to ubiquitous aeroallergens, such as house-dust mite (HDM) and pet dander. The ARIA guidelines proposed

shifting the paradigm of AR classification to that of symptom frequency (persistent or intermittent) (12). However, the seasonal/perennial approach is more applicable in countries, such as the UK, with well-defined pollinosis periods (13). AR disease prevalence is estimated to be as high as 43.9% in Europe, 22.8% in Africa, 54.5% in America and 47.9% in Asia, presenting as a global chronic condition (14). Longitudinal studies have demonstrated AR is one of the most prevalent pediatric ADs, with incidence often peaking during the teenage years and sustained until the fourth decade of life when incidence gradually declines (15, 16). Predisposition for AR development include a family history of atopic diseases and risk factors including heavy exposure to tobacco, including electronic cigarettes, air pollution, dietary changes, and obesity (17-20). AR is often under-recognised and underestimated, with many patients not seeking medical care despite burdensome symptoms. Studies have recorded 4% of adults have missed work and 36% had presenteeism due to AR, accounting indirectly for most of the AR economic cost, estimated at €30 billion-€50 billion annually within the European Union (21-23). Real-world studies have also demonstrated AR symptoms can detrimentally impact student exam grades, disrupt sleep, and decrease involvement in outdoor activities, thereby impairing patient QoL (24-26).

1.2.2 Common UK Allergic Rhinitis Causative Allergens

Molecular allergology studies have demonstrated that the spectrum of allergens is highly diverse, although common aeroallergens within the UK include pet dander, such as cat, GP, and HDM. Grasses (Poaceae) are near ubiquitous within the environmental and are found on all continents, with grass pollinosis being a leading cause of SAR within the UK. Within the UK, the GP season typically runs for 12-weeks between April/May and July/August dependent on various factors such as weather conditions and flora growth (27). GP allergens, such as *Phleum pratense* (*Phl p*), are subclassified into 13 allergen groups of similar allergenic relationships across GP species, with groups 1 and 5, i.e., *Phl p* 5, demonstrating the most potent allergenicity (28). HDM are ubiquitous and prevalent indoor allergen sources

worldwide, thereby representing one of the most common causative agents of PAR. HDM are arthropodal, with major allergenic HDMs including *Dermatophagoides pteronyssinus* (*Der p*), including the predominate *Der p 1* and *Der p 2* allergen components, and *Dermatophagoides farina* (*Der f*) (29). PAR sensitivity occurs predominantly in response to inhalation of HDM faecal pellets or bodies, with HDM allergen components capable of directly disrupting nasal epithelium integrity through activating protease and toll-like receptors (TLR) (30). Pet dander is a common allergy in the UK, with cat dander being amongst the leading causes of PAR. The major cat allergen, the secretoglobin *Felis domesticus* (*Fel d)* 1, confers the highest allergenicity of cat allergens and is produced in the skin, salivary and lacrimal glands of felines (31). Although homes of cat owners contain the highest concentrations of *Fel d* 1, studies have demonstrated cat allergens to be transported to cars, classrooms, and workspaces, where they can function as allergen reservoirs and become environmentally ubiquitous (32).

1.2.3 Clinical Diagnosis of Allergic Rhinitis

AR clinical diagnosis is based on evaluation of medical history, physical examination, and biomarker laboratory assessments. Initial assessment of patient medical history is critical to gain a detailed understanding of symptomatic history, including time, location, duration, frequency, seasonality, and suspected allergen exposures (33). Physical examination can include assessing the nasal cavity for structural abnormalities, such as nasal polyps, through nasendoscope examination. The cornerstone of AR laboratory diagnosis constitutes testing for elevated serum allergen specific IgE (sIgE) levels or positive wheal and flare responses during performance of a skin prick test (SPT) (34). Advancements in molecular biology have allowed for novel AR diagnostic approaches, such as allergen component-resolved diagnosis, advising therapeutic intervention response (35-37). Cellular diagnostic approaches, such as histamine-release assays and basophil or mast cell activation tests, may also be performed in specialised laboratories and provide further insight into the severity of AR disease (38, 39).

1.2.4 Allergic Rhinitis Pathophysiology

The nasal mucosa functions as the primary air conditioner, humidifier, and purifier of inspired air, and is the first line of defense against airborne foreign bodies, such as allergens, functioning to release alarmins to induce inflammation and initiate repair mechanisms. To optimally perform these functionalities, the nasal epithelium must retain its integrity and ability to regulate appropriate immune responses, both of which become dysregulated during allergic inflammation. Many features of allergic inflammation, notably the involvement of IgE and T_H2 cells, resemble inflammatory responses driven by enteric helminth or parasitic infection. Allergic inflammation pathophysiology is characterised into three temporal phases; sensitisation, early-phase response (EPR) and late-phase response (LPR).

1.2.4.1 Allergen Sensitisation Phase

The sensitisation phase represents first exposure to an allergen and reflects the allergens' ability to elicit a T_H2 cell response within a susceptible individual. Importantly, the allergen sensitisation phase is not associated with any clinical symptoms but represents the establishment of a pool of allergen-specific memory T_H2/T_H2A, IgE^+ B Cells and IgE-coated effector cells in preparation for the next encounter with the senstisising allergen. During initial aeroallergen inhalation, allergen components containing protease activity can directly compromise epithelial barrier integrity through cleaving tight junctions or directly activating pattern recognition receptors. Loss of epithelial barrier integrity causes 'leakiness', allowing allergens to penetrate and stimulate epithelial cell secretion of immunomodulatory cytokines, including IL-25, IL-33 and thymic stromal lymphopoietin (TSLP) (40-42). These alarmins have important roles in the propagation of the allergic inflammatory cascade through activating group 2 innate lymphoid cells (ILC2), that represent alternate sources of T_H2 cytokines (43, 44). In parallel, professional antigen-presenting cells (APC) such as submucosal immature

dendritic cells (DC), residing beneath the inflamed epithelial cells, capture and process allergen whilst simultaneously responding to epithelial-derived alarmins, inducing their activation, maturation, and differentiation into a pro-allergic type 2 DC subset (DC2), expressing CD141, GATA3 and RIPK4 (45, 46). ILC2 and DC cells propagate one another, as IL-13 derived from ILC2 cells promotes DC trafficking to the lymph node (LN), and DC secreted IL-33 activates ILC2 cells via the IL-33/ST-2 pathway (47). Activated DC2 migrate to the draining LN and present captured allergen-derived antigenic peptides in the context of major histocompatibility complex (MHC) II to naïve $CD4^+$ T_H cells (T_H0 cells), driving their activation and differentiation into T_H2, T_H2A or follicular helper T cell (T_{FH}) cells in the setting of an IL-4 rich milieu (45, 48). T_H2 and ILC2 cells accumulate within the nasal epithelium and play integral roles in allergic inflammation through rapidly secreting type-2 cytokines; IL-4, IL-5, IL-9, and IL-13 (48). Newly synthesized IL-4 can maintain the T_H2 lineage through recruiting further T_H0 cells, propagating the adaptive pro-allergic T cell response (48). IL-4, IL-13 and CD40 ligand (CD40L) from T_H2 and T_H2A cells, alongside T_{FH}-derived IL-4 and IL-21, promote B cell activation and immunoglobulin class switch recombination (CSR) towards IgE, driving differentiation into memory plasma cells that produce large volumes of allergen sIgE (49, 50). Soluble IgE diffuses locally, entering the circulatory system where it becomes systemically distributed and gains access to interstitial fluid where it can bind to high-affinity IgE receptors (FcεRI) on effector cells, such as mast cells or eosinophils (Figure 1.2.4.1, A).

1.2.4.2 Early-Phase Allergic Inflammation

The EPR is an IgE-mediated immediate hypersensitivity reaction which occurs within minutes of re-encountering the sensitising allergen. EPRs can last for 2-3 hours and are underscored by the secretion of immunomediators from effector cells at the allergen contact site. Allergen binds to sIgE-FcεRI complexes on effector cell surfaces, resulting in FcεRI cross-linking. Aggregation of two or more FcεRI molecules through cross-linking induces *de novo* gene transcription leading to cellular activation, degranulation, and the secretion of preformed and

newly synthesised immunomodulators including histamine, leukotrienes, cytokines, proteases, and prostaglandins. Studies utilisng nasal allergen challenge models have demonstrated histamine and tryptase levels peak as early as 5 minutes following mucosal allergen exposure (51, 52). Effector cell mediators interact with nasal sensory systems, glands, and local vasculature structures to drive vasodilation, vascular permeability, plasma exudation, stimulation of sensory nerves and mucus secretion. For example, the nasal mucosa is innervated through adrenergic and cholinergic nerve fibres that are activated by sensory nerves which express receptors for various mediators, such as histamine (53). Thus, effector cell mediators are responsible for driving the acute salient features of AR, such as nasal tissue swelling, tear formation, sneezing and a runny nose, and can contribute towards the development of the LPR (54) (Figure 1.2.4.1, B).

1.2.4.3 Late-Phase Allergic Inflammation

Although acute symptoms of the EPR may reduce within minutes, a proportion of patients sustain allergic inflammation at low levels for several hours following allergen exposure or recrudesce, constituting the LPR. The LPR occurs between 2-6 hours following allergen encounter, which often peaks between 6-9 hours and fully resolves in 1-2 days. Predominant LPR symptoms include nasal blockage and nasal discharge, due to prolonged tissue oedema. The LPR is coordinated in part due to persistent mediator production initiated during the EPR by nasal resident mast cells, resulting in influx and activation of a type 2 (T2) inflammatory infiltrate, including granulocytes (eosinophils, neutrophils, basophils), monocytes and T_H2 cells, to the site of allergen contact. Cell influx is facilitated through various cytokines, chemoattractant and adhesion molecules, including E-selectin, intracellular adhesion molecule 1 and vascular cell adhesion module-1 (13). In addition to further IgE-FcεRI complex activation and degranulation of newly recruited granulocytes, IgE-bound allergens bind to FCεRI on the surfaces of DC and mast cells, becoming internalised and facilitating pro-inflammatory cytokine production and allergen capture for presentation to T_H cells, driving their

differentiation into T_H2/T_H2A cells, augmenting allergic inflammation (55, 56). Moreover, IgE binding CD23 (FCεRIII) on B cells, allows efficient presentation of small amounts of allergen through facilitated antigen binding in the context of MHC II to T_H2 cells, stimulating their activation and subsequent production of large volumes of T2 cytokines (57). AR patients demonstrate increased frequencies of $CD23^+$ B cells compared to non-atopic individuals, possibly enhancing the incidence of allergen presentation to T_H cells (57, 58). T2 cytokines can propagate vascular permeability, immune cell infiltration, IgE production through B cell activation, mucus production, vascular leakage, and dilation (Figure 1.2.4.1, C).

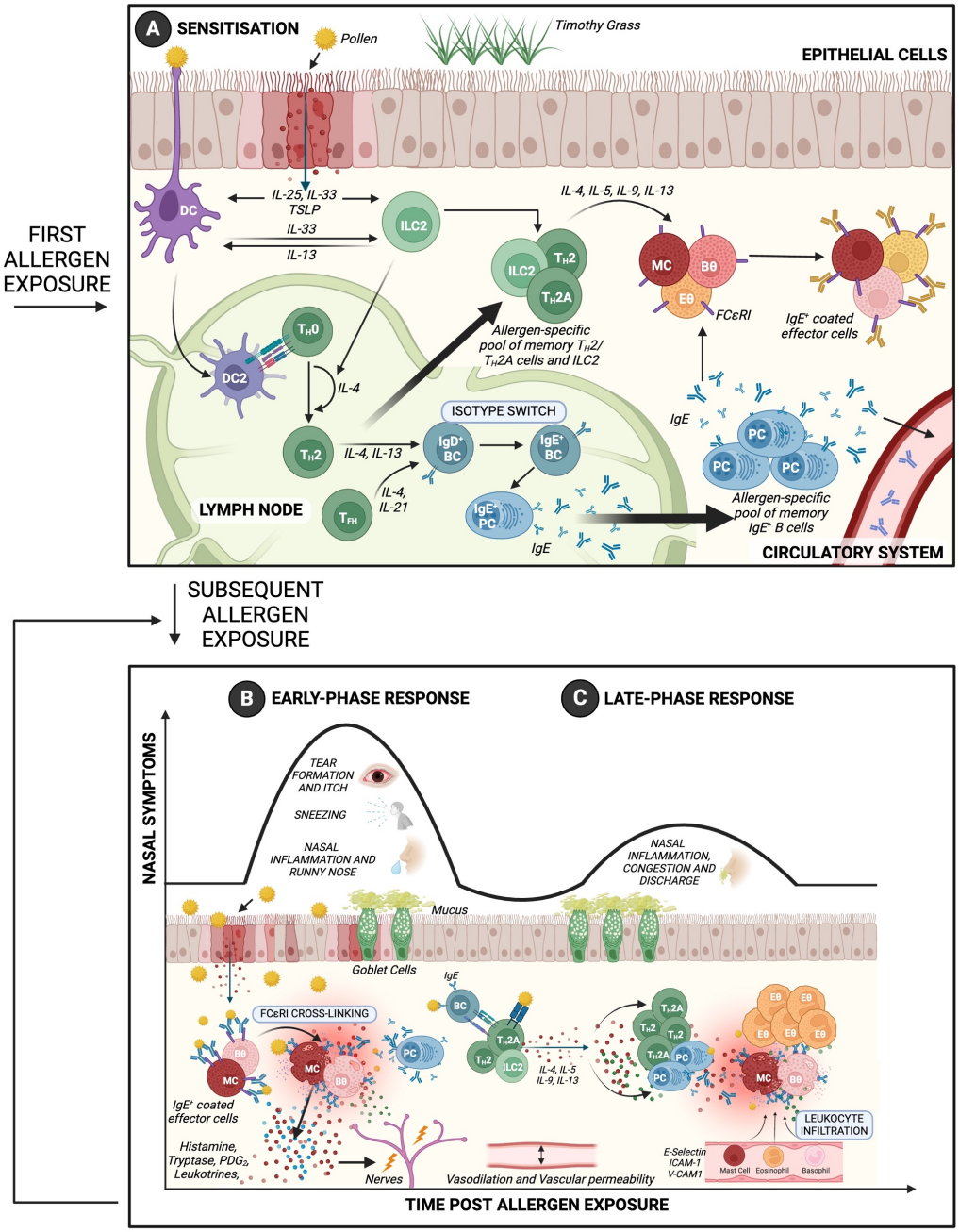


Figure 1.2.4.1 Temporal Phases of Allergic Rhinitis Pathogenesis.

A) Sensitisation Phase. First allergen exposure induces establishment of a pool of allergen-specific memory T_H2/T_H2A, IgE^+ B/PC Cells, IgE-coated effector cells and circulatory IgE. **B) Early-Phase Response**. Allergen-sIgE-FcεRI complex cross-linking upon effector cell surfaces induce cell activation and secretion of mediators, including histamine, which drive mucus production, nerve stimulation and vasodilation, responsible for AR cardinal symptoms. **C) Late-Phase Response.** Mediators released during the early-phase response alongside type-2 cytokines promote leukocyte infiltration, namely T cells, PC, MC, Bθ and Eθ, which undergo further degranulation and propagate the inflammatory response. DC, dendritic cell; T_H0, naïve T cell; $T_H2/2A$, T helper 2/2A cells; T_{FH}, T follicular helper cells; ILC2, innate lymphoid 2 cells; BC, B Cell; Eθ, eosinophil; Bθ, basophil; MC, mast cell; Ig, immunoglobulin; PC, plasma cell; TSLP, thymic stromal lymphopoietin; DC2, type 2 dendritic cell. Created on BioRender.com

1.2.5 Allergic Rhinitis Treatment and Management

1.2.5.1 Allergen Avoidance and Pharmacologic Management

First line adjunctive therapy in AR management is the minimisation of aeroallergen exposure, although this is not always feasible, especially for polysensitised patients or for ubiquitous perennial allergens. There are many pharmacologic treatment modalities, including oral and intranasal decongestants, available for management of AR that can provide symptomatic relief to patients and thereby demonstrate established benefit (59). For example, second generation H_1-antihistamines, such as fexofenadine, are effective at AR symptom alleviation, well tolerated, rapid, cost-effective, and safe, and are administered either prophylactically daily or at peak symptom onset (33). H_1-antihistamines are first line treatments for SAR and can be administered orally, intranasally, or ocularly, and block the effects of histamine by acting as antagonists or inverse agonists of H_1 and muscarinic receptors. Topical corticosteroids (TC), such as beclomethasone, are first-line treatments for mild persistent to moderate AR due to being superior to H_1-antihistamines in controlling rhinorrhea and nasal congestion (60). TC suppress allergic inflammation through enhancing local nasal mucosal anti-inflammatory effects in the absence of systemic effects due to the lack of systemic absorption, with common adverse effects including nasal irritation (33). TC should be administered sufficiently and regularly to effectively suppress AR symptoms and are often prescribed in a combination with H_1-antihistamines due to efficacy establishment taking several hours or days. Leukotriene receptor antagonists, such as motelukast, are often administered in combination with TC and H_1-antihistamines where they may provide additional therapeutic advantages, such as controlling ocular symptoms and symptoms at night-time, thus reducing sleep disturbance (61, 62).

1.2.5.2 Biological Treatment

Advancements in molecular biology have facilitated deeper understanding of allergic inflammatory pathways, allowing the development of various inhibitory biological therapeutics targeting specific elements, such as IgE, IL-4 and IL-5 (63). Omalizumab is an anti-IgE monoclonal antibody (mAb) indicated in the UK for treatment of moderate-severe uncontrolled allergic asthma and chronic idiopathic urticaria. Omalizumab efficacy has been well-demonstrated for AR treatment, with studies demonstrating a single dosage before the GP season achieves superior symptom control and reduces burdensome pharmacological treatment use (64, 65). Dupilumab is a fully humanised IgG_4 mAb directed against the α chain of the IL-4 receptor (IL-4Rα), which has been reported to improve AR nasal symptoms in patients suffering from chronic rhinosinusitis with nasal polyposis and asthma with comorbid AR (66, 67). Biologics targeting the IL-5 axis, such as mepolizumab, reslizumab and benralizumab suppress eosinophil production, maturation, and migration, although have not yet demonstrated clear efficacy in AR. Clinical trial data does yet support the ability of biologics to prevent, rescind or modify progression of AD upon discontinuation, preventing their costly routine application across the AR therapy area (63). Moreover, within the UK, currently no biologics are approved for the treatment of AR.

1.3 Allergen Immunotherapy

Conventional treatments for AD fail to elicit adequate symptomatic relief in all patients or alter underlying immunological perturbations, with treatment discontinuation resulting in symptom relapse in almost all patients. AIT is the only aetiological curative treatment approved for IgE-mediated AD such as AR, demonstrating the ability to establish long-term tolerance to the sensitising allergen following 3 years continuous administration in patients with uncontrolled moderate-severe symptoms. The classical AIT protocol was pioneered in 1911 by Noon and Freeman, following observations that prophylactic subcutaneous immunisation with GP

extracts mitigated symptomatic burden in SAR patients during the proceeding GP season (68, 69). Conventional AIT approaches consist of repeated provision of crude allergen extracts to establish clinical immunological tolerance to the administered allergen, compromising of an initial up-dosing phase of incremental allergen doses before a maintenance phase of high-dose exposure. Dosages of administered allergen during AIT protocols are markedly higher than natural environmental exposure to allergen, for example, delivering greater than four times the concentration of *Phl p* 5 per administration compared to that encountered during the whole GP season (70-72). Within Europe, aqueous allergen extracts utilised for AIT are alum-precipitated to suppress immediate hypersensitivity reactions through slowing allergen release on injection (73). Traditionally, AIT is administered through subcutaneous immunotherapy (SCIT) or sublingual immunotherapy (SLIT), through tablets or drops. SLIT is associated with greater safety but poor patient compliance, ranging between 18%-45%, and SCIT with greater efficacy and compliance, ranging between 50-89%, thereby remaining the gold standard AIT treatment (74, 75).

1.3.1 Allergen Immunotherapy for Allergic Rhinitis

Extensive studies have investigated AIT in the setting of AR, with recent systemic reviews reporting both SCIT and SLIT significantly reduce symptomatology and medication requirements in selected patients who are refractory to first line therapy with pharmacologics (76, 77). Moreover, numerous long-term studies have confirmed SLIT and SCIT administration for 3 years induces sustained tolerance to administered allergen, evidenced through lasting humoral compartment modifications, and persistent decrease in clinical symptoms following treatment cessation (78-83). For example, the recent REACT study investigating long-term real-world effectiveness of AIT in AR treatment in 46,024 AIT-treated subjects reported significant reduction of medication need and symptomatic burden in the AIT-treated group, indicating sustained effectiveness of AIT (84). The allergen specificity of AIT was recently confirmed by Durham *et al.* whereby AR patients administered either TG or birch-pollen AIT

demonstrated significant symptom reduction upon nasal provocation with their AIT targeted allergen, but not the untargeted allergen (85). An overview of seminal studies investigating AIT for AR treatment can be found in Table 1.3.1.1.

Table 1.3.1.1 Seminal Allergen Immunotherapy clinical studies

Year	Admin. Route	Allergen	Key Findings	Ref.
1911	SCIT	GP	Prophylactic administration suppressed immediate conjunctival sensitivity and AR symptoms during the GP season	(68, 69)
1954	SCIT	GP	First RDBPC trial, demonstrating efficacy of SCIT therapy	(86)
1996	SCIT	Cat	Synthesised T cell peptides containing dominant epitopes for *Fel d* 1, reduced nasal symptoms following cat exposure	(87)
1998	SLIT	HDM	Two-year administration with HDM allergoid is effective at reducing symptom score compared to placebo	(88)
1999	SLIT	GP	Prophylactic administration reduced clinical symptoms and modification need during preceding GP season	(89)
2007	SCIT	GP	AR subjects demonstrated long-term symptom reduction and preventative effect of asthma development (PAT study, 10-year follow-up)	(90)
2008	ILIT	GP	Direct administration of GP extract into LN effectively ameliorated AR symptom burden, sIgE levels and SPT reactivity	(91)
2009	ECIT	GP	Patches containing GP significantly reduced symptom scores following NAC	(92)
2011	SCIT	GP	Short-term AIT utilising adjuvant provided significant symptomatic relief compared to placebo after four weeks	(93)
2017	SCIT and SLIT	GP	Confirmation two years conventional therapy is not sufficient to confer long-term tolerance to administered allergen	(74)
2017	SCIT	GP	B cell targeted-epitope peptides reduced medication need and symptom scores alongside induction of allergen-sIgG	(94)
2018	SCIT	Cat	Passive immunotherapy with anti-*Fel d* 1 IgG_4 mAb reduces symptomatic burden and enhances serum blocking IgG levels	(95)
2021	SLIT and SCIT	GP	Differential induction of blocking antibodies following SCIT and SLIT suggest differential modes of action	(96)

Admin, administration; SCIT, subcutaneous immunotherapy; GP, grass pollen; SLIT, sublingual immunotherapy; HDM, house dust mite; ILIT, intralymphatic immunotherapy; ECIT, epicutaneous immunotherapy; NAC, nasal provocation test; mAB, monoclonal antibody; RDBPC, randomised double blinded placebo controlled.

1.3.2 Allergen Immunotherapy for Peanut Allergy

Peanut allergy is amongst the most common food hypersensitivity in children, affecting between 1-3% of children and persisting into adulthood in approximately 75-80% of those affected, presenting as a life-long condition (97, 98). 97% of peanut allergic (PA) individuals demonstrate sensitivity to the major peanut protein (*Arachis hypogaea)* components, *Ara h* 1, *Ara h* 2 or *Ara h* 3, although, patient sensitisation to *Ara h* 2 is often associated with the most severe symptomatic burden of peanut allergy (99, 100). PA exposure to peanut can lead to significant symptoms, including anaphylactic shock, and is often associated with more severe reactions than other food allergies, such as egg or soy (101). Therefore, peanut allergy can present as a serious healthcare burden to patients due to the significant efforts required to avoid inadvertent peanut particle ingestion and potentially traumatic accidental allergic reactions, detrimentally affecting patient QoL (97). Current therapeutic treatments for peanut allergy are lacking, with first line management involving strict allergen avoidance not always feasible, leading to the recommendation of AIT for the treatment of peanut sensitization to reinstate threshold tolerance (102). Although late phase oral immunotherapy, epicutaneous immunotherapy (ECIT) and SLIT peanut studies have reported strong clinical desensitisation rates, safety concerns remain due to the high number of reported adverse events, including anaphylaxis (103-107). For example, during the PALISADE clinical study, although 300mg encapsulated whole peanut administered daily led to 67.2% of patients reaching a predetermined threshold of tolerance, systemic side effects were observed in 14.2% of participants, including 1 case of anaphylaxis (108). Although the PALISADE trial led to an approved peanut AIT product, challenges with oral AIT for peanut allergy remain due to lack of sustained remission, with the recent IMPACT and POISED studies reporting loss of tolerance to peanut after three years treatment cessation in 13 and 21% of patients, respectively (103, 104, 109). Therefore, further research to generate safer AIT approaches for

peanut allergy able to reprogram underlying disease immunophysiology in a disease-curative manner are required.

1.3.3 Immunological Basis of Allergen Immunotherapy Treatment

Delineating the multifactorial immune compartment alterations underscoring AIT is critical to identify specific biomarkers of treatment which can monitor efficacy, desensitisation and stratify responders from non-responders. Despite various candidate humoral, cellular, and metabolic components being proposed, there is not yet an established and validated AIT biomarker. Although the exact immunomodulatory mechanisms of AIT remain uncertain, long-term efficacy is attributable to restoration of epithelial barrier integrity, reinstatement of regulatory immune cellular compartments and depletion of pro-allergenic effector cells.

1.3.3.1 AIT Modulation of Epithelial Barrier Integrity

During AR disease pathomechanism, allergen penetration of nasal epithelial barriers results in loss of epithelial integrity and induction of epithelial-derived cytokines, such as IL-33. Modular network analysis performed as part of the GRASS clinical study revealed molecules relating to epithelial integrity, such as epidermal growth factor receptor, and lipid metabolism were significantly altered following two years of SCIT or SLIT treatment (110). AIT-driven restoration of epithelial integrity was also proposed during the recent VITAL study of HDM-SLIT, whereby decreased IL-33 levels were reported following 24 weeks of daily Acarizax treatment (111).

1.3.3.2 AIT Modulation of Innate Immune Compartment

Abated allergic inflammation during AIT is associated with reduced eosinophil, mast cell and basophil infiltration and responsiveness, consequently depleting local levels of their associated immunomodulators, such as histamine (112, 113). Assays exploring modulation of

basophil activation have demonstrated AIT-mediated reduction of degranulation, and suppression of IL-4 and IL-13 production (114, 115). AIT significantly modulates the DC compartment, inducing tolerogenic regulatory DCs (DCreg) phenotyped based on CC1Q, FCγRII, and STAB1 expression and IL-10, IL-12, and IL-27 secretion, which correlate with therapeutic efficacy (116, 117). Moreover, evaluation of DC2 and DCreg markers 4 months after SLIT treatment allowed stratification of treatment responders (117). AIT also demonstrates ability to downregulate CD86 expression on DCs, suggested in murine models to be important for driving airway eosinophilia and hyperresponsiveness (118, 119). Numerous AIT studies have reported effective suppression of seasonal increases in circulatory ILC2 levels alongside durable restoration of $CD25^+$ ILC1 levels (120-122). Moreover, preclinical studies have demonstrated suppressive $IL\text{-}10^+$ ILC2 cells preferentially expressing KLRG1, induced by IL-33, IL-7, and IL-2, strongly associate with AIT clinical efficacy (123).

1.3.3.3 AIT Modulation of Adaptive Immune Compartment: T Cells

T cells develop from haemopoietic lymphoid progenitors within the bone marrow (BM) before undergoing maturation, central tolerisation and both positive and negative selection within the thymus. Peripheral T_H cell subsets are vast, with defective T_H2, T_H2A, type 1 T cells (T_H1), T_{FH}, and Treg cellular compartments attributable to allergy development. Extensive research to decipher T cell responses have revealed prominent and significant modulations following AIT therapy which may contribute towards tolerance reinstatement to allergen.

1.3.3.3.1 T_H2/T_H2A Cellular Modulations

Presence of T_H2 cells, expressing the GATA3-transcription marker and secreting T2 associated proinflammatory cytokines, IL-4, IL-5, IL-9, and IL-13, is a hallmark of AD, significantly enhanced in AR patients compared to healthy controls (124). AR patients also presented with pathogenic allergen specific T_H2A cells, constituting a terminally differentiated

subpopulation of T_H2 cells that preferentially express CRT_H2, CD161 and CD49d alongside little to no CD27 (125). Due to their increased expression of epithelial-cell-derived cytokine receptors, T_H2A cells secrete higher volumes of IL-5 and IL-9 and express greater IL-4 compared to T_H2 cells, highlighting their importance in AR disease pathophysiology (125, 126). Following initial transient increases, significant attenuation of T_H2 and T_H2A cellular responses have been reported in numerous SLIT and SCIT studies, evidenced through reductions in their frequency and associated cytokine levels in both peripheral blood and nasal mucosa as well as attenuation of IL-4 mRNA expression (74, 127-130). Moreover, transcriptomic analysis of AR patient peripheral blood mononuclear cells (PBMCs) revealed SCIT treatment preceding the GP season induced significant suppression of T_H2 signature cytokines (131). The recent GRASS clinical trial reported effects of SCIT and SLIT mediated attenuation of T_H2 and T_H2A cell compartments and reduction of nasal cytokine levels were lost 1 year after treatment cessation, highlighting that long-term treatment is required to constrain pro-allergenic T_H2 and T_H2A cellular responses (127). GP AIT may also enhance T_H2 cell susceptibility to apoptosis, understood through observations that IL-4^+ cells from AIT-treated patients undergo rapid apoptosis following exposure to GP allergen (132). Moreover, recent studies have reported that T_H2A cells are deleted following AIT treatment, potentially due to cell exhaustion (133).

1.3.3.3.2 T_H1 Cellular Modulations

T_H1 cells, a subset of $CD4^+$ T_H cells expressing the T-bet1 transcription factor and secreting IFN-γ, differentiate from T_H0 cells within an IFN-γ rich milieu, propagating further T_H1 cell expansion. Numerous AIT studies have reported immune deviation from T_H2 and T_H2A cells towards IFN-γ^+ T_H1 cells, although initiation of T_H1 deviation in peripheral blood and target organs is a delayed response, often occurring after 12 months treatment (112, 134). For example, following GP and birch AIT treatment, enhanced peripheral T_H1:T_H2 cell subset ratios were reported alongside increased local nasal IFN-γ levels and attenuation of IL-5:IFN-

γ mRNA ratios, which correlated with reduced symptomatic burden (112, 135). Supporting this notion further, AIT has also been demonstrated to drive IFN-γ in a time-dependent manner following AIT treatment (136). Transcriptomic analysis of AR patient PBMCs revealed SCIT treatment prior to the GP season significantly upregulated IL-12A and IFN-y (131). Interestingly, T_H1 cells have also been reported to demonstrate increased expression of the anti-apoptotic protein Bcl-2 following 1 year of AIT-treatment (137).

1.3.3.3.3 T_{FH}/T_{FR} Cellular Modulations

T_{FH} cells can be located within germinal centres (GC) in secondary lymphoid organs, or circulating within the peripheral blood, termed circulatory T_{FH} (cT_{FH}) cells (50). Both T_{FH} and cT_{FH} express PD-1 and preferentially produce IL-4 and IL-21, known to be important for driving B cell isotype switch towards IgE, with recent studies demonstrating cT_{FH} cell frequencies are significantly enhanced in AR patients, potentially contributing towards inappropriate excessive IgE^+ B cell establishment (138-141). Interestingly, when stimulated by HDM extract, $IL\text{-}4^+$ T_H2-like cT_{FH} but not T_H1-like cT_{FH} were enhanced and correlated with HDM-sIgE levels (142). T_{FR} expressing $CXCR5^+PD\text{-}1^+BCL\text{-}6^+FOXP3^+$ play important suppressive counterpart roles to T_{FH} within B cell follicles, with a dearth of $IL\text{-}10^+$ T_{FR} cells alongside impaired ability to suppress B cells observed within AR patients (58, 143-145). Recent studies have revealed pro-inflammatory $CXCR5^+$ cT_{FH} subsets are reduced following AIT in parallel to enhanced levels of T_{FR} (141, 145, 146) . Therefore, the paradigm shift in T_{FH}/T_{FR} cells may reduce T_{FH}-promoted IgE production from B-cells, supported through positive correlations between reduced serum sIgE levels and reduced T_{FH} cells (142, 147).

1.3.3.3.4 iTreg/Treg/iTR1, iTr35 Cellular Modulations

Treg cellular compartments play critical roles in inflammation suppression and maintenance of homeostasis and include 2 main subclassifications, $FOXP3^+$ thymus derived natural Treg

(nTreg) cells and peripheral inducible Treg (iTreg) cells. iTreg cell populations are further classified into IL-10^+ iTR1 and IL-35^+ iTR35, dependent on dominant cytokine secretion. All Treg cell subsets constrain inflammation through a multitude of similar suppressive mechanisms, such as production of anti-inflammatory cytokines, such as IL-10 and TGF-β, and are phenotyped by $CD127^{lo}CD25^{hi}$ expression. AIT is effective at restoring iTR1, iTR35, and nTreg cell subset frequencies and associated levels of IL-10, TGF-β and IL-35 in peripheral blood and nasal mucosa of AR patients, that possess suppressive capacity (148-151). AIT has also been demonstrated to drive epigenetic modifications within Treg cell populations, whereby reduction in CpG methylation within FOXP3-regions increased its transcript and thus frequencies of nTreg cells (150). Preclinical studies in cultured PBMCs have also demonstrated novel subsets of $SATB1^-CD125^+$ Treg cells which are induced following exposure to depigmented and polymerised native *Phl p* extract (152). Novel AIT approaches, such as treatment with Notch-2 expressing lentivirus, have been demonstrated to directly promote local nTreg cellular compartment differentiation in AR (153, 154). Gene knockout studies have also demonstrated that miR-146a may play a key role in inducing Treg cells in AR patients through STAT5b regulation (155).

1.3.3.4 AIT Modulation of Adaptive Immune Compartment: B Cells

One of the most important immunological effects observed following AIT is isotype switching in IgE^+ B-cells and consequent induction of allergen-specific blocking antibodies IgA_1, IgA_2, IgG_1 and IgG_4 (83, 156, 157). AIT also induces and maintains a distinct rare subset of B cells, coined Breg, which elicit potent immunosuppressive functions (158). Although initial studies have demonstrated Breg cells can propagate peripheral tolerance through IL-10 production, the full spectrum of their role in tolerance reinstatement during AIT remains to be elucidated. AIT modulation of B cell compartments and antibodies are discussed in depth in Section 1.4 and Section 1.5. A summary of cellular modulations during AIT is presented in Figure 1.3.3.1.

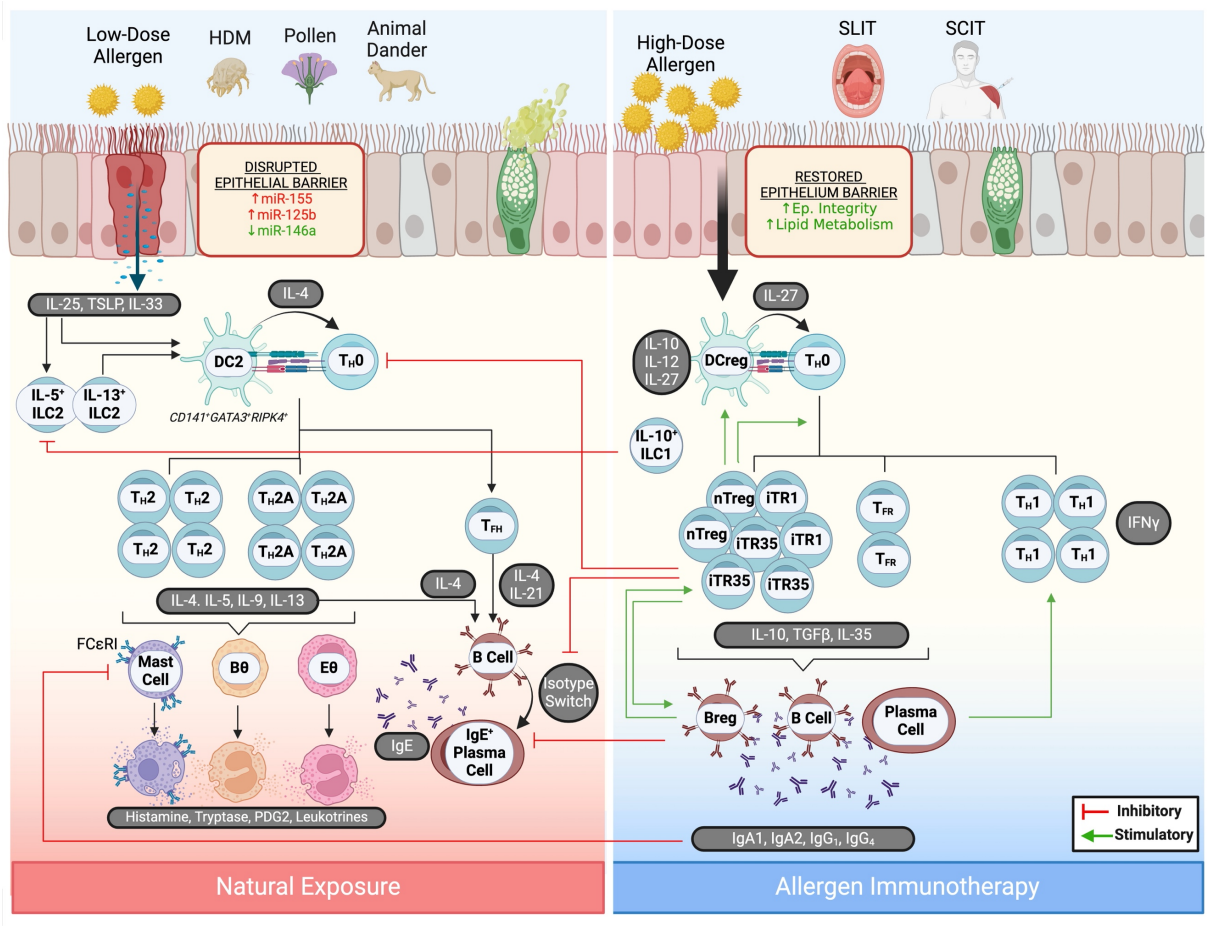


Figure 1.3.3.1 Allergen Immunotherapy Immunological Mechanism.

Natural low dose allergen exposure drives epithelial barrier dysregulation, activation of ILC2, DC2 and differentiation of pro-allergenic $T_H2/2A$ cells that promote IgE production by B cells. Allergen-sIgE-FcεRI complex cross-linking upon effector cell surfaces induce cell activation, degranulation, and secretion of immunomediators. High dose allergen exposure administered through allergen immunotherapy restores epithelial barriers and induces ILC1 subsets and DCreg cells, which promote T_H1 and T_{FR} differentiation and expansion of Treg subsets. IL-10, TGFβ and IL-35 drive B cells to produce inhibitory antibodies, IgA1, IgA2, IgG_1 and IgG_4. Inhibitory antibodies compete with IgE, preventing formation of allergen-IgE FCεRI complexes on effector cells. Red lines indicate inhibitory pathways and green lines indicate stimulatory pathways as mediated by allergen immunotherapy. DC2, type 2 dendritic cell; T_H0, naïve T cell; $T_H2/2A$, T helper 2/2A cells; T_{FH}, T follicular helper cells; ILC2, innate lymphoid 2 cells; BC, B Cell; Eθ, eosinophil; Bθ, basophil; MC, mast cell; TSLP, thymic stromal lymphopoietin; HDM, house-dust mite; SLIT, sublingual immunotherapy; SCIT, subcutaneous immunotherapy; DCreg, regulatory dendritic cell; T_{FR}, regulatory T follicular cell; Breg, regulatory B cell; nTreg, natural T regulatory cell; iTR1, inducible IL-10^+ T regulatory cell; iTR35, inducible IL-35^+ T regulatory cell; T_H1, type 1 helper T cell; PDG2, prostaglandin 2; Ep. Epithelial. Created on Biorender.com.

1.3.4 Allergen Immunotherapy Challenges and Alternative Approaches

Currently, routine use of AIT is limited due to its failure to confer clinical tolerance to the administered allergen in all treated patients, with a universally accepted prognostic and predictive biomarker facilitating identification of treatment responders yet to be identified (159). Moreover, AIT is expensive, associated with severe adverse effects, such as anaphylaxis, and is time-consuming, resulting in poor patient compliance to treatment (75, 160). As such, next generation AIT approach studies to resolve these challenges whilst maintaining clinical efficacy and mitigating risk of adverse effects are areas of extensive research. Despite numerous studies investigating alternative AIT administration routes, such as intralymphatic immunotherapy (ILIT), proposed to augment allergen presentation to T cell without local effector cell activation, and ECIT, proposed to target the high numbers of resident DC cells within the skin to facilitate efficient processing and presentation of low allergen dosages, neither approach has conferred any clinical advantage compared to SLIT or SCIT (92, 161, 162). Novel AIT approaches also include chemically modifying allergens to reduce allergenicity, utilising linear allergen peptides genetically modified to display distinct T and B cell epitopes and recombinant allergens, allowing medication standardisation and production of large quantities of stock for therapeutic usage (93, 163-165). However, no allergen modifications have yet demonstrated clear benefit over usage of standard crude allergen extracts, limiting their uptake (165, 166). Within Europe, aqueous crude allergen extracts are alum-precipitated, which can act as coadjuvants for T_H2 cell activation, increasing risks of therapy-related adverse effects. Thus, alternative depot formulations and adjuvants, like hydrogels or bioparticles (BP) are being investigated.

1.3.4.1 Novel Allergen Immunotherapy Approaches: Bioparticles

BP are amongst the most novel strategies to enhance AIT clinical efficacy and safety, proposed to enhance AIT immunogenicity by eliciting strong allergen-specific B and T cellular responses through the presentation of target allergen on their surfaces. Mounting evidence

has suggested BP can modulate immune responses, evidencing their potential benefit during AIT as highly immunogenic allergen carrier devices (167). BP-based vaccines have demonstrated success for the treatment of a variety of disease states, such as human papilloma virus and hepatitis-B (168). However, investigations into BP usage during AIT treatment remains in its infancy, with a scarcity of preclinical studies conducted to date. Virus-like particles (VLP) represent a specific-class of BP in which the structural and immunogenic constituents hail from viral origins, but without its genomic material. VLP are multimeric constructs which express repetitive displays of conformational allergen epitopes on their cell surfaces, proposed to result in activation of B cells through B cell receptor (BCR) cross-linking, highlighting their potential to enhance AIT immunogenicity (169-171). Clinical trials involving AR and allergic asthmatic patients have demonstrated VLP was tolerable, reduced symptom scores, and modulated eosinophil compartments (172, 173). Moreover, although VLP can be described as 'self-adjuvanted', additional adjuvants may confer further immunogenicity which could translate clinically to enhanced treatment efficacy. In addition to BP hailed from viruses, synthetic biology has produced artificial modular enveloped BP (eBP) comprised of elements from heterogenous biological sources in a 3D particulate ultrastructure, through coiled-coil hybrid assembly (174). Like VLP, eBP allow the presentation of multivalent high-density antigenic components to drive BCR cross-linking but, are devoid of viral immunogenic determinants which can drive anti-viral immune responses, making them attractive allergen-carrier systems for AD treatment.

1.4 B Cells

1.4.1 B Cell Ontology, Development and Central Tolerance

B cells, and their produced antibodies, constitute humoral immunity and are multifaceted in their contribution during homeostasis and inflammation, demonstrating capacity to differentiate into antibody-secreting plasma cells, act as potent APCs, produce a plethora of

cytokines and fine-tune T cell activation within GC. Human B cells arise from multipotent haemopoietic stem cells, located within BM microenvironmental stromal niches. Early B cell development is a tightly regulated maturation and selection programme, structured around successive rearrangements of antigen receptor genes, a unique mechanism premising B cells to generate diverse antigen-specific BCR repertoires from a restricted quantity of immunoglobulin variable (V) gene segments (175). Progenitor B cells undergo somatic recombination of V, diversity (D) and joining (J) gene segments within the *Igh* locus, synthesising an intact μ heavy chain (HC) protein that associates with a surrogate light chain (LC), constituting the pre-BCR complex. At this stage, CD19 is expressed on the surface of progenitor B cells, constituting a defining marker of the B cell lineage (175). Pre-BCR complex expression initiates progression into precursor B cells, which subsequently undergo LC (κ or λ), rearrangement of the V_L and D_L gene segments, forming a fully formed IgM BCR complex consisting of two functional HC and LC alongside the signal transducing heterodimer, Igα/Igβ (175). Precursor B cells which successfully form fully functional BCR are termed 'immature' B cells. HC include C regions expressed in the form of five immunoglobulin isotype classes: IgM, IgD, IgE, IgG (subclassified into IgG_1, IgG_2, IgG_3, IgG_4) and IgA (subclassified into IgA_1 and IgA_2), that modify BCR effector function whilst maintaining antigen specificity. Thus, the final BCR consists of two identical HC, including the C region determining antibody isotype, and two LC light chains, including a Fc region and a F(ab) region, responsible for antigen binding, separated by a disulphide bond. B cells have capacity to generate approximately $5x10^{13}$ different BCR specificities, termed its "repertoire" (176). Central tolerance ensures BCR specificities produced through somatic recombination are not autoreactive through stromal cell presentation of self-antigens to immature B cells, with autoreactive BCR-expressing B cells selectively eliminated through clonal deletion, anergy induction, resulting in functional inactivation due to downregulation of BCR expression, and receptor editing, generating a new BCR with a new specificity (177). Upon egressing from the BM immature IgM^+ B cells become 'transitional' (T) B cells, subdivided into T1 (IgM^{high}) and then T2 ($IgM^{high}IgD^+$) B cells,

expressing high CD24 and CD38 and consisting of 4% of the total B cell population (178). T1/T2 B cells migrate to the spleen to complete early-development, differentiating into either follicular B cells (FOB) or marginal zone B cells (MZB). MZB develop due to weak BCR signalling and reside within the margins of the spleen, responsible for rapidly responding to blood-borne antigens through both T-cell dependent and independent responses and differentiating into short-lived plasmablasts, producing large amounts of IgM (179). Tonic, or strong BCR signalling alongside a BAFF survival signal induces FOB, which recirculate throughout the blood and secondary lymphoid structures, and are responsible for interacting with T cells and responding to BCR and antigen cognate interactions, producing high affinity antibodies (180).

1.4.2 B Cell Germinal Centre Reactions

Upon recognition of their cognate antigen, resting FOB migrate to the T cell border of secondary lymphoid follicles and receive co-stimulatory signals from T_H cells, inducing their differentiation into large, rapidly proliferating, centroblasts (180, 181). Mitotically active centroblasts form a transient GC structure to undergo antibody affinity maturation, microanatomically defined by a ‘dark’ zone (DZ) and a ‘light’ zone (LZ). Centroblasts upregulate abundant expression of activation-induced cytidine deaminase (AID) and the master transcription factor Bcl6, required for entry to the GC programme. AID is a mutator enzyme that initiates somatic hypermutations (SHM) at a rate of 1/1000 base pairs per cell generation within the V region of the expressed immunoglobulin gene. AID-induced mutations can also trigger CSR, whereby the C region of IgM is replaced to either IgA, IgE or IgG. Post-mitotic centroblasts migrate to the LZ where they become centrocytes and interact with antigen-held in the form of immune complexes on follicular DC to test the affinity of their newly mutated BCR (182, 183). Centrocytes with strong BCR affinities capture the highest quantity of presented antigen, thereby presenting the highest amount of antigen on MHC II to T_{FH} cells. T_{FH} provide survival signals to high affinity centrocytes through cognate interactions mediated

by CD40L and various cytokines, including IL-4 and IL-21, which contribute towards isotype switch selection (184). Of note, allergen-primed T_{FH} cells secrete IL-13 which promotes expression of IgE (185). Competitive expansion of high affinity centrocytes for a limited pool of T_{FH} cells drives elimination of centrocytes with weak affinity by apoptosis, due to suppression of the anti-apoptotic gene Bcl2 by Bcl6 (180, 186). B cells can shuttle between the DZ and LZ to undergo further attempts at SHM and CSR to try and improve their BCR affinity to antigen, following a CXCR4 gradient. Positively selected centrocytes differentiate into plasmablasts and then plasma cells secreting large volumes of the same specific antigen or $CD27^+$ memory B cells, dependent on expression of Bcl6 (187). These antigen-specific memory B cells can reside in either secondary lymphoid structures or migrate to specific survival niches in the BM where they can persist for years and continue to produce antibodies to prime subsequent immune responses (175, 180).

1.4.3 B Cells in Allergic Inflammation

The contribution of pro-inflammatory B cells to allergic inflammation is well characterised, predominantly through the provision of large volumes of allergen sIgE. IgE contributes substantially to allergic pathogenesis through activating effector cell degranulation and facilitating antigen presentation by B cells, DC, and mast cells to T cells, driving T_H2 differentiation. Local mucosal tissue may represent survival niches for memory B cells and plasma cells responsible for IgE production, supported by observations that exposure to HDM enhances local HDM-sIgE levels in the nasal mucosa of AR patients before HDM-sIgE serum levels (188). Moreover, local AR is hallmarked by the presence of IgE^+ B cells and IgE^+ plasma cells in nasal biopsies and local allergen-sIgE alongside absence of systemic IgE responses (189-191). In addition to traditional GC reactions in secondary lymphoid organs, increasing evidence suggests the source of IgE^+ B cells at mucosal surfaces may arise from the development of local 'tertiary' GC structures at the tissue site. For example, C region isotype CSR to IgE is mediated through IL-4 and IL-13 secretion from allergen-activated cognate T_H2

cells, which are prevalent within nasal mucosa and can be indicated by expression of εGLT and εmRNA and AIT presence (192). Studies have also demonstrated mucosal B cells express enhanced levels of both εGLT and εMRNA following allergen exposure, indicating these B cells have potential to, or have undergone, CSR, with C region switch from IgM, IgG_1, IgG_3 and IgG_4 to IgE recorded in GP and ragweed SAR patients following allergen exposure, evidenced through identification of ε switch circle (193-197). The phenomenon of local CSR within nasal mucosa may explain how effector cell FCεRI remains fully saturated with IgE in the absence of high systemic IgE levels.

1.4.4 B Cells following Allergen Immunotherapy

AIT induces B cell isotype switching, resulting in increased serum and local levels of antigen $sIgA_1$, $sIgA_2$, $sIgG_1$ and $sIgG_4$ levels in parallel to reduction of tIgE and sIgE levels, following initial transient enhancement (96, 156, 198-202). The concept of serum blocking antibodies was first introduced in 1935 following observations that passive transfer of AIT-patient serum conferred sensitivity in untreated patients (203). Numerous studies have demonstrated inhibitory antibodies induced during AIT include IgG_1, IgG_2 and IgG_4, with peripheral and local levels of IgG_4 antibodies increasing up to 100-fold compared to baseline following AIT treatment (204). IgG upregulation is associated with repetitive and prolonged exposure to antigen, with recent studies confirming that AIT utilising high-dose extract, but not low-dose allergoid, induced protective IgG_1 responses (205). Allergen-$sIgG_2$ levels were also significantly enhanced in treatment responders following GP- and HDM- SLIT (206-208). IgG_4 antibodies partake in dynamic F(ab) arm exchange and demonstrate functional monovalency as bispecific antibodies that possess low affinities for Fcγ receptors and an inability to active complement (209). Therefore, IgG_4 antibodies are considered anti-inflammatory through exhibiting reduced ability to mediate antibody-dependent cellular cytotoxicity and antibody-dependent cellular phagocytosis. IgG_4 attenuates allergic inflammation during AIT through

competing with IgE for allergen binding, thereby impeding FcεRI-IgE-allergen cross-linking activation of effector cells and IgE-facilitated allergen presentation by B cells, to T cells, suppressing T_H2 and T_H2A cell development (51, 156, 157, 202, 210, 211). Interestingly, IgE-facilitated binding competitive studies demonstrated nasal fluid allergen $sIgG_4$ exhibits greater inhibitory capacity of IgE compared to systemic $sIgG_4$, suggesting local and peripheral IgG_4. may confer different functionalities (202). The potency of IgG_4 antibodies in mediating suppression of allergic inflammation are confirmed through the significant clinical efficacy of fully humanized IgG_4 mAbs directed against non-overlapping epitopes on *Fel d* 1 and *Bet v* 1, reducing clinical symptom scores and T_H2 cellular responses (95). Moreover, IgG_1 and IgG_4 functional inhibition of IgE peaks between 3-6 months of AIT administration and demonstrates sustained clinical effectiveness for greater than a year following treatment, suggesting establishment of allergen $sIgG_1$ and $sIgG_4^+$ memory B cell populations (83, 156). RNA sequencing approaches have indicated increased expression of *IGHG4* (IgG_4) expression occurs as early as 4-months GP-SLIT treatment, alongside increased proportions of allergen-$sIgG_4^+$ memory B cells (212). However, correlations between IgG_4 levels and clinical response remain inconsistent across studies, with some studies proposing that specifically functional, rather than immunoreactive, IgG_4 levels correlate with clinical response (156, 198, 204, 213, 214). Like IgG_4, IgA1 and IgA2 exhibit blocking properties through competing with IgE for allergen (96). Interestingly, the GRASS clinical trial recently reported that the dominant inhibitory antibody isotypes during SCIT and SLIT are IgG and IgA, respectively, proposing differential mechanisms of humoral modulation between the two administration processes, although recent reports have suggested blocking of IgE by IgG_4 may be more clinically important than IgA (96, 215). Two-year GP-SCIT treatment was associated with enhanced GP-$sIgA_2$, but not IgA_1 serum antibody levels compared to placebo, which attenuated allergic inflammation through inducing IL-10-expression from monocytes (216).

1.5 Regulatory B Cells

1.5.1 Discovery of Regulatory B Cells

Breg cells are a distinct subset of tolerogenic B cells and an important modulatory component of the immune system, acting to induce peripheral tolerance and maintain immune homeostasis. The first recorded studies demonstrating B cells possessed suppressive capabilities were during the mid-1970s whereby adoptive transfer of B cells resulted in suppression of delayed hypersensitivity to ovalbumin in guinea pigs (217, 218). However, interest in the Breg field wasn't reignited until over 20 years later when Wolf *et al.* reported genetically altered murine models lacking B cells were unable to resolve experimental autoimmune encephalitis (EAE), concluding B cells held a protective role against the autoimmune response (219). Moreover, another study in the early-1990s by O'Garra *et al.* evidenced the ability of murine B cells to produce IL-10, building the notion that B cells could exert suppression (220). Finally, two seminal studies in 2002 by Mizoguchi and Fillatreau demonstrating B cell deficient mice exhibited chronic inflammation cemented the understanding that subsets of B cells possessed immunosuppressive properties, leading Mizoguchi to coin the phrase 'regulatory B cells' (221, 222). The existence of human Breg cells were first indicated following reports that treatment with rituximab, an anti-CD20 B cell antibody, was associated with development of autoimmune diseases (223, 224). These first studies paved the way to the identification of the first two 'distinct' Breg subsets within humans less than 10 years later by the Tedder and Mauri laboratory groups (225, 226). These landmark studies formed the backbone of an expanding field aiming to understand Breg biology and their roles in immune homeostasis and inflammatory disease states, such as allergy (Table 1.5.1.1).

Table 1.5.1.1 Seminal regulatory B cell studies.

Year	Disease Model	Key Findings	Reference
1974	Murine Models of Delayed Hypersensitivity	Following immunisation, B cells suppress the expression of the delayed hypersensitivity reaction. Postulated B cell suppression of T cells	(217, 218)
1990	Murine Models of Lymphoma	B cells possess ability to express IL-10	(220)
1996	Murine Model of EAE	B cell-deficient mice were unable to recover from EAE as effectively as those with B cells	(219)
1997	Murine Model of Colitis	B cell-deficient mice developed more severe colitis compared to those with B cells	(227)
2002	Murine Model of Colitis	B cells secrete anti-inflammatory IL-10 which can suppress severe colitis. Coined the term 'Breg'	(221)
2002	Murine Model of EAE	In the absence of B-cell-derived IL-10 mice did not recover from EAE	(222)
2007	Murine Model of Experimental Arthritis	Transitional 2-marginal precursor B cells prevent and ameliorate arthritis and secrete IL-10.	(228)
2010	Human SLE Patients	Breg cells first described in human blood ($CD19^{+}CD24^{hi}CD38^{hi}$ B cells) and noted to be reduced in both frequency and functionality in SLE patients.	(225)
2011	Human Peripheral Blood	Characterisation of Breg cells in human blood ($CD19^{+}CD24^{hi}CD27^{+}$)	(226)
2014	CNS Autoimmune diseases	Bregs cells are stimulated by IL-35 and can secrete IL-35.	(229, 230)

SLE, systemic lupus erythematosus; CNS, central nervous system; Breg, regulatory B cells.

1.5.2 Regulatory B Cells Origins, Activation and Phenotypes

In humans, B cells comprise 10-15% of PBMCs, with Breg cells only accounting for 1-2% of this total B cell number under homeostatic conditions. Breg cell populations can be expanded substantially during *in vivo* inflammatory conditions or through *ex vitro* exogenous stimulation through appropriate stimulus. Numerous stimuli trigger robust Breg acquisition of suppressive functionality, including BCR activation, TLR activation, (TLR2, TLR4 and TLR9), CD40L and CD80/86 cognate co-stimulation, cytokine stimulation (IL-1β, IL-2, IL-6, IL-10, IL-21, IL-33, IL-35, IFN-α, IFN-β), GM-CSF, and proliferation inducing ligands (BAFF and APRIL) (225, 229,

231-238). Amongst these, CpG is one of the most routinely utilised as human B cells express several TLR, of which TLR9 is amongst the highest expressed. TLR9 is strongly stimulated by the high frequency of hypomethylated CpG oligonucleotide (CpG ODN) motifs that are enriched in bacterial and viral DNA but rare in mammalian DNA due to suppression and methylation of CpG islands, resulting in an inhibited status (239-241). CpG motifs are characterised by regions of DNA including a central unmethylated cysteine-phosphate-guanine sequence flanked by 5' purines and 3' pyrimidines. Synthetic CpG ODN mimics are short single-stranded synthetic sequences specifically designed to stimulate TLR9 and are widely utilised in research due to their ability to mount strong innate and adaptive T_H1-cellular immune responses. For example, CpG ODN 1018 has been utilised as an adjuvant in vaccine development, such as for hepatitis B (242, 243), cancer immunotherapy (244) and AIT (245). For investigation of Breg cells, various studies have also successfully utilised CD40L to generate IL-10^+ Breg cells, indicating involvement of adaptive T cell interactions (225, 246).

Although expansion of IL-10^+ Breg populations has allowed in-depth investigations, there is currently no universal phenotypic definition of Breg cells, with 'distinct' subsets commonly discriminated by cell surface marker expression, cytokine production or induction manner. The high phenotypic and functional heterogeneity of Breg subsets, alongside the absence of a specific lineage marker, has led to the commonly accepted hypothesis that Breg cells can arise from almost all B cells contingent on local microenvironmental stimuli to curtail local inflammation (247, 248). Supporting this concept, transitional, plasma and memory human B cells have all been induced to transform into Breg cells (225, 226, 232). Diverse Breg heterogeneity also suggests cells exist on a 'continuum', possessing different ranges of immunosuppressant functionality. For example, studies conducted by Tedder *et al*. identified 'progenitor' Breg cells that were transitioning towards a 'full' Breg phenotype, whereas Wang *et al.* postulated Breg cells expressing IL-35 may represent a Breg development phenotype before or after the acquisition IL-10 (226, 229). The absence of lineage marker also suggests

the Breg phenotype does not represent a terminally differentiated stable Breg cell state, allowing cells to transition back to a conventional 'pro-inflammatory' B cell state. Supporting this theory, a recent study expanding Breg cell populations in culture over the course of 7-14 days for therapeutic use demonstrated the Breg cell phenotype was no longer maintained following cessation of CD40L stimulation, returning to a conventional B cell state (246). Therefore, current Breg nomenclature across the literature is challenging, with further studies required to deepen our understanding of complex Breg phenotypes, functionality, and development pathways. As Breg cells display a predominant propensity to produce IL-10, intracellular IL-10 expression is now widely utilised to functionally classify the Breg phenotype. An overview of B cell development and IL-10^{+} Breg cell phenotypes can be found in Figure 1.5.2.1.

1.5.2.1 Transitional $CD24^{hi}CD38^{hi}$ Breg cells

The first Breg cell subset identified in humans were $CD24^{hi}CD38^{hi}$ T1/T2 B cells following stimulation with CD40L-expressing cell lines by Mauri and colleagues (225). IL-10^{+} producing-$CD24^{hi}CD38^{hi}$ Breg cells have since been demonstrated to induce tolerance in numerous disease models and can skew T_H cells towards regulatory cellular responses, through IL-10 production and CD80-CD86 coreceptor interactions (225, 249).

1.5.2.2 Activated $CD1d^{hi}CD5^{+}$ Breg cells

CD5, a marker of B cell activation, has also been associated with functionally suppressive Breg subsets. For example, paucity of splenic $CD5^{+}$ B cells expressing high levels of Fas ligand (FasL) was associated with increased rheumatoid arthritis (RA) severity (250). Breg cells highly expressing CD1d have also been characterised in numerous studies, able to constrain states of chronic inflammation through IL-10-mediated immunosuppression (221). $CD1d^{+}$ Breg cells may also mediate tolerance through maintaining suppressive natural killer

T cell populations through CD1d-mediated lipid-antigen presentation (251). Numerous studies have characterised a potent IL-10-producing $CD1d^{hi}CD5^{+}$ Breg subset which elicits important suppressive functions during chronic inflammatory conditions, normalising hypersensitivity driven immune responses upon adoptive transfer to B cell deficient mice (233, 252).

1.5.2.3 Activated $CD25^{+}CD71^{lo}CD73^{hi}$ Breg cells

B cells expressing $CD25^{+}CD71^{lo}CD73^{hi}$ were first described by Van de Veen and colleagues in 2013 in the context of bee venom allergy through miRNA microarray analysis of $IL\text{-}10^{+}$ and $IL\text{-}10^{-}$ B cells (253). $CD25^{+}CD71^{lo}CD73^{hi}$ Breg cells have since been characterised in the setting of HDM-mediated AR, murine skin transplant tolerance models and subcutaneous cell carcinoma, where they were found to be dysregulated compared to healthy controls (198, 246). IL-10-producing $CD25^{+}CD71^{lo}CD73^{hi}$ Breg cells have been demonstrated to upregulate IgG_4 production, express programmed death-ligand 1 (PD-L1) and induce Treg cells (253).

1.5.2.4 Memory $CD27^{+}$ and Plasmablast $CD138^{+}$ Breg cells

Various subsets of IL-10-producing $CD27^{+}$ memory and plasmablast B cells have been described to exert regulatory function, including $CD138^{+}$ plasma cells and $CD24^{hi}CD27^{+}$ (B10) B cells (226, 232). LN $CD138^{+}$ plasmablasts are reported to be important sources of IL-10 during EAE development and can constrain DC-mediated promotion of pathogenic T cells (232). Studies have also reported $CD138^{+}$ Breg plasmablast subsets express the suppressive molecules IL-35, PD-L1 and IgA^{+}, indicating their importance in immune tolerance (254-256). Progenitor B10 cells have been demonstrated to mature into 'full' B10 cells through LPS and CD40L stimulation and suppress immune responses through attenuating activation and TNF-α production from monocytes in addition to modulating T cell responses (226).

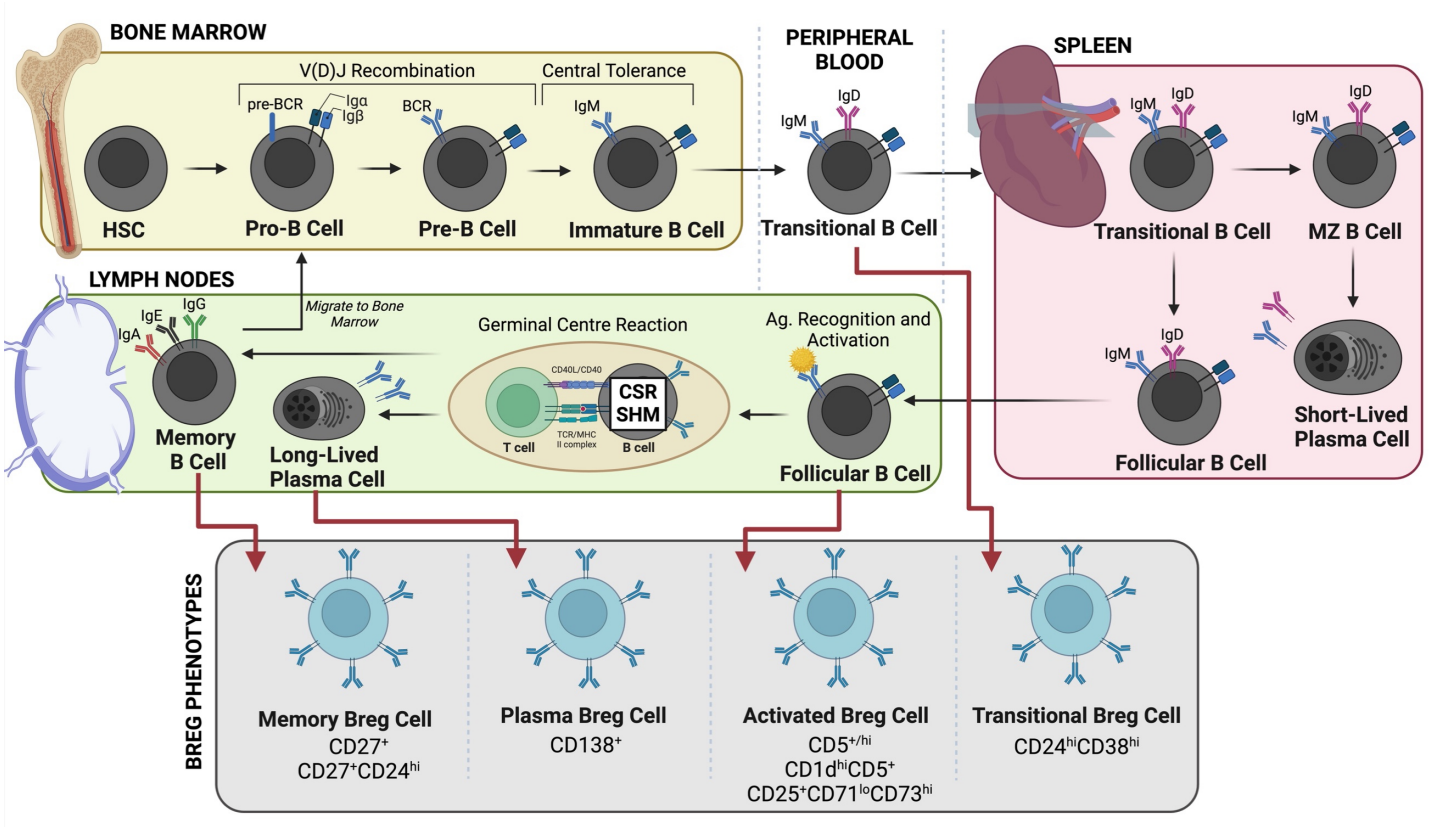


Figure 1.5.2.1 Regulatory B cell Phenotypes throughout the B cell development and maturation process.

In the bone marrow, HSC give rise to pro-B cells, pre-B cells and then immature B cells, who have undergone successful V(D)J recombination of their heavy and light chains and express a fully formed non-autoreactive BCR upon their cell surface. Transitional B cells migrate to the spleen where they complete development into MZ B cells, which differentiate into short-lived plasma cells, or follicular B cells. Follicular B cells recirculate around lymph nodes until activated through encountering their cognate antigen, driving germinal centre reactions, undergoing CSR and SHM to alter their antibody affinity and isotype and receiving T cell help. B cells exiting germinal centres become either long-lived plasma cells or memory B cells which can migrate back to the bone marrow. Memory B cells, plasma cells, activated B cells and transitional B cells, identifiable through cell surface marker expression, have all demonstrated ability to produce IL-10 upon treatment with stimuli. BCR, B cell receptor; MZ, marginal zone; Ag, antigen; CSR, class switch recombination; SHM, somatic hypermutation; pro-B cells, progenitor B cell; pre-B cell; precursor B cells.

1.5.3 Immunomodulatory Mechanisms of Regulatory B Cells

Despite their very low numbers, Breg cells elicit peripheral tolerance though an armamentarium of immunosuppressive mechanisms, including soluble mediators, cell contact dependent mechanisms and neutralising antibodies.

1.5.3.1 Breg Soluble Mediators

In addition to IL-10, Breg-mediated immunosuppression is also attributable to other regulatory secretory molecules, including TGF-β, IL-35, serine-protease granzyme B (GZ-B), adenosine and heat-shock proteins (257, 258).

1.5.3.1.1 IL-10

IL-10 is a member of the type II cytokine family, expressed by several cell types, including T cells, monocytes, and epithelial cells (259). The IL-10 receptor (IL-10R) complex comprises of two IL-10Rα and two IL-10Rβ molecules, constituting the ligand binding and signalling subunits, respectively (259). Upon IL-10 ligand binding, IL-10Rα oligomerises with IL-10Rβ and signals via the tyrosine kinases, Jak1 and Tyk2, driving receptor complex phosphorylation and recruitment of STAT3 (259, 260). Phosphorylation of STAT3 leads to its translocation to the nucleus, binding to STAT3-binding elements of IL-10 responsive genes (259, 260). The importance of Breg-derived IL-10 in mediating immunosuppression was first observed in animal models, whereby mice with B cell-specific IL-10 knockout presented with exacerbated chronic inflammation in numerous disease models, including colitis, RA and EAE (221, 222, 261). The IL-10 cytokine is multimodal in its immunosuppressive mechanisms to preserve immune homeostasis. For example, Breg-derived IL-10 dampens inflammatory responses through negative regulation of pathogenic $CD4^+$ and $CD8^+$ T cell activation, proliferation, and survival (249, 262-264), with recent studies reporting IL-10^+ Breg cells develop longer cognate interactions with T_H cells compared to IL-10^- B cells, which may inadvertently reduce their

opportunity to interact with pro-inflammatory DC (261). Breg-derived IL-10 also able induces Treg differentiation, expansion, and enhancement of suppressive capacity through STAT3 signalling activation and upregulation of PD-1 and CTLA-4 expression (249, 265-267). IL-10 is a potent regulator of B-cell survival, favouring plasma cell differentiation, skewing B-cell isotype-switching from IgE towards IgM and anti-inflammatory IgG and IgG_4 (268-270). IL-10 is also able to dampen IL-10^- B cell proliferation, inadvertently favoring B cells with regulatory capacity (271). IL-10 downregulates innate immune responses by attenuating cytokine production, such as TNF and IL-12, and antigen-presentation capacity of pro-inflammatory macrophages, DC, and other APC (226, 272-274). As DC cells are critical for priming antigen-specific T cell responses, IL-10^+ Breg mediation of the DC compartment, including promotion of monocyte differentiation towards DC phenotypes, and inducing DCreg, may indirectly contribute towards skewing T cell activation and differentiation (275, 276).

1.5.3.1.2 TGF-β

TGF-β is a pleiotropic cytokine produced by various cell types including Treg, DC and macrophages. Activated B cells produce relatively small volumes of TGF-β under normal physiological conditions, thereby increased propensity of Breg cells to produce TGF-β marks a significant departure from 'conventional' B cell activity (277). The role of Breg-derived TGF-β in immunosuppression can be understood from murine studies whereby mice with selective knockout of B cell derived-TGF-β developed advanced EAE progression compared to healthy controls (278). Breg-derived TGF-β has been demonstrated to promote conversion of $CD4^+$ T_H cells to Treg cells, even working independently from IL-10, and induce anergy in $CD4^+$ and $CD8^+$ T cells (279-282). TGF-β^+ Breg have also been reported to modulate innate immune responses through limitation of DC antigen presentation by induction of DCreg, and cooperate with anti-inflammatory macrophages, preventing downstream activation of effector T_H cells (283-285). Interestingly, a recent RNA sequencing study reported TGF-β^+ Breg cells were able to activate IL-35 expression but, did not produce IL-10. This contrasts with other studies

demonstrating human IL-10^{+} Breg cells have capacity to co-express TGF-β, with further work required to delineate the relationship between TGF-β and IL-10 (225, 286, 287).

1.5.3.1.3 IL-35

IL-35 is a potent anti-inflammatory heterodimeric cytokine in the IL-12 family, composed of the IL-12p35 and Ebi3 subunits, signaling dependently through IL-12β2 receptors via STAT1 and STAT3 signal transduction in B cells (288). IL-35 is expressed by a variety of cells including DCreg, iTR35 cells, endothelial cells, and macrophages (289-291). Two seminal studies demonstrated IL-35 induces Breg cells capable of secreting large volumes of IL-35, with recent studies revealing IL-35 production from Breg can be induced following CD40L and TLR4 stimulation (229, 230). Dysregulated peripheral IL-35^{+} Breg frequencies have been reported in numerous chronic inflammatory disease states, such as SLE and gastric cancer, highlighting their broad clinical importance in modulating appropriate immune responses (292, 293). IL-35^{+} Breg modulate T cell responses through inducing Treg cell subsets and suppressing proinflammatory CD4^{+} T_H cellular subsets to limit inflammation (229, 294, 295). IL-35 treatment also induced antigen-presentation capacity of B cells and expanded Breg populations alongside increasing IL-10 and IL-35 levels within the serum (230, 294). Interestingly, recent studies have highlighted the efficacy of IL-35^{+} Breg-derived exosomes containing bioactive IL-35 for treatment for EAU, highlighting their potential importance as novel therapies for inflammatory diseases (296). However, further evidence is required to characterise the phenotype and functionality of human IL-35^{+} Breg cells.

1.5.3.2 Contact-dependent Mechanisms

Breg promotion of immunosuppression can also be driven through membrane-associated molecules, such as T-cell immunoglobulin and mucin domain-1 (TIM-1), PD-L1, MHC II, CD80, CD86, and Fas-L (250).

1.5.3.2.1 TIM-1

TIM-1 is one of three TIM receptor family members (TIM-1, TIM-3 and TIM-4) and is a type I transmembrane glycoprotein containing an IgV and mucin domain important for the regulation of $CD4^+$ T_H cells (297). TIM-1 is expressed by various immune cells, such as T cells and DC, and binds to its ligand, TIM-4 (298). TIM-1 is an important activation signal, enhancing DC and T cell activation, maturation, and cytokine secretion (297-299). TIM-1 signaling has been reported to be required for optimum IL-10 expression through STAT3 axis activation, with TIM-1^+ B cells demonstrating ability to constrain states of chronic inflammation, such as colitis, EAE, and airway inflammation (246, 300-302). TIM-1^+ B cells are dysregulated in various inflammatory disease states, such as systemic sclerosis, coronary heart disease and RA (303-305). For example, in SLE patients, TIM-1 expression on B cells positively correlated with IL-10 expression, and dual positive TIM-1^+IL-10^+ Breg cells were reported to modulate T cell responses during HIV infection and cancer (306, 307). In addition to IL-10, TIM-1 can act as a master regulator of other suppressive molecules and cytokines, such as TGF-β, Ebi3 and LAG-3 (308).

1.5.3.2.2 PD-L1/PD-1

The suppressive transmembrane PD-1/PD-L1 axis is considered an immune checkpoint inhibitory receptor which modulates immune activation of various cells, including B cells, and exerts inhibition of TCR-mediated signaling through binding to PD-1 expressed upon T cell surfaces (158). Studies have demonstrated IL-10 overexpressing B cells increase transcriptional expression of PD-L1, and that PD-1^+ and PD-$L1^+$ B cells co-express IL-10 (276, 309). Interestingly, attenuation of PD-$L1^+$ B cells has been described in chronic inflammatory states such as RA and multiple sclerosis (309, 310). Upon triggering the PD-1/PD-L1 axis, Breg cells have been demonstrated to suppress $CD4^+$ T_H and $CD8^+$ T cells, and induce Treg cellular responses, through induction of IL-10 production and PD-1 mediated suppression

(309, 311, 312). Moreover, initial studies have reported that IgA^+ Breg cells require PD-L1 expression for dampening of macrophage responses (254, 313).

1.5.3.2.3 CD80 and CD86

The costimulatory ligands CD80 and CD86 are employed by APC during crosstalk with T cells to deliver activating or inhibitory signals through cognate interactions with CTLA-4 and CD28, respectively (314). BCR-antigen capture may enhance antigen specific Breg cell suppressive capacity through enabling cognate interactions with antigen-specific T cells, demonstrated through live imaging studies of IL-10^+ B cells (315). Therefore, CD80 and CD86 may enhance Breg suppressive capacity through mediating cognate interactions with T cells, with studies reporting that CD80 and CD86 work synergistically with IL-10^+ Breg cells to suppress T_H1 responses and regulate peripheral functionality of Treg cells (316, 317).

1.5.3.3 Antibody Production

A major biological function of B cells is the production of antibodies, with preliminary studies evidencing Breg cells can elicit regulatory function through the production of anti-inflammatory antibodies such as IgG_4 and IgA.

1.5.3.3.1 IgG_4

IgG_4 antibodies are considered anti-inflammatory through exhibiting reduced ability to mediate antibody-dependent cellular cytotoxicity and antibody-dependent cellular phagocytosis. Small scale studies have demonstrated that IL-10^+ B cells produce 10-100-fold higher IgG_4 quantities that IL-10^- B cells (253). Supporting this concept that IL-10^+ B cells are responsible for IgG_4 production, Breg cells have been reported to be dysregulated in IgG_4-related diseases, and both Breg and IgG_4 levels are enhanced during AIT treatment (318). However, conflicting data

was reported in IL-10 transfection murine models, whereby IL-10-overexpressing B cells did not demonstrate any changes in IgG_4 expression (276). Moreover, studies have noted that IL-10 may drive IgG_1 and IgG_4 antibody responses from B cells, however, their expression is likely to also depend on other factors within the local microenvironment (270). Therefore, further research to understand the relationship between IL-10^+ Breg cells and IgG_4 is required.

1.5.3.3.2 IgA

The mucosal immunoglobulin IgA elicits suppressive capacity in various disease states, such as colitis and cancer (319, 320). Enhancement of IgA1 and IgA2 levels are observed following AIT treatment, coinciding with an increase in IL-10^+ Breg cells, suggesting a relationship. Dual positive IgA^+IL-10^+ Breg cells have been characterised in numerous studies, constraining inflammatory states through both IL-10 and PD-L1-mediated suppression (256, 313). However, conflicting data in the relationship between IL-10 and IgA was reported in an IL-10 transfection model whereby IL-10-overexpressing B cells were associated with a reduction in IgA expression (276). Therefore, further research to decipher a clear relationship between IgA and IL-10^+ Breg cells is required.

1.5.4 Regulatory B Cells in Immune Homeostasis and Disease

Breg cell exertion of immunoregulation has been consistently demonstrated across various disease states, such as autoimmune diseases, cancer, infectious diseases, allograft tolerance, and AD, suggesting their broad clinical importance.

1.5.4.1 Regulatory B Cells in Autoimmune Disease

In parallel to the presence of autoreactive B cells, patients with immunocompromised immune systems due to autoimmune diseases, including SLE, RA, multiple sclerosis, and diabetes,

present with attenuated IL-10$^+$ Breg cell frequencies (225, 263, 321, 322). Moreover, CD38$^+$ and TGF-β^+ Breg cells are reduced in RA patients compared to healthy controls and are associated with positive treatment response (323, 324). Finally, peripheral IL-35$^+$ Breg cells have been associated with reduced disease activity and expansion of Treg subsets in SLE and EAU (292, 296).

1.5.4.2 Regulatory B Cells in Cancer

Breg cells promote tumour development and survival through secretion of anti-inflammatory factors, including IL-10 and IgG_4, suppressing CD8$^+$ T cell dependent tumour immunity (325-327). Numerous studies have demonstrated that various types of cancer, such as cutaneous squamous cell carcinoma, myeloma and gastric, are associated with elevated peripheral and tumour Breg cells and IgG_4 levels compared to healthy controls (246, 328). Moreover, gastric, and pancreatic cancer cells have demonstrated ability to promote unregulated growth through promoting induction of IL-35$^+$ Breg cell levels, dampening anti-tumour responses (293, 329).

1.5.4.3 Regulatory B Cells in Infectious Diseases

In chronic bacterial diseases, such as *listeria* and *Mycobacterium tuberculosis,* diseased murine models have demonstrated elevated frequencies of IL-10$^+$ Breg cells that prevent bacterial cell clearance through inhibition of macrophage function, CD4$^+$ T cell proliferation and T_H17 cell activation (330-332). Breg cells also exert negative immunoregulatory roles during viral infections, such as HIV and hepatitis B, whereby increased Breg frequencies are responsible for suppressing virus specific CD8$^+$ T cell responses, IFN-γ production and augmenting further Breg and Treg responses, preventing viral clearance (264, 333). Murine models studying enteric parasitic infection, such as helminths, reveal their capacity to stimulate Breg population expansion to assist in avoiding immune clearance (334).

1.5.4.4 Regulatory B Cells in Allograft Transplantation Tolerance

Dearth in IL-10$^+$ Breg frequency and functionality have been associated with increased risk of renal transplant rejection (335). However, enhanced IL-10$^+$ Breg frequencies are associated with effective lung and renal allograft tolerance through provision of IL-10 and TGF-β, requiring antigen recognition (336-338). Numerous studies have evidenced that adoptive transfer of Breg cells can prolong skin allograft survival, with recent preclinical studies aiming to expand Breg populations for therapeutic use in transplant patients able to maintain Breg populations in culture for 14 days (246, 339).

1.5.5 Regulatory B Cells in Allergy

1.5.5.1 Allergic Rhintis and Allergic Asthma

Animal allergic asthmatic models demonstrate attenuated peripheral and tissue-resident IL-10$^+$ Breg cell subsets, which are re-established alongside normalisation of airway inflammation following adoptive transfer of IL-10$^+$ Breg cells in *il10* reporter mice (340-344). Moreover, knock-out of DOCK8, a gene mutation known to increase susceptibility to AD, in B cells resulted in reduced Breg functionality and frequency (345). Paucity of IL-10$^+$ Breg frequency and functionality have also been reported in human asthmatic patients, demonstrating decreased CD5$^+$, CD24^{hi}CD27$^+$ and CD24^{hi}CD38^{hi} Breg cell subset frequencies and diminished IL-10 expression (346-348). Similarly, in the setting of AR, patients display significant Breg subset dysregulation compared to healthy controls, with a recent study by Shamji *et al.* more specifically reporting prominent reduction in IL-10$^+$ Breg cells in GP allergic SAR patients outside, but not during, the GP season (202, 349). In addition to attenuation of frequency, Breg functionality is also impaired during allergic asthma, exhibiting reduced IL-10 propensity during T:B co-cultures exposed to HDM allergen (346). Dysregulation of Breg cell subsets during allergic asthma causes an inability to inhibit T_H2 cell-mediated inflammation

and promote Treg cell subsets, resulting in exacerbated pulmonary inflammation (343, 350). IL-10$^+$ Breg cells also demonstrate ability to constrain IgE-mediated mast cell activation and pro-allergenic cytokine production through CD40L cognate interactions, thereby preventing EPR-associated allergic reactions (351). Clinical studies have reported attenuation of IL-35 levels during allergic airway diseases, which are negatively correlated with high IgE expression in children with asthma, indirectly suggesting diminution of IL-35$^+$ Breg cells (149, 352). Moreover, recent studies have demonstrated IL-35 constrains allergic inflammation through limitation of AR patient eosinophil activation and migration (353).

1.5.5.2 Atopic Dermatitis and Food Allergy

Studies have reported that patients suffering from atopic dermatitis demonstrate attenuated Breg frequencies compared to healthy counterparts, possessing dysregulated ability to inhibit T_{FH} differentiation or respond to TLR activation (354, 355). Food allergy can be interlinked with atopic dermatitis, occurring after food particle inhalation or contact with damaged skin. Studies have demonstrated TGF-β-producing CD5$^+$ Breg cells were significantly increased in milk-tolerant subjects compared to milk-allergic subjects and were associated with lower frequencies of eczematous reaction (356-358). TGF-β^+ Breg cell-mediated induction of FOXP3$^+$ nTreg and suppression of T_H2 cell differentiation have also been demonstrated in the setting of food-allergy induced intestinal inflammation (359).

1.5.6 Regulatory B Cells in Allergen Immunotherapy

AIT has demonstrated ability to significantly upregulate nasal mucosal IL-10 mRNA and IL-10-protein expressing cells and peripheral IL-10-producing PBMCs following allergen stimulation after two years treatment compared to placebo treated subjects (204). Moreover, AIT demonstrates capability to upregulate heterogenic IL-10$^+$ Breg subsets, suggesting their importance in tolerance reinstatement to administered allergen (198, 199). Long-term GP-AIT

progressively increased IL-10^{+} Breg cell subset frequencies, including those characterised by CD1d^{hi}CD5^{+}, in a time-dependent manner (199). Moreover, RNA-sequencing of allergen-specific B cell subsets following 4-months SLIT treatment in SAR demonstrated enhancement of two transcriptionally distinct memory B cell subsets which were both associated with upregulated CD29, CD23 and IgG_4 expression (212). Long-term HDM-AIT treatment is also associated with increased IL-10^{+} and dual-positive IL-10^{+}IL-1RA^{+} Breg cells which significantly correlated with improved clinical symptoms (198). Peripheral IL-10^{+} Breg:T2-T_{FH} ratios in patients with allergic asthma with AR have also been demonstrated to increase following AIT, and correlated with positive treatment response (146). In addition to IL-10^{+} Breg cells, murine models with local inhalational tolerance demonstrated a 5-fold increase in TGF-β^{+} Breg cells within the hilar LN, capable of differentiating naïve T cells to FOXP3^{+} nTreg cells and associated with inhibition of airway eosinophilia (360). AIT also drives expansion of TGF-$\beta1^{+}$ Breg cells in AR patients during a 2-year course of HDM-AIT in combination with oral corticosteroid treatment, with significant induction observed as early as 4 months (361). This study also demonstrated ten independent Breg phenotypes that were induced by AIT, including CD25^{+}CD71^{lo}CD73^{hi}TGF-$\beta1^{+}$ Breg cells. Akdis *et al.* reported B-cell IL-10 expression was enhanced in bee venom allergic individuals following a course of bee venom AIT, comparable to levels observed in naturally exposed healthy beekeepers during the beekeeping season (200). Building on these observations, more recent studies demonstrated that AIT in bee venom allergic individuals demonstrated increased frequencies of CD25^{+}CD71^{lo}CD73^{hi}IL-10^{+} Breg cells following treatment that were enhanced in PD-1 expression (253). In addition to conventional AIT approaches, preclinical novel AIT studies have reported the immunogenicity of LPP and depigmented and polymerised *Phl p* in expansion of *ex vivo* IL-10^{+} Breg cell populations in culture (152, 362). Data surrounding the frequency of TIM-1^{+} B cells following AIT remains scare and conflicting, with some pediatric HDM-SLIT studies drawing a negative correlation between TIM-1 expression and clinical symptom reduction, however, the cellular source was not confirmed. As previously described

in Section 1.4.4, AIT induces B cell isotype switching, resulting in increased systemic and local levels of antigen-specific IgA and sIgG_4 levels. Small scale-studies have indicated IL-10^+ Bregs are substantial producers of IgG_4, with IgG_4 secretion potentially being the most potent mechanism of Breg-mediated immunosuppression during AIT (253). Furthermore, following conflicting reports as to whether IL-10^+ Breg cells are associated with IgA production, it remains unclear whether IL-10^+ B cells are responsible for AIT-mediated enhancements in IgA_1 and IgA_2 levels. However, IgA_2 induction correlated with nasal TGF-β mRNA levels, potentially due to an increase in tissue-resident TGF-β^+ Breg cells, with other studies demonstrating TGF-β1 secretion from B cells increases CSR towards IgA production (363).

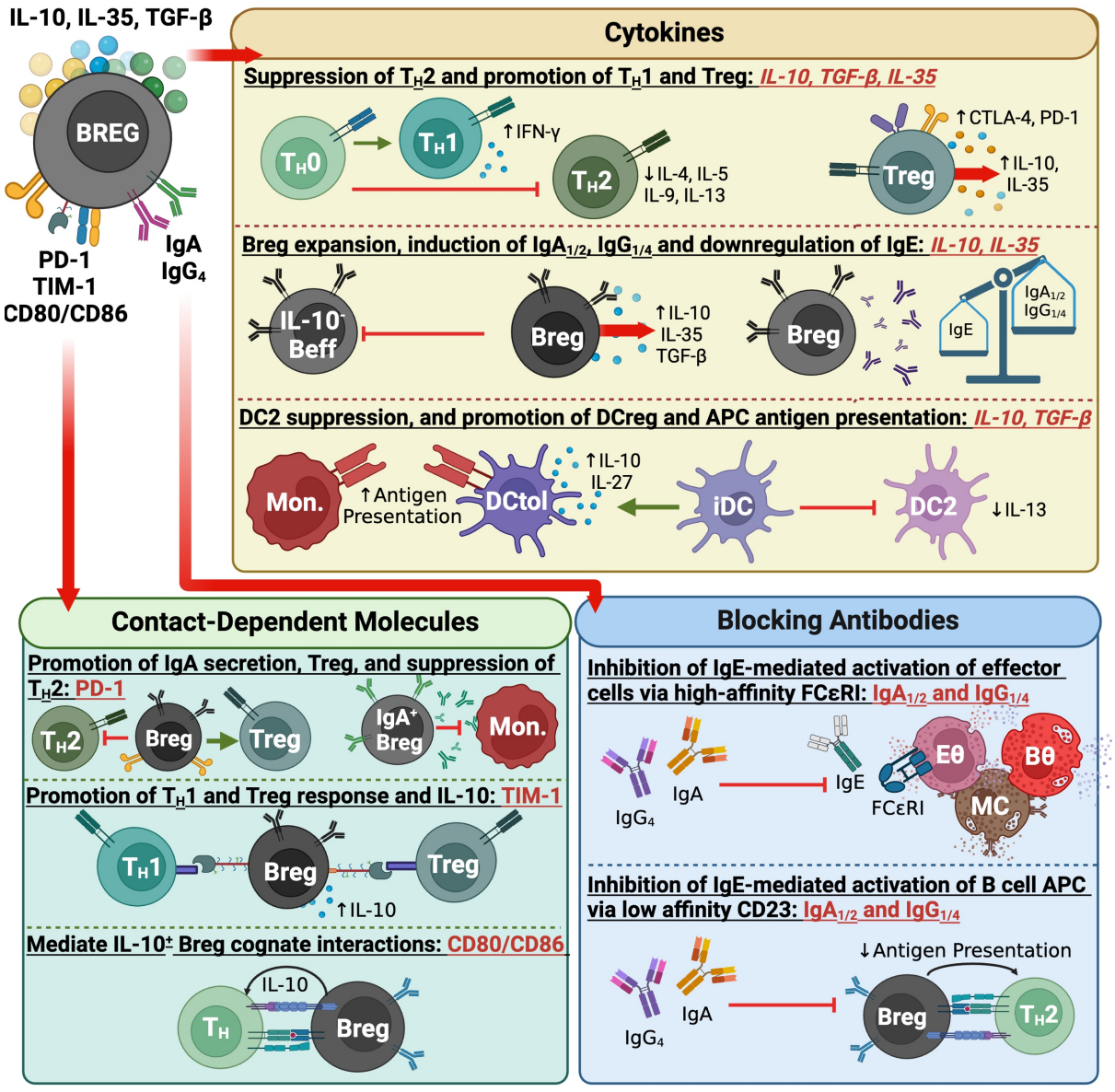


Figure 1.5.6.1 Proposed Breg-mediated Suppression during Allergen Immunotherapy.

Breg cells secrete cytokines include IL-10, TGF-β and IL-35, which can suppress T_H2 cells in parallel to induction of IFN-γ^+ T_H1 cells and Treg frequencies, expression of CTLA-4 and PD-1, and production of IL-10 and IL-35. IL-10, and IL-35 also induce class switch recombination in B cells towards IgA_1/IgA_2 and IgG_1/IgG_4, Breg cell frequencies and cytokine production. IL-10, TGF-β also enhance iDC differentiation to DCreg as opposed to DC2 phenotypes and enhance the APC of monocytes and DCtol. PD-1 expression is associated with enhanced secretion of IgA and regulation of T cell responses. TIM-1 and CD80/CD86 both enhance Breg-mediated regulation of T_H cell subsets. Blocking antibodies, $IgA_{1/2}$ and $IgG_{1/4}$, compete with IgE for allergen binding, thus preventing FCεRI activation of mon, Eθ, and Bθ, and CD23-mediated APC by B cells to T cells. T_H2, type 2 helper T cells; T_H1, type 1 helper T cells; Treg, regulatory T cells; Mon, monocytes, iDC, immature dendritic cell; DCtol, tolerogenic dendritic cell; DC2, type 2 dendritic cell; TIM-1, T cell immunoglobulin and mucin domain 1; MC, mast cell; Eθ, eosinophil; Bθ, basophil. Created on Biorender.com.

1.6 Thesis Hypotheses and Aims

1.6.1 Hypotheses

This study hypothesised that Breg cells are dysregulated in patients with AR and are modulated following AIT, including novel allergen immunotherapy approaches. Moreover, IL-10^+ Breg cells modulate allergen-driven T_H2, T_H2A and Treg responses. The study was performed in several sections, with individual hypotheses outlined as below:

1. Human peripheral blood IL-10^+ Breg cells are enriched within distinct phenotypic subsets of B cells and can be stimulated with TLR ligands, such as CpG ODN sequences and CD40L. Moreover, human peripheral blood Breg cells express TIM-1, IL-35, TGFβ1, CD80, CD86, PD-L1 and PD-1 upon stimulation.

2. IL-10^+ Breg cells are dysregulated in SAR and PAR patients compared to NAC and are associated with greater IgA and IgG_4 expression compared to IL-10^- B cells. Moreover, AR patients demonstrate dysregulated frequencies of TIM-1^+, IL-35^+ and TGF$\beta1^+$ Breg compared to NAC.

3. IL-10^+ Breg cells are restored in SAR patients following SCIT-treatment to similar levels observed in NAC. Moreover, GP-SCIT treatment modulates TIM-1 B cell expression and serum IgE and IgG_4 levels.

4. Novel allergen carrier systems, such as eBP or VLP, can generate IL-10^+ Breg cell responses in allergic individuals. Moreover, short-term administration of PQ Grass 27600 SU (GP allergoid adjuvanted with MPL-A and MCT) AIT treatment induces IgG, IgG_4 and $IgA_1/_2$ levels in serum and nasal fluid alongside the induction of IL-10^+ B cells in GPA patients.

5. SAR demonstrate increased T_H2/T_H2A cells and decreased IL-10^+ Breg and IL-10^+ iTreg cell frequencies compared to NAC in response to allergen stimulation. Moreover, IL-10^+ B cells suppress T_H2 and T_H2A cell proliferation in parallel to inducing IL-10^+ iTreg cells and anti-inflammatory cytokine production, in an IL-10 dependent manner.

1.6.2 Aims and Objectives in relation to Hypotheses

Hypothesis 1

1. To determine whether *ex vivo* CpG and CD40L stimulation promotes expression of IL-10 in human peripheral blood B cells and levels of IL-10 protein secretion in a dose- and time- dependent manner.
2. To determine whether human peripheral blood IL-10^+ Breg cells are associated with TIM-1, IL-35, TGFβ1, CD80, CD86, PD-L1 and PD-1 expression compared to IL-10^- B cells.

Hypothesis 2

1. To assess whether IL-10^+ Breg, TIM-1^+ B cell, TIM-1^+IL-10^+ Breg frequencies and IL-10 propensity are dysregulated in SAR (GP sensitised) and PAR (cat and HDM sensitised) patients.
2. To assess whether IgA and IgG_4 are significantly enhanced in IL-10^+ B cells and are dysregulated in SAR and PAR patients compared to NAC.
3. To evaluate whether IL-35^+, TGF$\beta1^+$ and IL-10^+IL-35^+TGFß1^+ Breg cells are dysregulated in SAR patients compared to NAC.

Hypothesis 3

1. To determine whether SCIT AIT treatment restores IL-10^+ Breg cell frequencies in SAR patients compared to NAC.
2. To evaluate whether SCIT-treatment modifies TIM-1 expression on SAR patient B cells.
3. To evaluate whether SCIT-treatment modifies serum TG-sIgE, tIgE and TG-sIgG_4 levels.

Hypothesis 4

1. To assess the ability of novel *Fel d* 1 eBP to amplify IL-10^+ B cell responses in cat allergic subjects and NAC.
2. To determine the ability of VLP-Peanut, adjuvanted with MCT, to generate IL-10^+ B cell responses in peanut allergic subjects.
3. To assess the effects of extended or conventional PQ Grass 27600 SU on IgA_1, IgA_2, IgG and IgG_4 immunoglobulin responses in serum and nasal fluid and peripheral blood IL-10^+ B cell responses during a RDBPC study in GPA patients.

Hypothesis 5

1. To characterise NAC peripheral blood T_H2/T_H2A cells and associated levels of IL-5, and IL-13 production through αCD3/CD28 stimulation.

2. To evaluate *Phl p* stimulated T_H2/T_H2A, IL-10^+ iTreg and IL-10^+ Breg cells in NAC and SAR patients.

3. To assess the ability of rIL-10 to suppress *Phl p* activated T_H2/T_H2A and IL-10^+ iTreg cells and IL-5 and IL-10 protein expression in SAR patients.

4. To determine the ability of enriched IL-10^{+} B cells to modulate T_H2/T_H2A and IL-10^{+} iTreg cell responses to *Phl p* stimulation, and whether this modulation relies on IL-10 or IL-35 mechanisms.

CHAPTER 2. METHODOLOGY

2.1 Ethical Statement

All blood sample collection within this thesis was approved by the national research ethics committee (South-West London committee, REC3) and the Research Office of the Royal Brompton and Harefied NHS Foundation Trust, other than samples provided during the PQGrass Phase III clinical study outlined in Chapter 6 where local regulatory authorities in the US and Germany granted approval (NCT04687059; EudraCT number: 2020-000408-13). All samples and data were processed following good clinical practice (GCP) and good laboratory practice (GLP) guidelines, including obtaining informed and written consent from all patients prior to sample collection. For all studies, participant samples were anonymised prior to laboratory processing and data was internally locked prior to unblinding.

2.2 Patient Recruitment

Unless stated otherwise, peripheral blood donors were recruited from the Royal Brompton and Harefield NHS Foundation Trust by research nurses and characterised based upon their atopic status. SPT were conducted on all study participants against common UK allergens, including house-dust mite, timothy grass, mugwort, silver birch, cat hair, dog hair, aspergillus fumigatus, cladosporium hebarum, and alternaria alternata. NAC study participants were defined by absence of any prior history of AD alongside a negative SPT and sIgE score (<0.35 kU_A/L) in response to tested allergen. Inclusion criteria for allergic subjects included a positive SPT (>3mm wheal diameter) alongside elevated serum sIgE (>0.70 kU_A/L) to HDM (*Der p*), TG pollen (GP; *Phl p*), cat dander (*Fel d*) and peanut (*Ara h*) allergens. GP-SCIT treated patients were identified as GP allergic (GPA) individuals who had received monthly subcutaneous injections of 100,000 SQ-U *Aquagen SQ*, ALK-Abelló for greater than one year prior to sample donation. Exclusion criteria included previous AIT for allergic subjects and a

clinical history of other significant diseases. Whole venous blood samples were collected in lithium-heparin blood collection tubes and transported to the Immune Tolerance Group (ITG) laboratory facilities at Imperial College London for processing. Relevant patient demographics of preclinical and clinical study participants can be found within Chapters 3-7.

2.2.1 Clinical Symptom Questionnaires

Retrospective total nasal symptom scores (TNSS) were provided by subjects during sample donation to assess their allergic rhinoconjunctivitis symptoms in response to allergen encounter. All participants were asked to respond to the question 'how were your nasal symptoms when at their most severe during the most recent GP season/upon encountering cat dander/HDM?', by indicating on a 4-point Likert scale (0-3) their individual nasal symptoms, including runny nose, blocked nose, sneezing, and itchy nose, resulting in a possible total score between 0 and 18. Subject's retrospective clinical symptom severity was also measured by a visual analogue scale (VAS) assessment, whereby in response to the question 'how do you rate your allergic rhinitis symptoms overall (for hayfever suffers during the season)?', subjects were asked to place a vertical mark on a linear scale from 0 to 10cm, where 0cm represents no symptoms at all and 10cm indicates the worst possible symptoms. A score from 0-100 was then delineated using a ruler whereby 1mm equals a score of 1; i.e., a mark at 6cm would equate to a score of 60. Patients were also asked to complete a Global Evaluation 2 (GE2) assessment, whereby subjects were asked to rank their hay fever symptom scores ranging from -3 (much worse) to +3 (much better) compared with either the preceding GP season or prior to commencing AIT treatment.

2.3 Peripheral Blood Cell Isolation and Cryopreservation

PBMC processing from heparinised human whole blood begun within 2 hours of phlebotomy. To isolate PBMCs, whole blood was centrifuged (750*g*, 10 minutes) to separate the plasma

layer which was subsequently stored at -20°C for serological analysis. Remaining blood was diluted in equal volume of medium (RPMI 1640 (-); Gibco; 31870-025) and layered onto 30% Ficoll-Paque™ PLUS (Cytiva; 17144003) for density gradient separation (750*g*, 25 minutes without brakes). Extracted PBMC layers were washed twice with medium prior to dilution 1:10 in trypan blue (Sigma; T8154-100) for cell counting and viability assessment on a haemocytometer. PBMCs were washed again in medium (RPMI 1640 (+); Gibco; 52400-025) before resuspension in cold Recovery™ Cell Culture medium (Life Technologies; 12648010) at a density of $20x10^6$ million cells/mL in cryovials. PBMCs were placed into Mr. Frosty™ Freezing containers (ThermoFisher) containing isopropyl alcohol at -80°C for 24 hours before cryopreservation in liquid nitrogen (-196°C) for long-term storage. Cryopreserved PBMCs were thawed by intermittent exposure to a 37°C water bath (Grant SUB Aqua 2S) until 75% thawed before dropwise dilution in medium (RPMI (+), Gibco). Following two washes in medium by centrifugation (400*g*, 10 minutes), PBMCs were resuspended in medium (RPMI (+), Gibco) and diluted as appropriate in trypan blue for cell counting and viability scoring.

2.4 B Cell and T Cell Enrichment

$CD19^+$ B cells and $CD4^+$ T cells were enriched from PBMCs by immunomagnetic negative selection utilising EasySep™ Isolation kits (StemCell Technologies, #17954 and #17952 respectively), according to manufactures instructions. PBMCs were placed in an EasySep™ magnet (StemCell Technologies, #18000) alongside B or T cell isolation/RapidSpheres™ cocktails as appropriate and incubated for 3 minutes at room temperature (RT) before the magnet and tube were inverted in one continuous motion and the enriched cell suspension collected in a fresh tube. Following B and T cell enrichment, purity was assessed immediately utilising flow-cytometry prior to cell culture. $CD19^+$ B cell purity was confirmed through dual staining with CD19 and CD3 antibodies and identified as pure if $CD19^+CD3^-$. $CD4^+$ T_H cell

purity was confirmed through single colour positive stain with CD4 antibody (Table 2.9.2.1). A purity threshold of 95% or higher was determined acceptable for downstream analysis.

2.5 B Cell Stimulation and Culture

PBMCs and enriched B cells were resuspended at a concentration of $22.2x10^6$ cells/mL in tissue culture media (TCM; RPMI (+/+) containing 5% heat inactivated human AB serum (Sigma; H3667) and 1% penicillin/streptomycin/glutamine (Gibco; 10378-016)) and seeded at a density of $4x10^6$ cells/well in 200μL of TCM in a 48-well flat-bottomed plate (ThemoScientific; 150687). To stimulate IL-10^+ Breg cells, cells were cultured in the presence of various stimulants; CpG (0.1μg/mL, 0.3μg/mL, 1μg/mL, 3μg/mL, 10μg/mL; InvivoGen; tlrl-2006) and recombinant CD40L (0.0625μg/mL, 1.25μg/mL, 2.5μg/mL, 3.75μg/mL, 5μg/mL; Biotechne; 6420-CL-025/CF). For *Phl p* dose response assays described in Chapter 7, PBMCs were cultured in the presence of *Phl p* (0.1μg/mL, 0.3μg/mL, 1μg/mL, 3μg/mL, 10μg/mL; ALK-Abello A/S, Hoersholm, Denmark). Descriptions of the novel eBP and VLP experimental stimulants and native allergen controls utilised in clinical studies are outlined in Chapter 6. Cells were incubated at 37°C, 5% CO_2 for 72 hours, unless stated otherwise, prior to supernatant extraction and cell staining for flow-cytometry.

2.6 T Cell Stimulation and Culture

2.6.1 Cell Trace Violet Cellular Proliferation Staining Kit

To investigate $CD4^+$ T cell proliferation, cells were stained with CellTrace Violet fluorescent dye (Life Technologies, C34557) reconstituted in DMSO to a stock solution of 5mM according to manufacturer's instructions. PBMCs or enriched $CD4^+$ T cells were resuspended at a density of $5x10^6$ cells/mL in 1x PBS (Gibco; 70013-016) and incubated with 1μL of reconstituted 5mM CellTrace dye per $5x10^6$ cells for 20 minutes in the dark at RT. To generate

an unstained sample control, $0.5x10^6$ cells were removed prior to addition of CellTrace Violet dye. TCM was added to cells for a further 5 minutes incubation at RT in the dark to dilute any free dye remaining in solution before washing by centrifugation (400*g*, 10 minutes). To confirm dye internalisation prior to cell culture set-up, 50μL of stained cells were taken for single-colour assessment by flow-cytometry. Cell trace-stained cells were resuspended in TCM and seeded at a density of $5x10^6$ cells/well in 96-well plates (ThemoScientific; 163320).

2.6.2 T cell Stimulants and Proliferation Assay

CellTrace labelled PBMCs and $CD4^+$ T cells were cultured in the presence of *Phl p* (0.1μg/mL, 0.3μg/mL, 1μg/mL, 3μg/mL, 10μg/mL; ALK-Abello A/S), recombinant IL-10 (rIL-10; 50ng/mL; BD Biosciences, 554611), neutralising IL-10 (αIL-10; 1μg/mL; Biolegend, 501427), or neutralising IL-35 (αIL-35; 10μg/mL; 2BScientific, 855660000-MDD). For polyclonal T cell stimulation, flat-bottomed 96-well plates were coated with αCD3 (1μg/mL; R&D Systems, MAB100) and αCD28 (2μg/mL; R&D Systems, MAB342) antibodies diluted in 200μL of 1X PBS (Gibco) or 1X PBS alone for negative controls. αCD3/αCD28 antibody coated plates were incubated overnight at 4°C before solution was tapped out in a sterile cabinet. CellTrace labelled PBMCs/$CD4^+$ T cells were cultured in αCD3/αCD28 antibody coated and uncoated wells at a density of $5x10^6$ cells/well. Cells were incubated at 37°C, 5% CO_2 for various timepoints prior to supernatant extraction and cell staining for flow-cytometry.

2.7 B and T Cell Co-Cultures

2.7.1 IL-10^+ B Cell Enrichment

To perform functional co-culture investigations, IL-10^+ B cells were enriched from $CD19^+$ B cells utilising an IL-10 Secretion, Cell Enrichment and Detection Kit (Miltenyi Biotech, 130-090-4335), according to the manufacturer's instructions. Enriched $CD19^+$ B cells stimulated

by 1μg/mL CpG and 2.5μg/mL CD40L for 72 hours were washed (400g, 5 minutes) and resuspended in 15mL cold buffer (2-8°C; MACS® BSA Stock Solution (130-091-376) diluted 1:20 with autoMACS® Rinsing Solution (130-091- 222). B cells were washed (300*g*, 10 minutes, 2-8°C) before resuspension in 160μL cold medium alongside IL-10 cytokine catch reagent for 5 minutes on ice. Cells were diluted in 10mL warm media (RPMI (+)) and allowed to secrete cytokines for 1 hour at 37°C under continuous rotation utilising a MACSmix Tube Rotator (Miltenyi Biotec, 130-090-753). Cells were placed on ice and washed with cold buffer (300*g*, 10 minutes, 2-8°C) before resuspension in 160μL cold medium alongside IL-10 cytokine detection reagent for a further 10 minutes. Cells were diluted in 10mL cold buffer and washed (300g, 10 minutes, 2-8°C) before magnetic labelling with anti-PE microbeads for 15 minutes at 2-8°C. Cells were washed in 10mL cold buffer (300*g*, 10 minutes, 2-8°C) prior to magnetic separation using LS Columns (Miltenyi Biotec, 130-042-401) placed into the magnetic field of a MidiMACS Seperator (Miltenyi Biotec, 130-042-301) and washed with 500μL cold buffer. Magnetically labelled B cell suspensions were placed directly onto the column and washed three times with 3mL cold buffer, with flow-through containing unlabeled IL-10$^-$ B cells collected. To elute labelled IL-10$^+$ B cells, 1mL cold buffer was added to the column and immediately flushed out by firmly applying the plunger. IL-10$^-$ and IL-10$^+$ B cell fractions were assessed immediately by flow-cytometry prior to culture set-up (Figure 2.7.1.1).

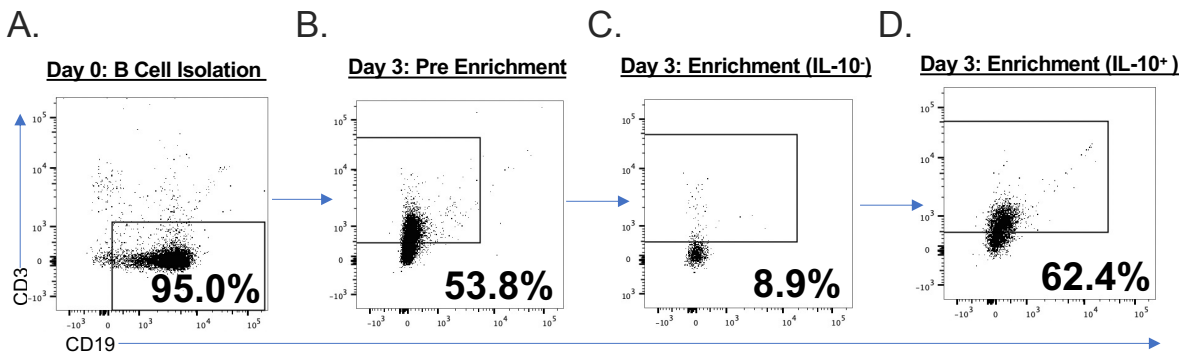


Figure 2.7.1.1 Enrichment of IL-10$^+$ B cells from human PBMCs.

A) CD19$^+$ B cells were isolated by negative immunomagnetic separation from human PBMCs. **B)** Following 3 days of CpG and CD40L stimulation, isolated CD19$^+$ B cells were stained with IL-10-labelled microbeads (PE fluorochrome). IL-10(PE)-microbead labelled B cells were separated by column separation into either **C)** IL-10$^-$ or **D)** IL-10$^+$ enriched B cells for use in downstream co-culture systems. PBMC, peripheral blood mononuclear cell.

2.7.2 B and T Cell Co-Culture Set-Up

To assess IL-10$^+$ Breg cell functionality, enriched IL-10$^-$ and IL-10$^+$ B cell fractions were co-cultured alongside autologous CellTrace-labelled PBMCs at a 1:1 ratio within 200μL TCM at a seeding density of 5x10^6 in a 96-well plate (e.g., 100μL B cells + 100μL PBMCs). Cells were stimulated with 1μg/mL *Phl p* (ALK-Abello A/S) and cultured alongside 10μg/mL nIL-10 (Biolegend) or 10μg/mL nIL-35 (2BScientific). CpG and CD40L stimulated (termed 'primed') and unstimulated (termed 'unprimed') enriched CD19$^+$ B cells were cultured alongside autologous CellTrace-labelled PBMCs at varying T:B cell ratios (primed: 1:1, 2:1, 4:1, 8:1, 16:1, 1:32, 1:64; unprimed: 1:1, 2:1, 4:1, 8:1, 16:1). CellTrace-labelled PBMCs were also cultured in supernatant from primed (1:1, 2:1, 4:1; TCM:B cell media) and unprimed (2:1; TCM:B-cell media) B cell co-cultures. Co-culture experiments were performed at 6, 10 or 13 days at 37°C, 5% CO_2 prior to flow cytometry staining.

2.8 Flow Cytometry

2.8.1 Flow-Cytometry Compensation

Prior to experiment commencement, flow-cytometry panels were subject to compensation to correct for fluorescence spill over. One drop of OneComp eBeads™ (Life Technologies, 01-1111-42) or reactive and negative ArC™ Amine Reactive compensation beads (Life Technologies, A10638) were incubated alongside 1μL antibody and 3μL of LIVE/DEAD™ dye, respectively, for 15 minutes at RT in the dark. Antibody/bead cocktails were washed with 2mL

cell staining buffer (CSB; 400*g*, 5 minutes) before resuspension in 250μL CSB. During flow-cytometry acquisition, positive and negative peaks of antibody fluorochrome expression were manually gated, with automated software compensation utilised to set compensation values. Acquisition of cells was performed utilising either FACSCanto II or Fortessa FACS machines (both BD Biosciences), with all flow cytometry data analysed using FlowJo™ v10.7 software.

2.8.2 Flow-Cytometry Cell Staining

Following culture incubation, cells were centrifuged (400*g*, 5 minutes) and culture supernatant was stored at -20°C for downstream ELISA analysis. Cells were restimulated in TCM containing 50ng/mL phorbol 12-myristate 13-acetate (PMA; Sigma) and 1μg/mL ionomycin (Sigma) diluted in 150μL (96-well plate) or 500μL (48-well plate) TCM for 5 hours at 37°C, 5% CO_2. For the final 4 hours, B cells were treated with 10μL Brefeldin A (BD Biosciences; 347688) and T cells were treated with 20μg/mL monensin (Biolegend; 420701). Cells were centrifuged (400g, 5 minutes) and resuspended in 75μL CSB (Biolegend, 420201) alongside 10μL FcR blocking solution (Miltenyi Biotec; 130-I59-901) for 15 minutes to prevent non-specific binding of antibodies. Cells were stained with a cocktail of cell surface antibodies (Table 2.8.2.1) for a further 30 minutes at RT before washing firstly in 150μL CSB and then 150μL 1X PBS (both 400g, 5 minutes). To differentiate live cells, cells were stained with 0.1% FVS780 (BD Biosciences, 565388), 0.1% LIVE/DEAD™ Fixable Green Dead Stain Kit (Life Technologies, L34969) or 1% Zombie Aqua™ Viability stain (Biolegend, 423101) diluted in 1X PBS for 10 minutes at RT. Cells were washed with 150μL CSB (400g, 5 minutes) before resuspension in 100μL fixation and permeabilisation solution (BD Biosciences; 51-2090KZ) for 20 minutes at 4°C. Cells were washed twice with BD Perm/Wash™ Buffer (BD Biosciences; 51-2091KZ; 400g, 5 minutes) before staining with intracellular antibodies for 30 minutes at 4°C (Table 2.8.2.1). Cells were washed a final time with 100μL BD Perm/Wash™ Buffer before resuspension in 200μL CSB for sample acquisition on the flow-cytometer.

Table 2.8.2.1 Antibodies used for cell staining by flow cytometry

Target	Fluorochrome	Clone	Company	Cat. Number
Cell Surface Markers				
CD1d	BV421	CD1d42	BD Biosciences	743604
CD3	APC/Cy7	SK7	Biolegend	344818
CD3	AF700	SK7	Biolegend	344818
CD4	BUV395	RPA-T4	BD Biosciences	564724
CD5	APC	UCHT2	BD Biosciences	555355
CD5	PE/Dazzle 594	UCHT2	Biolegend	300634
CD19	PerCP Cy5.5	HIB19	Biolegend	302230
CD24	BV510	ML5	Biolegend	311126
CD24	BV510	ML5	Biolegend	311126
CD25	PE-Cy5	M-AC51	Biolegend	356156
CD27	Pacific Blue	M-T271	Biolegend	356414
CD27	BV650	M-T271	Biolegend	302828
CD38	PE/Cy7	HIT2	Biolegend	303516
CD38	BV711	HIT2	Biolegend	303528
CD49d	BV711	9F10	Biolegend	304332
CD71	PE-Cy7	CY1G4	Biolegend	334112
CD73	BV785	AD2	Biolegend	344028
CD80 (B7-1)	BV605	L307.4	BD Biosciences	563315
CD86 (B7-2)	BUV737	2331	BD Biosciences	612784
CD127	PE-Cy7	HIL-7R-M21	BD Biosciences	560822
CD161	BV605	HP-3G10	Biolegend	339916
CD274 (PD-L1)	PE	29E.2.A3	Biolegend	329706
CD279 (PD-1)	BUV737	EH12.1	BD Biosciences	565299
CD294 (CRTH2)	PE/Dazzle 594	BM16	Biolegend	350126
TIM-1	BV605	1D12	BD Biosciences	742541
Intracellular Markers				
IgA	APC-Vio770	REA1014	Miltenyi Biotech	130-116-88
IgG_4	APC	SAG4	ThermoFisher	CYT-IGG4AP
IL-10	BV786	JES3-9D7	BD Biosciences	564049
IL-10	PE	JES3-19F1	BD Biosciences	559330
IL-12/IL-35 p35	PE	27537	R&D Systems	MAB1570
IL-12/IL-35 Ebi3	APC	607201	R&D Systems	MAB6456
TGFb1	PE-Cy7	TW4-2F8	Biolegend	349610

Cat, Catalogue.

2.9 Nasal Fluid Extraction

During the exploratory PQGrass Phase III clinical study described in Chapter 6, nasal fluid was collected from study participants at primary study sites for antibody quantification. To collect nasal fluid, research nurses inserted nasosorption FX-i devices (Hunt Developments, UK; NSFL-FXI-11) containing a synthetic absorptive matrix into each subject's right and left nostrils for 50 seconds to absorb mucosal lining fluid from within the nasal cavity. Nasosorption FX-i devices were weighed and cryopreserved in liquid nitrogen and shipped at study completion to the ITG laboratories at Imperial College London. For quantitative and atraumatic

processing of nasal secretions, nasosorption FX-i devices were transferred into Costar™ Spin-X™ centrifuge tubes containing a membrane 0.22μM filter unit to remove bacteria, cells, and particles from liquids (Corning, 10104101). Next, 300μL sterile elution buffer (4°C; Merck Millipore, AB-33K) was added onto the membrane within the filter tube and vortexed before immediate centrifugation (16000g, 20 minutes, 4°C). Filter inserts containing nasosorption FX-i devices were discarded and nasal fluid from both nostrils were pooled whilst on ice and weighed. Processed nasal fluid samples were placed in Protein LoBind Tubes (Eppendorf, 0030108116) and stored at -80°C until downstream analysis by ImmunoCAP or ELISA.

2.10 ImmunoCAP100 Antibody Quantification

Sensitive quantitative assessment of tIgE and allergen-specific sIgE, sIgG, $sIgG_4$, IgA_1 and IgA_2 antibody levels were conducted utilising the ImmunoCAP100 system (Phadia, Inc., Uppsala, Sweden), according to manufactures instructions. Allergens investigated included GP (g6; Phadia Inc., 14-4100-01) cat dander (e1; Phadia Inc., 14-4109-01), HDM (d1; Phadia Inc., 14-4107-01), peanut (f13; Phadia Inc.,14-4126-01), *Ara h 1* (f422; Phadia Inc., 14-4963-01) and *Ara h 2* (f423, Phadia Inc., 14-4964-01).

2.11 Enzyme-linked immunosorbent assay (ELISA)

2.11.1 Cell Culture Supernatant Cytokine Measurements

Cell culture supernatant samples were analysed for levels of IL-5, IL-10, and IL-13 protein utilising R&D Systems sandwich ELISA kits, according to the manufactures' instructions (R&D Systems; IL-5, DY-205; IL-10, DY217B; IL-13, DY213). MaxiSorp 96-well microplates (ThermoFisher Scientific, 442404) were utilised alongside ancillary kit-supplied (R&D Systems, DY008B) coating buffer, wash buffer (diluted 1:24 in diH_20), reagent diluent (RD; diluted 1:10 in diH_20), streptavidin-HRP (diluted 1:40 in RD), substrate solution (1:1 Solution

A: Solution B) and stop solution. Optical densities (OD) were read utilising a microplate reader (Molecular Devices; Emax Plus) at the appropriate wavelength and analysis conducted on SoftMax Pro software (Molecular Devices). Unknown sample protein concentrations were determined in relation to a kit-supplied standard-generated hyperbola curve.

2.11.2 Antibody Measurements - IgA, IgA2 and IgG ELISA

Before ELISA experiments on study samples were performed, ELISA conditions were optimised for IgA_1, IgA_2 and IgG assessment on a biobank serum sample collected from a GP-AIT treated subject to provide the most accurate comparison to the PQGrass AIT study samples. Assay conditions to be optimised included concentration of *Phl p 5* utilised to coat ELISA plates, volume of samples, and concentration of secondary detection antibody. Although these experiments were not utilised to determine the final ELISA conditions described below, they have been included in this thesis appendix for completeness and reference (Supplementary Figure 18.1).

During the exploratory PQGrass Phase III clinical study described in Chapter 6, quantification of *Phl p 5* $sIgA_1$, $sIgA_2$ and sIgG within participant nasal fluid and serum was determined through in-house optimised ELISA. MaxiSorp 96-well microplates (ThermoFisher Scientific) were coated with 100μL diluted *Phlp 5* in 1X PBS for 1 hour at 37°C, before being washed three times with 200μL wash buffer (1x PBS with 0.05% Tween) and blocked with ChonBlock™ (Chondrex Inc., 9068) for 1 hour at 37°C. Following another three washes, 100μL samples diluted in 1X PBS were added to duplicate wells in an appropriate concentration to allow their identification within the remits of the standard curve concentration. To generate a hyperbola standard curve, 100μL serum samples with known IgA_1 and IgA_2 and IgG concentrations as measured by ImmunoCAP analysis were serially diluted and added to duplicate wells. Following sample addition, ELISA plates were sealed and incubated overnight

at 4°C. Following three washes with wash buffer, 100μL biotinylated primary secondary antibodies diluted in 1x PBS were added (IgA1: Southern Biotech, 9130-08; IgA2: Southern Biotech, 9140-08; IgG: Sigma, B6775). Plates were washed three times and treated with 100μL diluted streptavidin-HRP (Biolegend, 405210) for 30 minutes at RT in the dark. Following a final three washes, 100μL of TMB solution (Merck Millipore, CL07) was added until significant colour change was observed in the highest standard concentrations. Reactions were stopped with 50μL of 1M H2S04 and OD were read utilising a microplate reader at 450nm with analysis occurring on SoftMax Pro software (both, Molecular Devices). Sample concentrations were determined in relation to the standard-generated hyperbola curve. All tested dilutions and reaction times can be found in Table 2.11.2.1.

Table 2.11.2.1 Sandwich ELISA assay conditions for assessment of serum *Phl p 5* specific IgA$_1$, IgA2 and IgG.

Antibody	*Phl p 5* Coating Concentration	Sample Dilution	Secondary Antibody	HRP	Time Developed
IgA1	1μg/mL	1:4	1:1000	1:1000	8 minutes
IgA2	5μg/mL	1:4	1:500	1:1000	8 minutes
IgG	1μg/mL	1:4	1:200,000	1:1000	12 minutes

2.12 Unbiased Visualisation Machine Learning Algorithms

Multi-parametric high dimensional flow cytometry data was interrogated further by the unbiased visualisation machine learning algorithms viSNE, SPADE and FlowSOM, utilsing Cytobank software (Cytobank Inc., Santa Clara, CA, USA). To create concatenated FCS files from subjects within the same experimental groups, files were concatenated using FCSConcat 2 software (Cytobank Inc) or within Cytobank.

2.12.1 viSNE

viSNE is a non-linear dimensionality reduction algorithm that allows the visualisation of high dimensional single cell data in a two-dimensional format to reveal phenotypic heterogeneity of samples (Figure 2.12.3.1, A). viSNE uses Barnes-Hut implementation of the *tSNE*-1 algorithm and is developed based on Stochastic Neighbor Embedding, utilising probability value to model similarity between two data points in the Euclidian space. Thus, phenotypically cells cluster together to form 'islands' whereby red expression represents high and blue low expression according to channel key. viSNE analyses were run on pre-gated $CD19^+$ B cells or $CD4^+$ T cells as indicated on equal event sampling. All viSNE analyses were run on 3000 iterations (the number of times the algorithm adjusts the placement of single cells within the two-dimensional space to best reflect similarity of single cells), perplexity of 30 (estimation of the number of similar neighbors any given single cell will have) and theta of 0.5 (controls similarity between Barnes-Hut implementation of *tSNE* (created for data-sets greater than a few thousand events total) to the original *tSNE* algorithm).

2.12.2 FlowSOM

FlowSOM is a powerful unsupervised clustering algorithm which firstly assigns viSNE single cell data into cell clusters, and then clusters phenotypically similar cell clusters into metaclusters (MC; population of cell clusters) in the form of a self-organising maps (SOM; (Figure 2.12.3.1, B). Cluster node size represents population abundance, with parameter expression within each node represented in the form of a pie chart whereby distance from the outer border represents parameter fluorescent intensity (the closer the segment is to the outer border, the higher the intensity). FlowSOM analyses were performed at an appropriate MC setting per flow-cytometry panel with quality assessed by overlaying FlowSOM MC upon viSNE maps. MC population abundance and marker intensity can be assessed between experimental groups to explore novel aberrations in cell subsets, with heatmap illustration of FlowSOM MC allowing for phenotypic evaluation of distinct MC cellular subsets.

2.12.3 SPADE

SPADE (Spanning-tree Progression Analysis of Density-normalised events) represents entire datasets through clustering phenotypically similar cells into hierarchies in the form of two-dimensional clustered trees which are connected by ‘steps’, allowing multi-dimensional analysis of heterogenous samples (Figure 2.12.3.1, C). The number of steps between clusters determine the differences between the cells within the clusters. For instance, 10 steps between cluster A and cluster B would insinuate these cells demonstrate greater phenotypic similarities than cells in cluster A and cluster C which are separated by 100 steps. Moreover, the size of each SPADE cluster is proportional to the number of cells within the cluster and phenotypes are deciphered through cluster channel colour according to an asymmetric scale. Phenotypically similar cells can thus be placed into ‘bubbles’ to define populations.

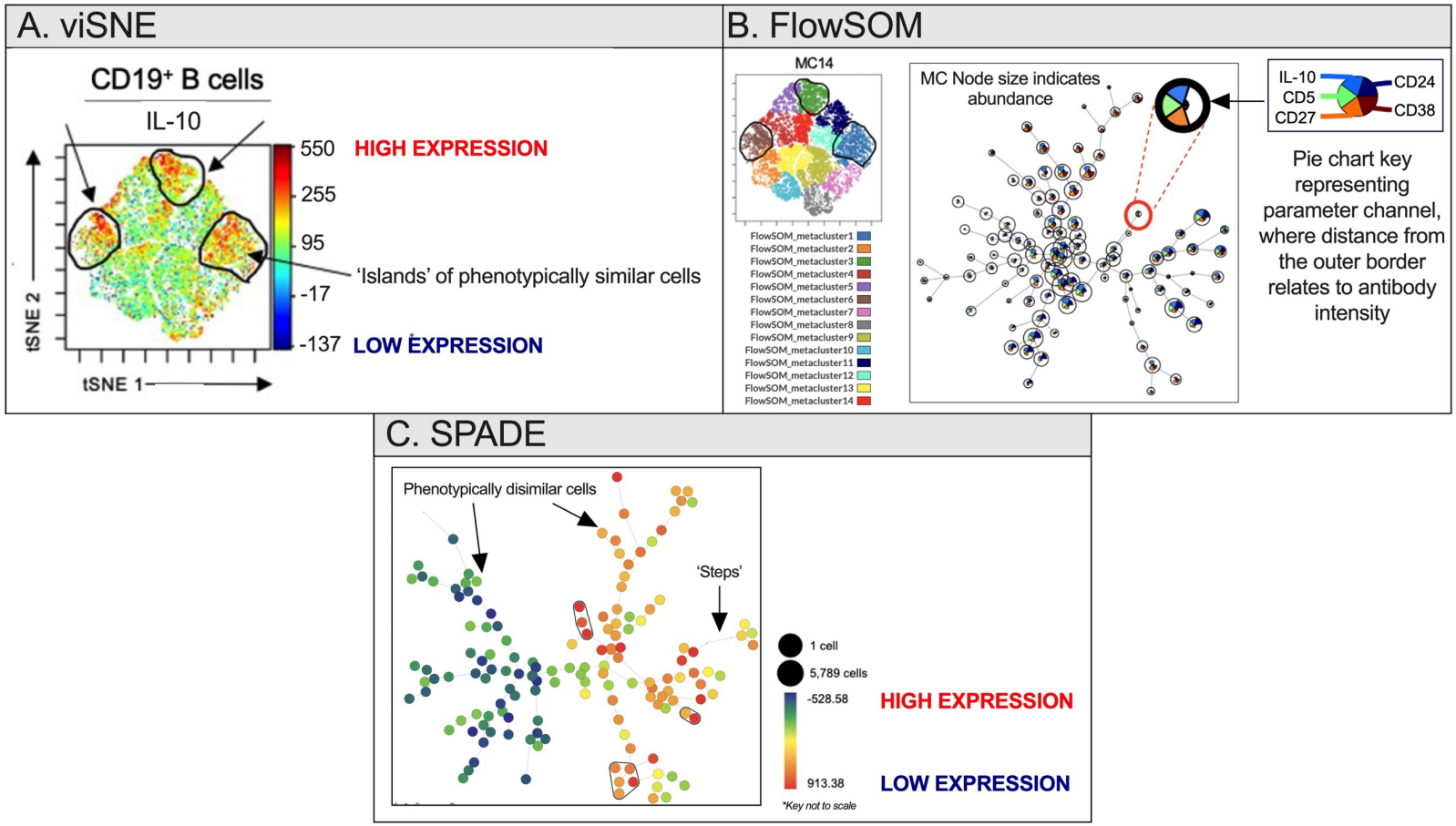


Figure 2.12.3.1 viSNE, FlowSOM and SPADE.

A) viSNE map of CD19^{+} B Cells allows identification of phenotypically similar cells, which form 'islands' based upon marker expression by colour. **B)** FlowSOM of viSNE whereby maps are divided into MC as represented in self-organising maps. MC node size represents abundance and marker expression is represented within node pie charts. **C)** SPADE allows hierarchical clustering of cells divided by steps, allowing for identification of clusters of phenotypically cells based upon step number in distance and marker expression by colour. MC, metacluster.

2.13 Statistical Analysis

Statistical analyses were performed using GraphPad Prism 9.0 (GraphPad Software, La Jolla, USA). Error bars in graphs represent standard error of the mean (SEM). Analysis between different experimental groups were performed using non-parametric Mann-Whitney U tests and within the same experimental groups utilising non-parametric Wilcoxon-paired rank sums test as appropriate. The non-parametric ANOVA Friedmann test with multiple comparisons was utilised to compare the difference between more than two related groups (e.g., dose responses). Small datasets are rarely non-normally distributed, in addition to normality tests having less power to detect non-gaussian distributions with smaller sample sizes. To confirm this within this thesis, normality testing was performed on two of the datasets in this thesis of highest value (n=18) utilised in the cross-sectional analyses in Chapter 4, which demonstrated that the data was not normally distributed (NAC, n=18: Shapiro Wilk normality test, W = 0.822; $P = 0.0032$, and, GPA, n=18, Shapiro Wilk normality test, W = 0.890; $P = 0.0381$). As such, non-parametric analyses were used throughout this thesis, without the check for normal distribution on every dataset. Data was defined as statistically significant at $P < 0.05$, termed in all data graphs as $*P < 0.05$, $**P < 0.01$ and $***P < 0.001$.

CHAPTER 3. DEEP IMMUNOPHENOTYPING OF IL-10$^+$ REGULATORY B CELLS

3.1 Introduction

Breg cells are an important modulatory component of the immune system, acting to suppress inflammation and maintain immune homeostasis (221, 222). In humans, B cells comprise 10-15% of PBMCs, with Breg cells accounting for 1-2% of this total B cell number under homeostatic conditions. IL-10$^+$ Breg cell populations can be expanded greatly through *ex vivo* stimulation with both innate and adaptive induction stimuli, such as the TLR9 agonist, CpG, and the costimulatory molecule, CD40L, allowing for in-depth investigations of Breg immunophenotypes (225, 239, 240, 246). Currently, there is no consensus of unequivocal cellular surface markers or transcriptional lineage marker capable of defining the Breg phenotype, with 'subsets' of Breg cells instead defined based on dynamic cell surface marker expression, cytokine production and induction manner (247, 248). Thereby, further studies to decode IL-10$^+$ B cell immunophenotypes are required to develop methodology to identify and investigate Breg cells to gain greater understanding of the role suppressive IL-10$^+$ Breg cells play during inflammatory diseases, such as allergy. As Breg cells are often associated with increased anti-inflammatory IL-10 propensity, intracellular IL-10 expression is now widely utilised across the literature to define the functionally suppressive Breg cellular phenotype (225, 226). Recent studies have reported that Breg-mediated suppression may not be exclusive to IL-10 secretion, with further studies revealing distinct phenotypic subsets of Breg cells possessing capability to express other known suppressive molecules, such as CD80, CD86, PD-1, PD-L1, TIM-1, IL-35 and TGF-β (229, 230, 246, 278, 316). Therefore, research to delineate the relationship between IL-10$^+$ Breg cells and co-expression of other suppressive molecules is required.

3.1.1 Hypothesis and Aims

3.1.1.1 Hypothesis

1. Stimulation with TLR ligands, such as CpG sequences and CD40L, can result in the generation of IL-10^{+} Breg cells.
2. Human peripheral blood IL-10^{+} Breg cells are enriched within distinct phenotypic subsets of B cells.

3.1.1.2 Aims

3. To determine whether *ex vivo* CpG and CD40L stimulation promotes expression of IL-10 in B cells and levels of IL-10 protein secretion in a dose- and time- dependent manner.
4. To determine whether IL-10^{+} Breg cells are associated with TIM-1, IL-35, TGFβ1, CD80, CD86, PD-L1 and PD-1 expression compared to IL-10^{-} B cells.
5. To validate flow-cytometry analysis using unbiased mathematical machine learning algorithms, viSNE, FlowSOM and SPADE.

3.2 Results

3.2.1 Identification of IL-10$^+$ Breg cells in human peripheral blood

To perform deep immunophenotyping of Breg cells, PBMCs were isolated from whole blood of *n*=45 NAC (Table 3.2.1.1). As per inclusion criteria (described in section 2.2), NAC donors were confirmed to have a negative SPT to tested allergen and low tIgE levels. Although participant age range was wide and well distributed, there was a gender bias towards females. Phenotypic composition of IL-10$^+$ Breg cells was evaluated through multi-parametric flow-cytometry. Lymphocytes were first differentiated from PBMCs based on side and forward scatter area (Figure 3.2.1.1, A) before doublet exclusion based on forward scatter height and area (Figure 3.2.1.1, B). Next, live cells were isolated based on a negative L/D viability stain (Figure 3.2.1.1, C) before B cells were classified based on positive expression of the pan B cell marker CD19 and negative CD3 cell surface marker expression (Figure 3.2.1.1, D). CD19$^+$ B cells that produced IL-10 were then identified (Figure 3.2.1.1, E). IL-10$^+$ B cells were further identified within four putative peripheral B cell subsets: activated B cells (CD19$^+$CD5$^{+/hi}$; Figure 3.2.1.1, F-H), memory B cells (CD19$^+$CD27$^+$; Figure 3.2.1.1, I-J) and transitional B cells (CD19$^+$CD24hiCD38^{hi}; Figure 3.2.1.1, K-L).

Table 3.2.1.1 Patient Demographics of NAC used in IL-10$^+$ Breg culture optimisation experiments

Characteristic	Non-Atopic Control (n=45)
Gender, M:F	15:30
Age (years), range	25-70 (mean: 42.9)
tIgE (kU_A/L), mean ± SD	31 ±33*
Skin Prick Test (mm^2) ± SD	0 ± 0

*N.B. tIgE data not available for *n*=4 samples.

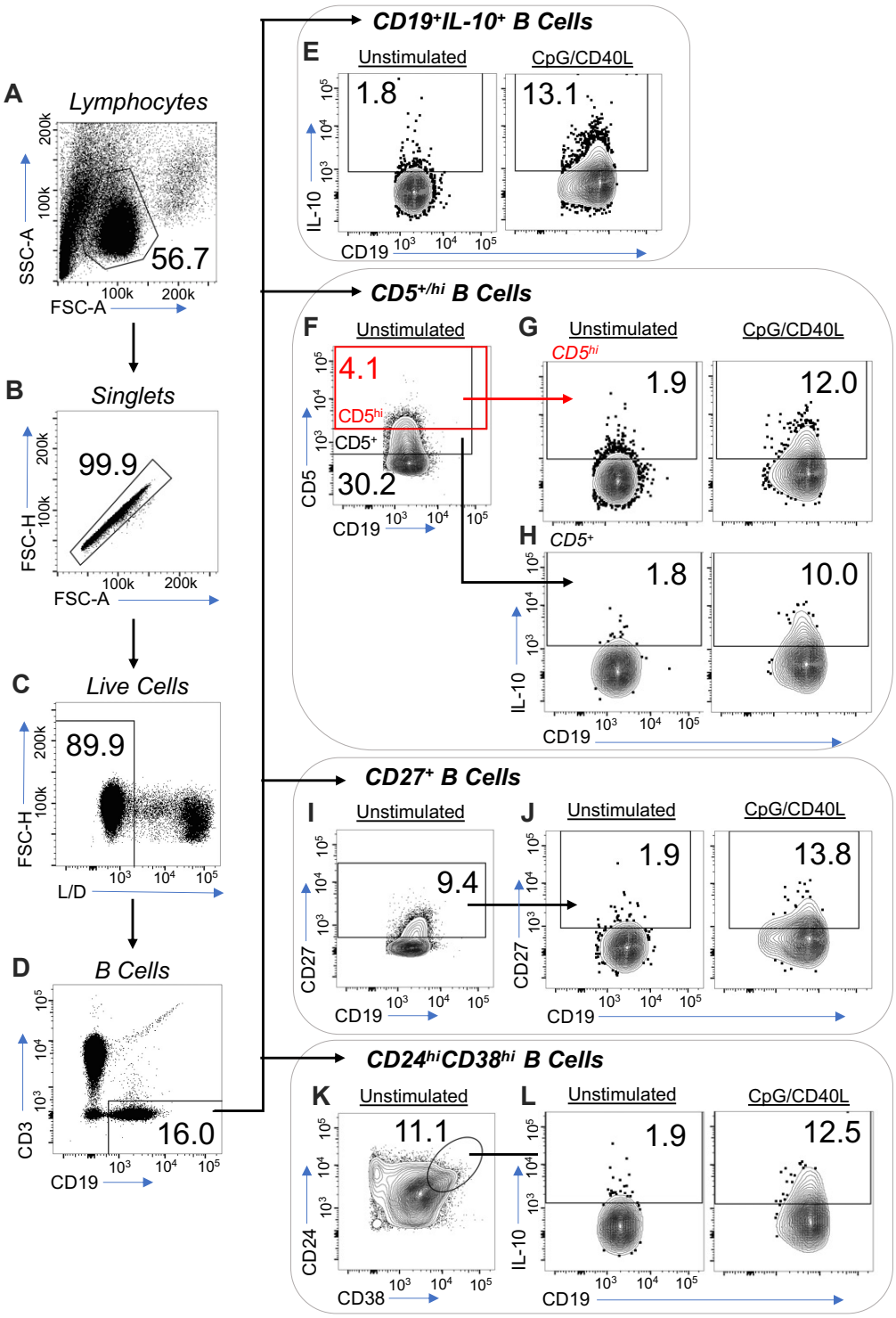


Figure 3.2.1.1 Flow cytometry gating strategy to identify IL-10$^+$ Breg cells from PBMCs

A) Lymphocytes were phenotyped from PBMCs based on FSC and SSC before **B)** doublet exclusion based on FSC-H and FSC-A. **C)** Viable cells were selected based on negative L/D stain before **D)** CD3$^-$CD19$^+$ B cells were categorised. B cells were differentiated into **E)** CD19$^+$IL-10$^+$, **F-H)** CD19$^+$CD5$^{+/hi}$IL-10$^+$, **I-J)** CD19$^+$CD27$^+$IL-10$^+$ and **K-L)** CD19$^+$CD24^{hi}CD38^{hi}IL-10$^+$ B cells. Plots in **E**, **G, H, J and L** represent unstimulated and 1μg/mL CpG and 2.5μg/mL CD40L stimulated samples. FSC-A, forward scatter-area; FSC-H, forward scatter-height, SSC-A, side scatter area; L/D, Live Dead viability stain.

3.2.2 Ex vivo CpG and CD40L stimulation induces significant IL-10$^+$ Breg cell frequencies from human peripheral blood in a dose-dependent manner

To determine the ability of CD40L to induce IL-10$^+$ Breg cells, PBMCs were stimulated with increasing concentrations of CD40L (0.625μg/mL, 1.25μg/mL, 2.5μg/mL, 3.75μg/mL and 5μg/mL) for 72 hours. CD40L stimulation at 2.5μg/mL (P = 0.0214), 3.75μg/mL (P = 0.0039) and 5μg/mL (P = 0.0065) significantly induced CD19$^+$IL-10$^+$ Breg cells (Figure 3.2.2.1, A-B and Table 3.2.2.1). Stimulation with 2.5μg/mL CD40L also significantly enhanced activated CD5$^+$ (P = 0.0107), memory CD27$^+$ (P = 0.0170) and transitional CD24^{hi}CD38^{hi} (P = 0.0411) IL-10$^+$ Breg cells. Moreover, ELISA analysis revealed IL-10 protein levels were increased in cell culture supernatant in a CD40L dose-dependent manner (2.5μg/mL: P = 0.0010; 3.75μg/mL: P = 0.0030; 5μg/mL: P = 0.0003; Figure 3.2.2.1, C). To determine the ability of CpG to induce IL-10$^+$ Breg cells, PBMCs were stimulated with increasing concentrations of CpG (0.1μg/mL, 0.3μg/mL, 1μg/mL, 3μg/mL and 10μg/mL) alongside 2.5μg/mL CD40L. Flow cytometry analysis revealed, in the presence of CD40L, CpG stimulation resulted in a dose-dependent induction of all IL-10$^+$ Breg subsets, with peak responses observed at 1μg/mL (all, P = 0.0020) and 3μg/mL CpG (all, P < 0.01; Figure 3.2.2.1, E-I and Table 3.2.2.2). Similar trends were observed utilising a multiple comparison statistical approach, with all IL-10$^+$ Breg cell subsets significantly induced at 3μg/mL CpG (all P < 0.05; Table 3.2.2.3). ELISA analysis supported flow-cytometry observations through demonstrating a CpG dose-dependent increase in secreted IL-10 quantities, optimal at 1μg/mL (234pg/mL, P = 0.0195) and 3μg/mL (368pg/mL, P = 0.0078) CpG (Figure 3.2.2.1, J). For all experiments, basal percentages of IL-10$^+$ Breg cells within unstimulated samples were between 1.5 and 2.6%.

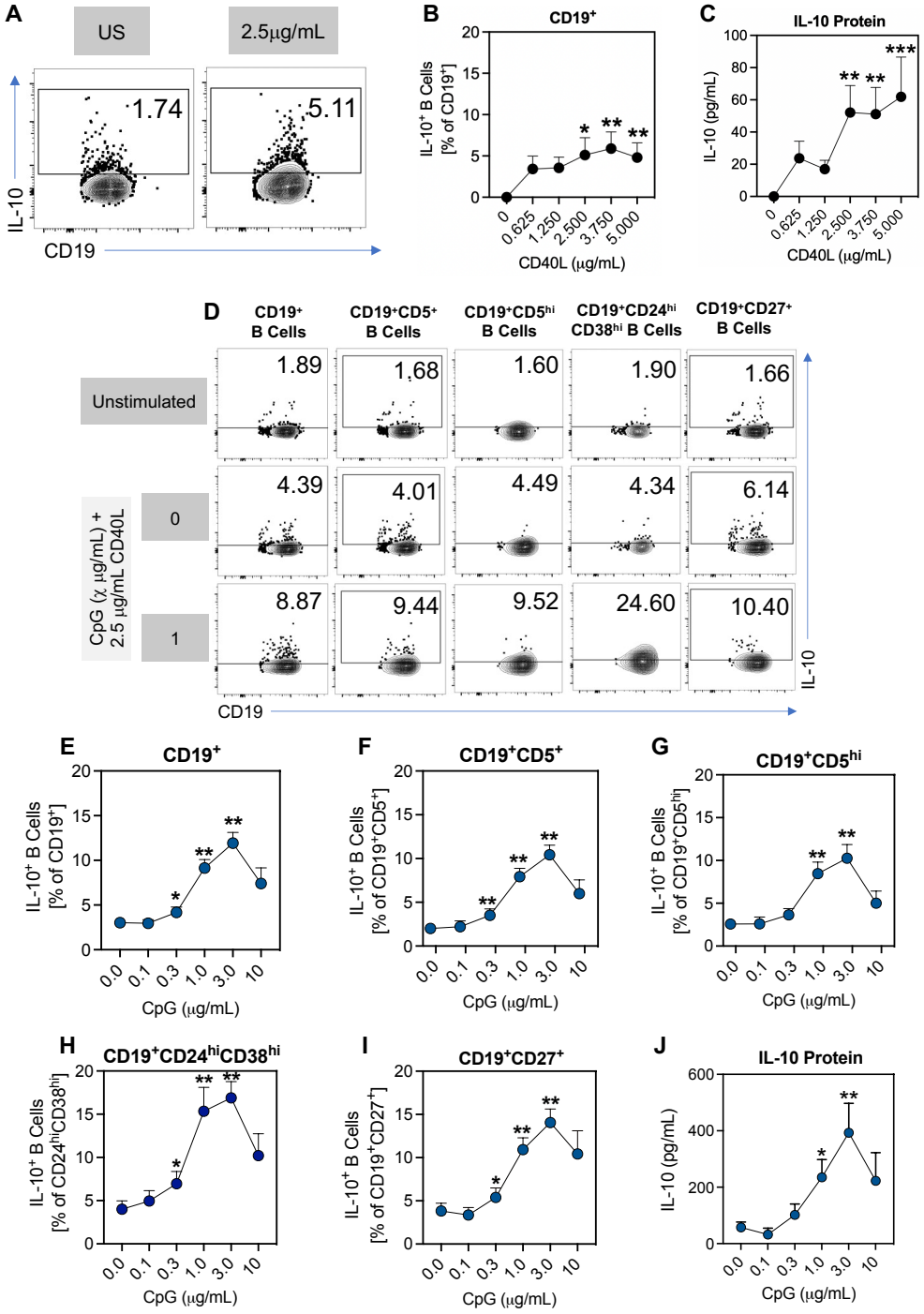


Figure 3.2.2.1 CD40L and CpG stimulation induces IL-10$^+$ Breg cells.

A) Flow cytometry representative plots from n=1 NAC illustrating induction of CD19$^+$IL-10$^+$ B cells in response to CD40L stimulation. Effect of increasing doses of CD40L on **B)** CD19$^+$IL-10$^+$ B cell frequencies and **C)** IL-10 levels in culture supernatant. **D)** Flow cytometry representative plots from n=1 NAC illustrating the induction of IL-10$^+$ Breg cell subsets in response to CpG stimulation. Effect of increasing doses of CpG in the presence of CD40L on **E)** IL-10$^+$CD19$^+$, **F)** CD5$^+$ **G)** CD5^{hi} **H)** CD24^{hi}CD38^{hi} and **I)** CD27$^+$ IL-10$^+$ B cells. **J)** IL-10 levels in culture supernatant quantified by ELISA. Data representative of **B-C)** n=7, **E-I)** n=10 NAC [10μg/mL, n=6; 0.1μg/mL, n=7] and **J)** n=9 NAC and presented as mean ±SEM. **B-C)** Friedman Test with Dunn's Multiple Comparisons. **E-J)** Wilcoxon paired signed-rank test.. *P < 0.05, **P < 0.01, ***P < 0.001. CD40 ligand, CD40L; Non-Atopic Control, NAC; US, unstimulated.

Table 3.2.2.1 IL-10^{+} Breg Cell Subset Expression Following Stimulation with increasing dosages of CD40L

CD40 Ligand Concentration (μg/mL)	B Cell Subset	Raw				Delta 0 (Unstimulated)			*P* value vs 0μg/mL CD40L
		n	mean	SD	SEM	mean	SD	SEM	
0 (Unstimulated)	CD19^{+}IL-10^{+}	7	1.75	0.09	0.03	NA	NA	NA	NA
	CD19^{+}CD5^{+}IL-10^{+}	7	1.76	0.07	0.03	NA	NA	NA	NA
	CD19^{+}CD5^{hi}IL-10^{+}	7	2.60	2.48	0.94	NA	NA	NA	NA
	CD19^{+}CD27^{+}IL-10^{+}	7	1.85	0.48	0.18	NA	NA	NA	NA
	CD19^{+}CD24^{hi}CD38^{hi}IL-10^{+}	7	1.79	0.12	0,04	NA	NA	NA	NA
0.625	CD19^{+}IL-10^{+}	7	5.04	4.14	1.57	3.43	4.08	1.54	0.1916
	CD19^{+}CD5^{+}IL-10^{+}	7	5.52	5.88	2.22	3.87	5.81	2.20	0.1340
	CD19^{+}CD5^{hi}IL-10^{+}	7	5.91	5.14	1.94	3.62	5.14	1.94	0.5804
	CD19^{+}CD27^{+}IL-10^{+}	7	4.27	2.41	0.91	2.45	2.48	0.94	0.0921
	CD19^{+}CD24^{hi}CD38^{hi}IL-10^{+}	7	8.17	7.66	2.90	6.39	7.68	2.90	0.1340
1.25	CD19^{+}IL-10^{+}	7	5.31	3.36	1.27	3.56	3.42	1.29	0.1340
	CD19^{+}CD5^{+}IL-10^{+}	7	4.78	3.17	1.20	3.09	3.12	1.18	0.3707
	CD19^{+}CD5^{hi}IL-10^{+}	7	6.25	3.93	1.48	3.84	3.33	1.26	**0.0411**
	CD19^{+}CD27^{+}IL-10^{+}	7	4.97	2.37	0.89	3.13	2.49	0.94	**0.0214**
	CD19^{+}CD24^{hi}CD38^{hi}IL-10^{+}	7	9.19	7.53	2.85	7.41	7.54	2.85	**0.0332**
2.5	CD19^{+}IL-10^{+}	7	6.82	5.56	2.10	5.10	5.57	2.11	**0.0214**
	CD19^{+}CD5^{+}IL-10^{+}	7	6.18	5.20	1.97	4.44	5.24	1.98	**0.0107**
	CD19^{+}CD5^{hi}IL-10^{+}	7	5.43	4.22	1.59	3.19	4.41	1.67	0.0621
	CD19^{+}CD27^{+}IL-10^{+}	7	5.72	4.18	1.58	3.96	4.26	1.61	**0.0170**
	CD19^{+}CD24^{hi}CD38^{hi}IL-10^{+}	7	8.50	5.24	1.98	6.71	5.27	1.99	**0.0411**
3.75	CD19^{+}IL-10^{+}	7	7.64	5.27	1.99	5.89	5.31	2.01	**0.0039**
	CD19^{+}CD5^{+}IL-10^{+}	7	7.12	4.65	1.76	5.36	4.68	1.77	**0.0051**
	CD19^{+}CD5^{hi}IL-10^{+}	7	7.25	5.61	2.12	4.70	5.76	2.18	**0.0267**
	CD19^{+}CD27^{+}IL-10^{+}	7	5.61	2.78	1.05	2.82	2.96	1.12	**0.0107**
	CD19^{+}CD24^{hi}CD38^{hi}IL-10^{+}	7	11.50	7.49	2.83	9.73	7.54	2.85	**0.0003**
5	CD19^{+}IL-10^{+}	7	6.55	4.64	1.75	4.80	4.69	1.77	**0.0065**
	CD19^{+}CD5^{+}IL-10^{+}	7	6.19	3.92	1.48	4.50	3.85	1.45	**0.0170**
	CD19^{+}CD5^{hi}IL-10^{+}	7	6.83	3.62	1.37	4.27	3.90	1.47	0.0621
	CD19^{+}CD27^{+}IL-10^{+}	7	4.83	2.96	1.12	3.01	3.11	1.18	0.1916
	CD19^{+}CD24^{hi}CD38^{hi}IL-10^{+}	7	9.80	4.65	1.76	8.01	4.70	1.78	**0.0030**

Bolded Values Represent significant ***P*** Values. Friedman Test, Dunn's Multiple Comparisons test.

Table 3.2.2.2 IL-10$^+$ Breg Cell Subset Expression Following Stimulation with increasing dosages of CpG alongside CD40L.

CpG Concentration (μg/mL)	CD40 Ligand Concentration (μg/mL)	B Cell Subset	Raw				Delta 0 (Unstimulated)			*P* value vs 0μg/mL CpG
			n	mean	SD	SEM	mean	SD	SEM	
0 (Unstimulated)	0	CD19$^+$IL-10$^+$	10	1.73	0.22	0.07	NA	NA	NA	NA
		CD19$^+$CD5$^+$IL-10$^+$	10	1.99	0.58	0.19	NA	NA	NA	NA
		CD19$^+$CD5^{hi}IL-10$^+$	10	1.75	0.14	0.05	NA	NA	NA	NA
		CD19$^+$CD27$^+$IL-10$^+$	10	2.21	1.44	0.48	NA	NA	NA	NA
		CD19$^+$CD24^{hi}CD38^{hi}IL-10$^+$	10	1.89	0.09	0.03	NA	NA	NA	NA
0	2.5	CD19$^+$IL-10$^+$	10	4.65	2.22	0.70	3.03	1.85	0.58	NA
		CD19$^+$CD5$^+$IL-10$^+$	10	3.84	1.87	0.59	2.01	1.77	0.56	NA
		CD19$^+$CD5^{hi}IL-10$^+$	10	4.18	1.92	0.61	2.58	1.67	0.53	NA
		CD19$^+$CD27$^+$IL-10$^+$	10	5.88	3.04	0.96	3.83	2.82	0.89	NA
		CD19$^+$CD24^{hi}CD38^{hi}IL-10$^+$	10	5.77	3.29	1.04	4.01	3.04	0.96	NA
0.1	2.5	CD19$^+$IL-10$^+$	7	4.71	1.07	0.40	2.95	1.03	0.39	0.6875
		CD19$^+$CD5$^+$IL-10$^+$	7	4.16	1.71	0.65	2.21	1.75	0.66	>0.9999
		CD19$^+$CD5^{hi}IL-10$^+$	7	4.77	2.07	0.78	2.59	2.14	0.81	0.8438
		CD19$^+$CD27$^+$IL-10$^+$	7	5.79	1.84	0.69	3.36	2.30	0.87	0.8125
		CD19$^+$CD24^{hi}CD38^{hi}IL-10$^+$	7	6.89	3.16	1.19	4.96	3.16	1.20	0.5938
0.3	2.5	CD19$^+$IL-10$^+$	10	5.91	2.02	0.64	4.18	1.88	0.60	**0.0371**
		CD19$^+$CD5$^+$IL-10$^+$	10	5.42	2.29	0.73	3.51	2.31	0.73	**0.0039**
		CD19$^+$CD5^{hi}IL-10$^+$	10	5.67	2.52	0.80	3.64	2.32	0.74	0.0977
		CD19$^+$CD27$^+$IL-10$^+$	10	7.60	3.18	1.01	5.39	3.46	1.09	**0.0195**
		CD19$^+$CD24^{hi}CD38^{hi}IL-10$^+$	10	8.84	4.51	1.43	6.95	4.51	1.43	**0.0273**
1	2.5	CD19$^+$IL-10$^+$	10	10.90	3.11	0.98	9.14	3.01	0.95	**0.0020**
		CD19$^+$CD5$^+$IL-10$^+$	10	9.91	2.94	0.93	7.92	3.02	0.96	**0.0020**
		CD19$^+$CD5^{hi}IL-10$^+$	10	10.80	4.32	1.37	8.46	4.26	1.35	**0.0020**
		CD19$^+$CD27$^+$IL-10$^+$	10	13.10	4.11	1.30	10.90	4.30	1.36	**0.0020**
		CD19$^+$CD24^{hi}CD38^{hi}IL-10$^+$	10	17.20	8.82	2.79	15.30	8.77	2.77	**0.0020**
3	2.5	CD19$^+$IL-10$^+$	10	13.70	3.88	1.23	11.93	3.80	1.20	**0.0020**
		CD19$^+$CD5$^+$IL-10$^+$	10	12.40	3.20	1.01	10.40	3.48	1.10	**0.0020**
		CD19$^+$CD5^{hi}IL-10$^+$	10	13.20	3.83	1.21	10.30	5.07	1.60	**0.0039**
		CD19$^+$CD27$^+$IL-10$^+$	10	16.30	4.45	1.41	10.90	4.30	1.36	**0.0020**
		CD19$^+$CD24^{hi}CD38^{hi}IL-10$^+$	10	18.80	6.00	1.90	16.90	5.96	1.89	**0.0020**
10	2.5	CD19$^+$IL-10$^+$	6	9.18	4.32	1.76	7.41	4.29	1.75	0.0625
		CD19$^+$CD5$^+$IL-10$^+$	6	7.82	3.76	1.53	6.00	3.82	1.56	0.0625
		CD19$^+$CD5^{hi}IL-10$^+$	6	6.78	3.37	1.38	5.01	3.44	1.40	0.0938
		CD19$^+$CD27$^+$IL-10$^+$	6	12.20	6.62	2.70	14.10	4.93	1.56	0.0938
		CD19$^+$CD24^{hi}CD38^{hi}IL-10$^+$	6	12.10	6.20	2.52	10.20	6.17	2.52	0.0625

Bolded Values Represent significant ***P*** Values. Wilcoxon paired signed-rank Test.

Table 3.2.2.3 IL-10$^+$ Breg Cell Subset Expression Following Stimulation with increasing dosages of CpG alongside CD40L.

CpG Concentration (μg/mL)	CD40 Ligand Concentration (μg/mL)	B Cell Subset	Raw				Delta 0 (Unstimulated)			*P* value vs 0μg/mL CpG
			n	mean	SD	SEM	mean	SD	SEM	
0 (Unstimulated)	0	$CD19^+IL\text{-}10^+$	6	1.77	0.21	0.09	NA	NA	NA	NA
		$CD19^+CD5^+IL\text{-}10^+$	6	1.82	0.10	0.04	NA	NA	NA	NA
		$CD19^+CD5^{hi}IL\text{-}10^+$	6	1.76	0.13	0.05	NA	NA	NA	NA
		$CD19^+CD27^+IL\text{-}10^+$	6	1.79	0.13	0.05	NA	NA	NA	NA
		$CD19^+CD24^{hi}CD38^{hi}IL\text{-}10^+$	6	1.86	0.09	0.04	NA	NA	NA	NA
0	2.5	$CD19^+IL\text{-}10^+$	6	4.50	2.46	1.00	2.91	1.97	0.81	NA
		$CD19^+CD5^+IL\text{-}10^+$	6	3.57	2.19	0.90	2.01	1.83	0.75	NA
		$CD19^+CD5^{hi}IL\text{-}10^+$	6	3.44	1.98	0.81	1.93	1.57	0.64	NA
		$CD19^+CD27^+IL\text{-}10^+$	6	5.74	3.88	1.59	4.21	3.43	1.40	NA
		$CD19^+CD24^{hi}CD38^{hi}IL\text{-}10^+$	6	5.33	2.88	1.17	3.69	2.39	0.98	NA
0.3	2.5	$CD19^+IL\text{-}10^+$	6	5.47	2.31	0.94	3.70	2.15	0.88	>0.9999
		$CD19^+CD5^+IL\text{-}10^+$	6	4.90	2.69	1.10	3.20	2.54	1.04	>0.9999
		$CD19^+CD5^{hi}IL\text{-}10^+$	6	4.33	2.46	1.00	2.73	2.23	0.91	>0.9999
		$CD19^+CD27^+IL\text{-}10^+$	6	7.73	4.24	1.73	5.95	4.24	1.73	>0.9999
		$CD19^+CD24^{hi}CD38^{hi}IL\text{-}10^+$	6	7.72	3.22	1.31	5.89	3.25	1.33	>0.9999
1	2.5	$CD19^+IL\text{-}10^+$	6	9.47	2.62	1.07	7.70	2.50	1.02	0.0705
		$CD19^+CD5^+IL\text{-}10^+$	6	8.35	2.25	0.92	6.53	2.28	0.93	0.0548
		$CD19^+CD5^{hi}IL\text{-}10^+$	6	7.82	2.24	0.91	6.06	2.23	0.91	0.0899
		$CD19^+CD27^+IL\text{-}10^+$	6	12.60	5.29	2.16	10.80	5.19	2.12	0.0705
		$CD19^+CD24^{hi}CD38^{hi}IL\text{-}10^+$	6	13.70	6.67	2.72	11.90	6.60	2.70	0.2716
3	2.5	$CD19^+IL\text{-}10^+$	6	14.10	4.60	1.88	12.35	4.57	1.87	**0.0002**
		$CD19^+CD5^+IL\text{-}10^+$	6	12.30	3.70	1.51	10.50	3.75	1.53	**0.0002**
		$CD19^+CD5^{hi}IL\text{-}10^+$	6	11.30	3.08	1.26	9.51	3.17	1.29	**0.0003**
		$CD19^+CD27^+IL\text{-}10^+$	6	17.20	5.54	2.26	15.40	5.51	2.25	**0.0021**
		$CD19^+CD24^{hi}CD38^{hi}IL\text{-}10^+$	6	17.60	4.32	1.76	15.80	4.27	1.75	**0.0021**
10	2.5	$CD19^+IL\text{-}10^+$	6	9.18	4.32	1.76	7.41	4.29	1.75	0.1784
		$CD19^+CD5^+IL\text{-}10^+$	6	7.82	3.76	1.53	6.00	3.82	1.56	0.1431
		$CD19^+CD5^{hi}IL\text{-}10^+$	6	6.78	3.37	1.38	5.01	3.44	1.40	0.2209
		$CD19^+CD27^+IL\text{-}10^+$	6	12.20	6.62	2.70	10.40	6.58	2.68	0.1784
		$CD19^+CD24^{hi}CD38^{hi}IL\text{-}10^+$	6	12.10	6.20	2.52	10.20	6.17	2.52	0.4014

Bolded Values Represent significant ***P*** Values. Friedman Test, Dunn's Multiple Comparisons test.

3.2.3 Combined CpG and CD40L stimulation induces greater IL-10$^+$ Breg cell frequencies than singular stimulation

To differentiate the importance of CpG or CD40L for the induction of IL-10$^+$ Breg cells, stimulants were administered singularly or in combination and evaluated by multi-parametric flow-cytometry. Singular stimulation with 1μg/mL CpG induced significant IL-10$^+$ Breg cells in all investigated subsets (all, $P = 0.0006$; Figure 3.2.3.1 and Table 3.2.3.1). Moreover, singular stimulation with 2.5μg/mL CD40L induced significant CD19$^+$IL-10$^+$ ($P = 0.0239$), memory CD27$^+$ ($P = 0.0202$) and transitional CD24^{hi}CD38^{hi} ($P = 0.0251$) IL-10$^+$ Breg cells, with similar trends observed in activated CD5$^{+/hi}$IL-10$^+$ Breg cells. However, CD40L stimulation alone induced significantly fewer IL-10$^+$ Breg cell frequencies compared to singular CpG stimulation (all, $P < 0.05$) and combined CpG and CD40L stimulation (all, $P < 0.01$). Moreover, combination of CpG and CD40L stimulation demonstrated a trend of increased IL-10$^+$ Breg subsets compared to singular CpG stimulation, although no significance was reached (Figure 3.2.3.1, A-E). ELISA revealed secreted IL-10 levels in culture supernatant were increased in CpG (624pg/mL, $P = 0.0111$) and combined CpG and CD40L (824pg/mL, $P = 0.0070$) stimulated samples compared to unstimulated samples (Figure 3.2.3.1, F). Moreover, combined CpG and CD40L stimulation significantly increased supernatant IL-10 protein levels compared to singular CD40L alone ($P = 0.0262$).

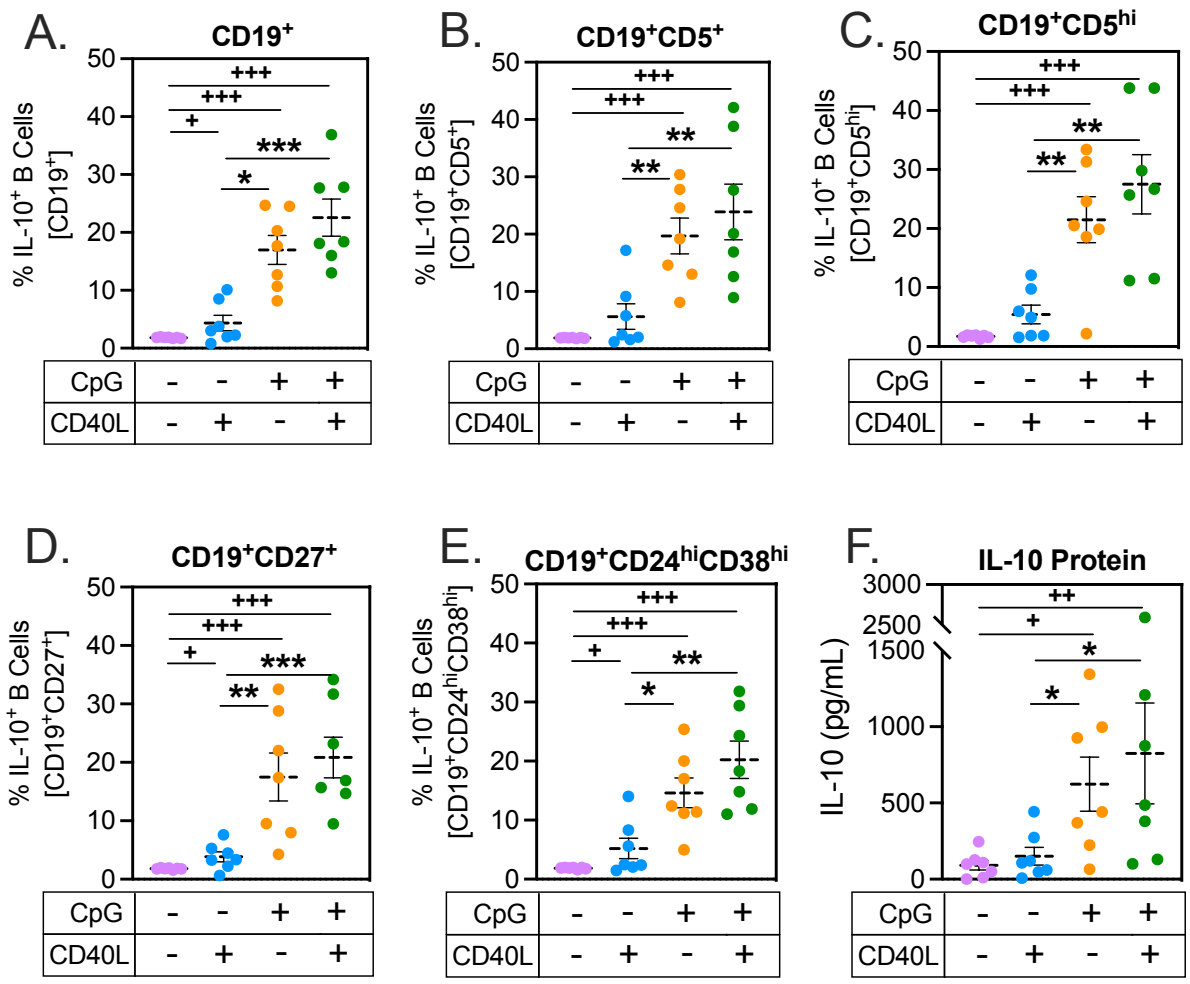


Figure 3.2.3.1 Combination of CpG and CD40L stimulation induces greater IL-10$^+$ Breg cell frequencies compared to singular stimulation.

Effect of CpG and CD40L stimulation on the induction of **A)** IL-10$^+$CD19$^+$, **B)** CD5$^+$, **C)** CD5^{hi}, **D)** CD27$^+$ and **E)** CD24^{hi}CD38^{hi} IL-10$^+$ Breg cell subsets. **F)** IL-10 protein levels in culture supernatants as measured by ELISA. Data representative of n=7 NAC and presented as mean ±SEM. Mann-Whitney U Test. *P < 0.05, **P < 0.01, ***P < 0.001. +, denotes significance between CD40L, CpG or CpG/CD40L stimulated samples and unstimulated samples. *, denotes significance between singular CD40L and CpG or CpG+CD40L stimulated samples. Non-atopic control, NAC.

CpG and CD40L-mediated induction of IL-10$^+$ Breg cells was validated through visualisation mathematical models developed to interrogate high-dimensional data. Initially, CD19$^+$ B cells were examined through viSNE analysis represented according to known B cell subset markers, CD5, CD24, CD27, CD38 and IL-10. viSNE maps confirmed the presence of IL-10$^+$ Breg cell populations in peripheral human blood and revealed phenotypically similar IL-10-expressing Breg cells formed two distinct islands (Figure 3.2.3.2, A, black arrows). IL-10 expression was enhanced in the two islands following singular CpG or CD40L stimulation compared to unstimulated samples, but was greatest when stimulation was combined, validating flow cytometry observations. A proportion of the two islands of IL-10 expressing CD19$^+$ B cells resided within high CD5, CD24, CD27 and CD38 expressing B cells.

To divulge the IL-10 expressing islands further and substantiate viSNE observations, another unbiased approach, FlowSOM, which groups phenotypically similar cell subsets into MC was layered on top of viSNE analysis. FlowSOM analysis identified two distinct IL-10 MC (MC 5 and MC 6) to be associated with the IL-10$^+$ islands observed in the viSNE map (Figure 3.2.3.2, B). Moreover, FlowSOM star plots confirmed MC 5 and MC 6 were differentially expressed between singular CpG, CD40L and combined CpG and CD40L stimulated samples (Figure 3.2.3.2, C). MC 6 population abundance and MC 5 and MC 6 IL-10 expression strongly supported flow cytometry observations that CpG, with and without CD40L, induces IL-10 expression from B cells (Figure 3.2.3.2, D-E). Heat-map analysis revealed MC 5 and MC 6 were phenotypically similar, representing CD5$^+$CD24$^-$CD27^{lo}CD38$^+$IL-10$^+$ and CD5^{hi}CD24$^-$CD27^{lo}CD38^{hi}IL-10$^+$ B cells, respectively (Figure 3.2.3.2, F).

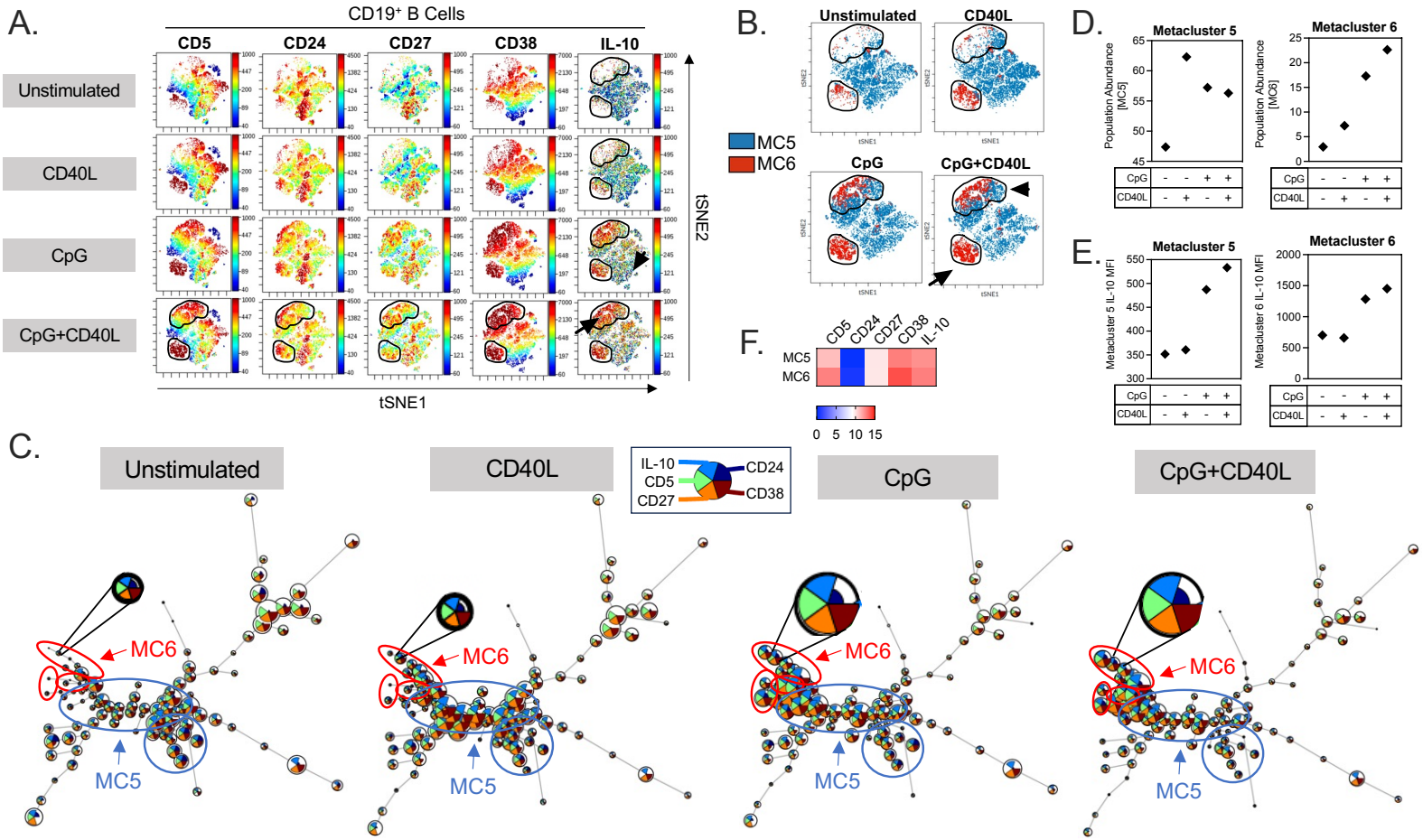


Figure 3.2.3.2 viSNE and FlowSOM confirm induction of IL-10$^+$ Breg cells in response to CpG and CD40L stimulation.

A) viSNE maps demonstrating islands of CD19$^+$ B cells expressing CD5, CD24, CD27 and CD38 and IL-10. **B)** Overlayed viSNE maps demonstrating FlowSOM identified MC 5 and MC 6. **C)** FlowSOM star plots demonstrating effect of CpG and CD40L stimulation on CD19$^+$ B cells, whereby MC 5 and MC 6 are highlighted by blue and red islands, respectively. **D)** Population abundance and **E)** Mean fluorescent intensity of IL-10 in MC 5 and MC 6. **F)** Heatmap of CpG/CD40L stimulated PBMCs. Data representative of n=3 concatenated FCS files per condition. MC, metaclusters.

Table 3.2.3.1 Comparison of CpG and CD40L stimulation of IL-10$^+$ Breg cells.

Parameter/Condition	B Cell Subset	Raw				*P* value vs Unstimulated	*P* value vs CD40L	*P* value vs CpG
		n	mean	SD	SEM			
Unstimulated	CD19$^+$IL-10$^+$	7	1.82	0.11	0.04	NA	NA	NA
	CD19$^+$CD5$^+$IL-10$^+$	7	1.90	0.09	0.03	NA	NA	NA
	CD19$^+$CD5^{hi}IL-10$^+$	7	1.71	0.24	0.09	NA	NA	NA
	CD19$^+$CD27$^+$IL-10$^+$	7	1.82	0.14	0.05	NA	NA	NA
	CD19$^+$CD24^{hi}CD38^{hi}IL-10$^+$	7	1.87	0.14	0.05	NA	NA	NA
CD40L	CD19$^+$IL-10$^+$	7	4.35	3.54	1.34	**0.0239**	NA	NA
	CD19$^+$CD5$^+$IL-10$^+$	7	5.62	5.85	2.21	0.2086	NA	NA
	CD19$^+$CD5^{hi}IL-10$^+$	7	5.44	4.17	1.58	0.0781	NA	NA
	CD19$^+$CD27$^+$IL-10$^+$	7	3.84	2.23	0.84	**0.0262**	NA	NA
	CD19$^+$CD24^{hi}CD38^{hi}IL-10$^+$	7	5.19	4.59	1.73	**0.0251**	NA	NA
CpG	CD19$^+$IL-10$^+$	7	17.0	6.61	2.50	**0.0006**	**0.0023**	NA
	CD19$^+$CD5$^+$IL-10$^+$	7	19.7	8.27	3.12	**0.0006**	**0.0070**	NA
	CD19$^+$CD5^{hi}IL-10$^+$	7	21.5	10.3	3.88	**0.0006**	**0.0070**	NA
	CD19$^+$CD27$^+$IL-10$^+$	7	17.5	10.8	4.09	**0.0006**	**0.0041**	NA
	CD19$^+$CD24^{hi}CD38^{hi}IL-10$^+$	7	14.6	6.72	2.54	**0.0006**	**0.0175**	NA
CpG+CD40L	CD19$^+$IL-10$^+$	7	22.6	8.48	3.20	**0.0006**	**0.0006**	0.2086
	CD19$^+$CD5$^+$IL-10$^+$	7	23.9	12.8	4.84	**0.0006**	**0.0070**	0.7104
	CD19$^+$CD5^{hi}IL-10$^+$	7	27.5	13.3	5.03	**0.0006**	**0.0023**	0.4330
	CD19$^+$CD27$^+$IL-10$^+$	7	20.8	9.22	3.49	**0.0006**	**0.0006**	0.6200
	CD19$^+$CD24^{hi}CD38^{hi}IL-10$^+$	7	20.2	8.39	3.17	NA	**0.0023**	0.3176

CD40L, CD40 Ligand. Bolded Values Represent significant ***P*** Values. Mann-Whitney U Test.

3.2.4 CpG and CD40L stimulate IL-10$^+$ Breg cells in a time-dependent manner

To determine optimal kinetics for generation of IL-10$^+$ Breg cells, PBMCs were stimulated with 1μg/mL CpG and 2.5μg/mL CD40L for 24, 48, 72 and 96 hours. Flow cytometry analysis revealed CpG and CD40L stimulation induced significant IL-10$^+$ Breg cell frequencies at all investigated time-points compared to respective unstimulated controls, with peak induction of IL-10$^+$ Breg cells observed at 72 hours (all subsets, $P < 0.05$; Figure. 3.2.4.1, A-F and Table 3.2.4.1). ELISA assessment of culture supernatant revealed IL-10 protein production was significantly enhanced in 48 (417pg/mL, $P = 0.0039$), 72 (628pg/mL, $P = 0.0078$) and 96 (978pg/mL, $P = 0.0039$) hour stimulated samples compared to respective unstimulated controls (Figure. 3.2.4.1, G). Moreover, IL-10 protein levels were significantly enhanced in stimulated samples at 72 ($P = 0.0115$) and 96 hours ($P < 0.0001$) compared to 24 hours (Figure. 3.2.4.1, G). To determine whether time-dependent increases in IL-10 protein levels were due to enhanced B cell IL-10 secretion or accumulative addition of IL-10 protein over time, PBMCs were stimulated with CpG and CD40L and media was replenished daily. ELISA analysis revealed the highest quantity of IL-10 secretion by cells occurred between 48 to 72 hours (24 hours: 38.1pg/mL; 48 hours: 97.7pg/mL; 72 hours: 394pg/mL; Figure. 3.2.4.1, H).

Flow cytometry analysis was corroborated by unbiased viSNE analysis on CD19$^+$ B cells, revealing a distinct IL-10$^+$ island that was enhanced within 72 hours stimulated PBMCs (Figure 3.2.4.2, A, black arrow). To investigate the IL-10$^+$ island in further detail, FlowSOM was employed, revealing three distinct IL-10$^+$ MC that were modulated in relation to stimulation duration: MC 6, MC 13 and MC 14 (Figure 3.2.4.2, B-C). Validating flow cytometry data, population abundance of all three IL-10$^+$ B cell MC were increased in a time-dependent manner (Figure 3.2.4.2, D). IL-10 expression from each MC was also enhanced in a time-dependent manner, with MC 13 and MC 14 demonstrating peak IL-10 expression at 72 hours (Figure 3.2.4.2, E). Heatmap analysis revealed the phenotypic classification of MC 6, 13 and 14 to be CD5^{lo}CD24^{lo}, CD5$^+$CD24$^+$ CD38^{hi} and CD27$^+$CD38^{hi} respectively (Figure 3.2.4.2, F).

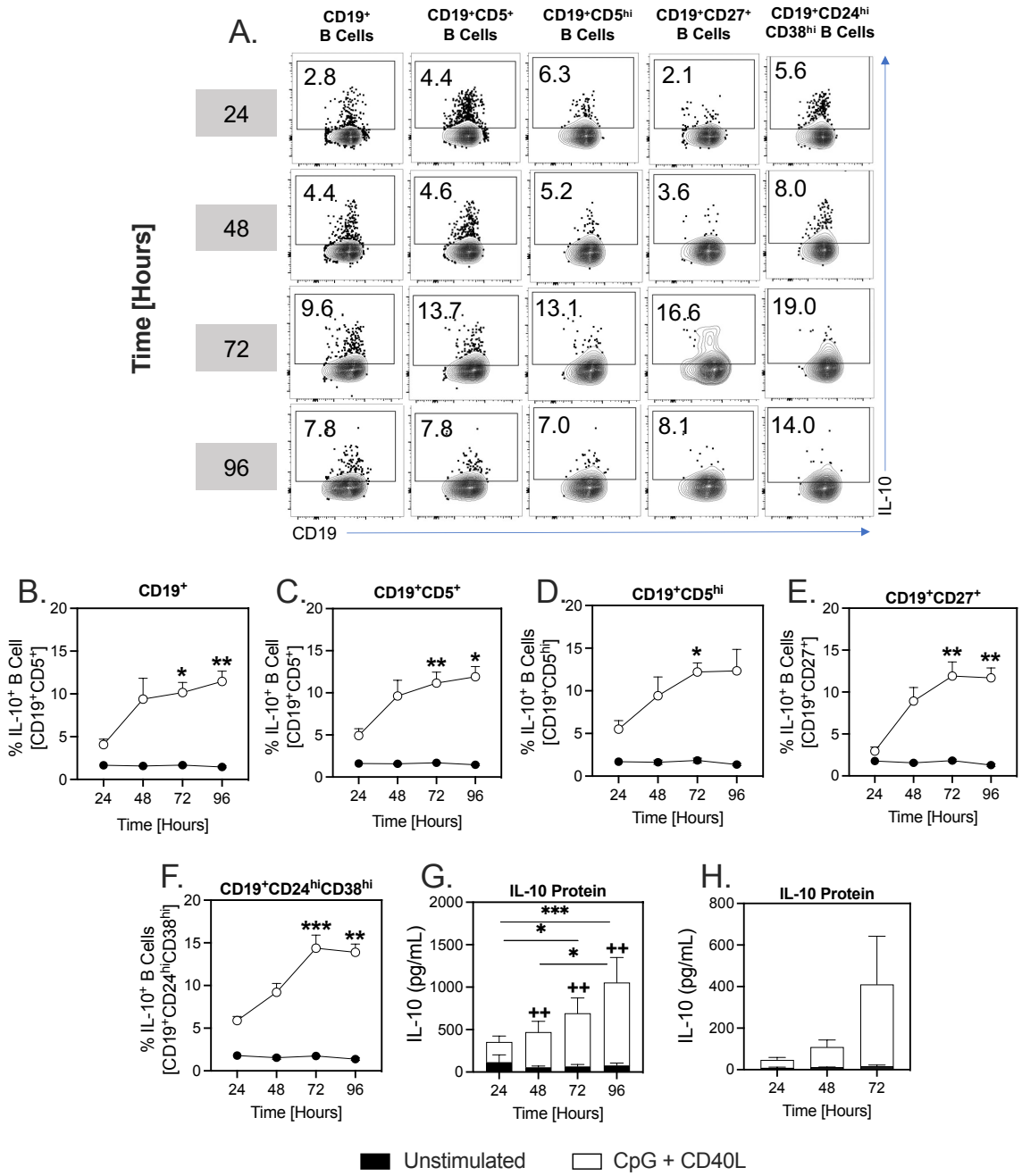


Figure 3.2.4.1 IL-10^{+} B cells are induced by CpG and CD40L stimulation in a time-dependent manner.

A) Flow cytometry representative plots from n=1 NAC illustrating induction of IL-10^{+} Breg cell subsets. Effect of increasing duration of CpG and CD40L stimulation on **B)** CD19^{+}IL-10^{+} **C)** CD5^{+} **D)** CD5^{hi}, **E)** CD27^{+} and **F)** CD24^{hi}CD38^{hi} IL-10^{+} Breg cells. **G)** ELISA quantification of IL-10 levels in culture supernatant. **H)** ELISA quantification of IL-10 in culture supernatant whereby media was replenished daily. Data representative of **B-G)** n=9, **G)** n=7 and **H)** n=3 NAC and presented as mean ±SEM. *, denotes Friedmann Test with Dunn's Multiple Comparisons. +, denotes Wilcoxon-signed pairs test. *P < 0.05, **P < 0.01, ***P < 0.001.

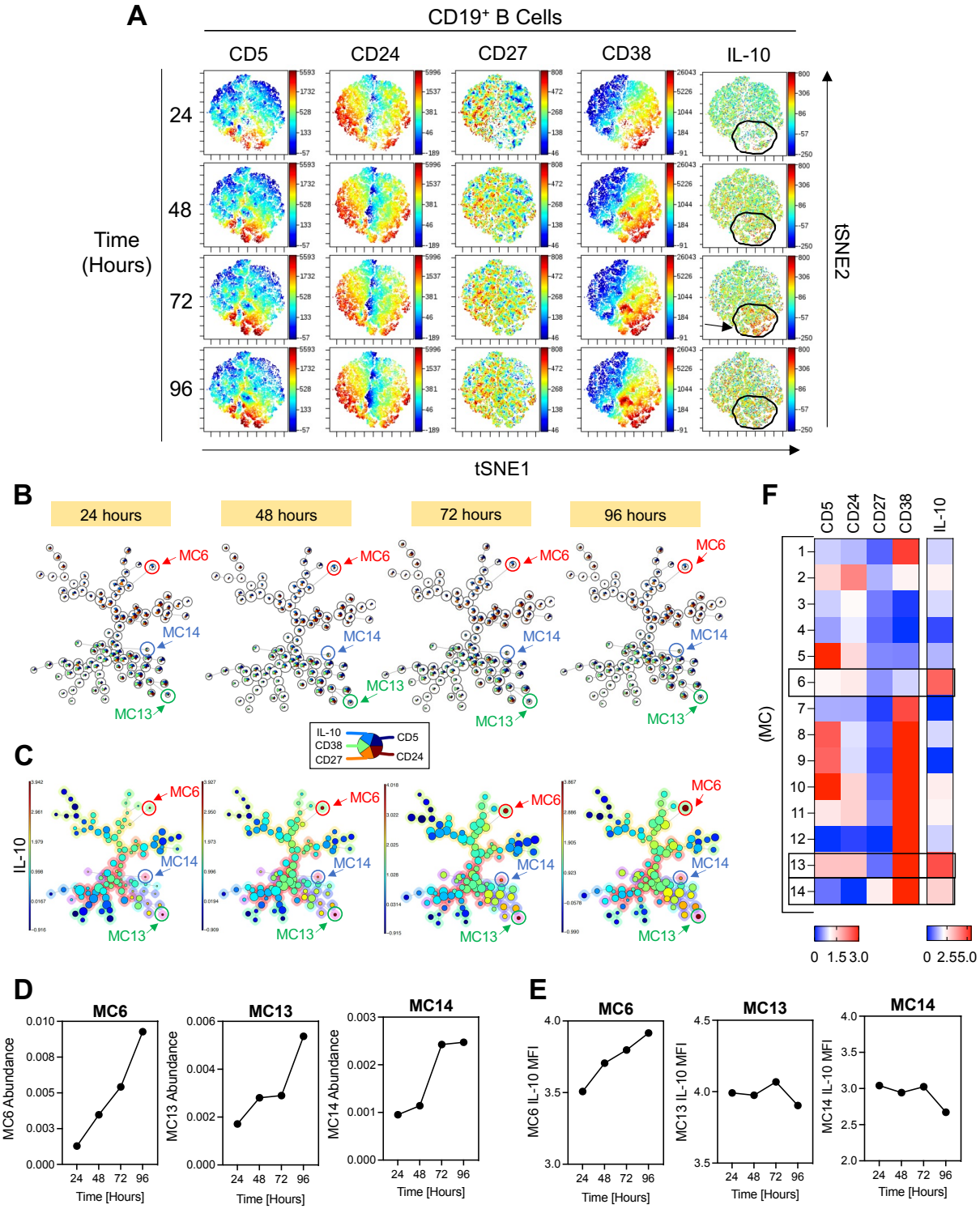


Figure 3.2.4.2 viSNE and FlowSOM confirm IL-10$^+$ Breg cells are induced by CpG and CD40L stimulation in a time-dependent manner.

A) viSNE map of CD19$^+$ B cells with a black arrow highlighting an IL-10 positive island. **B)** FlowSOM star plots and **C)** MST-coloured channels representing IL-10 expression, whereby three distinct MC (6, 13 and 14) are highlighted. **D)** Quantification of population abundance and **E)** IL-10 MFI for MC 6, MC 13, and MC 14. **F)** Heatmap of 72-hour stimulated PBMCs, whereby MC 6, 13 and 14 are highlighted. Data representative of n=3 concatenated FCS files per condition. MC, metacluster; MFI, mean fluorescent intensity.

Table 3.2.4.1 IL-10$^+$ Breg Subsets are induced by CpG and CD40L stimulation in a time-dependent manner.

Time In Culture (hours)	Culture Conditions	B Cell Subset	Raw				*P* value vs relative unstimulated[1]	*P* value vs 24 hours[2]
			n	mean	SD	SEM		
24	Unstimulated	CD19$^+$IL-10$^+$	9	1.66	0.27	0.09	NA	NA
		CD19$^+$CD5$^+$IL-10$^+$	9	1.61	0.26	0.09	NA	NA
		CD19$^+$CD5^{hi}IL-10$^+$	9	1.69	0.23	0.08	NA	NA
		CD19$^+$CD27$^+$IL-10$^+$	9	1.78	0.16	0.05	NA	NA
		CD19$^+$CD24^{hi}CD38^{hi}IL-10$^+$	9	1.79	0.21	0.07	NA	NA
	CpG/CD40L	CD19$^+$IL-10$^+$	9	4.07	1.92	0.64	**0.0117**	NA
		CD19$^+$CD5$^+$IL-10$^+$	9	4.93	2.45	0.82	**0.0078**	NA
		CD19$^+$CD5^{hi}IL-10$^+$	9	5.51	2.99	1.00	**0.0117**	NA
		CD19$^+$CD27$^+$IL-10$^+$	9	2.96	1.42	0.47	**0.0078**	NA
		CD19$^+$CD24^{hi}CD38^{hi}IL-10$^+$	9	5.89	1.45	0.48	**0.0039**	NA
48	Unstimulated	CD19$^+$IL-10$^+$	9	1.58	0.18	0.06	NA	NA
		CD19$^+$CD5$^+$IL-10$^+$	9	1.57	0.35	0.12	NA	NA
		CD19$^+$CD5^{hi}IL-10$^+$	9	1.63	0.73	0.78	NA	NA
		CD19$^+$CD27$^+$IL-10$^+$	9	1.55	0.42	0.15	NA	NA
		CD19$^+$CD24^{hi}CD38^{hi}IL-10$^+$	9	1.53	0.50	0.17	NA	NA
	CpG/CD40L	CD19$^+$IL-10$^+$	9	9.39	7.31	2.44	**0.0039**	0.1708
		CD19$^+$CD5$^+$IL-10$^+$	9	9.62	5.60	1.87	**0.0039**	0.2677
		CD19$^+$CD5^{hi}IL-10$^+$	9	9.43	6.62	2.21	**0.0078**	>0.9999
		CD19$^+$CD27$^+$IL-10$^+$	9	8.92	4.88	1.63	**0.0039**	0.0635
		CD19$^+$CD24^{hi}CD38^{hi}IL-10$^+$	9	9.20	3.13	1.04	**0.0039**	0.6021
72	Unstimulated	CD19$^+$IL-10$^+$	9	1.67	0.28	0.09	NA	NA
		CD19$^+$CD5$^+$IL-10$^+$	9	1.69	0.18	0.06	NA	NA
		CD19$^+$CD5^{hi}IL-10$^+$	9	1.84	0.82	0.27	NA	NA
		CD19$^+$CD27$^+$IL-10$^+$	9	1.83	0.49	0.16	NA	NA
		CD19$^+$CD24^{hi}CD38^{hi}IL-10$^+$	9	1.75	0.12	0.04	NA	NA
	CpG/CD40L	CD19$^+$IL-10$^+$	9	10.20	3.55	1.18	**0.0039**	**0.0209**
		CD19$^+$CD5$^+$IL-10$^+$	9	11.20	3.92	1.31	**0.0039**	**0.0061**
		CD19$^+$CD5^{hi}IL-10$^+$	9	12.20	3.21	1.07	**0.0039**	**0.0370**
		CD19$^+$CD27$^+$IL-10$^+$	9	11.90	5.08	1.69	**0.0039**	**0.0061**
		CD19$^+$CD24^{hi}CD38^{hi}IL-10$^+$	9	14.40	4.62	1.54	**0.0039**	**0.0002**
96	Unstimulated	CD19$^+$IL-10$^+$	9	1.47	0.31	0.10	NA	NA
		CD19$^+$CD5$^+$IL-10$^+$	9	1.54	0.33	0.11	NA	NA
		CD19$^+$CD5^{hi}IL-10$^+$	9	1.35	0.40	0.13	NA	NA
		CD19$^+$CD27$^+$IL-10$^+$	9	1.29	0.46	0.15	NA	NA
		CD19$^+$CD24^{hi}CD38^{hi}IL-10$^+$	9	1.38	0.44	0.15	NA	NA
	CpG/CD40L	CD19$^+$IL-10$^+$	9	11.5	3.58	1.19	**0.0039**	**0.0061**
		CD19$^+$CD5$^+$IL-10$^+$	9	12.2	3.51	1.17	**0.0039**	**0.0115**
		CD19$^+$CD5^{hi}IL-10$^+$	9	12.30	7.55	2.52	**0.0039**	0.4073
		CD19$^+$CD27$^+$IL-10$^+$	9	11.70	3.56	1.19	**0.0039**	**0.0061**
		CD19$^+$CD24^{hi}CD38^{hi}IL-10$^+$	9	13.90	2.93	0.98	**0.0039**	**0.0061**

Bolded Values Represent significant ***P*** Values. [1]Wilcoxon Test and [2]Friedman Test with Dunn's Multiple Comparison.

3.2.5 Validation of IL-10$^+$ Breg Culture Model Conditions

To validate the comparability of PBMCs and enriched B cells for immunophenotyping IL-10$^+$ Breg cells, autologous enriched CD19$^+$ B cells and PBMCs were stimulated with 1μg/mL CpG and 2.5μg/mL CD40L and evaluated by multi-parametric flow-cytometry. CpG and CD40L stimulation induced significant IL-10$^+$ Breg cells in both enriched B cells and PBMCs (all, $P < 0.001$; Figure 3.2.5.1, A, and Table 3.2.5.1). Importantly, no significant differences in any IL-10$^+$ Breg cell subset frequencies were observed between autologous enriched B cells and PBMCs following stimulation (all, $P > 0.05$). In line with these results, ELISA analysis revealed IL-10 protein levels in cell culture supernatant were significantly induced by CpG and CD40L stimulation (both, $P < 0.01$) and comparable between PBMC and enriched B cells ($P = 0.0781$; Figure 3.2.5.1 B).

To validate the use of cryopreserved PBMCs to investigate IL-10$^+$ Breg cells, cell surface and intracellular marker expression was assessed on autologous fresh and cryopreserved PBMC samples following 1μg/mL CpG and 2.5μg/mL CD40L stimulation by multi-parametric flow-cytometry (Figure 3.2.5.2, A). Fresh PBMCs were defined as those cultured immediately following PBMC isolation and cryopreserved PBMCs were defined as those stored in liquid nitrogen for greater than 7 days before thawing and culture set-up. B cell expression of CD1d, CD5, CD24, CD25, CD27, CD71, CD73, TIM-1 and intracellular IL-10 expression were not significantly affected by the cryopreservation process in either unstimulated or CpG and CD40L stimulated samples (all, $P > 0.05$, Figure 3.2.5.2, B-C and Table 3.2.5.2). Although B cell CD38 expression was downregulated following cryopreservation in CpG and CD40L stimulated samples ($P = 0.0312$), frequencies of all IL-10$^+$ Breg cell subsets, including CD24^{hi}CD38^{hi}IL-10$^+$ T1/2 B cells, were comparable between autologous fresh and cryopreserved PBMC samples (all subsets, $P > 0.05$; Figure 3.2.5.2, D and Table 3.2.5.3). ELISA quantification of cell culture supernatant confirmed IL-10 protein in cultured supernatant was not significantly different between cryopreserved and fresh PBMC samples ($P = 0.8438$,

Figure 3.2.5.2, E). To combat the dysregulation observed in B cell CD38 expression and ensure comparability across experiments, all experiments hereafter in this thesis were performed utilising cryopreserved PBMCs.

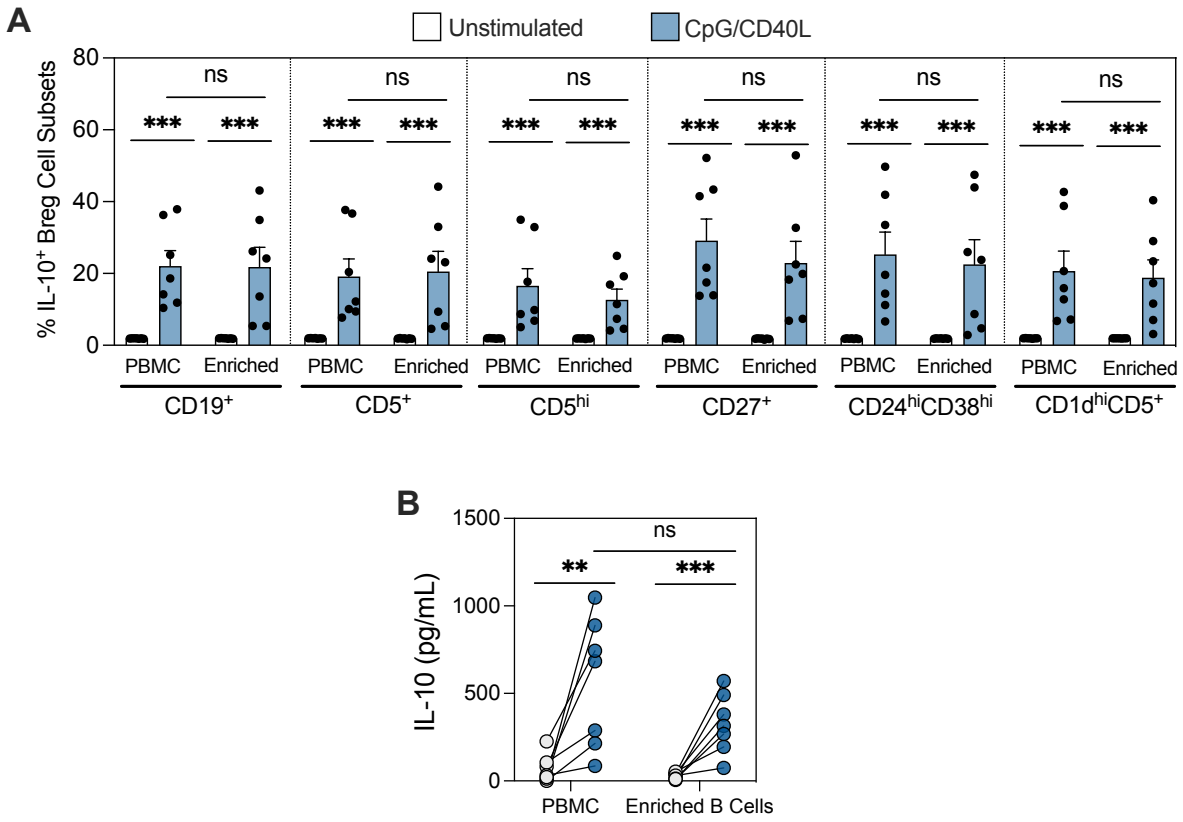


Figure 3.2.5.1 Comparison of IL-10$^+$ Breg Subsets in autologous PBMC and enriched CD19$^+$ B cells

A) Flow cytometry evaluation of IL-10$^+$ Breg cell subsets in PBMC and enriched CD19$^+$ B Cells following CpG and CD40L stimulation. B) IL-10 protein levels in culture supernatants as measured by ELISA. Data representative of n=7 NAC and presented as mean ±SEM. *, detonates significance between unstimulated and CpG/CD40L stimulated samples, Mann Whitney Test. ns, detonates significance between paired enriched B cells and PBMC samples, Wilcoxon paired signed-rank test. **P < 0.01, ***P < 0.001.

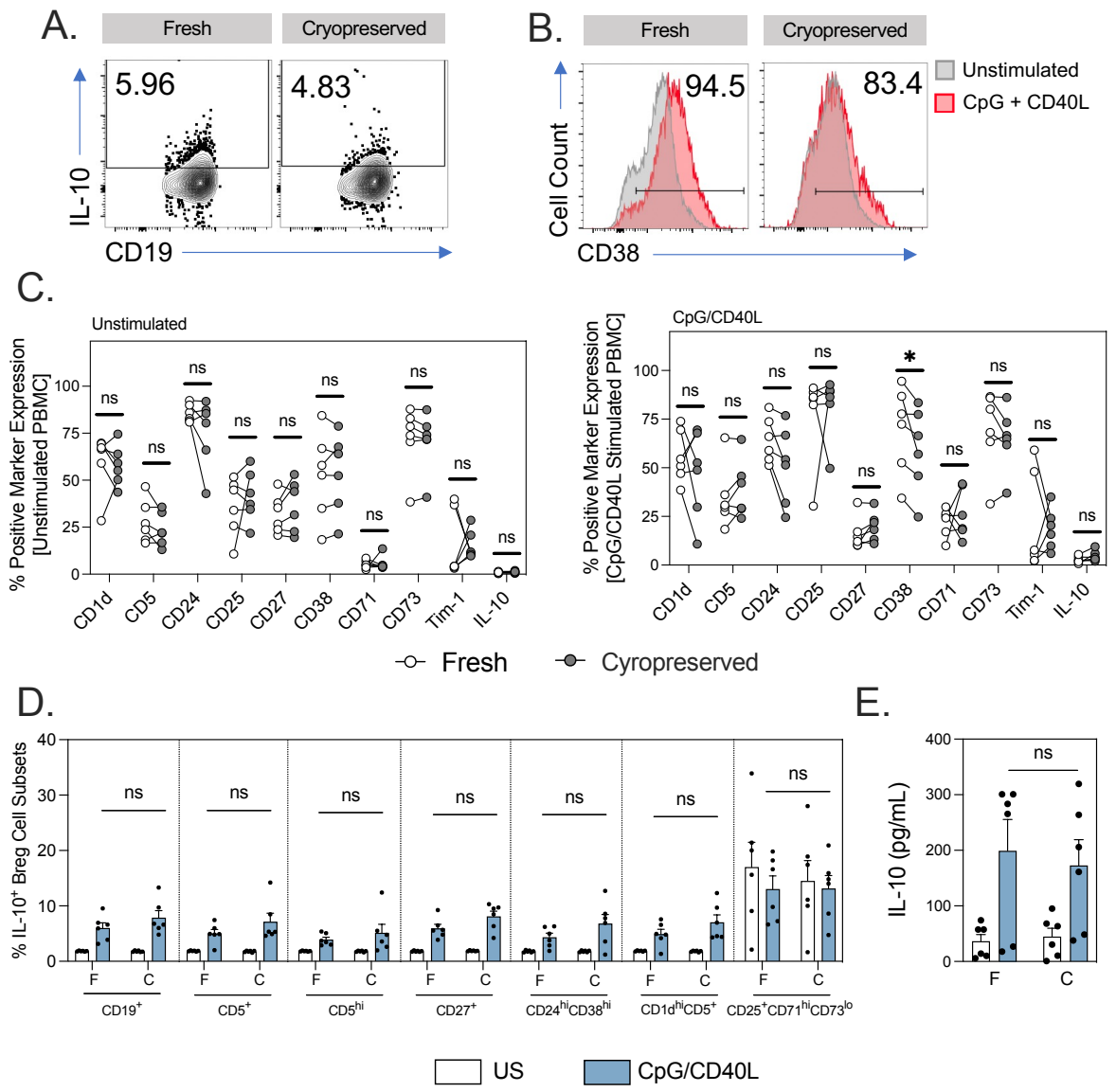


Figure 3.2.5.2 B Cell marker expression in fresh and cryopreserved PBMC samples.

Representative flow cytometry plots from n=1 NAC illustrating A) IL-10$^+$ B cell frequencies and B) CD38 expression on CD19$^+$ B cells. Flow cytometric analysis of C) marker expression on unstimulated and CpG/CD40L treated samples and D) IL-10$^+$ Breg subset expression. E) ELISA analysis of IL-10 protein levels in culture supernatant. Data representative of n=6 NAC. *P < 0.05, Wilcoxon paired signed-rank test. F, Fresh; C, Cryopreserved. PBMC, peripheral blood mononuclear cells.

Table 0.1 Comparison of IL-10$^+$ Breg Subsets in autologous PBMC and enriched CD19$^+$ B cell samples

IL-10$^+$ Breg Subsets	PBMC				Enriched B Cell				*P* value PBMC v. Enriched B Cell[1]	*P* value US v. CpG/CD40L [PBMC][2]	*P* value US v. CpG/CD40L [Enriched B Cell][2]
	n	mean	SD	SEM	n	mean	SD	SEM			
Unstimulated											
CD19$^+$IL-10$^+$	7	1.89	0.07	0.02	7	1.92	0.08	0.03	0.3438	NA	NA
CD19$^+$CD5$^+$IL-10$^+$	7	1.93	0.06	0.02	7	1.88	0.11	0.04	0.2188	NA	NA
CD19$^+$CD5^{hi}IL-10$^+$	7	1.94	0.05	0.02	7	1.89	0.07	0.02	0.3125	NA	NA
CD19$^+$CD27$^+$IL-10$^+$	7	1.90	0.06	0.02	7	1.82	0.14	0.05	0.4062	NA	NA
CD19$^+$CD24^{hi}CD38^{hi}IL-10$^+$	7	1.86	0.09	0.03	7	1.90	0.07	0.03	0.2031	NA	NA
CD19$^+$CD1d^{hi}CD5$^+$IL-10$^+$	7	1.94	0.07	0.03	7	1.94	0.02	0.01	0.9375	NA	NA
CpG/CD40L Stimulated											
CD19$^+$IL-10$^+$	7	22.10	11.40	4.30	7	21.80	14.50	5.47	>0.9999	**0.0006**	**0.0006**
CD19$^+$CD5$^+$IL-10$^+$	7	19.20	13.00	4.90	7	20.50	15.00	5.66	>0.9999	**0.0006**	**0.0006**
CD19$^+$CD5^{hi}IL-10$^+$	7	16.60	12.50	4.74	7	12.70	7.94	3.00	0.2188	**0.0006**	**0.0006**
CD19$^+$CD27$^+$IL-10$^+$	7	29.10	16.10	6.07	7	22.90	15.90	6.03	0.2969	**0.0006**	**0.0006**
CD19$^+$CD24^{hi}CD38^{hi}IL-10$^+$	7	25.30	16.50	6.24	7	22.50	18.20	6.89	0.8125	**0.0006**	**0.0006**
CD19$^+$CD1d^{hi}CD5$^+$IL-10$^+$	7	20.70	14.60	5.50	7	18.80	13.10	4.95	0.5781	**0.0006**	**0.0006**

Bolded Values Represent significant ***P*** Values. [1]Wilcoxon paired signed-rank test, [2]Mann Whitney test. US, unstimulated; PBMC, peripheral blood mononuclear cells.

Table 0.2 B Marker Expression Following Stimulation with CD40L and CpG in fresh and cryopreserved PBMC samples.

B Cell Surface Marker Expression	Fresh				Frozen				*P* value Fresh v. Frozen
	n	mean	SD	SEM	n	mean	SD	SEM	
Unstimulated									
CD1d	6	60.07	15.98	6.53	6	57.75	10.80	4.41	0.6875
CD5	6	27.92	11.38	4.65	6	23.73	8.86	3.62	0.4062
CD24	6	85.65	4.70	1.92	6	75.72	18.37	7.50	0.3125
CD25	6	35.73	15.53	6.34	6	41.60	13.65	5.57	0.8438
CD27	6	32.07	10.24	4.18	6	36.32	13.75	5.61	0.4375
CD38	6	52.55	23.34	9.53	6	53.68	21.12	8.62	0.8438
CD71	6	5.23	2.20	0.88	6	5.71	3.84	1.57	0.6875
CD73	6	72.00	17.59	7.18	6	70.75	15.78	6.44	0.4375
Tim-1	6	15.38	17.86	7.29	6	15.46	7.65	3.12	>0.9999
IL-10	6	0.89	0.43	0.18	6	1.14	0.55	0.22	0.8438
CpG/CD40L Stimulated									
CD1d	6	55.73	13.49	5.51	6	46.55	22.71	9.27	0.4375
CD5	6	34.65	16.14	6.59	6	39.13	15.03	6.14	0.4375
CD24	6	64.22	11.54	4.72	6	50.92	19.95	8.14	0.0625
CD25	6	77.37	23.24	9.49	6	81.77	16.05	6.55	0.8438
CD27	6	16.05	8.31	3.39	6	19.83	7.48	3.05	0.1562
CD38	6	69.72	22.42	9.15	6	59.15	21.64	8.83	**0.0312**
CD71	6	22.14	7.30	2.98	6	26.18	12.65	5.17	0.5625
CD73	6	69.25	20.80	8.49	6	64.95	16.19	6.61	0.3125
Tim-1	6	20.80	25.69	10.49	6	18.51	10.43	4.26	0.8438
IL-10	6	2.82	1.70	0.70	6	4.60	2.70	1.10	0.1562

Bolded Values Represent significant ***P*** Values. PBMC, peripheral blood mononuclear cells. Wilcoxon paired-signed rank test.

Table 0.3 IL-10$^+$ Breg Cell Expression Following Stimulation with CD40L and CpG in fresh and cryopreserved PBMC samples.

Cell Surface Marker Expression	Fresh				Frozen				*P* value Fresh v Frozen
	n	mean	SD	SEM	n	mean	SD	SEM	
Unstimulated									
CD19$^+$IL-10$^+$	6	1.84	0.07	0.03	6	1.81	0.13	0.05	NA
CD19$^+$CD5$^+$IL-10$^+$	6	1.86	0.08	0.03	6	1.78	0.14	0.06	NA
CD19$^+$CD5^{hi}IL-10$^+$	6	1.84	0.08	0.03	6	1.80	0.12	0.05	NA
CD19$^+$CD27$^+$IL-10$^+$	6	1.82	0.10	0.04	6	1.89	0.08	0.03	NA
CD19$^+$CD1d^{hi}CD5+	6	1.86	0.09	0.03	6	1.80	0.20	0.05	NA
CD19$^+$CD24^{hi}CD38^{hi}IL-10$^+$	6	1.81	0.17	0.07	6	1.80	0.14	0.06	NA
CD19$^+$CD25$^+$CD71^{hi}CD73^{lo}	6	17.02	10.95	4.47	6	14.51	9.03	3.69	NA
CpG/CD40L Stimulated									
CD19$^+$IL-10$^+$	6	6.01	2.30	0.94	6	7.88	3.11	1.30	0.1562
CD19$^+$CD5$^+$IL-10$^+$	6	5.03	1.78	0.73	6	7.15	3.73	1.52	0.1562
CD19$^+$CD5^{hi}IL-10$^+$	6	3.92	1.06	0.43	6	5.15	3.79	1.56	>0.9999
CD19$^+$CD27$^+$IL-10$^+$	6	5.95	1.84	0.75	6	8.1	2.36	0.96	0.0938
CD19$^+$CD1d^{hi}CD5+	6	4.91	2.15	0.88	6	7.04	3.32	1.37	0.3125
CD19$^+$CD24^{hi}CD38^{hi}IL-10$^+$	6	4.34	1.82	0.74	6	6.80	4.02	1.64	0.0625
CD19$^+$CD25$^+$CD71^{hi}CD73^{lo}	6	13.06	5.83	2.38	6	13.17	5.69	2.32	0.8438

Bolded Values Represent significant ***P*** Values. PBMC, peripheral blood mononuclear cells. Wilcoxon paired-signed rank test.

3.2.6 Co-expression of suppressive molecules on IL-10$^+$ Breg Cells

To evaluate additional suppressive molecules which may be induced by 1μg/mL CpG and 2.5μg/mL CD40L stimulation and delineate their potential relationship between IL-10$^+$ Breg cells, PBMCs were stimulated and assessed by multi-parametric flow-cytometry. CpG and CD40L stimulation significantly induced PD-L1, CD80 and CD86 expression on all B cell subsets and PD-1 expression in overall CD19$^+$ B cells and transitional CD24^{hi}CD38^{hi} B cells compared to respective unstimulated controls (all, $P < 0.05$, Figure 3.2.6.1, A-F and Table 3.2.6.1). Moreover, CpG and CD40L stimulation significantly enhanced B cell surface expression of TIM-1 on CD5$^+$ ($P = 0.0064$), CD5^{hi} ($P = 0.0062$) and transitional CD24^{hi}CD38^{hi} B cells ($P = 0.0138$; Figure 3.2.6.1, G). Although PD-L1 and PD-1 expression demonstrated a trend of enhancement on IL-10$^+$ B cells compared to IL-10$^-$ B cells, no significant differences were observed due to the low sample number (Figure 3.2.6.1, H-I). CD80 expression was not preferential on either IL-10$^-$ B cells or IL-10$^+$ Breg cells (Figure 3.2.6.1, J). On the other hand, CD86 expression was significantly enhanced on activated CD5$^+$ (10% increase, $P = 0.0078$) and CD5^{hi} (13% increase, $P = 0.0078$) IL-10$^+$ Breg cells compared to their respective IL-10$^-$ B cell counterparts (Figure 3.2.6.1, K). TIM-1 expression was significantly enhanced on CD19$^+$IL-10$^+$ (27% increase, $P = < 0.0001$), CD5$^+$ (47% increase, $P = <0.0001$) and CD5^{hi} (38% increase, $P = 0.0008$) B cells compared to respective IL-10$^-$ B cells, demonstrating the existence of dual-positive IL-10$^+$TIM-1$^+$ Breg cells (Figure 3.2.6.1, L).

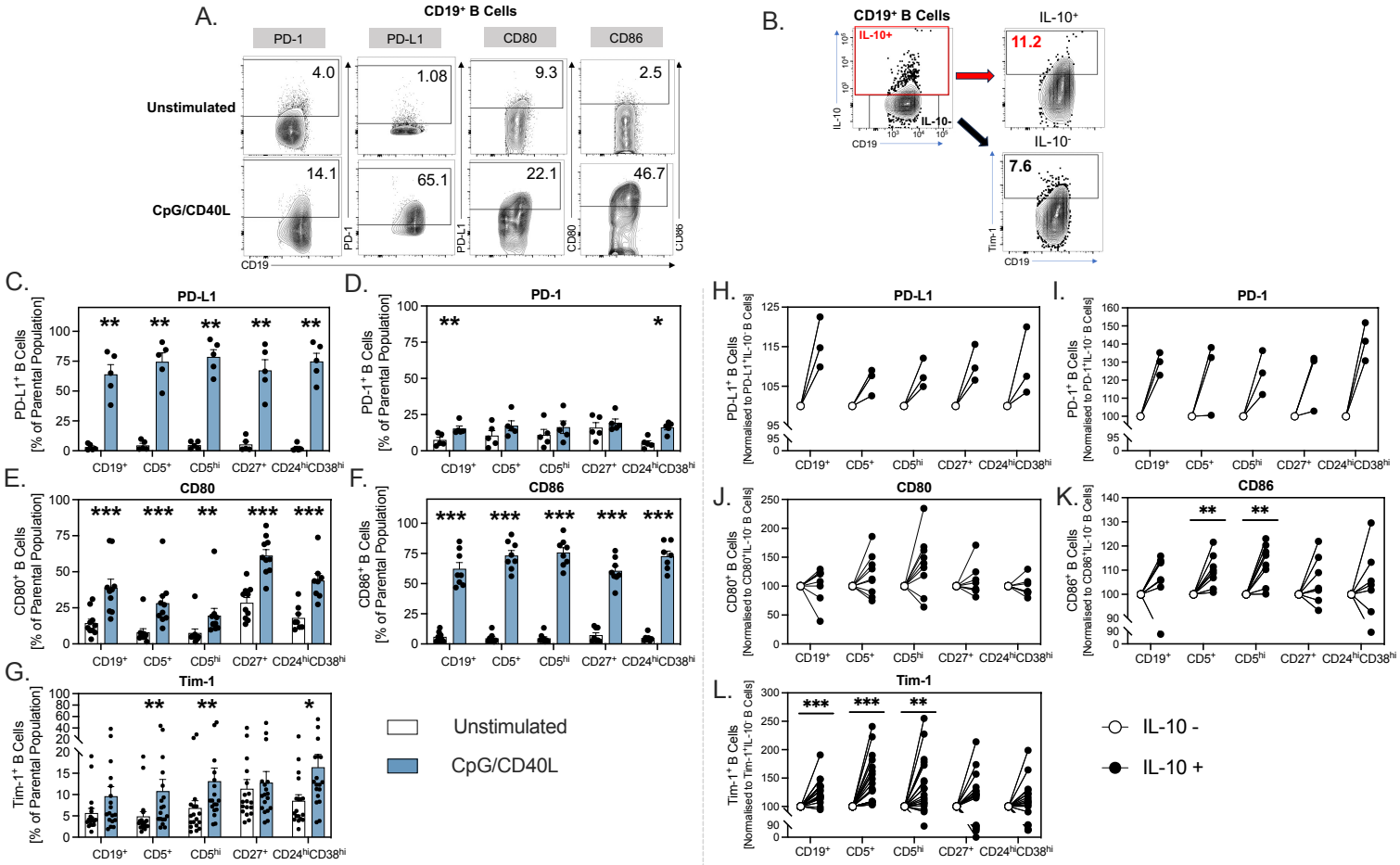


Figure 3.2.6.1 CpG and CD40L stimulation induces PD-L1, PD-1, CD80, CD86 and TIM-1 expression on B cells.

Representative flow-cytometry plots demonstrating **A)** PD-1$^+$, PD-L1$^+$, CD80$^+$ and CD86$^+$ B cells in unstimulated and CpG/CD40L stimulated PBMCs and **B)** TIM-1$^+$ B cells in CpG/CD40L stimulated PBMCs. Effect of CpG/CD40L stimulation on **C)** PD-L1$^+$, **D)** PD-1$^+$, **E)** CD80$^+$, **F)** CD86$^+$ and **G)** TIM-1$^+$ B cell frequencies, and **H)** PD-L1, **I)** PD-1, **J)** CD80, **K)** CD86 and **L)** TIM-1 expression on IL-10$^-$ and IL-10$^+$ B cell subsets. Data representative of **C-D)** n=5, **E)** n=10, **F and K)** n=8, **G and L)** n=18, **H-I)** n=3, **J)** n=9 and is represented as mean ± SEM. Whitney Test utilised in **C-G)** and Wilcoxon paired signed-rank test utilised in **H-L)**. *P < 0.05, **P < 0.01, ***P < 0.001.

Next, efforts were made to immunophenotype TGFβ1$^+$ and IL-35$^+$ Breg cells and ascertain whether they were contained within IL-10$^+$ Breg cell subsets or represented independent Breg phenotypes. Flow cytometry revealed CpG and CD40L induced significant TGFβ1 and IL-35 expression from all investigated B cells subset (all, $P < 0.001$; Figure 3.2.6.2, A-E, and Table 3.2.6.2). Although trends indicated that TGFβ1 and IL-35 were enhanced on IL-10$^+$ B cells compared to IL-10$^-$ B cells, no significance was reached, and this relationship was not mutually exclusive. Thus, flow cytometry data revealed the presence of TGFβ1$^+$IL-10$^-$ and IL-35$^+$IL-10$^-$ B cells in addition to dual positive TGFβ1$^+$IL-10$^+$ and IL-35$^+$IL-10$^+$ Breg cells within human peripheral blood. To interrogate these Breg phenotypes further, unbiased computational algorithms were employed to perform deep immunophenotyping of CD19$^+$ B cells. viSNE analysis corroborated flow-cytometry findings through revealing CD19$^+$ B cells were enhanced in IL-10, IL-12p35, Ebi3 and TGFβ1 expression following CpG and CD40L stimulation (Figure 3.2.6.2, F). Although the expression of each marker was not mutually exclusive with one another, three distinct islands which co-expressed IL-10, IL-12p35, Ebi3 and TGFβ1 were identified (Figure 3.2.6.2, F, black islands). SPADE analysis, which connects hierarchically clustered cells of similar phenotype allowing for rapid visualisation of cell phenotypes, was performed independently of viSNE analysis as another method through which to validate the presence of triple positive IL-10$^+$IL-35$^+$TGFβ1$^+$ Breg cells. SPADE analysis corroborated previous observations through revealing three clusters of CD19$^+$ B cells which co-expressed IL-10, IL-12p35, Ebi3 and TGF-β1 (Figure 3.2.6.2, H, black clusters).

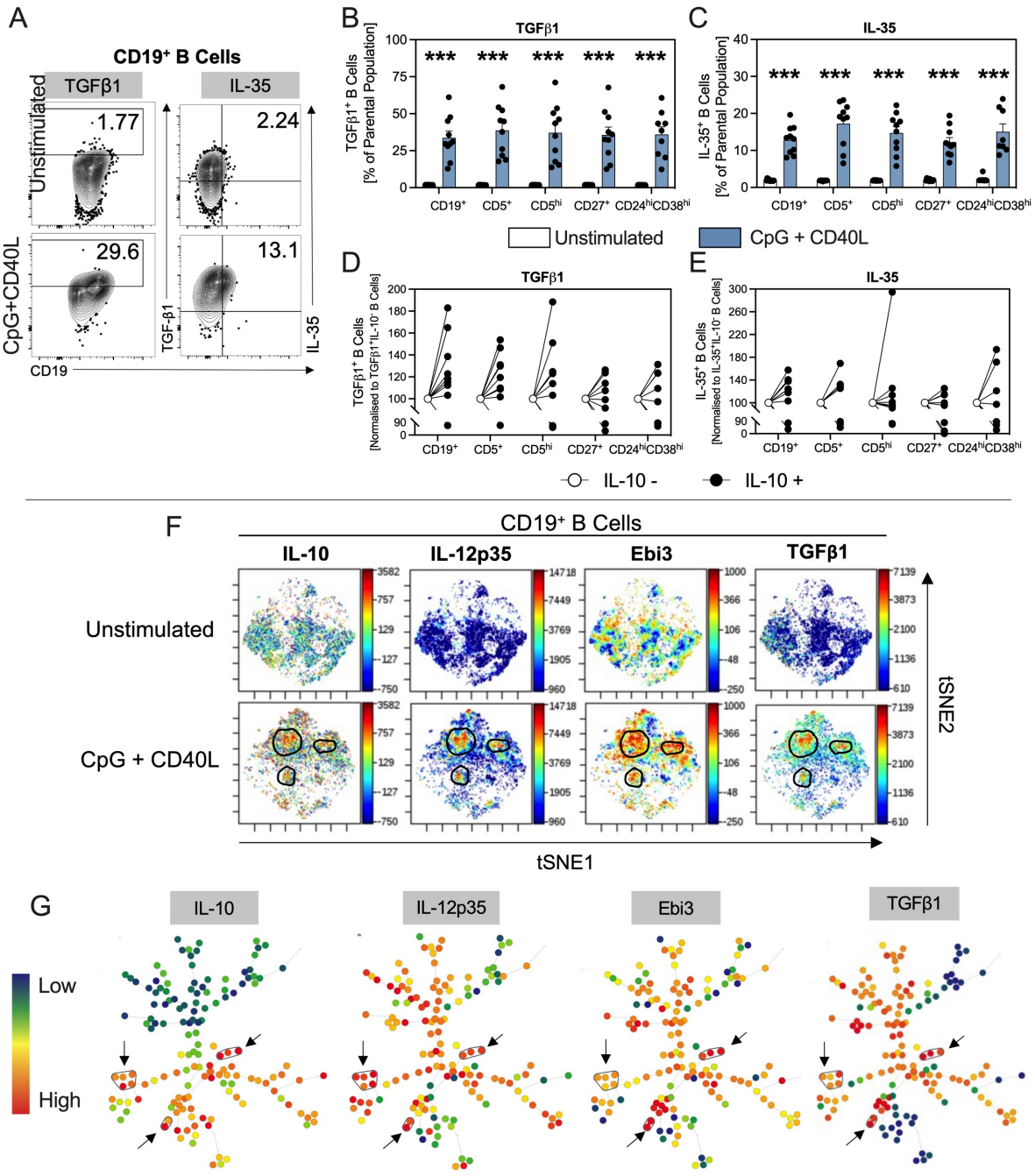


Figure 3.2.6.2 TGF-β1 and IL-35 expression is induced on B cells by CpG and CD40L and co-expressed with IL-10.

A) Representative flow-cytometry plots demonstrating TGFβ1$^+$ and IL-35$^+$ B cells frequencies. Flow-cytometry data demonstrating **B)** TGF-β1$^+$ and **C)** IL-35$^+$ B cells in unstimulated and CpG/CD40L stimulated PBMCs, and **D)** TGFβ1$^+$ and **E)** IL-35$^+$ expression on IL-10$^-$ and IL-10$^+$ B cell subsets. **F)** viSNE analysis of CD19$^+$ B cells. Black islands represent CD19$^+$ B cells co-expressing TGF-β1, Ebi3, IL-12p35 and IL-10. **G)** SPADE tree demonstrating three clusters of CD19$^+$ B cells co-expressing TGF-β1, Ebi3, IL-12p35 and IL-10. Data representative of n=10 non-atopic controls [N.B. **D-E)**, n=9]. Mann Whitney Test (**B-C)** and Wilcoxon paired signed-rank test (**D-E)**. ***$P < 0.001$.

Table 3.2.6.1 PD-L1, PD-1, CD80, CD86 and TIM-1 expression on B cells induced by CpG and CD40L stimulation.

	Culture Conditions	B Cell Subset	Raw				Normalised to IL-10⁻ B cells			*P* value Unstimulated vs CpG/CD40L[1]	*P* value IL-10⁻ vs IL-10⁺[2]
			n	mean	SD	SEM	mean	SD	SEM		
PD-L1	Unstimulated	$CD19^+PD\text{-}L1^+$	5	3.01	2.55	1.14	NA	NA	NA	NA	NA
		$CD19^+CD5^+PD\text{-}L1^+$	5	4.47	3.89	1.74	NA	NA	NA	NA	NA
		$CD19^+CD5^{hi}PD\text{-}L1^+$	5	4.66	3.04	1.36	NA	NA	NA	NA	NA
		$CD19^+CD27^+PD\text{-}L1^+$	5	5.24	5.63	2.52	NA	NA	NA	NA	NA
		$CD19^+CD24^{hi}CD38^{hi}PD\text{-}L1^+$	5	2.44	2.89	1.29	NA	NA	NA	NA	NA
	CpG/CD40L	$CD19^+PD\text{-}L1^+$	5	64.0	18.3	8.19	NA	NA	NA	**0.0079**	NA
		$CD19^+CD5^+PD\text{-}L1^+$	5	74.4	16.9	7.55	NA	NA	NA	**0.0079**	NA
		$CD19^+CD5^{hi}PD\text{-}L1^+$	5	78.6	13.5	6.06	NA	NA	NA	**0.0079**	NA
		$CD19^+CD27^+PD\text{-}L1^+$	5	67.3	20.0	8.93	NA	NA	NA	**0.0079**	NA
		$CD19^+CD24^{hi}CD38^{hi}PD\text{-}L1^+$	5	74.7	15.4	6.89	NA	NA	NA	**0.0079**	NA
	CpG/CD40L (IL-10⁻ Cells)	$CD19^+PD\text{-}L1^+$	3	59.5	21.5	12.4	100	100	100	NA	NA
		$CD19^+CD5^+PD\text{-}L1^{+\,-}$	3	71.1	20.0	11.5	100	100	100	NA	NA
		$CD19^+CD5^{hi}PD\text{-}L1^+$	3	75.5	15.0	8.64	100	100	100	NA	NA
		$CD19^+CD27^+PD\text{-}L1^+$	3	61.6	22.7	13.1	100	100	100	NA	NA
		$CD19^+CD24^{hi}CD38^{hi}PD\text{-}L1^+$	3	71.5	20.7	12.0	100	100	100	NA	NA
	CpG/CD40L (IL-10⁺ Cells)	$CD19^+PD\text{-}L1^+$	3	67.9	21.4	12.4	116	6.38	3.68	NA	0.2500
		$CD19^+CD5^+PD\text{-}L1^+$	3	75.5	21.1	12.2	106	3.38	1.95	NA	0.2500
		$CD19^+CD5^{hi}PD\text{-}L1^+$	3	81.5	16.2	9.33	108	3.67	2.12	NA	0.2500
		$CD19^+CD27^+PD\text{-}L1^+$	3	67.4	22.6	13.1	111	4.59	2.65	NA	0.2500
		$CD19^+CD24^{hi}CD38^{hi}PD\text{-}L1^+$	3	77.7	17.3	9.99	110	8.59	4.96	NA	0.2500
PD-1	Unstimulated	$CD19^+PD\text{-}1^+$	5	7.49	4.15	1.86	NA	NA	NA	NA	NA
		$CD19^+CD5^+PD\text{-}1^+$	5	10.5	7.75	3.46	NA	NA	NA	NA	NA
		$CD19^+CD5^{hi}PD\text{-}1^+$	5	11.0	8.52	3.81	NA	NA	NA	NA	NA
		$CD19^+CD27^+PD\text{-}1^+$	5	15.9	7.88	3.53	NA	NA	NA	NA	NA
		$CD19^+CD24^{hi}CD38^{hi}PD\text{-}1^+$	5	5.38	3.56	1.59	NA	NA	NA	NA	NA
	CpG/CD40L	$CD19^+PD\text{-}1^+$	5	15.3	4.13	1.85	NA	NA	NA	**0.0079**	NA
		$CD19^+CD5^+PD\text{-}1^+$	5	17.3	7.70	3.44	NA	NA	NA	0.2222	NA
		$CD19^+CD5^{hi}PD\text{-}1^+$	5	16.3	9.65	4.32	NA	NA	NA	0.4206	NA
		$CD19^+CD27^+PD\text{-}1^+$	5	19.3	5.90	2.64	NA	NA	NA	0.4206	NA
		$CD19^+CD24^{hi}CD38^{hi}PD\text{-}1^+$	5	16.1	3.75	1.68	NA	NA	NA	**0.0159**	NA
	CpG/CD40L (IL-10⁻ Cells)	$CD19^+PD\text{-}1^+$	3	15.5	5.03	2.91	100	100	100	NA	NA
		$CD19^+CD5^+PD\text{-}1^+$	3	19.8	8.88	5.13	100	100	100	NA	NA
		$CD19^+CD5^{hi}PD\text{-}1^+$	3	20.7	9.07	5.24	100	100	100	NA	NA
		$CD19^+CD27^+PD\text{-}1^+$	3	21.4	6.58	3.80	100	100	100	NA	NA
		$CD19^+CD24^{hi}CD38^{hi}PD\text{-}1^+$	3	16.1	2.55	1.47	100	100	100	NA	NA
	CpG/CD40L (IL-10⁺ Cells)	$CD19^+PD\text{-}1^+$	3	20.2	7.47	4.31	129	6.26	3.62	NA	0.2500
		$CD19^+CD5^+PD\text{-}1^+$	3	24.9	13.9	8.03	124	20.2	11.7	NA	0.2500
		$CD19^+CD5^{hi}PD\text{-}1^+$	3	25.5	11.0	6.37	124	12.1	7.01	NA	0.2500
		$CD19^+CD27^+PD\text{-}1^+$	3	26.4	10.3	5.96	122	16.5	9.5	NA	0.2500
		$CD19^+CD24^{hi}CD38^{hi}PD\text{-}1^+$	3	22.8	3.65	2.11	141	10.5	6.08	NA	0.2500
CD80	Unstimulated	$CD19^+CD80^+$	10	14.4	8.74	2.77	NA	NA	NA	NA	NA
		$CD19^+CD5^+CD80^+$	10	7.93	8.29	2.62	NA	NA	NA	NA	NA
		$CD19^+CD5^{hi}CD80^+$	10	7.52	9.06	2.86	NA	NA	NA	NA	NA
		$CD19^+CD27^+CD80^+$	10	28.5	11.5	3.62	NA	NA	NA	NA	NA
		$CD19^+CD24^{hi}CD38^{hi}CD80^+$	9	17.6	7.94	2.65	NA	NA	NA	NA	NA
	CpG/CD40L	$CD19^+CD80^+$	10	39.0	18.8	5.94	NA	NA	NA	**0.0003**	NA
		$CD19^+CD5^+CD80^+$	10	28./2	16.9	5.34	NA	NA	NA	**0.0005**	NA
		$CD19^+CD5^{hi}CD80^+$	10	19.6	16.1	5.1	NA	NA	NA	**0.0011**	NA

		$CD19^+CD27^+CD80^+$	10	61.2	13.1	4.13	NA	NA	NA	**<0.0001**	NA
		$CD19^+CD24^{hi}CD38^{hi}CD80^+$	8	43.9	14.1	4.97	NA	NA	NA	**0.0003**	NA
	CpG/CD40L (IL-10$^-$ Cells)	$CD19^+CD80^+$	9	35.4	16.7	5.56	100	100	100	NA	NA
		$CD19^+CD5^+CD80^+$	9	28.0	18.5	6.18	100	100	100	NA	NA
		$CD19^+CD5^{hi}CD80^+$	9	19.3	18.0	6.01	100	100	100	NA	NA
		$CD19^+CD27^+CD80^+$	8	61.1	15.3	5.43	100	100	100	NA	NA
		$CD19^+CD24^{hi}CD38^{hi}CD80^+$	8	43.9	14.2	5.01	100	100	100	NA	NA
	CpG/CD40L (IL-10$^+$ Cells)	$CD19^+CD80^+$	9	34.6	13.3	4.44	105	29.2	9.72	NA	0.2500
		$CD19^+CD80^+$Tim-1$^+$	9	29.2	11.2	3.75	119	35.9	12.0	NA	0.1641
		$CD19^+CD5^{hi}CD80^+$	9	22.0	10.7	3.55	138	50.4	16.8	NA	0.0547
		$CD19^+CD27^+CD80^+$	8	65.4	16.3	5.78	109	28.2	9.97	NA	0.6406
		$CD19^+CD24^{hi}CD38^{hi}CD80^+$	8	42.6	14.3	5.07	97.5	15.7	5.55	NA	0.3828
CD86	Unstimulated	$CD19^+CD86^+$	8	5.88	4.12	1.46	NA	NA	NA	NA	NA
		$CD19^+CD5^+CD86^+$	8	4.66	3.86	1.36	NA	NA	NA	NA	NA
		$CD19^+CD5^{hi}CD86^+$	8	4.63	3.80	1.34	NA	NA	NA	NA	NA
		$CD19^+CD27^+CD86^+$	8	7.20	5.71	2.02	NA	NA	NA	NA	NA
		$CD19^+CD24^{hi}CD38^{hi}CD86^+$	7	4.91	2.99	1.13	NA	NA	NA	NA	NA
	CpG/CD40L	$CD19^+CD86^+$	8	62.2	14.8	5.22	NA	NA	NA	**0.0002**	NA
		$CD19^+CD5^+CD86^+$	8	73.3	11.8	4.18	NA	NA	NA	**0.0002**	NA
		$CD19^+CD5^{hi}CD86^+$	8	75.7	11.5	4.07	NA	NA	NA	**0.0002**	NA
		$CD19^+CD27^+CD86^+$	8	60.6	10.9	3.86	NA	NA	NA	**0.0002**	NA
		$CD19^+CD24^{hi}CD38^{hi}CD86^+$	7	72.7	11.4	4.29	NA	NA	NA	**0.0006**	NA
	CpG/CD40L (IL-10$^-$ Cells)	$CD19^+CD86^+$	8	58.5	11.6	4.12	100	100	100	NA	NA
		$CD19^+CD5^+CD86^+$	8	72.2	12.0	4.24	100	100	100	NA	NA
		$CD19^+CD5^{hi}CD86^+$	8	74.7	11.7	4.13	100	100	100	NA	NA
		$CD19^+CD27^+CD86^+$	7	60.7	11.7	4.43	100	100	100	NA	NA
		$CD19^+CD24^{hi}CD38^{hi}CD86^+$	7	72.5	11.6	4.37	100	100	100	NA	NA
	CpG/CD40L (IL-10$^+$ Cells)	$CD19^+CD86^+$	8	61.3	14.3	5.06	105	15.3	5.40	NA	0.1953
		$CD19^+CD5^+CD86^+$	8	79.0	12.2	4.33	110	6.83	2.41	NA	**0.0078**
		$CD19^+CD5^{hi}CD86^+$	8	83.7	10.5	3.7	113	8.22	2.91	NA	**0.0078**
		$CD19^+CD27^+CD86^+$	7	63.9	12.1	4.58	106	10.1	3.82	NA	0.2188
		$CD19^+CD24^{hi}CD38^{hi}CD86^+$	7	75.2	13.3	5.05	104	14.8	5.59	NA	0.5781
TIM-1	Unstimulated	$CD19^+$Tim-1$^+$	18	5.66	4.71	1.11	NA	NA	NA	NA	NA
		$CD19^+CD5^+$Tim-1$^+$	18	4.88	4.82	1.14	NA	NA	NA	NA	NA
		$CD19^+CD5^{hi}$Tim-1$^+$	18	6.85	7.30	1.72	NA	NA	NA	NA	NA
		$CD19^+CD27^+$Tim-1$^+$	18	11.3	9.21	2.17	NA	NA	NA	NA	NA
		$CD19^+CD24^{hi}CD38^{hi}$Tim-1$^+$	18	8.55	6.07	1.43	NA	NA	NA	NA	NA
	CpG/CD40L	$CD19^+$Tim-1$^+$	18	9.61	9.52	2.24	NA	NA	NA	0.1201	NA
		$CD19^+CD5^+$Tim-1$^+$	18	10.8	11.7	2.76	NA	NA	NA	**0.0064**	NA
		$CD19^+CD5^{hi}$Tim-1$^+$	18	13.1	13.1	3.1	NA	NA	NA	**0.0062**	NA
		$CD19^+CD27^+$Tim-1$^+$	18	12.8	11.1	2.61	NA	NA	NA	0.5680	NA
		$CD19^+CD24^{hi}CD38^{hi}$Tim-1$^+$	18	16.4	12.9	3.03	NA	NA	NA	**0.0138**	NA
	CpG/CD40L (IL-10$^-$ Cells)	$CD19^+$Tim-1$^+$	18	9.15	9.08	2.14	100	100	100	NA	NA
		$CD19^+CD5^+$Tim-1	18	10.6	11.6	2.73	100	100	100	NA	NA
		$CD19^+CD5^{hi}$Tim-1$^+$	18	12.9	13.1	3.1	100	100	100	NA	NA
		$CD19^+CD27^+$Tim-1$^+$	18	12.7	10.9	2.58	100	100	100	NA	NA
		$CD19^+CD24^{hi}CD38^{hi}$Tim-1$^+$	18	16.4	12.7	2.98	100	100	100	NA	NA
	CpG/CD40L (IL-10$^+$ Cells)	$CD19^+$Tim-1$^+$	18	11.4	11.8	2.78	127	21.9	5.16	NA	**<0.0001**
		$CD19^+CD5^+$Tim-1$^+$	18	13.5	13.6	3.19	147	41.5	9.79	NA	**<0.0001**
		$CD19^+CD5^{hi}$Tim-1$^+$	18	15.7	14.0	3.3	138	48.1	11.3	NA	**0.0013**
		$CD19^+CD27^+$Tim-1$^+$	18	13.7	13.2	3.11	108	49.6	11.7	NA	0.4683
		$CD19^+CD24^{hi}CD38^{hi}$Tim-1$^+$	18	17.3	13.9	3.27	108	36.9	8.7	NA	0.3692

Bolded values represent significant ***P*** values. [1]Mann Whitney Test and [2]Wilcoxon paired signed-rank test.

Table 3.2.6.2 TGFβ1 and IL-35 expression on B cells is induced by CpG and CD40L stimulation.

	Culture Conditions	B Cell Subset	Raw				Normalised to IL-10⁻ B			*P* value Unstimulated vs CpG/CD40L[1]	*P* value IL-10⁻ vs IL-10⁺ [2]
			n	mean	SD	SEM	mean	SD	SEM		
TGF-ß1	Unstimulated	$CD19^+TGF\text{-}ß1^+$	10	1.88	0.06	0.02	NA	NA	NA	NA	NA
		$CD19^+CD5^+TGF\text{-}ß1^+$	10	1.80	0.11	0.04	NA	NA	NA	NA	NA
		$CD19^+CD5^{hi}TGF\text{-}ß1^+$	10	1.86	0.10	0.03	NA	NA	NA	NA	NA
		$CD19^+CD27^+TGF\text{-}ß1^+$	10	1.88	0.10	0.03	NA	NA	NA	NA	NA
		$CD19^+CD24^{hi}CD38^{hi}TGF\text{-}ß1^+$	9	1.86	0.08	0.03	NA	NA	NA	NA	NA
	CpG/CD40L	$CD19^+TGF\text{-}ß1^+$	10	33.7	14.4	4.56	NA	NA	NA	**<0.0001**	NA
		$CD19^+CD5^+TGF\text{-}ß1^+$	10	38.7	17.2	5.44	NA	NA	NA	**<0.0001**	NA
		$CD19^+CD5^{hi}TGF\text{-}ß1^+$	10	37.2	19.1	6.04	NA	NA	NA	**<0.0001**	NA
		$CD19^+CD27^+TGF\text{-}ß1^+$	10	35.6	16.8	5.32	NA	NA	NA	**<0.0001**	NA
		$CD19^+CD24^{hi}CD38^{hi}TGF\text{-}ß1^+$	9	36.0	15.6	5.19	NA	NA	NA	**<0.0001**	NA
	CpG/CD40L (IL-10⁻ Cells)	$CD19^+TGF\text{-}ß1^+$	9	31.1	13.9	4.63	100	100	100	NA	NA
		$CD19^+CD5^+TGF\text{-}ß1^+$	9	36.0	16.4	5.45	100	100	100	NA	NA
		$CD19^+CD5^{hi}TGF\text{-}ß1^+$	9	35.6	19.6	6.53	100	100	100	NA	NA
		$CD19^+CD27^+TGF\text{-}ß1^+$	8	33.8	17.9	6.35	100	100	100	NA	NA
		$CD19^+CD24^{hi}CD38^{hi}TGF\text{-}ß1^+$	8	34.4	15.3	5.41	100	100	100	NA	NA
	CpG/CD40L (IL-10⁺ Cells)	$CD19^+TGF\text{-}ß1^+$	9	40.0	21.0	7.01	125	33.8	11.3	NA	0.0547
		$CD19^+CD5^+TGF\text{-}ß1^+$	9	43.1	22.6	7.54	119	25.6	8.53	NA	0.0742
		$CD19^+CD5^{hi}TGF\text{-}ß1^+$	9	37.4	24.3	8.09	109	44.3	14.8	NA	0.6523
		$CD19^+CD27^+TGF\text{-}ß1^+$	8	35.5	23.7	8.39	96.4	31.5	11.1	NA	0.9453
		$CD19^+CD24^{hi}CD38^{hi}TGF\text{-}ß1^+$	8	36.3	21.8	7.72<	102	24.0	8.49	NA	0.8438
IL-35	Unstimulated	$CD19^+IL\text{-}35^+$	10	1.93	0.26	0.08	NA	NA	NA	NA	NA
		$CD19^+CD5^+IL\text{-}35^+$	10	1.84	0.08	0.03	NA	NA	NA	NA	NA
		$CD19^+CD5^{hi}IL\text{-}35^+$	10	1.88	0.09	0.03	NA	NA	NA	NA	NA
		$CD19^+CD27^+IL\text{-}35^+$	10	2.02	0.30	0.09	NA	NA	NA	NA	NA
		$CD19^+CD24^{hi}CD38^{hi}IL\text{-}35^+$	8	2.23	0.85	0.30	NA	NA	NA	NA	NA
	CpG/CD40L	$CD19^+IL\text{-}35^+$	10	12.8	3.77	1.19	NA	NA	NA	**<0.0001**	NA
		$CD19^+CD5^+IL\text{-}35^+$	10	17.2	6.09	1.93	NA	NA	NA	**<0.0001**	NA
		$CD19^+CD5^{hi}IL\text{-}35^+$	10	14.7	5.36	1.69	NA	NA	NA	**<0.0001**	NA
		$CD19^+CD27^+IL\text{-}35^+$	10	12.3	3.92	1.24	NA	NA	NA	**<0.0001**	NA
		$CD19^+CD24^{hi}CD38^{hi}IL\text{-}35^+$	8	15.0	6.01	2.13	NA	NA	NA	**0.0002**	NA
	CpG/CD40L (IL-10⁻ Cells)	$CD19^+IL\text{-}35^+$	9	12.1	3.82	1.27	100	100	100	NA	NA
		$CD19^+CD5^+IL\text{-}35^+$	9	17.7	6.38	2.13	100	100	100	NA	NA
		$CD19^+CD5^{hi}IL\text{-}35^+$	9	15.0	6.93	2.31	100	100	100	NA	NA
		$CD19^+CD27^+IL\text{-}35^+$	8	16.2	7.85	2.78	100	100	100	NA	NA
		$CD19^+CD24^{hi}CD38^{hi}IL\text{-}35^+$	8	13.7	7.01	2.48	100	100	100	NA	NA
	CpG/CD40L (IL-10⁺ Cells)	$CD19^+IL\text{-}35^+$	9	14.3	7.78	2.59	113	38.2	12.7	NA	0.2500
		$CD19^+CD5^+IL\text{-}35^+$	9	17.7	8.97	2.99	103	38.5	12.8	NA	0.8203
		$CD19^+CD5^{hi}IL\text{-}35^+$	9	16.1	7.66	2.55	117	69.0	23.0	NA	0.9102
		$CD19^+CD27^+IL\text{-}35^+$	8	12.5	8.04	2.84	81.0	46.7	16.5	NA	0.5781
		$CD19^+CD24^{hi}CD38^{hi}IL\text{-}35^+$	8	13.0	8.13	2.87	105	55.4	19.6	NA	>0.9999

Bolded values represent significant ***P*** values. [1]Mann Whitney Test and [2]Wilcoxon pared signed-rank test.

3.3 Summary

In this chapter, I confirm distinct and heterogenous IL-10$^+$ Breg cell subsets are present in human peripheral blood and can be expanded in *ex vivo* through CpG and CD40L stimulation in both a dose and time-dependent manner (225, 226). Mathematical visualisation and clustering algorithms supported these findings, revealing combined stimulation with 1μg/mL CpG and 2.5μg/mL CD40L for 72 hours and beyond yielded significant IL-10$^+$ Breg cell subsets, consistent with accounts in previous literature (249). I reveal CpG and CD40L stimulation significantly upregulates PD-L1, PD-1, CD80, CD86 and TIM-1 expression on CD19$^+$ B cells. Moreover, activated CD5$^+$ and CD5^{hi} IL-10$^+$ Breg cells express significantly enhanced CD86 and TIM-1 expression compared to CD5$^+$ and CD5^{hi} IL-10$^-$ B cells, with similar trends observed in PD-L1 and PD-1 expression. CpG and CD40L stimulation also induces TGF-β1 and IL-35 cytokine production from B cell subsets, with some, but not all, IL-10$^+$ Breg cells exhibiting enhanced TGF-β1 and IL-35 expression compared to IL-10$^-$ B cells, highlighting the existence of dual positive IL-10$^+$TGF-β1$^+$ and IL-10$^+$IL-35$^+$ Breg cells. Computational algorithms confirmed the existence of triple positive IL-10$^+$IL-35$^+$TGFβ1$^+$ Breg cells which were induced by CpG and CD40L stimulation. Collectively, this chapter demonstrates significant heterogenous IL-10$^+$ Breg cell phenotypes can be induced during *ex vivo* culture models which may mediate immunoregulation through CD86, PD-L1, PD-1, TIM-1, TGFβ1 and IL-35 mechanisms in addition to IL-10 secretion.

CHAPTER 4. DYSREGULATION OF IL-10$^+$ BREG CELLS IN SEASONAL AND PERENNIAL ALLERGIC RHINITIS

4.1 Introduction

AR is driven by IgE-mediated T2 hypersensitivity immune reactions and characterised by loss of peripheral tolerance to allergen (9). AR can be subclassified into SAR and PAR, with SAR patients sensitive to allergens that are present only at distinct times of the year, such as GP, and PAR patients sensitive to allergens that are present all year round, such as HDM and cat dander (13). Previous studies have reported a dysregulation in IL-10$^+$ Breg cells in AR patients, which may contribute towards disease pathogenesis and loss of peripheral tolerance to allergen (202, 348). However, it remains to be determined whether similar IL-10$^+$ Breg cell compartment dysregulation underlies SAR and PAR. TIM-1 is an important regulator of IL-10 provision from B cells via STAT3 signaling (246). Although TIM-1$^+$ Breg cells have demonstrated important roles in mediating immune tolerance during allograft transplantation their role in AD remains uncertain (246). For example, genetic studies have highlighted that *tim-1* gene polymorphisms are associated with atopic populations, with TIM-1 contributing towards development of T_H2-driven allergic responses (364). However, treatment with TIM-1-specific blocking antibodies, and adoptive transfer of TIM-1$^+$, but not TIM-1$^-$, B cells, reduced tissue inflammation and goblet cell hyperplasia, ameliorating allergic inflammation (302, 365). Thus, studies of TIM-1$^+$ and TIM-1$^+$IL-10$^+$ Breg cell subsets in SAR and PAR are warranted. Although initial small-scale experiments have eluded IL-10$^+$ Breg cell subsets significantly upregulate IgG_4 antibody production compared to IL-10$^-$ B cells, this is yet to be robustly confirmed during a large cross-sectional study (253). Additionally, previous studies have published conflicting reports relating to IL-10$^+$ Breg cell association with IgA production, with

further investigations warranted (256, 276). Finally, it remains to be determined whether SAR GPA patients present with altered frequencies of IL-35$^+$, TGFß1$^+$, and the newly characterised IL-10$^+$IL-35$^+$TGFß1$^+$ Breg cells compared to NAC.

4.1.1 Hypotheses and Aims

4.1.1.1 Hypotheses

1. IL-10$^+$ Breg cells are dysregulated in SAR and PAR patients compared to NAC.
2. IL-10$^+$ Breg cells are associated with IgA and IgG$_4$ expression compared to IL-10$^-$ B cells.
3. SAR patients display dysregulated IL-35$^+$, TGFβ1$^+$ and IL-10$^+$IL-35$^+$TGFß1$^+$ Breg cells compared to NAC.

4.1.1.2 Aims

4. To confirm distinct IL-10$^+$ Breg cell subsets are aberrated in AR patients compared to NAC.
5. To assess whether IL-10$^+$ Breg cell frequencies and IL-10 propensity are dysregulated in SAR (GP sensitised) and PAR (cat and HDM sensitised) patients.
6. To examine CD19$^+$ B cell surface phenotype within IL-10$^+$ and IL-10$^-$ B cells to determine potential dysregulation between NAC, GPA, HDM allergic and cat allergic patients.
7. To assess whether TIM-1$^+$ and TIM-1$^+$IL-10$^+$ Breg cell frequencies are modified in SAR and PAR patients compared to NAC.
8. To assess whether IgA and IgG$_4$ are significantly enhanced in IL-10$^+$ B cells and are dysregulated in SAR and PAR patients compared to NAC.
9. To confirm multi-parametric flow-cytometry evaluations of IL-10$^+$, IgA$^+$, IgG$_4^+$ and TIM-1$^+$ Breg cells in NAC, SAR, and PAR patients through viSNE and FlowSOM analysis.
10. To assess correlations between IL-10$^+$ Breg cell frequencies and AR patient clinical symptom severity, sIgE levels, tIgE levels, SPT scores, age, and gender.

11. To evaluate whether IL-35^{+}, TGFβ1^{+} and IL-10^{+}IL-35^{+}TGFß1^{+} Breg cells are dysregulated in SAR patients compared to NAC.

4.2 Results

4.2.1 IL-10^{+} Regulatory B Cells in AR Patients and NAC

To confirm IL-10^{+} Breg cells are dysregulated in AR individuals compared to NAC, isolated PBMCs were cultured alongside 1μg/mL CpG and 2.5μg/mL CD40L before assessment of IL-10^{+} Breg cell subsets by multi-parametric flow-cytometry. AR patients were clinically sensitised to either GP, cat dander or HDM allergens. In addition to the Breg cell subsets investigated in Chapter 3 (CD19^{+}, CD5$^{+/hi}$, CD27^{+} and CD24^{hi}CD38^{hi}), two additional IL-10^{+} Breg subsets described previously in literature to be dysregulated in allergic individuals were investigated: CD19^{+}CD1d^{hi}CD5^{+} and CD19^{+}CD25^{+}CD71^{lo}CD73^{hi} (Figure 4.2.1.1, A and B). CpG and CD40L stimulation generated significantly diminished CD19^{+}, CD5^{+}, CD5^{hi}, CD24^{hi}CD38^{hi}, and CD27^{+} IL-10^{+} Breg cell frequencies in AR patients compared to NAC (all, $P < 0.001$; Figure 4.2.1.1, C-H and Table 4.2.1.1). Interestingly, no dysregulation in IL-10^{+} Breg frequencies were observed in either AR CD1d^{hi}CD5^{+} or CD25^{+}CD71^{lo}CD73^{hi} IL-10^{+} Breg subsets compared to NAC (both, $P > 0.05$; Figure 4.2.1.1, I-J). Corroborating flow-cytometry data, ELISA analysis demonstrated cell culture supernatants from AR patients had significantly reduced IL-10 levels compared to NAC (NAC: 347pg/mL v. AR: 224pg/mL, $P = 0.0198$; Figure 4.2.1.1, K).

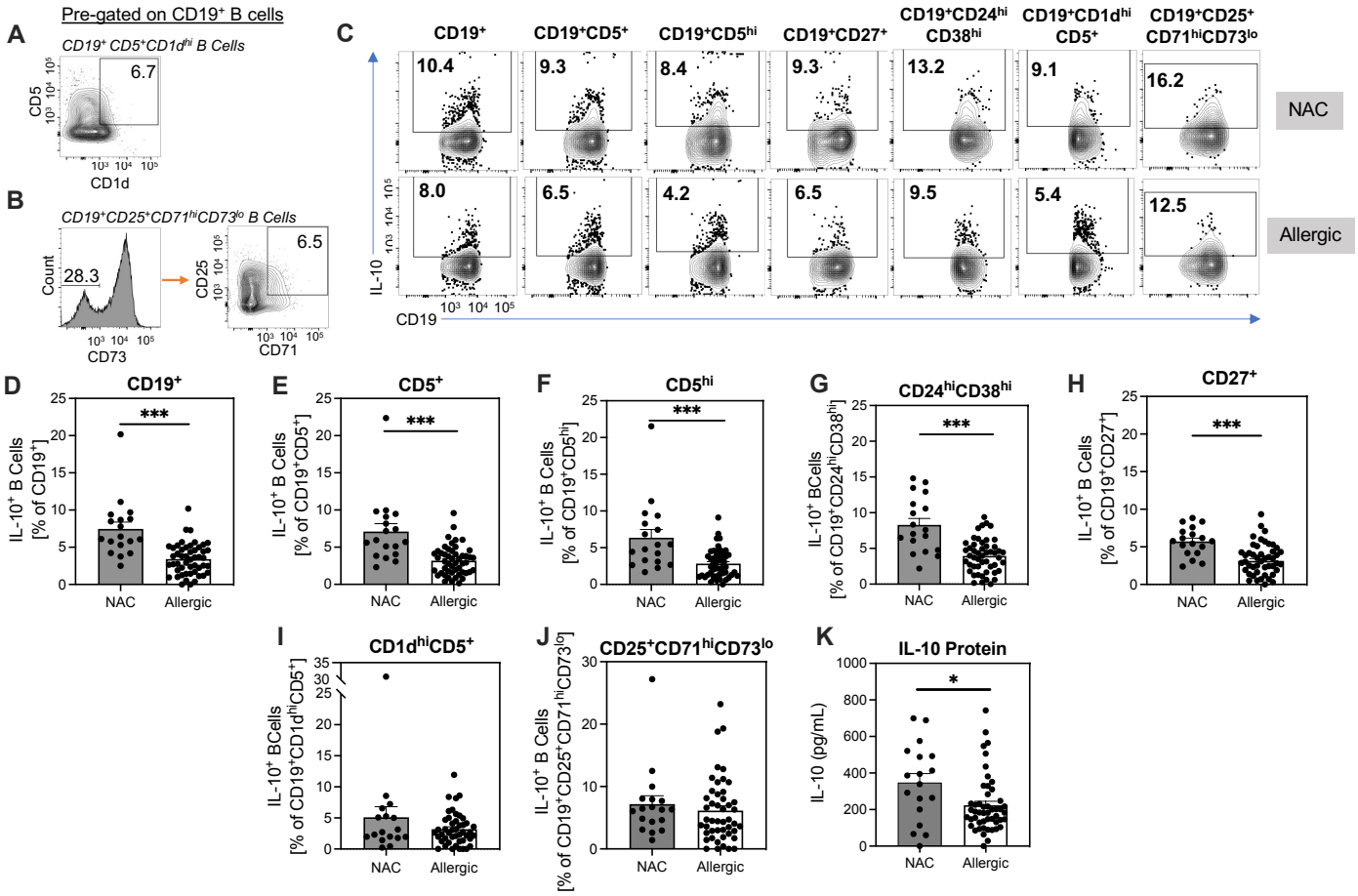


Figure 4.2.1.1 AR patients demonstrate reduced peripheral IL-10$^+$ Breg Cell subsets compared to NAC.

Flow cytometry gating strategy to identify **A)** CD1d^{hi}CD5$^+$ and **B)** CD25$^+$CD71^{hi}CD73^{lo} B cells. **C)** Representative flow cytometry plots from n=3 concatenated FCS files illustrating IL-10$^+$ B cells. Flow-cytometric analysis of **D)** CD19$^+$, **E)** CD5$^+$, **F)** CD5^{hi}, **G)** CD24^{hi}CD38^{hi} **H)** CD27$^+$, **I)** CD1d^{hi}CD5$^+$ and **J)** CD25$^+$CD71^{hi}CD73^{lo} IL-10$^+$ Breg subset expression. **K)** ELISA analysis of IL-10 protein in culture supernatants. Data shown as mean ± SEM [N.B. **J)** represented as raw values of CpG/CD40L stimulated samples] and representative of NAC, n=18 and AR, n= 50 [N.B. **I)** NAC, n=17; AR, n=46 and **J)** AR, n=47]. *P < 0.05, **P < 0.01, ***P < 0.001, Mann Whitney Test. PBMC, peripheral blood mononuclear cells; NAC, non-atopic controls; AR, allergic rhinitis.

Table 4.2.1.1 IL-10$^+$ Breg cell subset frequencies in NAC and AR Patients.

Atopic Status	Culture Conditions	B Cell Subset	Raw				Delta (Unstimulated)			*P* value NAC vs AR
			n	mean	SD	SEM	mean	SD	SEM	
NAC	Unstimulated	CD19$^+$IL-10$^+$	18	1.87	0.08	0.02	NA	NA	NA	NA
		CD19$^+$CD5$^+$IL-10$^+$	18	1.87	0.09	0.02	NA	NA	NA	NA
		CD19$^+$CD5^{hi}IL-10$^+$	18	1.88	0.10	0.02	NA	NA	NA	NA
		CD19$^+$CD27$^+$IL-10$^+$	18	1.85	0.09	0.02	NA	NA	NA	NA
		CD19$^+$CD24^{hi}CD38^{hi}IL-10$^+$	18	1.82	0.14	0.03	NA	NA	NA	NA
		CD19$^+$CD1d^{hi}CD5$^+$IL-10$^+$	17	1.85	0.11	0.03	NA	NA	NA	NA
		CD19$^+$CD25$^+$CD71^{hi}CD73^{lo}IL-10$^+$	18	7.62	5.14	1.21	NA	NA	NA	NA
	CpG/CD40L	CD19$^+$IL-10$^+$	18	9.34	3.93	9.92	7.46	3.92	0.93	NA
		CD19$^+$CD5$^+$IL-10$^+$	18	8.97	4.50	1.06	7.10	4.50	1.06	NA
		CD19$^+$CD5^{hi}IL-10$^+$	18	8.24	4.71	1.11	6.35	4.72	1.11	NA
		CD19$^+$CD27$^+$IL-10$^+$	18	7.56	1.87	0.44	5.72	1.91	0.45	NA
		CD19$^+$CD24^{hi}CD38^{hi}IL-10$^+$	18	10.10	3.85	0.91	8.28	3.87	0.91	NA
		CD19$^+$CD5$^+$CD1d^{hi}IL-10$^+$	17	6.95	7.03	1.71	5.09	7.09	1.72	NA
		CD19$^+$CD25$^+$CD71^{hi}CD73^{lo}IL-10$^+$	18	7.17	5.69	1.34	NA	NA	NA	NA
AR	Unstimulated	CD19$^+$IL-10$^+$	50	1.63	0.08	0.01	NA	NA	NA	NA
		CD19$^+$CD5$^+$IL-10$^+$	50	1.66	0.11	0.02	NA	NA	NA	NA
		CD19$^+$CD5^{hi}IL-10$^+$	50	1.66	0.12	0.02	NA	NA	NA	NA
		CD19$^+$CD27$^+$IL-10$^+$	50	1.65	0.10	0.01	NA	NA	NA	NA
		CD19$^+$CD24^{hi}CD38^{hi}IL-10$^+$	50	1.69	0.09	0.01	NA	NA	NA	NA
		CD19$^+$CD1d^{hi}CD5$^+$IL-10$^+$	46	1.78	0.66	0.10	NA	NA	NA	NA
		CD19$^+$CD25$^+$CD71^{hi}CD73^{lo}IL-10$^+$	47	9.61	6.27	0.91	NA	NA	NA	NA
	CpG/CD40L	CD19$^+$IL-10$^+$	50	5.01	2.10	0.30	3.40	2.08	0.29	**<0.0001**
		CD19$^+$CD5$^+$IL-10$^+$	50	4.84	1.94	0.28	3.18	1.96	0.28	**<0.0001**
		CD19$^+$CD5^{hi}IL-10$^+$	50	4.48	1.88	0.27	2.82	1.93	0.27	**0.0001**
		CD19$^+$CD27$^+$IL-10$^+$	50	4.77	2.16	0.31	3.13	2.18	0.31	**<0.0001**
		CD19$^+$CD24^{hi}CD38^{hi}IL-10$^+$	50	5.63	2.31	0.33	3.95	2.32	0.33	**<0.0001**
		CD19$^+$CD1d^{hi}CD5$^+$IL-10$^+$	46	4.84	2.64	0.39	3.19	2.59	0.38	0.4446
		CD19$^+$CD25$^+$CD71^{hi}CD73^{lo}IL-10$^+$	47	6.15	5.20	0.76	NA	NA	NA	0.3943

Bolded values represent significant ***P*** values. Mann Whitney Test. NAC, non-atopic control; AR, allergic rhinitis.

4.2.2 Evaluation of IL-10$^+$ Breg cell subsets in SAR and PAR

Following confirmation IL-10$^+$ Breg cells are dysregulated in AR individuals, a large blinded cross-sectional study was performed to investigate potential IL-10$^+$ Breg cells aberrations between SAR and PAR patients. SAR patients were defined as GPA, and PAR were defined as HDM allergic (HDMA) and cat allergic (CA) patients. Both clinical symptoms and allergen sensitisation were taken into consideration when defining cross-sectional study groups, with allergic patients displaying clinical symptoms in response to the allergen in their assigned study group only, regardless of potential sensitisation to additional allergens. Although tree allergens, such as birch pollen, and other perennial allergens, such as dog allergens, are also prominent UK allergens indicated in SAR and PAR disease pathogenesis, respectively, these were not investigated within this thesis due to limited availability of sensitised patients during the recruitment process. As per inclusion criteria (described in section 2.2), NAC (*n*=18), GPA (*n*=18), HDMA (*n*=16) and CA (*n*=16) donors were recruited, with allergic individuals demonstrating significantly increased positive SPT, elevated sIgE to the relevant sensitising allergen (GPA, TG; HDMA, HDM; CA, cat dander) and tIgE compared to NAC (all, $P < 0.0001$; Table 4.2.2.1). Study participants completed a self-assessment questionnaire to assess their symptom severity, with SAR and PAR patients recording significantly increased VAS scores compared to NAC (all, $P < 0.0001$).

Table 4.2.2.1 Patient Demographics of NAC, SAR and PAR patients enrolled for a cross-sectional study of IL-10$^+$ B cells.

Characteristic	NAC (n=18)	SAR	PAR	
		GPA (n=18)	HDMA (n=16)	CA (n=16)
Gender, M:F	6:12	10:8	8:8	8:8
Age (years), range	31-70	25-64	23-60	23-56
Allergen-specific sIgE (kU_A/L), mean ± SD	0.0 ±0.0	22.6 ±29.4^{+++}	13.2 ±20.4*,$^{+++}$	5.3 ±7.6*,$^{+++}$
Allergen-specific SPT (mm^2) mean ± SD	0.0 ±0.0	8.3 ±4.3^{+++}	7.1 ±2.3^{+++}	10.7 ± 3.3^{+++}
tIgE (kU/L), mean ± SD	28.3 ±33.2	312.0 ± 522.8^{+++}	432.8 ± 754.3**,$^{+++}$	373.0 ± 909.7^{+++}
VAS, mean ± SD	0.0 ±0.0	74.9 ±10.7^{+++}	62.5 ±16.5^{+++}	63.1 ±17.8^{+++}
Monosensitised	-	11	4	0
Polysensitised	-	7	12	18

*sIgE for n=1 HDMA and n=1 CA subject not available. **tIgE for n=1 HDMA not available. $^+$, denotes statistical analysis compared to NAC. ***P < 0.001, Mann Whitney Test. SPT, skin prick test; HDMA, house-dust mite allergic; NAC, non-atopic control; GPA, grass pollen allergic; CA, cat allergic; SAR, seasonal allergic rhinitis; PAR, perennial allergic rhinitis; sIgE, specific IgE; tIgE, total IgE; VAS, visual analogue scale.

To evaluate IL-10$^+$ Breg cells in SAR and PAR patients, PBMCs were stimulated with 1μg/mL CpG and 2.5μg/mL CD40L for 72 hours and enumerated by multi-parametric flow-cytometry. GPA, HDMA and CA patients demonstrated significant dysregulation in CD19$^+$, CD5$^+$, CD5^{hi}, CD24^{hi}CD38^{hi} and CD27$^+$ IL-10$^+$ Breg cell subsets compared to NAC (all, P > 0.0001; Figure 4.2.2.1, A-F and Table 4.2.2.2). In line with observations in the pilot study, CD1d^{hi}CD5$^+$ and CD25$^+$CD71^{lo}CD73^{hi} IL-10$^+$ B cells were not significantly reduced in NAC compared to CA, GPA or HDMA (all, P > 0.05, Figure 4.2.2.1, G-H). No aberrations in any IL-10$^+$ Breg cell subset frequencies were observed between GPA, HDMA and CA (all, P > 0.05). ELISA analysis demonstrated a significant reduction in IL-10 levels in culture supernatant from NAC compared to HDMA (NAC: 347pg/mL v. HDMA: 169pg/mL, P = 0.0099), with similar trends observed in GPA (NAC v. GPA: 253pg/mL, P = 0.1516) and CA (NAC v. CA: 244pg/mL, P = 0.1110; Figure 4.2.2.1, I).

To assess whether SAR and PAR IL-10^{+} B cells are associated with dysregulated B cell surface marker expression compared to NAC and assess the stability of B cell subsets, CD1d, CD5, CD24, CD25, CD27, CD38, CD71 and CD73 expression were evaluated on IL-10^{-} B Cells and IL-10^{+} Breg cells in stimulated PBMC samples. The average expression of CD1d, CD5, CD24, CD25, CD27, CD38, CD71 and CD73 was similar on IL-10^{+} Breg and IL-10^{-} B cells in all groups (Figure 4.2.2.2 and Table 4.2.2.3). However, CD1d, CD5, CD25 and CD71 expression was significantly upregulated in IL-10^{+} compared to IL-10^{-} CD19^{+} B cells in all groups (all $P < 0.05$). Interestingly, CD27 was also significantly upregulated in IL-10^{+} compared to IL-10^{-} B cells in NAC ($P = 0.0010$), GPA ($P = 0.0001$) and HDMA ($P = <0.0001$), but not CA (Figure 4.2.2.2, B and F). However, CA were the only group to demonstrate significant upregulation in CD24 expression on IL-10^{+} Breg cells ($P = 0.0042$). All groups demonstrated a strong significant decrease in CD73 expression on IL-10^{+} Breg cells compared to IL-10^{-} B cells (all, $P < 0.01$).

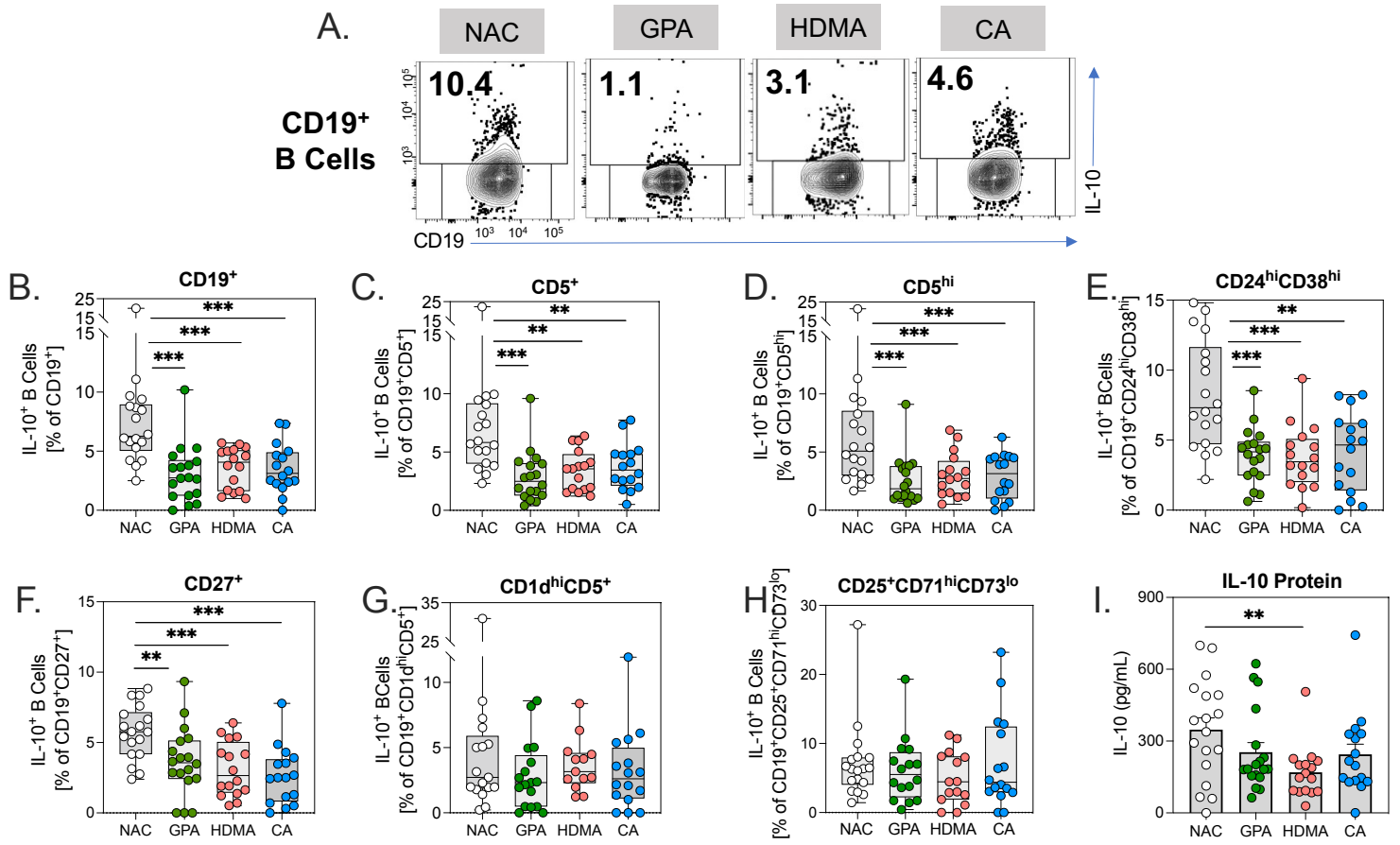


Figure 4.2.2.1 SAR and PAR demonstrate significantly reduced IL-10⁺ Breg cell frequencies and IL-10 provision compared to NAC.

A) Representative flow cytometry plots illustrating CD19⁺IL-10⁺ B cell subsets. Flow-cytometric analysis of **B)** CD19⁺, **C)** CD5⁺, **D)** CD5^{hi}, **E)** CD24^{hi}CD38^{hi}, **F)** CD27⁺, **G)** CD1d^{hi}CD5⁺ and **H)** CD25⁺CD71^{hi}CD73^{lo} IL-10⁺ Breg subset expression. **I)** ELISA analysis of IL-10 protein levels in culture supernatant. Data presented as mean ± SEM and representative of NAC, n=18, GPA, n=18, HMDA, n=16 and CA, n=16 [N.B. **G)** NAC and GPA, n=17; HDMA, n=13. **H)** GPA, n=16 and HDMA, n=15]. $^{**}P < 0.01$, $^{***}P < 0.001$, Mann Whitney Test. PBMC, peripheral blood mononuclear cells; NAC, non-atopic controls; GPA, grass pollen allergic; HDMA, house dust mite allergic; CA, cat allergic; SAR, seasonal allergic rhinitis; PAR, perennial allergic rhinitis.

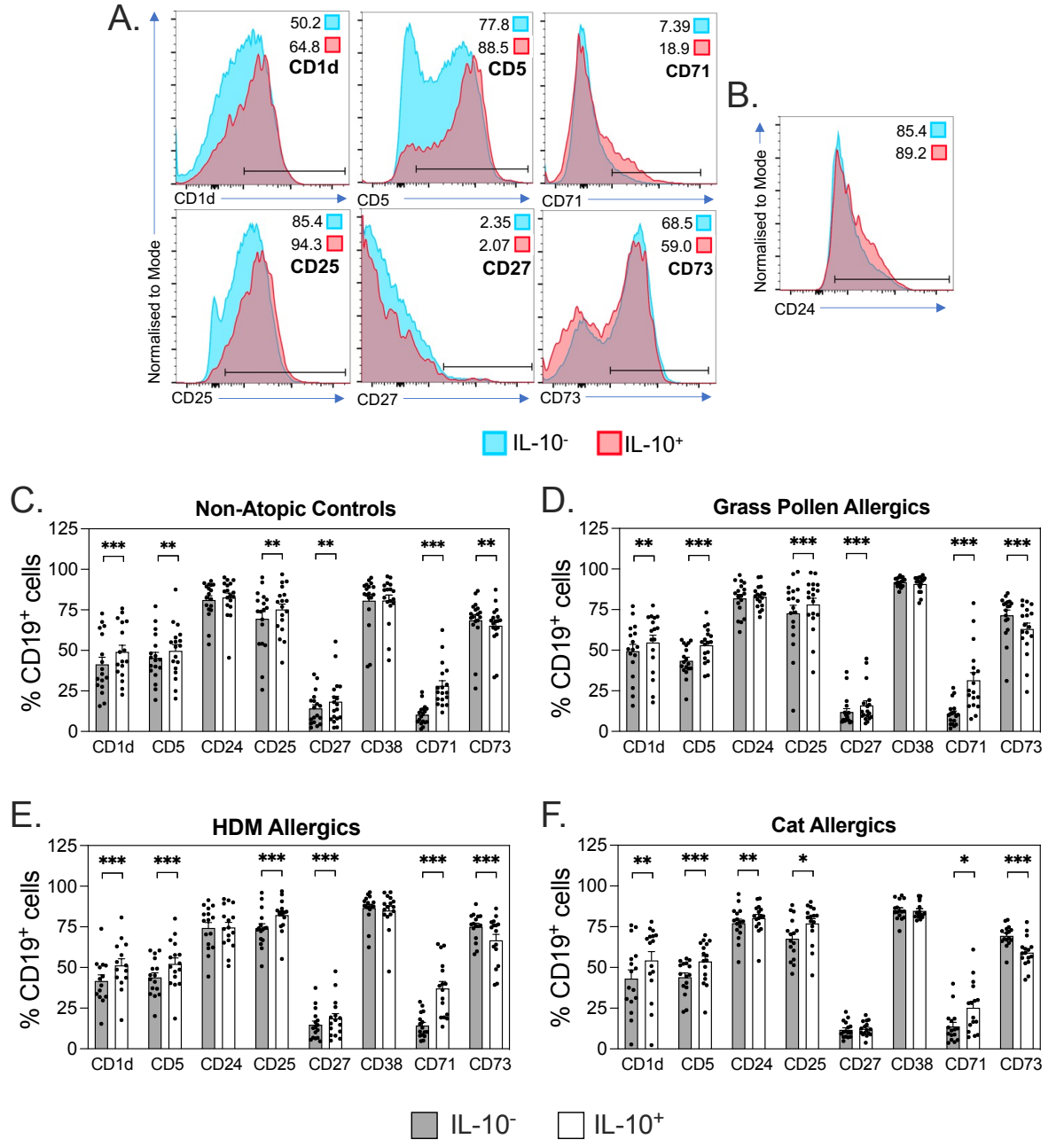


Figure 4.2.2.2 Cell Surface Marker Expression in IL-10$^-$ and IL-10$^+$ B cells in NAC, GPA, HDMA and CA.

A) Representative histograms from n=1 NAC demonstrating CD1d, CD5, CD25, CD27, CD71 and CD73 expression in IL-10$^-$ (blue) and IL-10$^+$ (red) CD19$^+$ B cells. **B)** Representative histograms from n=1 CA demonstrating CD24 expression in IL-10$^-$ (red) and IL-10$^+$ (blue) B cells. Flow cytometry data demonstrating the effect of CpG and CD40L stimulation on cell surface marker expression on CD19$^+$IL-10$^-$ and CD19$^+$IL-10$^+$ B cells in **C)** NAC, **D)** GPA, **E)** HDM allergic and **F)** CA. Data is presented as mean ±SEM and representative of n=18 NAC; n=18 GPA [CD1d, n=17]; n=16 HDMA [CD1d, n=14] and n=16 CA. *P < 0.05, **P < 0.01, ***P < 0.001, Wilcoxon Signed Pairs-Rank Test. NAC, non-atopic control; GPA, grass pollen allergic; HDM, House Dust Mite; CA, cat allergic.

Table 4.2.2.2 IL-10$^+$ Breg Cell subset frequencies in GPA, HDMA, CA and NAC

Atopic Status	Culture Conditions	CD19$^+$ B Cell Subset	Raw				Delta (Unstimulated)			*P* value vs NAC	*P* value vs GPA	*P* value vs HDMA
			n	mean	SD	SEM	mean	SD	SEM			
NAC	Unstimulated	IL-10$^+$	18	1.87	0.08	0.02	NA	NA	NA	NA	NA	NA
		CD5$^+$IL-10$^+$	18	1.87	0.09	0.02	NA	NA	NA	NA	NA	NA
		CD5^{hi}IL-10$^+$	18	1.88	0.10	0.02	NA	NA	NA	NA	NA	NA
		CD27$^+$IL-10$^+$	18	1.85	0.09	0.02	NA	NA	NA	NA	NA	NA
		CD24^{hi}CD38^{hi}IL-10$^+$	18	1.82	0.14	0.03	NA	NA	NA	NA	NA	NA
		CD1d^{hi}CD5$^+$IL-10$^+$	17	1.85	0.11	0.03	NA	NA	NA	NA	NA	NA
		CD25$^+$CD71^{lo}CD73^{hi}	18	7.62	5.14	1.2	NA	NA	NA	NA	NA	NA
	CpG/CD40L	IL-10$^+$	18	9.34	3.93	9.92	7.46	3.92	0.93	NA	NA	NA
		CD5$^+$IL-10$^+$	18	8.97	4.50	1.06	7.10	4.50	1.06	NA	NA	NA
		CD5^{hi}IL-10$^+$	18	8.24	4.71	1.11	6.35	4.72	1.11	NA	NA	NA
		CD27$^+$IL-10$^+$	18	7.56	1.87	0.44	5.72	1.91	0.45	NA	NA	NA
		CD24^{hi}CD38^{hi}IL-10$^+$	18	10.10	3.85	0.91	8.28	3.87	0.91	NA	NA	NA
		CD1d^{hi}CD5$^+$IL-10$^+$	17	6.95	7.03	1.71	5.09	7.09	1.72	NA	NA	NA
		CD25$^+$CD71^{lo}CD73^{hi}	18	7.17	5.69	1.34	NA	NA	NA	NA	NA	NA
GPA	Unstimulated	IL-10$^+$	18	1.62	0.08	0.02	NA	NA	NA	NA	NA	NA
		CD5$^+$IL-10$^+$	18	1.69	0.12	0.03	NA	NA	NA	NA	NA	NA
		CD5^{hi}IL-10$^+$	18	1.63	0.11	0.03	NA	NA	NA	NA	NA	NA
		CD27$^+$IL-10$^+$	18	1.63	0.08	0.02	NA	NA	NA	NA	NA	NA
		CD24^{hi}CD38^{hi}IL-10$^+$	18	1.67	0.10	0.02	NA	NA	NA	NA	NA	NA
		CD1d^{hi}CD5$^+$IL-10$^+$	17	1.95	1.08	0.26	NA	NA	NA	NA	NA	NA
		CD25$^+$CD71^{lo}CD73^{hi}	16	11.47	7.99	1.99	NA	NA	NA	NA	NA	NA
	CpG/CD40L	IL-10$^+$	18	4.68	2.46	0.58	3.09	2.41	0.57	**<0.0001**	NA	NA
		CD5$^+$IL-10$^+$	18	4.57	2.15	0.51	2.88	2.18	0.52	**<0.0001**	NA	NA
		CD5^{hi}IL-10$^+$	18	4.19	2.03	0.48	2.56	2.05	0.48	**0.0003**	NA	NA
		CD27$^+$IL-10$^+$	18	5.23	2.45	0.58	3.65	2.43	0.57	**0.0077**	NA	NA
		CD24^{hi}CD38^{hi}IL-10$^+$	18	5.58	1.94	0.46	3.91	1.97	0.47	**0.0003**	NA	NA
		CD1d^{hi}CD5$^+$IL-10$^+$	17	4.56	2.55	0.62	2.84	2.60	0.63	0.3266	NA	NA
		CD25$^+$CD71^{lo}CD73^{hi}	16	6.12	4.67	1.68	NA	NA	NA	0.6212	NA	NA
HDMA	Unstimulated	IL-10$^+$	16	1.64	0.09	0.02	NA	NA	NA	NA	NA	NA
		CD5$^+$IL-10$^+$	16	1.64	0.11	0.03	NA	NA	NA	NA	NA	NA
		CD5^{hi}IL-10$^+$	16	1.71	0.14	0.03	NA	NA	NA	NA	NA	NA
		CD27$^+$IL-10$^+$	16	1.69	0.11	0.03	NA	NA	NA	NA	NA	NA
		CD24^{hi}CD38^{hi}IL-10$^+$	16	1.69	0.08	0.02	NA	NA	NA	NA	NA	NA
		CD1d^{hi}CD5$^+$IL-10$^+$	13	1.67	0.08	0.02	NA	NA	NA	NA	NA	NA
		CD25$^+$CD71^{lo}CD73^{hi}	15	8.41	4.97	1.28	NA	NA	NA	NA	NA	NA
	CpG/CD40L	IL-10$^+$	16	5.22	1.72	0.43	3.60	1.74	0.44	**0.0001**	0.2272	NA
		CD5$^+$IL-10$^+$	16	5.08	1.72	0.43	3.43	1.73	0.43	**0.0012**	0.3089	NA
		CD5^{hi}IL-10$^+$	16	4.72	1.80	0.45	3.01	1.87	0.49	**0.0051**	0.3653	NA
		CD27$^+$IL-10$^+$	16	4.81	1.91	0.48	3.11	1.93	0.48	**0.0007**	0.5972	NA
		CD24^{hi}CD38^{hi}IL-10$^+$	16	5.48	2.22	0.56	3.80	2.23	0.56	**0.0002**	0.7791	NA
		CD1d^{hi}CD5$^+$IL-10$^+$	13	5.34	2.02	0.56	3.66	2.03	0.56	0.9755	0.1868	NA
		CD25$^+$CD71^{lo}CD73^{hi}	15	4.96	3.77	0.97	NA	NA	NA	0.2863	0.6328	NA
CA	Unstimulated	IL-10$^+$	16	1.64	0.08	0.02	NA	NA	NA	NA	NA	NA
		CD5$^+$IL-10$^+$	16	1.66	0.09	0.02	NA	NA	NA	NA	NA	NA
		CD5^{hi}IL-10$^+$	16	1.66	0.11	0.03	NA	NA	NA	NA	NA	NA
		CD27$^+$IL-10$^+$	16	1.63	0.11	0.03	NA	NA	NA	NA	NA	NA
		CD24^{hi}CD38^{hi}IL-10$^+$	16	1.70	0.10	0.02	NA	NA	NA	NA	NA	NA
		CD1d^{hi}CD5$^+$IL-10$^+$	16	1.68	0.11	0.03	NA	NA	NA	NA	NA	NA
		CD25$^+$CD71^{lo}CD73^{hi}	16	8.87	5.29	1.32	NA	NA	NA	NA	NA	NA
	CpG/CD40L	IL-10$^+$	16	5.17	2.08	0.52	3.56	2.08	0.52	**0.0002**	0.4790	0.8381
		CD5$^+$IL-10$^+$	16	4.92	1.99	0.50	3.71	2.00	0.5	**0.0024**	0.1643	0.6893
		CD5^{hi}IL-10$^+$	16	4.58	1.86	0.47	2.92	1.93	0.48	**0.0063**	0.3653	0.9852

	$CD27^{+}IL\text{-}10^{+}$	16	4.22	2.05	0.51	2.62	2.03	0.51	**0.0001**	0.1891	0.4068
	$CD24^{hi}CD38^{hi}IL\text{-}10^{+}$	16	5.83	2.84	0.71	4.15	2.84	0.71	**0.0039**	0.7463	0.7520
	$CD1d^{hi}CD5^{+}IL\text{-}10^{+}$	16	4.72	3.22	0.81	3.19	3.05	0.76	0.4436	0.8519	0.3510
	$CD25^{+}CD71^{lo}CD73^{hi}$	16	7.28	6.73	1.68	NA	NA	NA	0.6146	>0.9999	0.3947

Bolded values represent significant ***P*** values. Mann Whitney Test. NAC, non-atopic control; GPA, grass pollen allergic; HDMA, house dust mite allergic; CA, cat allergic.

Table 4.2.2.3 Surface Marker Expression on $IL\text{-}10^{+/-}$ B Cells in NAC, GPA, CA and HDMA

Atopic Status	Cell Surface Marker	$IL\text{-}10^{-}$ B cell				$IL\text{-}10^{+}$ Breg cell			*P* value vs $IL\text{-}10^{-}$ B cell
		n	mean	SD	SEM	mean	SD	SEM	
NAC	CD1d	18	41.4	18.3	4.43	49.1	17.1	4.15	**<0.0001**
	CD5	18	45.4	14.8	3.48	49.7	16.2	3.82	**0.0056**
	CD24	18	81.1	11.1	2.62	82.7	11.7	2.75	0.2645
	CD25	18	69.5	18.8	4.44	75.2	14.6	3.43	**0.0038**
	CD27	18	14.2	9.95	2.35	18.4	14.4	3.4	**0.0010**
	CD38	18	80.6	16.1	3.79	80.8	14.1	3.32	0.8407
	CD71	18	10.3	6.16	1.45	28.2	12.4	3.15	**<0.0001**
	CD73	18	68.6	15.0	3.54	65.3	13.4	3.15	**0.0046**
GPA	CD1d	17	49.45	17.13	4.16	54.76	18.26	4.43	**0.0046**
	CD5	18	43.47	9.58	2.26	53.08	10.67	2.52	**<0.0001**
	CD24	18	81.92	10.07	2.37	82.89	6.76	1.59	0.4617
	CD25	18	72.72	20.93	4.93	78.17	16.25	3.83	**0.0004**
	CD27	18	11.89	9.11	2.15	16.04	11.86	2.80	**0.0001**
	CD38	18	91.91	2.84	0.67	90.77	4.89	1.15	0.3230
	CD71	18	10.86	7.15	1.69	31.48	19.84	4.68	**<0.0001**
	CD73	18	71.56	13.32	3.14	63.06	15.54	3.66	0.0001
HDM	CD1d	14	41.7	14.0	3.74	51.3	15.4	4.12	**0.0001**
	CD5	16	43.9	11.5	2.87	52.2	14.7	3.68	**0.0002**
	CD24	16	74.3	13.4	3.34	74.6	12.7	3.18	0.7532
	CD25	16	74.1	11.3	2.82	82.2	9.64	2.41	**0.0003**
	CD27	16	14.8	9.14	2.29	18.7	11.8	2.96	**<0.0001**
	CD38	16	86.6	8.92	2.23	85.0	11.7	2.91	0.2476
	CD71	16	14.3	7.59	1.90	37.2	17.0	4.24	**<0.0001**
	CD73	16	75.1	8.46	2.11	66.7	14.9	3.71	0.0008
CA	CD1d	16	43.2	21.2	5.30	54.3	21.9	5.47	**0.0010**
	CD5	16	44.0	10.4	2.61	53.7	12.9	3.23	**0.0004**
	CD24	16	77.1	10.1	2.54	80.2	9.10	2.28	**0.0042**
	CD25	16	67.7	12.6	3.15	77.0	12.6	3.00	**0.0131**
	CD27	16	11.7	5.01	1.25	12.3	4.42	1.10	0.2689
	CD38	16	85.1	5.84	1.46	84.8	5.17	1.29	0.3029
	CD71	16	13.8	10.0	2.50	25.3	15.6	3.90	**0.0182**
	CD73	16	69.5	6.37	1.59	59.1	9.21	2.30	**0.0008**

Bolded values represent significant ***P*** values. Wilcoxon-signed pairs rank test. NAC, non-atopic control; GPA, grass pollen allergic; HDMA, house dust mite allergic; CA, cat allergic.

4.2.3 Evaluation of TIM-1$^+$ Breg Cell Subsets in SAR and PAR

Following observations that IL-10$^+$ Breg cells are associated with significant expression of TIM-1 (described in section 3.2.5), the frequency of TIM-1$^+$ B cells and dual positive IL-10$^+$TIM-1$^+$ Breg cells were assessed in NAC, GPA, HDMA and CA by multi-parametric flow-cytometry to assess potential novel aberrations between SAR, PAR and NAC. Although no dysregulation was observed in any allergic group compared to NAC, CA patients demonstrated significantly reduced TIM-1$^+$ B cells compared to HDMA (P = 0.0349; Figure 4.2.3.1, A-B and Table 4.2.3.1). Similarly, no aberration in dual positive CD19$^+$IL-10$^+$TIM-1$^+$ or CD5$^+$IL-10$^+$TIM-1$^+$ Breg cells were observed between NAC and any allergic group (all, P > 0.05, Figure 4.2.3.1, C-D). However, activated CD5^{hi}IL-10$^+$TIM-1$^+$ Breg cells were significantly reduced in CA compared to NAC (P = 0.0389; Figure 4.2.3.1, E). Strikingly, HDMA subjects demonstrated significantly increased frequencies of CD19$^+$IL-10$^+$TIM-1$^+$ (P = 0.0075), CD5$^+$IL-10$^+$TIM-1$^+$ (P = 0.0039) and CD5^{hi}IL-10$^+$TIM-1$^+$ (P = 0.0015) Breg cell subsets compared to CA, and significantly increased CD19$^+$IL-10$^+$TIM-1$^+$ Breg cells compared to GPA (P = 0.0326).

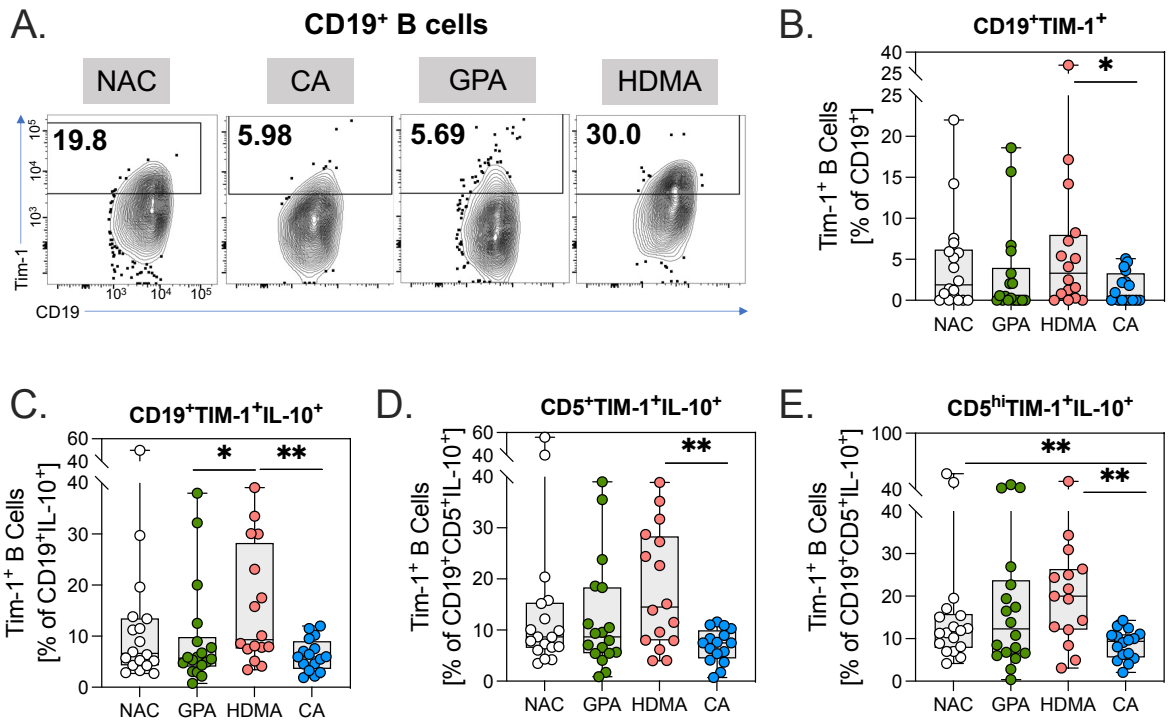


Figure 4.2.3.1 TIM-1⁺ B cells and IL-10⁺TIM-1⁺ Breg cells are significantly reduced in CA compared to HDMA.

A) Representative flow-cytometry plots from n=1 each NAC, GPA, CA and HDMA showing expression of TIM-1⁺ B cells. Flow cytometry data demonstrating Tim-1 expression on **B)** CD19⁺ B cells and **C)** CD19⁺, **D)** CD5⁺ and **E)** CD5^{hi} IL-10⁺ Breg subsets. Data representative of n=18 NAC, n=18 GPA, n=16 HDMA and n=16 CA. [N.B **B)** GPA, n=17; **E)** HDMA, n=15] and presented as mean ± SEM. * < *P*.0.05, ***P* < 0.01, Mann Whitney Test. NAC, non-atopic controls; GPA, grass pollen allergic; HDMA, house dust mite allergic; CA, cat allergic.

Table 4.2.3.1 TIM-1$^+$ B cells and TIM-1$^+$IL-10$^+$ Breg cells in NAC, GPA, HDMA and CA.

Atopic Status	Culture Conditions	B Cell Subset	Raw				Delta			*P* value vs NAC	*P* value vs GPA	*P* value vs CA
			n	mean	SD	SEM	mean	SD	SEM			
NAC	Unstimulated	CD19$^+$TIM-1$^+$	18	5.66	4.71	1.11	NA	NA	NA	NA	NA	NA
	CpG/CD40L	CD19$^+$TIM-1$^+$	18	9.61	9.52	2.24	4.34	5.82	1.37	NA	NA	NA
	CpG/CD40L	CD19$^+$TIM-1$^+$IL-10$^-$	18	11.38	11.79	2.78	NA	NA	NA	NA	NA	NA
	(IL-10$^+$ Cells)	CD19$^+$CD5$^+$TIM-1$^+$IL-10$^-$	18	13.53	13.56	3.20	NA	NA	NA	NA	NA	NA
		CD19$^+$CD5^{hi}TIM-1$^+$IL-10$^-$	18	15.69	13.98	3.30	NA	NA	NA	NA	NA	NA
GPA	Unstimulated	CD19$^+$TIM-1$^+$	17	5.46	4.81	1.17	NA	NA	NA	NA	NA	NA
	CpG/CD40L	CD19$^+$TIM-1$^+$	17	8.4	9.82	1.28	3.10	5.53	1.30	0.2397	NA	NA
	CpG/CD40L	CD19$^+$TIM-1$^+$IL-10$^+$	18	9.54	10.29	2.42	NA	NA	NA	0.5418	NA	NA
	(IL-10$^+$ Cells)	CD19$^+$CD5$^+$TIM-1$^+$IL-10$^+$	18	12.26	10.87	2.56	NA	NA	NA	0.7193	NA	NA
		CD19$^+$CD5^{hi}TIM-1$^+$IL-10$^+$	18	16.71	13.97	3.29	NA	NA	NA	0.9378	NA	NA
HDMA	Unstimulated	CD19$^+$TIM-1$^+$	16	6.89	5.19	10.2	NA	NA	NA	NA	NA	NA
	CpG/CD40L	CD19$^+$TIM-1$^+$	16	12.9	10.2	2.55	6.17	8.35	2.09	0.5537	0.0958	NA
	CpG/CD40L	CD19$^+$TIM-1$^+$IL-10$^+$	16	15.73	11.72	2.93	NA	NA	NA	0.1540	**0.0326**	NA
	(IL-10$^+$ Cells)	CD19$^+$CD5$^+$TIM-1$^+$IL-10$^+$	16	18.07	11.70	2.93	NA	NA	NA	0.1985	0.1258	NA
		CD19$^+$CD5^{hi}TIM-1$^+$IL-10$^+$	15	20.43	12.05	3.11	NA	NA	NA	0.0810	0.2586	NA
CA	Unstimulated	CD19$^+$TIM-1$^+$	16	3.86	1.49	0.37	NA	NA	NA	NA	NA	NA
	CpG/CD40L	CD19$^+$TIM-1$^+$	16	4.89	3.00	0.75	1.55	1.89	0.47	0.0991	0.7801	**0.0349**
	CpG/CD40L	CD19$^+$TIM-1$^+$IL-10$^+$	16	6.31	3.17	0.79	NA	NA	NA	0.3009	0.8782	**0.0075**
	(IL-10$^+$ Cells)	CD19$^+$CD5$^+$TIM-1$^+$IL-10$^+$	16	6.97	3.27	0.82	NA	NA	NA	0.1258	0.2811	**0.0039**
		CD19$^+$CD5^{hi}TIM-1$^+$IL-10$^+$	16	8.63	3.50	0.85	NA	NA	NA	**0.0389**	0.1371	**0.0015**

Bolded values represent significant ***P*** values. Mann Whitney Test. NAC, non-atopic control; GPA, grass pollen allergic; HDMA, house dust mite allergic; CA, cat allergic.

4.2.4 Evaluation of IgA$^+$ and IgG4$^+$ Breg Cell Subsets in SAR and PAR

To determine whether IgA and IgG_4 antibodies are associated with IL-10$^+$ Breg cells, the expression of IgG_4 and IgA were assessed on IL-10$^-$ and IL-10$^+$ Breg cells by multi-parametric flow-cytometry. Although no significant aberration in IgA expression was observed between IL-10$^+$ and IL-10$^-$ B cells, memory CD27$^+$IL-10$^+$ Breg cells demonstrated significantly reduced IgA expression compared to IL-10$^-$ B cells in GPA (24% reduction, *P* = 0.0135), HDMA (30% reduction, *P* = 0.0085) and CA (28% reduction, *P* = 0.0007; Figure 4.2.4.1, A-C and Table 4.2.4.1). In contrast, no differential IgA expression was observed between CD27$^+$IL-10$^-$ and CD27$^+$IL-10$^+$ Breg cells in NAC (1% reduction, *P* = 0.2306). CD19$^+$IL-10$^+$ B cells expressed greater than double IgG_4 expression compared to CD19$^+$IL-10$^-$ B cells in NAC (58% increase, *P* = 0.0085), GPA (59% increase, *P* = 0.0046), HDMA (51% increase, *P* = <0.0001) and CA (51% increase, *P* = 0.0007; Figure 4.2.4.1, D). However, memory CD27$^+$IL-10$^+$ Breg cells were not significantly associated with IgG_4 expression compared to CD27$^+$IL-10$^-$ B cells in any subject group (all, *P* > 0.05), although IgG_4 expression on IL-10$^+$ compared to IL-10$^-$ Breg cells was enhanced in NAC (48% increase) compared to AR groups (all, <10% increase; Figure 4.2.4.1, E). The frequency of IL-10$^+$IgG$_4^+$ and IL-10$^+$IgA$^+$ Breg cells were assessed in NAC, GPA, HDMA and CA individuals to assess potential novel aberrations between allergic sensitisation status, with dual positive IL-10$^+$IgA$^+$ and IL-10$^+$IgG$_4^+$ B cells frequencies similar across all groups (all, *P* > 0.05, Figure 4.2.4.1, F-I).

The frequency of CD27$^+$IL-10$^+$IgA$^+$ and CD27$^+$IL-10$^+$IgG$_4^+$ Breg cells in NAC were significantly positively correlated (*P* = 0.0015), with similar trends observed in allergic groups (Figure 4.2.4.2, A-D) Moreover, CD27$^+$IL-10$^+$IgG$_4^+$ B cells were significantly negatively correlated with serum cat dander-sIgE in CA (*P* = 0.0217; Figure 4.2.4.2, I). No correlation was observed between any other dual positive IL-10$^+$IgA$^+$ or IL-10$^+$IgG$_4^+$ B cells subsets or with allergen-sIgE across GPA, HDMA and CA (Figure 4.2.4.2).

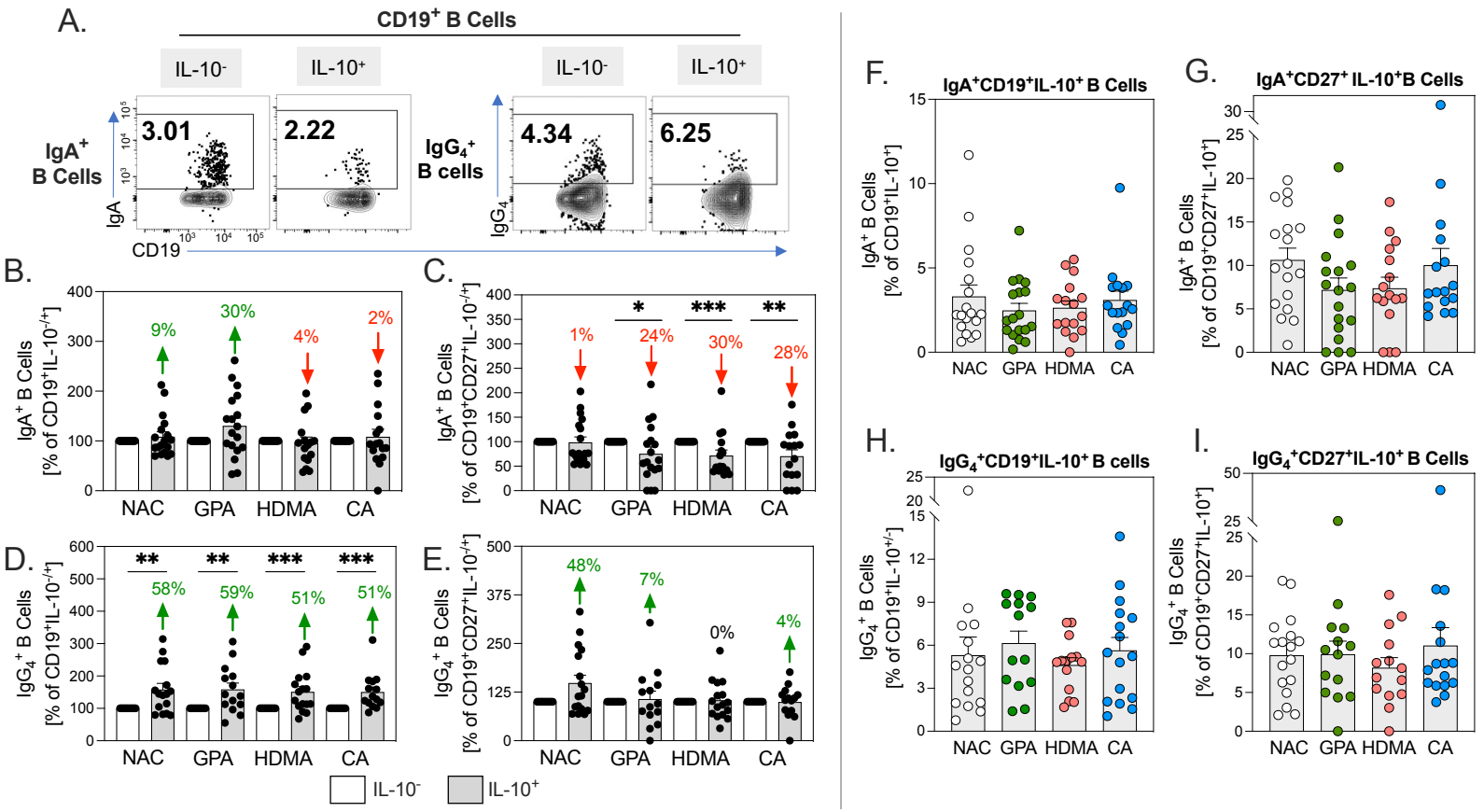


Figure 4.2.4.1 IgG$_4$, but not IgA, expression is significantly enhanced on IL-10$^+$ Breg cells compared to IL-10$^-$ B cells.

A) Representative flow-cytometry plots from n=1 NAC showing IgA and IgG$_4$ expression in CD19$^+$IL-10$^{+/-}$ B cells. Flow cytometry data demonstrating percentage change in IgA expression on IL-10$^+$ B cells compared to IL-10$^-$ B cells in **B)** CD19$^+$ and **C)** CD27$^+$ B cell subsets, and percentage change in IgG$_4$ expression on IL-10$^+$ B cells compared to IL-10$^-$ B cells in **D)** CD19$^+$ and **E)** CD27$^+$ B cell subsets. Flow cytometry data demonstrating dual positive **F)** IgA$^+$IL-10$^+$, **G)** CD27$^+$IgA$^+$IL-10$^+$, **H)** IgG$_4^+$IL-10$^+$ and **I)** CD27$^+$IgG$_4^+$IL-10$^+$ B cells. Data representative of NAC [IgA data, n=18; IgG$_4$ data, n=16], GPA [IgA data, n=18; IgG$_4$ data, n=14], CA, n=16 and HDMA [IgA data, n=16; IgG$_4$ data, n=14] and presented as mean ± SEM. *P < 0.05, ** P < 0.01, *** P < 0.001, Mann Whitney Test. NAC, non-atopic controls; GPA, grass pollen allergic; HDMA, house dust mite allergic; CA, cat allergic.

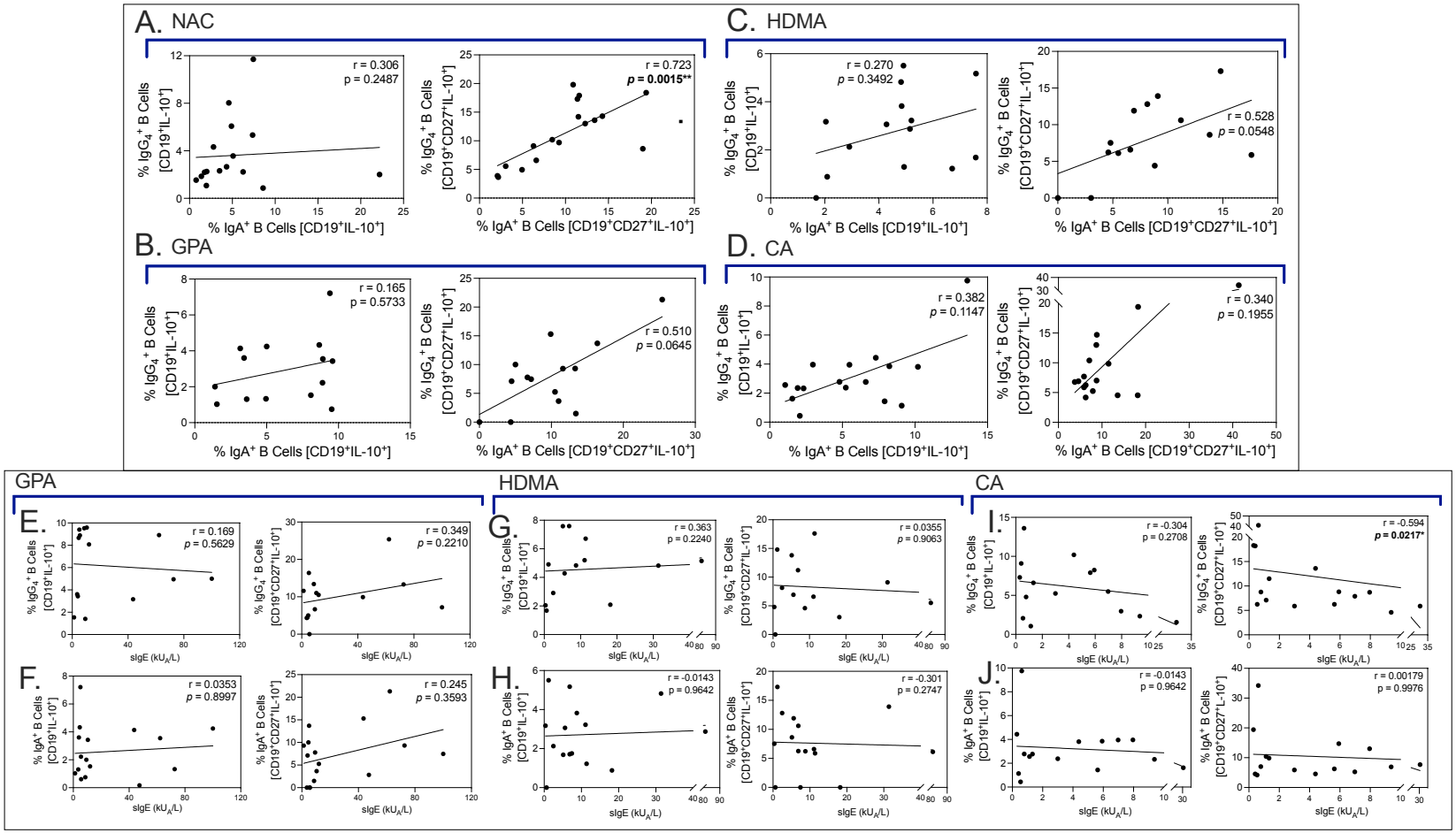


Figure 4.2.4.2 Correlation between IL-10$^+$IgA$^+$ and IL-10$^+$IgG$_4^+$ Breg cells and serum sIgE in GPA, HDMA and CA.

Correlation between IL-10$^+$IgA$^+$ and IL-10$^+$IgG$_4^+$ Breg cells, and CD27$^+$IL-10$^+$IgA$^+$ and CD27$^+$IL-10$^+$IgG$_4^+$ Breg cells in **A)** NAC, **B)** GPA, **C)** HDMA and **D)** CA. Correlation between IL-10$^+$IgA$^+$ and IL-10$^+$IgG$_4^+$ B cells and **E-F)** GP-sIgE in GPA, **G-H)** cat dander-sIgE in CA, and **I-J)** HDM-sIgE in HDMA. Data representative of NAC: IgA data, n=18; IgG$_4$ data, n=17 [N.B CD19$^+$ B cell IgG$_4$, n=16], GPA: IgA data, n=18 (sIgE, n=16); IgG$_4$ data, n=14, HDMA: IgA data, n=14 (sIgE, n=15); IgG$_4$ data, n=14 (sIgE, n=13), CA: IgA data, n=16; IgG$_4$ data, n=16 (sIgE, both n=15). Spearman Correlation. *P < 0.05. NAC, non-atopic control; GPA, grass pollen allergic; HDMA, house dust mite allergic; CA, cat allergic.

Table 4.2.4.1 IgG_4 expression is significantly enhanced on IL-10^+ Breg cells

	Atopic Status	Culture Conditions	B Cell Subset	Raw				Normalised to IL-10^-			*P value vs. IL-10^+ (Norm)*	*P value vs. NAC IL-10^+ (Raw)*
				n	mean	SD	SEM	mean	SD	SEM		
IgA	NAC	CpG/CD40L	$CD19^+IgA^+IL\text{-}10^-$	18	3.11	2.58	0.61	NA	NA	NA	NA	NA
			$CD19^+CD27^+IgA^+IL\text{-}10^-$	18	12.45	8.1	1.9	NA	NA	NA	NA	NA
		CpG/CD40L	$CD19^+IgA^+IL\text{-}10^+$	18	3.31	2.90	0.68	109	41.7	9.83	0.7718	NA
			$CD19^+CD27^+IgA^+IL\text{-}10^+$	18	10.65	5.71	1.34	99	45.8	10.8	0.2306	NA
	GPA	CpG/CD40L	$CD19^+IgA^+IL\text{-}10^-$	18	1.97	1.13	0.27	NA	NA	NA	NA	NA
			$CD19^+CD27^+IgA^+IL\text{-}10^-$	18	10.53	6.94	1.64	NA	NA	NA	NA	NA
		CpG/CD40L	$CD19^+IgA^+IL\text{-}10^+$	18	2.48	1.79	0.42	131	64.7	15.2	0.2306	0.3758
			$CD19^+CD27^+IgA^+IL\text{-}10^+$	18	7.19	5.81	1.37	75.6	58.2	13.7	**0.0135**	0.5574
	HDM	CpG/CD40L	$CD19^+IgA^+IL\text{-}10^-$	16	2.52	1.74	0.44	NA	NA	NA	NA	NA
			$CD19^+CD27^+IgA^+IL\text{-}10^-$	16	11.08	5.55	1.39	NA	NA	NA	NA	NA
		CpG/CD40L	$CD19^+IgA^+IL\text{-}10^+$	16	2.64	1.56	0.40	96.1	46.5	11.6	0.1074	0.7984
			$CD19^+CD27^+IgA^+IL\text{-}10^+$	16	7.38	5.05	1.26	70.4	51.9	13	**0.0085**	0.9794
	CA	CpG/CD40L	$CD19^+IgA^+IL\text{-}10^-$	16	3.32	1.48	0.37	NA	NA	NA	NA	NA
			$CD19^+CD27^+IgA^+IL\text{-}10^-$	16	14.63	6.41	1.60	NA	NA	NA	NA	NA
		CpG/CD40L	$CD19^+IgA^+IL\text{-}10^+$	16	3.10	2.11	0.53	108	60.3	15.1	0.2048	0.5060
			$CD19^+CD27^+IgA^+IL\text{-}10^+$	16	10.04	7.69	1.92	71.9	45.2	11.3	**0.0007**	0.4062
IgG_4	NAC	CpG/CD40L	$CD19^+IgG_4^+IL\text{-}10^-$	16	4.17	3.96	0.99	NA	NA	NA	NA	NA
			$CD19^+CD27^+IgG_4^+IL\text{-}10^-$	16	8.85	6.12	1.48	NA	NA	NA	NA	NA
		CpG/CD40L	$CD19^+IgG_4^+IL\text{-}10^+$	16	5.31	5.08	1.27	158	74.4	18.6	**0.0085**	NA
			$CD19^+CD27^+IgG_4^+IL\text{-}10^+$	16	9.81	5.23	1.27	148	83.3	20.2	0.3685	NA
	GPA	CpG/CD40L	$CD19^+IgG_4^+IL\text{-}10^-$	14	4.03	1.91	0.511	NA	NA	NA	NA	NA
			$CD19^+CD27^+IgG_4^+IL\text{-}10^-$	14	11.5	5.48	1.47	NA	NA	NA	NA	NA
		CpG/CD40L	$CD19^+IgG_4^+IL\text{-}10^+$	14	6.15	3.14	0.84	159	72.3	19.3	**0.0046**	0.1536
			$CD19^+CD27^+IgG_4^+IL\text{-}10^+$	14	9.94	6.27	1.68	107	75.2	20.1	0.5089	0.3997
	HDM	CpG/CD40L	$CD19^+IgG_4^+IL\text{-}10^-$	16	3.56	2.23	0.59	NA	NA	NA	NA	NA
			$CD19^+CD27^+IgG_4^+IL\text{-}10^-$	14	8.34	5.03	1.34	NA	NA	NA	NA	NA
		CpG/CD40L	$CD19^+IgG_4^+IL\text{-}10^+$	14	4.62	1.91	0.51	151	56.6	15.1	**<0.0001**	0.6084
			$CD19^+CD27^+IgG_4^+IL\text{-}10^+$	14	8.21	4.83	1.29	99.8	42.2	11.3	0.1766	0.6090
	CA	CpG/CD40L	$CD19^+IgG_4^+IL\text{-}10^-$	16	3.94	2.42	0.61	NA	NA	NA	NA	NA
			$CD19^+CD27^+IgG_4^+IL\text{-}10^-$	16	11.0	5.39	1.35	NA	NA	NA	NA	NA
		CpG/CD40L	$CD19^+IgG_4^+IL\text{-}10^+$	16	5.65	3.60	0.90	151	63.9	16.0	**0.0007**	0.4230
			$CD19^+CD27^+IgG_4^+IL\text{-}10^+$	16	11.1	9.19	2.30	104	49.3	12.3	0.5340	0.9100

Bolded values represent significant ***P*** values. Mann Whitney Test. NAC, non-atopic control; GPA, grass pollen allergic; HDMA, house dust mite allergic; CA, cat allergic.

4.2.5 Computational algorithms confirm dysregulation of TIM-1$^+$ and IL-10$^+$ Breg Cell Subsets in SAR and PAR

Flow cytometry data was interrogated further utilising unbiased mathematical tools, viSNE and FlowSOM, to distinguish distinct IL-10$^+$ Breg subsets in NAC, SAR, and PAR. viSNE analysis revealed four distinct IL-10$^+$ B cell islands that were reduced in allergic groups compared to NAC (Figure 4.2.5.1, A, black islands). Although there was a distinct island of TIM-1$^+$ B cells enhanced in CA and HDMA compared to NAC and GPA (Figure 4.2.5.1, A, blue islands), two additional TIM-1$^+$ islands were increased in CA compared to all other groups (Figure 4.2.5.1, black islands). Supporting previous observations, cell surface marker expression was not aberrated between NAC, GPA, HDMA and CA (Figure 4.2.5.1, B). Upon overlaying IL-10$^+$ islands across cell surface marker channels, it was observed that CD71^{hi} B cells were strongly co-localised with IL-10$^+$ islands (Figure 4.2.5.1, B, black islands). FlowSOM identified four distinct MC (MC 1, MC 5, MC 27 and MC 32) that were dysregulated in allergic patients compared to NAC (Figure 4.2.5.2, A). Heatmap analysis revealed MC 1 to be IL-10$^+$TIM-1$^+$ Breg cells, which were significantly reduced in abundance in HDMA (NAC, $P = 0.0031$; GPA, $P = 0.0079$) and CA (NAC, $P = 0.0039$; GPA, $P = 0.0136$) compared to GPA and NAC (Figure 4.2.5.2, B-C). Although no aberration in IL-10 was observed, HDMA demonstrated increased TIM-1 expression compared to GPA ($P = 0.0389$) and CA ($P = 0.0468$). Heatmap analysis phenotyped MC 5 as memory CD27$^+$IgA$^+$IgG$_4^+$ B cells, which were significantly reduced in frequency in HDMA compared to NAC ($P = 0.0245$; Figure 4.2.5.2, D). Moreover, MC 5 IL-10 expression was significantly reduced in HDMA compared to NAC ($P = 0.0237$) and GPA ($P = 0.0272$). Although no difference in IgA expression was observed between groups, IgG$_4$ expression was significantly reduced in HDMA compared to GPA ($P = 0.0275$). Two IL-10$^{lo/-}$ TIM-1$^{lo/-}$ B cell populations, MC 27 and MC 32, were significantly increased in abundance in CA compared to NAC (both, $P < 0.0001$), GPA (MC 27, $P = 0.0136$; MC 32, $P = 0.0016$) and HDMA (MC 27, $P < 0.0001$; MC 32, $P = 0.0038$). MC 32 abundance was also significantly higher in HDMA compared to NAC ($P = 0.0003$).

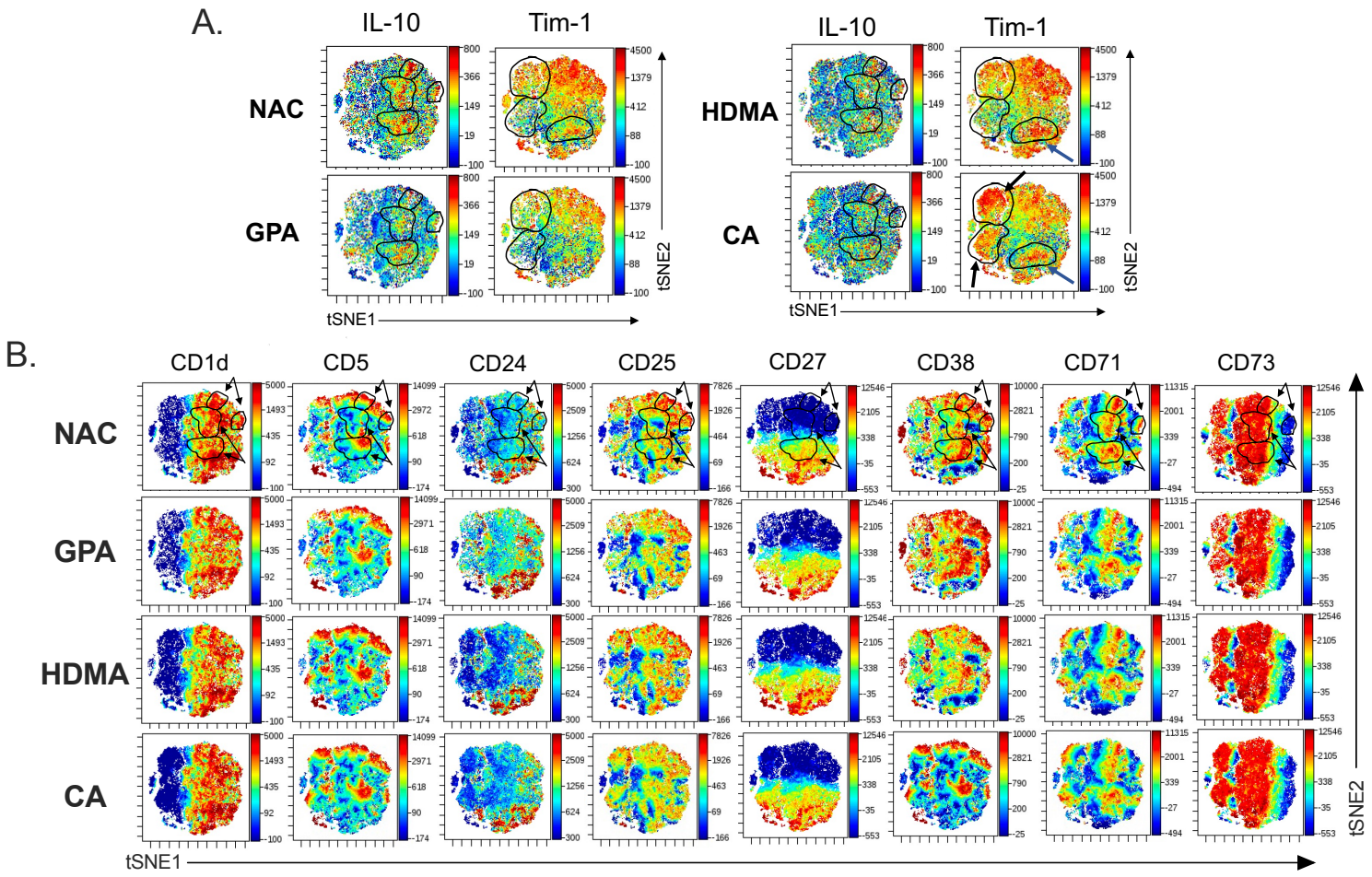


Figure 4.2.5.1 viSNE Analysis of CD19^{+} B cells reveals IL-10 and Tim-1 are dysregulated between GPA, CA, HDMA and NAC.

A) viSNE map of IL-10^{+} and Tim-1^{+}positive populations, indicated by black islands. Black arrows in Tim-1 channel represent a distinct Tim-1^{+} population absent in NAC, GPA and HDMA. **B)** Black arrows indicate overlay of IL-10^{+} islands over cell surface marker. viSNE data representative of n=5 concatenated FCS files per condition. NAC, non-atopic control; GPA, grass pollen allergic; CA, cat allergic; HDMA, house dust mite allergic.

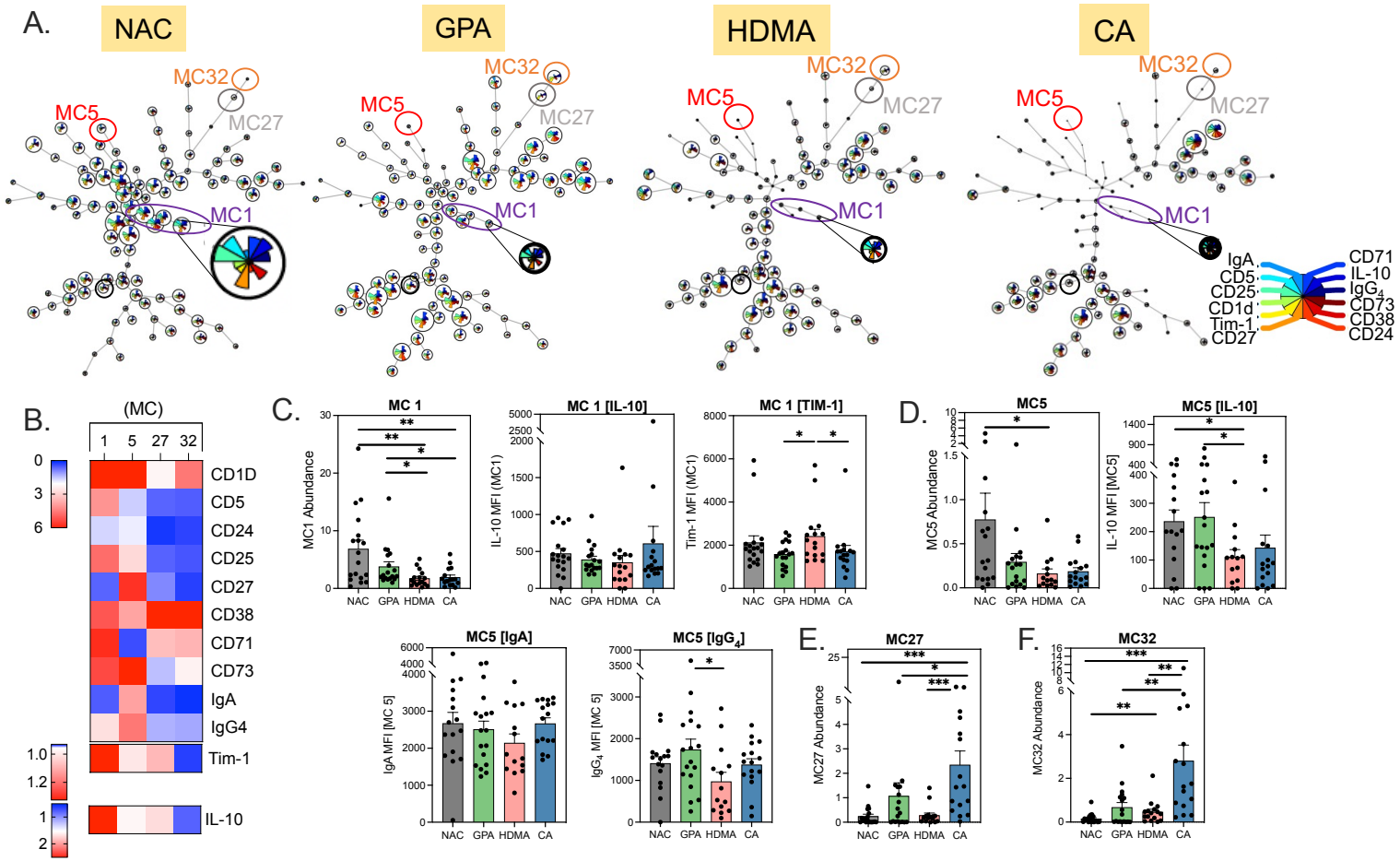


Figure 4.2.5.2 FlowSOM Analysis reveals IL-10$^+$ and Tim-1$^+$ Breg cells are dysregulated between GPA, CA, HDMA and NAC.

A) Representative FlowSOM star plots representing marker expression in NAC, GPA, HDMA and CA. Four distinct MC that are differentially expressed across allergic groups are highlighted: MC 1, 5, 27, 32. **B)** Heatmap of n=3 CpG/CD40L stimulated NAC samples. Quantification of population abundance and MFI expression for **C)** MC1, **D)** MC5, **E)** MC27 and **E)** MC32. Data representative of NAC, n=18; GPA, n=18; CA, n=16; HDMA, n=16. *P < 0.05, **P < 0.001, ***P < 0.0001, Mann Whitney Test. NAC, non-atopic control; GPA, grass pollen allergic; CA, cat allergic; HDMA, house dust mite allergic.

4.2.6 Correlation between IL-10$^+$ Breg Cells, Clinical Symptom Severity, Age and Gender

Correlation analysis of IL-10$^+$ Breg cells subset frequencies with clinical symptom scores (VAS), SPT scores and serological allergen-sIgE and tIgE levels, were performed to evaluate the relationship between IL-10$^+$ Breg cells and AR disease severity. Surprisingly, CD19$^+$IL-10$^+$ Breg cell frequencies were significantly correlated with enhanced VAS (P = 0.0111) and SPT (P = 0.0326) scores in GPA, with similar trends observed in other IL-10$^+$ Breg subsets (Figure 4.2.6.1, A and D and Appendix Figure 18.2). Although IL-10$^+$ Breg cell frequencies were not correlated with TG-sIgE, tIgE was positively correlated with memory CD27$^+$IL-10$^+$ Breg cell frequencies in GPA (P = 0.0047; Figure 4.2.6.1, G and Appendix Figure 13.1.1.2). Neither HDMA or CA demonstrated significant correlations between IL-10$^+$ Breg cell frequencies and any investigated patient demographic score (Figure 4.2.6.1, B-I and Appendix Figures 13.1.1.3 and 13.1.1.4). IL-10$^+$ Breg cell frequencies were also correlated with participant age and gender to identify any additional relationships that may have interfered with the observations of dysregulation observed with allergic status. Interestingly, CD19$^+$IL-10$^+$ Breg cell frequencies demonstrated a weak correlation with age, observed across all cross-sectional subjects and within the NAC group alone, although no significance was reached (Figure 4.2.6.1 J-K). Females demonstrated a slight trend of increased IL-10$^+$ Breg cell frequencies, although no significant difference between the male and female sex were observed between the pooled cross-sectional participants (P = 0.2857) or within NAC subjects alone (P = 0.1797; Figure 4.2.6.1, L-M). Finally, as there was an uneven distribution between monosensitised and polysensitised patients between GPA, HDMA and CA, IL-10$^+$ Breg cell frequencies were evaluated to determine whether polysensitisation to multiple allergens may drive further dysregulation. Although no significant difference between CD19$^+$IL-10$^+$ Breg cell frequencies were observed between monosensitised and polysensitized AR patients, it was noted that polysensitized individuals demonstrated a trend of increased Breg frequencies (Figure 4.2.6.1, N).

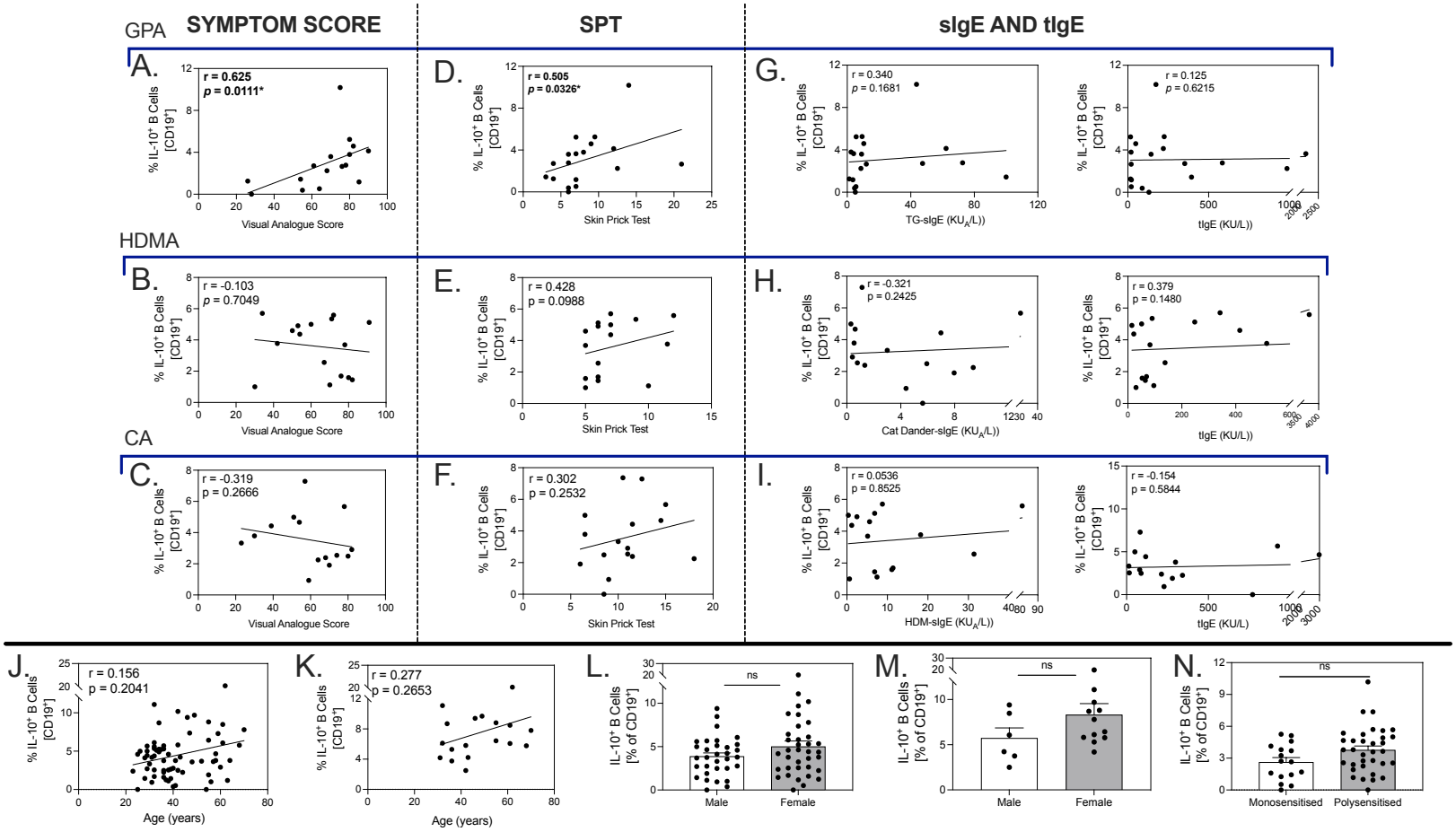


Figure 4.2.6.1 Correlation between IL-10$^+$ B cells and AR patient demographics.

Correlation between IL-10$^+$ Breg cells and VAS in **A)** GPA, **B)** HDMA and **C)** CA, and SPT in **D)** GPA, **E)** HDMA, **F)** CA, and allergen-sIgE and tIgE in **G)** GPA, **H)** HDMA and **I)** CA. Correlation between **J)** pooled NAC, GPA, HDMA and CA and **K)** NAC only, IL-10$^+$ Breg cells and age. Correlation between **L)** pooled NAC, GPA, HDMA and CA and **M)** NAC only, IL-10$^+$ Breg cells and gender. **N)** Correlation between pooled GPA, HDMA and CA IL-10$^+$ Breg cells and sensitisation status. *P < 0.05, **P < 0.001, Spearman Correlation test. Data representative of NAC, n=18; GPA, n=18; CA, n=16 and HDMA, n=16 subjects.

4.2.7 SAR IL-10$^+$ Breg cell demonstrate reduced sensitivity to CpG stimulation and IL-35$^+$IL-10$^+$TGFβ1$^+$ Breg cell frequencies compared to NAC.

Following confirmation IL-10$^+$ Breg cells are dysregulated in SAR individuals, two smaller studies characterising IL-10$^+$ Breg cell subset dysregulation further was performed. As per inclusion criteria (described in section 2.2), *n*=26 NAC and *n*=18 GPA were recruited, with GPA demonstrating significantly enhanced TG-sIgE, tIgE, SPT and VAS ($P < 0.001$) scores compared to NAC (Table 4.2.7.1).

To determine the sensitivity of SAR IL-10$^+$ Breg cells to respond to CD40L and CpG stimulation compared to NAC, PBMCs were stimulated with CpG (0.1μg/mL, 0.3μg/mL, 1μg/mL, 3μg/mL, 10μg/mL), with or without CD40L stimulation (2.5μg/mL) and evaluated by multi-parametric flow-cytometry. In the presence of CD40L, CpG stimulation resulted in a dose-dependent induction of SAR IL-10$^+$ Breg subsets which were significantly reduced compared to NAC at 1μg/mL (CD5$^+$IL-10$^+$, $P = 0.0266$; CD24^{hi}CD38^{hi}IL-10$^+$, $P = 0.0343$; CD27$^+$IL-10$^+$, $P = 0.0155$) and 3μg/mL (CD5$^+$IL-10$^+$, $P = 0.0044$; CD24^{hi}CD38^{hi}IL-10$^+$, $P = 0.0003$; CD27$^+$IL-10$^+$, $P = 0.0030$) CpG (Figure 4.2.7.1, A-C and Table 4.2.7.2). Moreover, CpG stimulation alone or in combination with CD40L induced significantly fewer CD19$^+$IL-10$^+$ (CpG alone, $P = 0.0022$; CpG+CD40L, $P = 0.0037$) and activated CD5^{hi}IL-10$^+$ (CpG alone, $P = 0.0065$; CpG+CD40L, $P = 0.0541$) Breg cells in SAR compared to NAC, with similar trends observed in other IL-10$^+$ Breg cell subsets (Figure 4.2.7.2, D-H and Table 4.2.7.3). SAR also demonstrated significantly reduced basal levels of CD19$^+$IL-10$^+$ ($P = 0.0012$), CD5$^+$ ($P = 0.0003$), and CD24^{hi}CD38^{hi} ($P = 0.0037$) IL-10$^+$ Breg cells within unstimulated samples compared to NAC. ELISA analysis revealed IL-10 protein was reduced in SAR cell culture supernatant compared to NAC in response to singular or combined stimulation with CpG and CD40L, however, no statistical significance was achieved due to the small sample size (Figure 4.2.7.1, I).

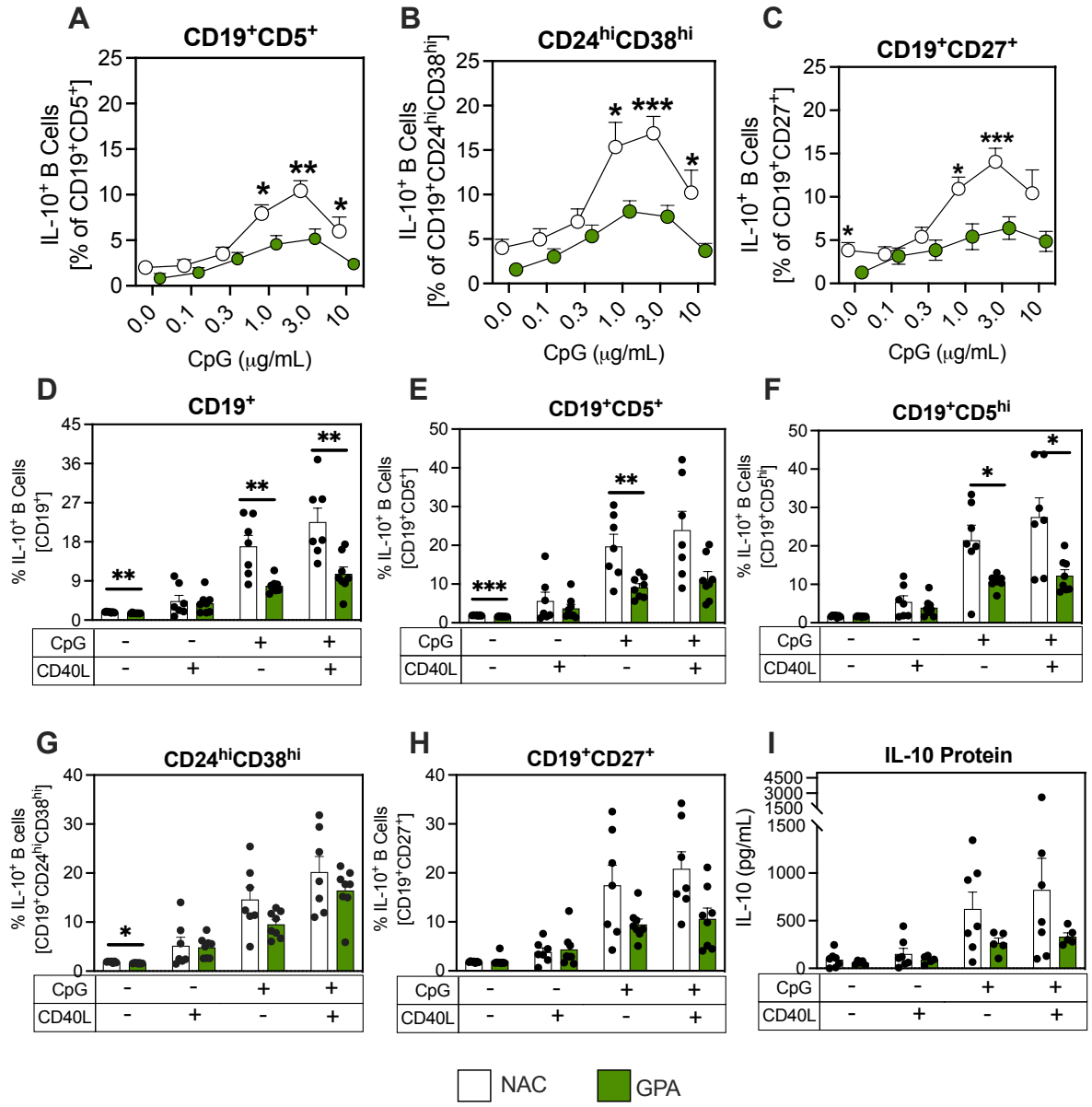


Figure 4.2.7.1 GPA demonstrate significantly reduced capability to induce IL-10$^+$ Breg cells in response to CD40L and CpG stimulation compared to NAC.

Effect of increasing doses of CpG in the presence of CD40L on **A)** CD5$^+$ **B)** CD24^{hi}CD38^{hi} and **C)** CD27$^+$ IL-10$^+$ Breg cells. Effect of singular and combined CpG and CD40L stimulation on the induction of **D)** CD19$^+$, **E)** CD5$^+$, **F)** CD5^{hi}, **G)** CD24^{hi}CD38^{hi} and **H)** CD27$^+$ IL-10$^+$ Breg cell subsets. **I)** IL-10 protein levels in culture supernatants as measured by ELISA. Data representative of n=8 GPA and n=10 NAC [**A-C)** 10μg/mL, n=6; 0.1μg/mL, n=7; **D-I)** n=7] and presented as mean ±SEM. *P<0.05, **P < 0.01, ***P < 0.001, Mann-Whitney Test. NAC, non-atopic control; GPA, grass pollen allergic,

Table 4.2.7.1 Patient Demographics of subjects enrolled for B cell culture stimulation experiments in NAC and SAR.

Characteristic	NAC (n=26)	GPA (n=18)
Gender. M:F	10:16	7:11
Age (years), range	25-68	27-63
Allergen-specific sIgE (kU_A/L), mean ± SD	0.0 ± 0.0*	33.4 ±29.3*,$^{+++}$
Allergen-specific SPT (mm^2) ± SD	0 ± 0	8.5 ±2.6^{+++}
tIgE (kU_A/L), mean ± SD	35.3 ±32.9**	402.7 ±516.2**,$^{+++}$
Visual Analogue Score	0 ±0	77 ±12^{+++}

*sIgE missing for n=2 NAC and n=1 GPA. **tIgE missing for n=4 NAC and n=1 GPA. SPT, skin prick test; NAC, non-atopic control; GP, grass pollen; sIgE,specific immunoglobulin E; tIgE, total IgE. $^{+}$, denotes significance between GPA and NAC, Mann Whitney Test, *** $P < 0.001$.

Table 4.2.7.2 IL-10^{+} Breg Cell Subsets in SAR and NAC Following stimulation with increasing dosages of CpG alongside CD40L

CpG Concentration	CD40L Concentration.	B Cell Subset	NAC Delta Unstimulated				GPA Delta Unstimulated				*P* value vs GPA
			n	mean	SD	SEM	n	mean	SD	SEM	
0	2.5	$CD19^{+}CD5^{+}IL\text{-}10^{+}$	10	2.01	1.77	0.56	8	0.823	1.46	0.52	0.1679
		$CD19^{+}CD24^{hi}CD38^{hi}IL\text{-}$	10	5.77	3.29	1.04	8	1.62	1.38	0.49	0.0639
		$CD19^{+}CD27^{+}IL\text{-}10^{+}$	10	5.88	3.04	0.96	8	1.26	1.45	0.51	**0.0339**
0.1	2.5	$CD19^{+}CD5^{+}IL\text{-}10^{+}$	7	2.21	1.75	0.66	8	1.44	1.52	0.54	0.5882
		$CD19^{+}CD24^{hi}CD38^{hi}IL\text{-}$	7	5.79	1.84	0.69	8	3.01	2.55	0.90	0.1520
		$CD19^{+}CD27^{+}IL\text{-}10^{+}$	7	2.59	2.14	0.81	8	3.16	2.67	0.95	0.9259
0.3	2.5	$CD19^{+}CD5^{+}IL\text{-}10^{+}$	10	3.51	2.31	0.73	8	2.94	2.01	0.71	0.7618
		$CD19^{+}CD24^{hi}CD38^{hi}IL\text{-}$	10	8.84	4.51	1.43	8	5.33	3.50	1.24	0.6334
		$CD19^{+}CD27^{+}IL\text{-}10^{+}$	10	7.60	3.18	1.01	8	3.84	3.28	1.16	0.5726
1	2.5	$CD19^{+}CD5^{+}IL\text{-}10^{+}$	10	7.92	3.02	0.96	8	4.56	2.66	0.94	**0.0266**
		$CD19^{+}CD24^{hi}CD38^{hi}IL\text{-}$	10	17.20	8.82	2.79	8	8.10	3.44	1.22	**0.0343**
		$CD19^{+}CD27^{+}IL\text{-}10^{+}$	10	13.10	4.11	1.30	8	5.40	4.19	1.48	**0.0155**
3	2.5	$CD19^{+}CD5^{+}IL\text{-}10^{+}$	10	10.4	3.48	1.1	8	5.16	3.06	1.08	**0.0044**
		$CD19^{+}CD24^{hi}CD38^{hi}IL\text{-}$	10	18.80	6.00	1.90	8	7.51	3,56	1.26	**0.0003**
		$CD19^{+}CD27^{+}IL\text{-}10^{+}$	10	16.30	4.45	1.41	8	6.39	3.69	1.31	**0.0003**
10	2.5	$CD19^{+}CD5^{+}IL\text{-}10^{+}$	6	6.00	3.82	1.56	8	2.38	1.05	0.37	**0.0273**
		$CD19^{+}CD24^{hi}CD38^{hi}IL\text{-}$	6	12.1	6.20	2.52	8	3.69	2.31	0.82	**0.0283**
		$CD19^{+}CD27^{+}IL\text{-}10^{+}$	6	12.20	6.62	2.70	8	4.86	3.26	1.15	0.1812

Bolded Values Represent significant ***P*** Values. Mann Whitney U Test. NAC, non-atopic control; GPA, grass pollen allergic.

Table 4.2.7.3 Comparison of CpG and CD40L stimulation of IL-10$^+$ Breg cells in SAR and NAC

Parameter/Condition	B Cell Subset	NAC				GPA				*P* value vs NAC
		n	mean	SD	SEM	n	mean	SD	SEM	
Unstimulated	CD19$^+$IL-10$^+$	7	1.82	0.11	0.04	8	1.58	0.09	0.03	**0.0012**
	CD19$^+$CD5$^+$IL-10$^+$	7	1.90	0.09	0.03	8	1.60	0.07	0.03	**0.0003**
	CD19$^+$CD5^{hi}IL-10$^+$	7	1.71	0.24	0.09	8	1.64	0.11	0.04	0.4434
	CD19$^+$CD27$^+$IL-10$^+$	7	1.82	0.14	0.05	8	2.00	1.04	0.37	0.0939
	CD19$^+$CD24^{hi}CD38^{hi}IL-10$^+$	7	1.87	0.14	0.05	8	1.61	0.07	0.25	**0.0037**
CD40L	CD19$^+$IL-10$^+$	7	4.35	3.54	1.34	8	3.84	2.33	0.83	>0.9999
	CD19$^+$CD5$^+$IL-10$^+$	7	5.62	5.85	2.21	8	3.75	2.89	1.02	0.7789
	CD19$^+$CD5^{hi}IL-10$^+$	7	5.44	4.17	1.58	8	3.95	2.45	0.87	0.6126
	CD19$^+$CD27$^+$IL-10$^+$	7	3.84	2.23	0.84	8	4.38	3.51	1.24	0.8424
	CD19$^+$CD24^{hi}CD38^{hi}IL-10$^+$	7	5.19	4.59	1.73	8	4.84	2.09	0.74	0.3969
CpG	CD19$^+$IL-10$^+$	7	17.0	6.61	2.50	8	7.86	1.63	0.58	**0.0022**
	CD19$^+$CD5$^+$IL-10$^+$	7	19.7	8.27	3.12	8	9.16	2.70	0.95	**0.0065**
	CD19$^+$CD5^{hi}IL-10$^+$	7	21.5	10.3	3.88	8	10.7	1.73	0.61	**0.0205**
	CD19$^+$CD27$^+$IL-10$^+$	7	17.5	10.8	4.09	8	9.47	3.13	1.11	0.2319
	CD19$^+$CD24^{hi}CD38^{hi}IL-10$^+$	7	14.6	6.72	2.54	8	9.54	2.66	0.94	0.1520
CpG+CD40L	CD19$^+$IL-10$^+$	7	22.6	8.48	3.20	8	10.6	4.39	1.55	**0.0037**
	CD19$^+$CD5$^+$IL-10$^+$	7	23.9	12.8	4.84	8	11.3	5.51	1.95	0.0541
	CD19$^+$CD5^{hi}IL-10$^+$	7	27.5	13.3	5.03	8	12.3	4.34	1.53	0.4330
	CD19$^+$CD27$^+$IL-10$^+$	7	20.8	9.22	3.49	8	10.6	6.16	2.18	0.0541
	CD19$^+$CD24^{hi}CD38^{hi}IL-10$^+$	7	20.2	8.39	3.17	8	16.4	4.79	1.70	0.6723

Bolded Values Represent significant ***P*** Values. Mann-Whitney Test. CD40L, CD40 Ligand; NAC, non-atopic control; GPA, grass pollen allergic.

Following observations IL-10$^+$ B cells are associated with additional suppressive molecules (described in Section 3.2.5), SAR PBMCs were stimulated with 1μg/mL CpG and 2.5μg/mL CD40L, and B cell expression of CD80, CD86, IL-35 and TGFβ1 was evaluated by multi-parametric flow cytometry. There were no strong aberrations between CD80$^+$, CD86$^+$, CD80$^+$IL-10$^+$ or CD86$^+$IL-10$^+$ B cell frequencies between SAR and NAC (all, $P > 0.05$; Figure 4.2.7.2, A-B and Table 4.2.7.4). Although SAR demonstrated a weak trend of increased TGF-β1$^+$ B cell frequencies compared to NAC, no differences in dual positive TGF-β1$^+$IL-10$^+$ Breg cells were observed. Memory CD27$^+$IL-35$^+$ B cells were significantly reduced in SAR compared to NAC ($P = 0.0185$), with similar trends of attenuation observed in CD19$^+$ and CD5$^+$/^{hi} B cell subsets and dual-positive IL-10$^+$IL-35$^+$ Breg subsets. Relationships between IL-10$^+$ Breg cells and expression of IL-35 and TGF-β1 in NAC and SAR were interrogated further utilising unbiased dimensionality reduction tools, with viSNE analysis supporting flow cytometry observations through revealing three distinct islands of CD19$^+$ B cells which expressed IL-12p35 and Ebi3 that were reduced in expression in SAR compared to NAC, which co-localised with IL-10$^+$ islands (Figure 4.2.7.2, C, black islands). viSNE map also revealed a TGF-β1$^+$ island which was upregulated in SAR compared to NAC (Figure 4.2.7.2, C, red islands). Interestingly, three further TGF-β1$^+$ islands which co-localised with IL-12p35$^+$, Ebi3$^+$ and IL-10$^+$ B cell islands were downregulated in SAR compared to NAC, revealing a smaller population of IL-10$^+$IL-35$^+$TGFβ1$^+$ Bregs cells (Figure 4.2.7.2, C, black islands). FlowSOM heatmap analysis revealed two MC representing IL-35$^+$ B cells: MC 8 and MC 17 (Figure 4.2.7.2, D). Interestingly, although abundance of MC 8 and MC 17 was slightly increased in SAR patients, both IL-12p35 and Ebi3 subunit expression was higher in NAC (Figure 4.2.7.2, E-F). Heatmap analysis revealed MC 24 to represent the IL-10$^+$IL-35$^+$TGF-β1$^+$ Breg cell subset, phenotyped as CD5^{hi}CD24$^-$CD27^{hi}CD38$^+$CD80^{hi}CD86^{hi} B cells, which was reduced in abundance in SAR compared to NAC, alongside attenuation of IL-12p35 and IL-10 expression (Figure 4.2.7.2, G).

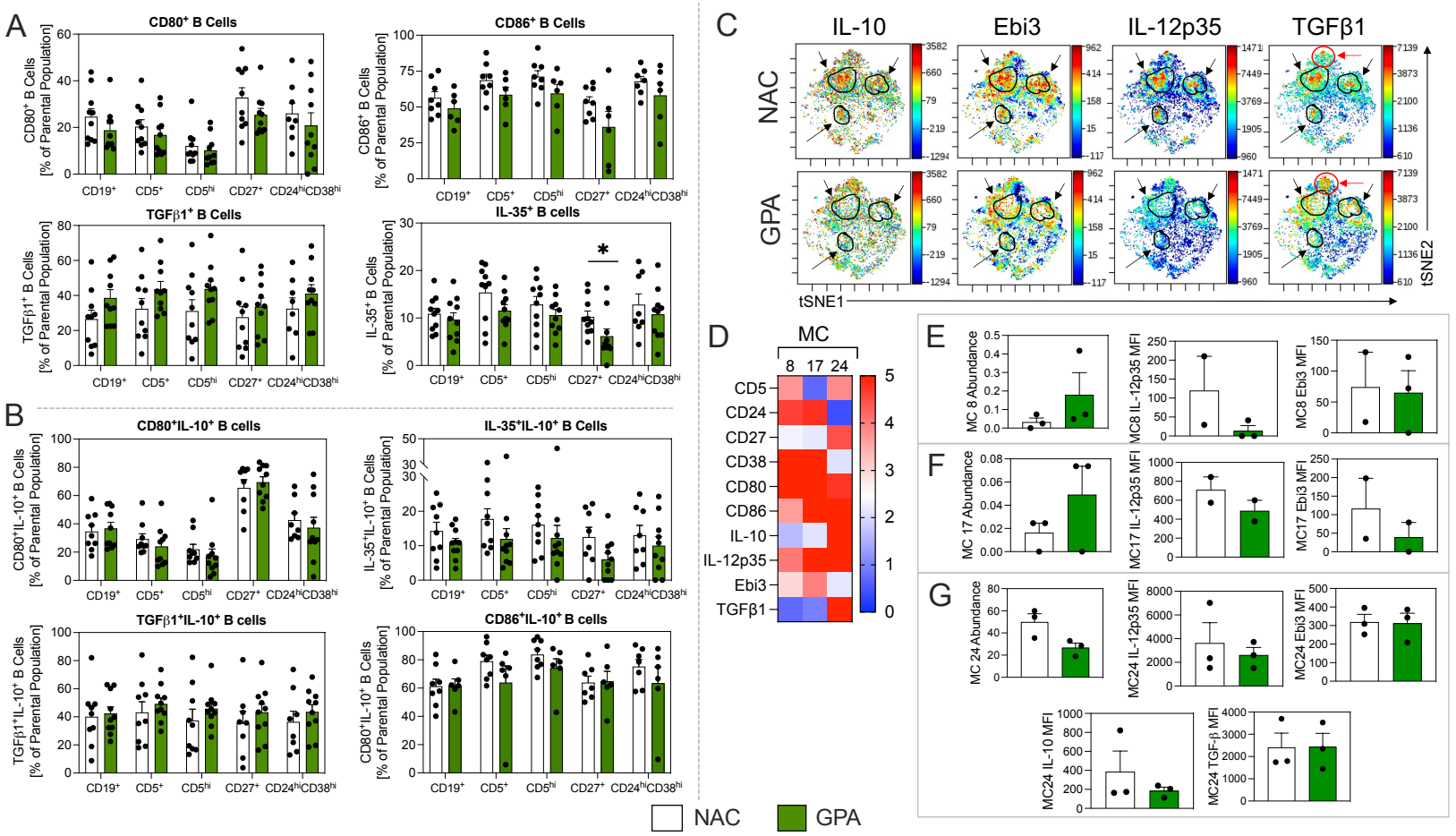


Figure 4.2.7.2 IL-35$^+$ B cells and IL-35$^+$IL-10$^+$TGFβ1$^+$ Breg cell B cells are reduced in GPA compared to NAC.

Flow-cytometry data demonstrating **A)** CD80$^+$, CD86$^+$, IL-35$^+$ and TGF-β1$^+$ B cells, and **B)** CD80$^+$IL-10$^+$, CD86$^+$IL-10$^+$, IL-35$^+$IL-10$^+$ and TGF-β1$^+$IL-10$^+$ Breg cells. **C)** viSNE map of CD19$^+$ B cells where IL-12p35$^+$IL-10$^+$Ebi3$^+$TGFβ1$^+$ and TGFβ1$^+$ expressing islands are highlighted by black islands and red arrows, respectively. **D)** Heatmap analysis of FlowSOM-derived MC. Population abundance and MFI expression for **E)** MC 8, **F)** MC 17 and **G)** MC 24. Data representative of **A-B)** NAC, n=10 and GPA, n=10, **C)** n=3 concatenated files per patient group and **D-G)** NAC, n=3 and GPA, n=3, and presented as mean ±SEM. *P < 0.05, Mann Whitney Test. NAC, non-atopic control. GPA, grass pollen allergic.

Table 4.2.7.4. IL-35$^+$ B cells are significantly reduced in SAR compared to NAC.

	Culture Conditions	B Cell Subset	NAC Delta				GPA Delta				*P* value NAC v GPA
			n	mean	SD	SEM	n	mean	SD	SEM	
TGF-ß1	CpG/CD40L	CD19$^+$TGF-1$^+$	10	33.7	14.4	4.56	10	38.6	15.2	4.82	0.1051
		CD19$^+$CD5$^+$TGF-ß1$^+$	10	38.7	17.2	5.44	10	43.6	13.9	4.40	0.2475
		CD19$^+$CD5^{hi}TGF-ß1$^+$	10	37.2	19.1	6.04	10	43.7	14.5	4.59	0.1230
		CD19$^+$CD27$^+$TGF-ß1$^+$	10	35.6	16.8	5.32	10	33.6	15.8	4.99	0.3527
		CD19$^+$CD24^{hi}CD38^{hi}TGF-ß1$^+$	9	36.0	15.6	5.19	10	41.1	16.1	5.10	0.4082
	CpG/CD40L (IL-10$^+$ Cells)	CD19$^+$TGF-ß1$^+$IL-10$^+$	9	40.0	21.0	7.01	10	42.4	14.9	4.71	0.7802
		CD19$^+$CD5$^+$TGF-ß1$^+$IL-10$^+$	9	43.1	22.6	7.54	10	49.2	12.9	4.08	0.4967
		CD19$^+$CD5^{hi}TGF-ß1$^+$IL-10$^+$	9	37.4	24.3	8.09	10	45.8	13.4	4.23	0.2775
		CD19$^+$CD27$^+$TGF-ß1$^+$IL-10$^+$	8	35.5	23.7	8.39	10	43.2	18.6	5.87	0.4082
		CD19$^+$CD24^{hi}CD38^{hi}TGF-ß1$^+$IL-10$^+$	8	36.3	21.8	7.72	10	43.5	16.2	5.11	0.4598
IL-35	CpG/CD40L	CD19$^+$IL-35$^+$	10	12.8	3.77	1.19	10	9.65	4.65	1.47	0.5288
		CD19$^+$CD5$^+$IL-35$^+$	10	17.2	6.09	1.93	10	11.5	4.01	1.27	0.0753
		CD19$^+$CD5^{hi}IL-35$^+$	10	14.7	5.36	1.69	10	10.6	3.84	1.21	0.3150
		CD19$^+$CD27$^+$IL-35$^+$	10	12.3	3.92	1.24	10	6.15	4.91	1.55	**0.0185**
		CD19$^+$CD24^{hi}CD38^{hi}IL-35$^+$	8	15.0	6.01	2.13	10	10.8	5.42	1.42	0.6965
	CpG/CD40L (IL-10$^+$ Cells)	CD19$^+$IL-35$^+$IL-10$^+$	9	14.3	7.78	2.59	10	10.7	4.48	1.42	0.3562
		CD19$^+$CD5$^+$IL-35$^+$IL-10$^+$	9	17.7	8.97	2.99	10	11.9	9.56	3.02	0.1333
		CD19$^+$CD5^{hi}IL-35$^+$IL-10$^+$	9	16.1	7.66	2.55	10	12.2	11.7	3.68	0.1564
		CD19$^+$CD27$^+$IL-35$^+$IL-10$^+$	8	12.5	8.04	2.84	10	6.05	5.98	1.89	0.1053
		CD19$^+$CD24^{hi}CD38^{hi}IL-35$^+$IL-10$^+$	8	13.0	8.13	2.87	10	10.0	8.26	2.61	0.4449
CD80	CpG/CD40L	CD19$^+$IL-35$^+$	10	24.6	11.0	3.48	10	18.8	9.20	2.91	0.1378
		CD19$^+$CD5$^+$IL-35$^+$	10	20.3	9.56	3.02	10	16.8	8.96	2.83	0.3527
		CD19$^+$CD5^{hi}IL-35$^+$	10	12.0	7.56	2.39	10	10.2	6.25	1.98	0.3527
		CD19$^+$CD27$^+$IL-35$^+$	10	32.8	13.5	4.26	10	25.4	8.68	2.74	0.2549
		CD19$^+$CD24^{hi}CD38^{hi}IL-35$^+$	8	26.0	12.7	4.49	10	20.9	17.1	5.41	0.3527
	CpG/CD40L (IL-10$^+$ Cells)	CD19$^+$IL-35$^+$IL-10$^+$	9	34.6	13.3	4.44	10	36.8	13.8	4.38	0.7639
		CD19$^+$CD5$^+$IL-35$^+$IL-10$^+$	9	29.2	11.2	3.75	10	24.0	14.1	4.45	0.4002
		CD19$^+$CD5^{hi}IL-35$^+$IL-10$^+$	9	22.0	10.7	3.55	10	17.3	15.5	4.91	0.7802
		CD19$^+$CD27$^+$IL-35$^+$IL-10$^+$	8	65.4	16.3	5.78	10	69.5	12.0	3.79	0.5298
		CD19$^+$CD24^{hi}CD38^{hi}IL-35$^+$IL-10$^+$	8	42.6	14.3	5.07	10	37.3	23.4	7.41	0.3154
Cd86	CpG/CD40L	CD19$^+$IL-35$^+$	8	56.3	12.5	4.4	6	49.0	11.7	4.78	0.3450
		CD19$^+$CD5$^+$IL-35$^+$	8	68.6	11.9	4.2	6	58.5	13.0	5.31	0.2284
		CD19$^+$CD5^{hi}IL-35$^+$	8	71.1	11.8	4.17	6	59.5	15.5	6.32	0.1419
		CD19$^+$CD27$^+$IL-35$^+$	8	53.4	10.6	3.74	6	36.1	26.4	10.8	0.1812
		CD19$^+$CD24^{hi}CD38^{hi}IL-35$^+$	7	67.8	9.46	3.57	6	58.1	20.8	8.48	0.5338
	CpG/CD40L (IL-10$^+$ Cells)	CD19$^+$IL-35$^+$IL-10$^+$	6	61.3	14.2	5.06	6	61.8	11.5	4.69	0.8518
		CD19$^+$CD5$^+$IL-35$^+$IL-10$^+$	6	79.0	12.2	4.33	6	63.9	28.9	11.8	0.4136
		CD19$^+$CD5^{hi}IL-35$^+$IL-10$^+$	6	83.7	10.5	3.7	6	74.1	16.2	6.6	0.2824
		CD19$^+$CD27$^+$IL-35$^+$IL-10$^+$	6	63.9	12.1	4.58	6	64.8	17.5	7.13	0.6282
		CD19$^+$CD24^{hi}CD38^{hi}IL-35$^+$IL-10$^+$	6	75.2	13.3	5.05	6	63.4	28.3	11.5	0.6282

Bolded values represent significant ***P*** values. Mann Whitney Test

4.3 Summary

In this chapter, I confirmed IL-10$^+$ Breg cell frequencies and IL-10 propensity are reduced in SAR and PAR patients compared to NAC during a large blinded cross-sectional study, confirmed by unbiased computational algorithms and in line with previous studies (202). TIM-1$^+$ B cells and distinct subsets of dual positive TIM-1$^+$IL-10$^+$ Breg cell frequencies were significantly enhanced in HDMA and CA patients compared to SAR and NAC patients, highlighting potential discrepancies underlying SAR and PAR disease pathophysiology. IL-10$^+$ Breg cells were significantly enhanced in IgG_4 expression compared to IL-10$^-$ Breg cells, corroborating findings in smaller scale studies (253), although no clear aberration in IgA expression between IL-10$^-$ and IL-10$^+$ B cells was found in any group. Frequencies of IgG_4^+ and IgA$^+$ memory CD27$^+$IL-10$^+$ Breg cell subsets were strongly positively correlated, with IgG_4^+IL-10$^+$ Breg cell frequencies negatively correlated with serum allergen-sIgE levels in CA. Interestingly, a strong correlation between IL-10$^+$ Breg cell frequencies and clinical symptom severity was observed in SAR but not PAR patients. Finally, SAR patients demonstrated significantly attenuated IL-35$^+$ B cells compared to NAC, with similar trends observed in dual positive IL-10$^+$IL-35$^+$ Breg cells. Computational algorithms confirmed triple positive IL-10$^+$IL-35$^+$TGFß1$^+$ Breg cells were downregulated in SAR compared to NAC. Collectively, this chapter confirms IL-10$^+$ Breg cells are dysregulated in AR patients and highlights potential nuances in IL-10$^+$ Breg cell aberration between SAR and PAR, in addition to the identification of novel IL-10$^+$IL-35$^+$TGFß1$^+$ B cell subsets which are reduced in SAR patients.

CHAPTER 5. ALLERGEN IMMUNOTHERAPY RESTORES IL-10$^+$ BREG CELLS IN GPA SAR PATIENTS

5.1 Introduction

AIT remains the only disease modifying treatment for AR, establishing long-term clinical tolerance to administered allergen, allowing for symptom elevation and QoL improvement (74, 159). SCIT has been associated with restoration of IL-10$^+$ Breg cell frequencies, enhancement of serum allergen-sIgG$_4$ and suppression of allergen-sIgE levels (96, 198-200, 204). However, the exact IL-10$^+$ Breg cell frequencies which are targeted during SCIT and whether they are responsible for the enhancement of allergen-sIgG$_4$ remains to be fully elucidated. To date, no studies have evaluated the ability of SCIT to modulate TIM-1$^+$ B cell or dual positive TIM-1$^+$IL-10$^+$ Breg frequencies, which may provide insight into AIT mechanism of action. As GP allergy is a SAR, occurring in response to seasonal allergies, it is imperative to investigate B cell modulations during and outside of the GP season to decipher whether potential AIT-induction of Breg cell frequencies is modulated by natural seasonal exposure to allergen. There is not yet a universally accepted biomarker of AIT efficacy able to predict patient efficacy and allow accurate stratification of responders and non-responders (159). For example, modulation of humoral biomarkers, such as tIgE, sIgE, IgG and IgA isotypes and IgE blocking factors, are often deemed one of the hallmarks of successful AIT. However, correlation of tIgE, allergen sIgE and sIgG$_4$ levels with clinical response to treatment has been inconsistent across studies (213, 214, 366, 367). Moreover, following novel observations during the recent GRASS trial that IgA and IgG$_4$ are preferentially induced by SLIT and SCIT respectively, it must be considered that various administration routes of AIT may elicit differentially immunomodulatory effects, complicating identification of a reliable humoural biomarker further (96). Although numerous innate and adaptive cellular biomarkers understood to be involved in AR disease pathogenesis have been identified in small experimental studies, namely T$_H$2 cells, Tregs,

ILC2s, DCs and IL-10$^+$ Bregs, the lack of large clinical trial data to support these findings, in addition to the absence of consistent trends with clinical response across studies remains a challenge in validating these biomarkers (117, 123, 253, 368). It is also important to note additionally that widespread investigation of cellular biomarkers is limited by the complexity of the experimental procedures required to investigate these cells. Several candidate cytokines (IFN-β, IFN-λ, IL-33 and IL-25 (111)) and metabolic (lactic acid, ornithine, creatinine, nitric acid (369, 370)) biomarkers have also been proposed to date, however findings are either inconsistent across studies or limited to small-scale trials. In addition to measuring antibody and cellular levels, functional assays, such as IgE-facilitated binding assays and basophil and mast cell activation tests have also been described to investigate the function of candidate biomarkers, although their correlation with clinical response and validity remains to be assessed (38, 39, 371). Finally, *in vivo* biomarkers such as SPT, intradermal dilution testing, and skin patch tests, have also been described as potential biomarkers of AIT (372, 373). Therefore, further studies are required to decipher prognostic and predictable markers associated with AIT treatment.

5.1.1 Hypotheses and Aims

5.1.1.1 Hypotheses

1. IL-10$^+$ Breg cells are restored in SAR patients following SCIT-treatment to similar levels observed in NAC.

5.1.1.2 Aims

4. To determine whether SCIT-treatment restores IL-10$^+$ Breg cell frequencies in SAR patients compared to NAC.
5. To evaluate whether SCIT-treatment modifies TIM-1 expression on SAR B cells.

6. To evaluate whether SCIT-treatment modifies serum TG-sIgE, tIgE and TG-sIgG$_4$ levels.
7. To interrogate flow-cytometry evaluations of IL-10$^+$ and Tim-1$^+$ Breg cells in NAC, SAR, and SCIT-treated samples through viSNE and FlowSOM mathematical algorithms
8. To assess whether IL-10$^+$ Breg cells correlate with symptom severity or length of SCIT administration.

5.2 Results

5.2.1 Dysregulation of IL-10$^+$ Breg cells in SAR are restored following GP-SCIT treatment

Following confirmation in Chapter 4 that IL-10$^+$ Breg cell subsets are dysregulated in SAR compared to NAC, the ability of SCIT treatment to restore IL-10$^+$ Breg cells abnormalities in SAR patients was confirmed during a blinded cross-sectional study. As GPA is a seasonal allergy, recruited NAC, GPA and SCIT-treated subjects were differentiated into 'in season' (IS; May-July) or 'out season' (OS; August-April) donors dependent on donation date (Table 5.2.1.1). SCIT-treated donors received treatment for a minimum of 1 year prior to sample donation, with a median treatment duration of 21.3 months for IS samples and 29 months for OS donors. Of note, one SCIT-treated OS donor had completed treatment 19 months prior to sample donation. GPA and SCIT-treated subjects reported significantly increased VAS and TNSS scores compared to NAC (all, $P < 0.05$; Figure 5.2.1.1, A and B). SCIT patients also reported decreased VAS ($P < 0.05$) and TNSS compared to GPA during the GP season. Patients completed GE2 self-assessment clinical questionnaires (described in section 2.2.1) to assess their symptom severity in relation to either the previous GP season (NAC and GPA) or before SCIT administration (SCIT-treated patients) with both IS ($P < 0.05$) and OS SCIT donors recording improvement in symptom severity following treatment compared to GPA, suggestive of clinical efficacy (Figure 5.2.1.1, C).

Table 5.2.1.1 Patient Demographics and clinical characteristics of subjects enrolled for cross-sectional study of IL-10$^+$ B cell culture stimulation in GP-SCIT-treated subjects.

Characteristic	NAC IS (n=10)	NAC OS (n=8)	GPA IS (n=7)	GPA OS (n=11)	SCIT IS (n=4)	SCIT OS (n=12)
Gender, M:F	3:7	3:5	5:2	5:6	1:3	6:6
Age (years), range	32-68	31-70	25-64	29-63	39-60	32-68
TG-sIgE (kU$_A$/L), mean ± SD	0.0 ±0.0	0.0 ±0.0	20.4 ±23.0	24.1 ±33.9	12.1 ±7.9	27.3 ±29.9
Allergen-specific SPT	0.0 ±0.0	0.0 ±0.0	9.4 ±2.8	7.6 ±5.1	8.9 ±6.2	7.4 ±4.0
tIgE (kU$_A$/L), mean ± SD	23 ±19	23 ±46	121 ±92	433 ± 646	90 ±37*	277 ± 343
VAS, mean ± SEM	0.0 ±0.0	0.0 ±0.0	80.8 ±8.0**,$^{+++}$	72.8 ±12.1**,$^{+++}$	31.5 ±31.9$^{\phi}$,$^{+++}$	55.1 ±34.7**,$^{+++}$
TNSS, mean ± SEM	0.0 ±0.0	0.0 ±0.0	11.3 ±5.8^{+++}	3.9 ±5.1^{+}	4.0 ±2.8^{+}	6.2 ±4.6^{+++}
GE2 (-3 to +3), mean ± SEM	0.0 ±0.0	0.0 ±0.0	-0.75 ±0.96	0.89 ±1.3	1.0 ±1.6^{+}	2.2 ±0.87$^{\phi}$,$^{+++}$
Monosensitised	-	-	4	8	2	2
Polysensitised	-	-	3	3	2	10
Duration of SCIT (Months), mean ± SD	-	-	-	-	21.3 ±6.0	29±13.2
Duration of SCIT Withdrawal (Months)	-	-	-	-	-	19 (n=1)

*tIgE for n=1 GP-SCIT IS donor, and **, VAS for n=1 GPA IS, n=1 GPA OS, n=4 SCIT OS not available. $^{+}$, detonates statistical significance between NAC IS/OS and respective GPA and SCIT IS/OS. $^{\phi}$, detonates statistical significance between SCIT IS/OS and respective GPA IS/OS. *P < 0.05, **P < 0.001, Mann Whitney test. IS, in season; OS, out season; SPT, skin prick test; NAC, non-atopic control; GPA, grass pollen allergic; SCIT, subcutaneous immunotherapy, sIgE, specific immunoglobulin E; tIgE, total IgE; TG, timothy grass.

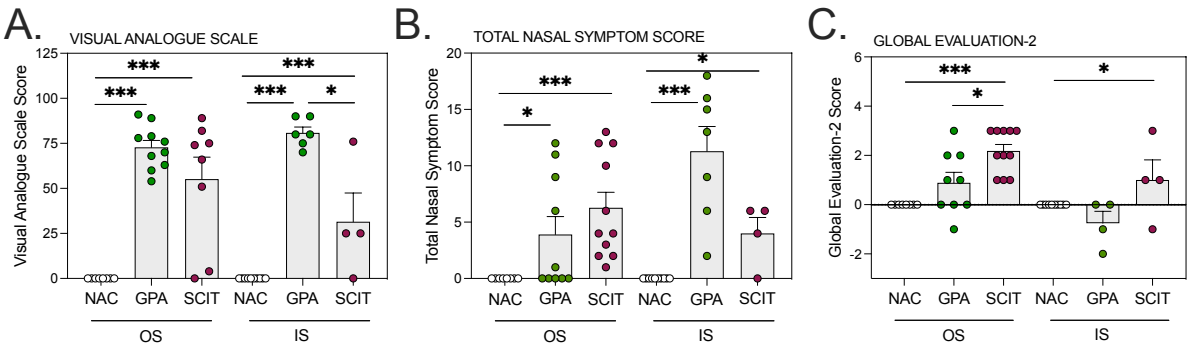


Figure 5.2.1.1 Clinical symptom scores from patients enrolled for cross-sectional study of IL-10$^+$ B cell culture stimulation in GP-SCIT-treated subjects.

A) VAS, **B)** TNSS, and **C)** GE2 scores**.** Data representative of NAC IS, n=10, NAC OS, n=8, GPA IS, n=7, GPA OS, n=11, SCIT IS, n=4 and SCIT OS, n=12 [N.B. **A)** VAS for n=1 GPA IS, n=1 GPA OS, n=4 SCIT OS; **B)** TNSS for n=1 GPA OS; and **C)** n=3 GPA IS, n=2 GPA OS not available].Presented as mean ±SEM. *P < 0.05, **P < 0.001, Mann Whitney test. IS, in season; OS, out season; NAC, non-atopic control; GPA, grass pollen allergic; SCIT, subcutaneous immunotherapy; VAS, visual analogue scale; GE, global evaluation.

To assess the effects of SCIT on IL-10$^+$ Breg cells, NAC, GPA, and SCIT patient PBMCs were stimulated with 1μg/mL CpG and 2.5μg/mL CD40L and evaluated by multi-parametric flow-cytometry. NAC demonstrated no aberration in any IL-10$^+$ Breg cell subset frequencies between IS or OS donors (all subsets, $P > 0.05$; Figure 5.2.1.2, A-F and Table 5.2.1.2). However, GPA demonstrated significant increases in CD19$^+$ ($P = 0.0001$), CD5$^+$ ($P = 0.0012$) and CD25$^+$CD71^{hi}CD73^{lo} ($P = 0.0164$) IL-10$^+$ Breg cell frequencies during the GP season, with similar trends observed in other Breg subsets (Figure 5.2.1.2, A-G). In contrast, IS SCIT patients demonstrated significant decreases in CD5^{hi} ($P = 0.0401$) and CD1d^{hi}CD5$^+$ IL-10$^+$ Breg cells ($P = 0.0162$) compared to OS SCIT donors. Although only CD24^{hi}CD38^{hi} IL-10$^+$ Breg cells were significantly reduced in GPA compared to NAC ($P = 0.0460$) during the GP season, all investigated IL-10$^+$ Breg cell subsets were significantly reduced in GPA compared to NAC outside of the GP season (all, $P < 0.05$). SCIT patients demonstrated no increase in IL-10$^+$ Breg cell subsets compared to GPA during the GP season, with CD1d^{hi}CD5$^+$IL-10$^+$ Breg cells significantly reduced compared to GPA ($P = 0.0460$). However, outside of the GP season IL-10$^+$ Breg cell subsets apart were significantly restored in SCIT-treated patients compared to GPA (all, $P < 0.05$), apart from memory CD27$^+$ and CD25$^+$CD71^{hi}CD73^{lo} IL-10$^+$ Breg cells, although similar trends were observed. Apart from CD1d^{hi}CD5$^+$ and CD25^{hi}CD71^{hi}CD73^{lo} IL-10$^+$ Breg cells, IL-10$^+$ Breg cell frequencies were attenuated in SCIT patients compared to NAC during the GP season ($P < 0.05$). However, only CD5$^+$IL-10$^+$ Breg cells were reduced compared to NAC outside of the GP season ($P = 0.0252$). ELISA analysis revealed IL-10 protein levels in culture supernatant was significantly reduced in GPA compared to NAC outside of the GP season (NAC OS: 372pg/mL v. GPA OS: 174pg/mL, $P = 0.0203$; Figure 5.2.1.2, H). However, SCIT-treated patients did not demonstrate any dysregulation compared to NAC ($P = 0.1153$) or GPA ($P = 0.9759$). The SCIT-treated subject who had withdrawn from treatment demonstrated trends of lower IL-10$^+$ Breg cell frequencies compared to other SCIT OS patients, with frequencies instead like OS GPA (Figure 5.2.1.2, red open square).

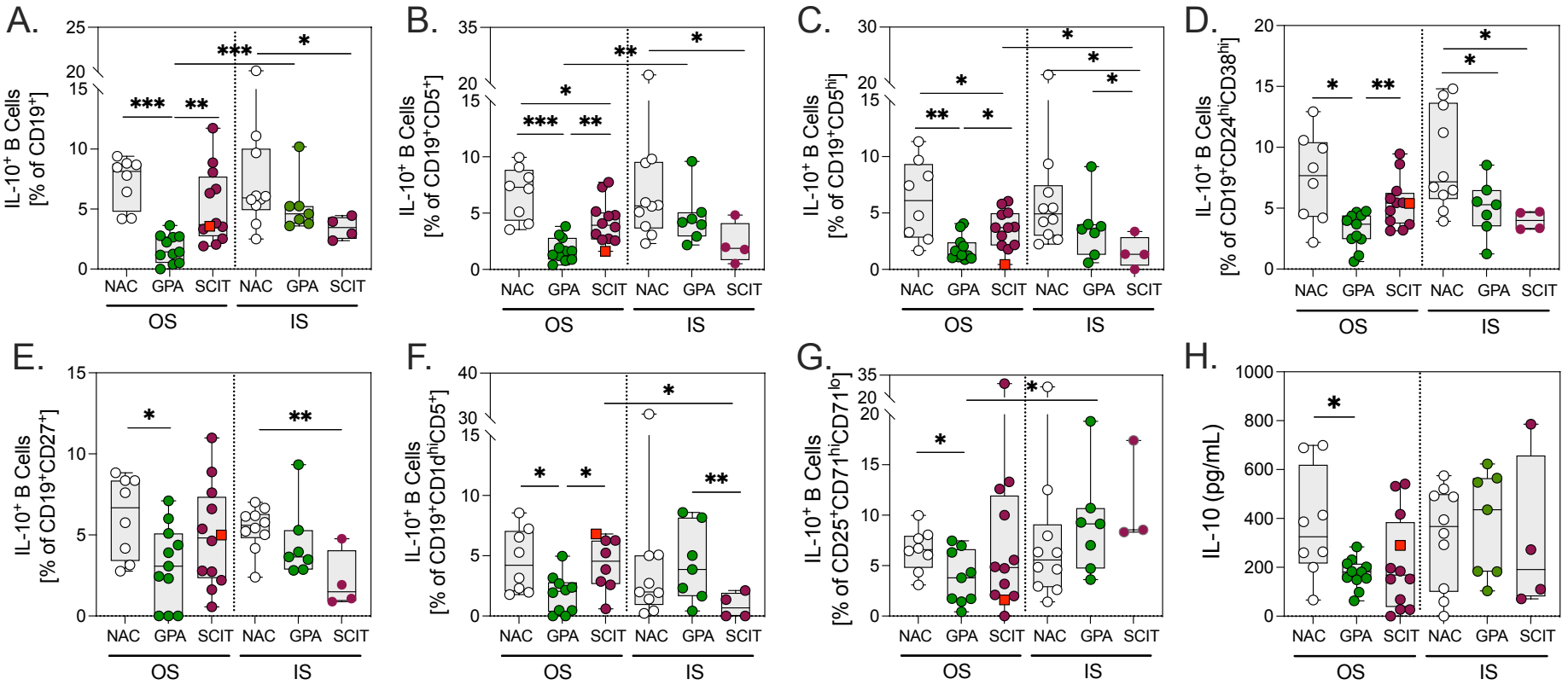


Figure 5.2.1.2 SCIT-treated GPA demonstrate significantly increased IL-10$^+$ Breg cell frequencies compared to GPA outside of the grass pollen season.

Flow-cytometric analysis of **A)** CD19$^+$, **B)** CD5$^+$, **C)** CD5^{hi}, **D)** CD24^{hi}CD38^{hi}, **E)** CD27$^+$ and **F)** CD1d^{hi}CD5$^+$ and **G)** CD25$^+$CD71^{hi}CD73^{lo} IL-10$^+$ Breg subset expression in NAC, GPA and GP-SCIT, IS and OS samples. **H)** ELISA analysis of IL-10 protein levels in cell culture supernatant. Red square represents n=1 GP-SCIT OS season who had withdrawn from treatment. Data representative of NAC (IS, n=10; OS, n=8), GPA (IS, n=7; OS, n=11) and GP-SCIT treated (IS, n=4; OS, n=12) [N.B. **F)** NAC IS, n=9; GPA OS, n=10, GP-SCIT, OS n=8; **G)** GPA OS, n=9, GP-SCIT IS, n=3] and presented as mean ± SEM. *P < 0.05, ** P < 0.01, *** P < 0.001, Mann Whitney Test. PBMC, peripheral blood mononuclear cells; NAC, non-atopic controls; GPA, grass pollen allergic; SCIT, subcutaneous immunotherapy; IS, in season; OS, out season.

Table 5.2.1.2 IL-10^{+} Breg Cell subsets in IS and OS NAC, GPA and SCIT-treated patients.

Atopic Status	Culture Conditions	B Cell Subset	Raw				Delta (Unstimulated)			*P* value vs NAC	P Value vs GP-SCIT	P Value IS v OS
			n	mean	SD	SEM	mean	SD	SEM			
NAC IS	Unstimulated	CD19^{+}IL-10^{+}	10	1.84	0.06	0.02	NA	NA	NA	NA	NA	NA
		CD19^{+}CD5^{+}IL-10^{+}	10	1.88	0.11	0.03	NA	NA	NA	NA	NA	NA
		CD19^{+}CD5^{hi}IL-10^{+}	10	1.92	0.08	0.02	NA	NA	NA	NA	NA	NA
		CD19^{+}CD27^{+}IL-10^{+}	10	1.86	0.10	0.03	NA	NA	NA	NA	NA	NA
		CD19^{+}CD24^{hi}CD38^{hi}IL-10^{+}	10	1.84	0.14	0.04	NA	NA	NA	NA	NA	NA
		CD19^{+}CD1d^{hi}CD5^{+}IL-10^{+}	9	1.84	0.13	0.04	NA	NA	NA	NA	NA	NA
	CpG/CD40L	CD19^{+}IL-10^{+}	10	9.46	5.08	1.60	7.63	5.07	1.60	NA	NA	NA
		CD19^{+}CD5^{+}IL-10^{+}	10	9.20	5.82	1.84	732	5.82	1.84	NA	NA	NA
		CD19^{+}CD5^{hi}IL-10^{+}	10	8.44	5.64	1.78	6.52	5.68	1.80	NA	NA	NA
		CD19^{+}CD27^{+}IL-10^{+}	10	7.25	1.31	0.42	5.40	1.34	0.42	NA	NA	NA
		CD19^{+}CD24^{hi}CD38^{hi}IL-10^{+}	10	10.80	4.07	1.29	8.94	4.11	1.30	NA	NA	NA
		CD19^{+}CD5^{+}CD1d^{hi}IL-10^{+}	9	7.36	9.61	3.20	5.53	9.69	3.23	NA	NA	NA
		CD19^{+}CD25^{+}CD71^{hi}CD73^{lo}	10	7.67	7.55	2.39	NA	NA	NA	NA	NA	NA
NAC OS	Unstimulated	CD19^{+}IL-10^{+}	8	1.92	0.06	0.02	NA	NA	NA	NA	NA	NA
		CD19^{+}CD5^{+}IL-10^{+}	8	1.87	0.07	0.03	NA	NA	NA	NA	NA	NA
		CD19^{+}CD5^{hi}IL-10^{+}	8	1.84	0.10	0.04	NA	NA	NA	NA	NA	NA
		CD19^{+}CD27^{+}IL-10^{+}	8	1.83	0.08	0.03	NA	NA	NA	NA	NA	NA
		CD19^{+}CD24^{hi}CD38^{hi}IL-10^{+}	8	1.80	0.16	0.05	NA	NA	NA	NA	NA	NA
		CD19^{+}CD1d^{hi}CD5^{+}IL-10^{+}	8	1.87	0.06	0.02	NA	NA	NA	NA	NA	NA
	CpG/CD40L	CD19^{+}IL-10^{+}	8	9.18	2.06	0.73	7.25	2.07	0.73	NA	NA	0.6334
		CD19^{+}CD5^{+}IL-10^{+}	8	8.68	2.34	0.83	6.81	2.35	0.83	NA	NA	0.6334
		CD19^{+}CD5^{hi}IL-10^{+}	8	7.98	3.59	1.27	6.14	3.54	1.25	NA	NA	0.7618
		CD19^{+}CD27^{+}IL-10^{+}	8	7.96	2.44	0.86	6.12	2.50	0.88	NA	NA	0.4725
		CD19^{+}CD24^{hi}CD38^{hi}IL-10^{+}	8	9.26	3.65	1.29	7.46	3.66	1.29	NA	NA	0.5148
		CD19^{+}CD1d^{hi}CD5^{+}IL-10^{+}	8	6.47	2.65	0.94	4.60	2.65	0.94	NA	NA	0.1996
		CD19^{+}CD25^{+}CD71^{hi}CD73^{lo}	8	6.55	2.15	0.76	NA	NA	NA	NA	NA	0.5148
GPA IS	Unstimulated	CD19^{+}IL-10^{+}	7	1.65	0.06	0.02	NA	NA	NA	NA	NA	NA
		CD19^{+}CD5^{+}IL-10^{+}	7	1.61	0.08	0.03	NA	NA	NA	NA	NA	NA
		CD19^{+}CD5^{hi}IL-10^{+}	7	1.56	0.08	0.03	NA	NA	NA	NA	NA	NA
		CD19^{+}CD27^{+}IL-10^{+}	7	1.60	0.05	0.02	NA	NA	NA	NA	NA	NA
		CD19^{+}CD24^{hi}CD38^{hi}IL-10^{+}	7	1.62	0.07	0.03	NA	NA	NA	NA	NA	NA
		CD19^{+}CD1d^{hi}CD5^{+}IL-10^{+}	7	1.65	0.10	0.04	NA	NA	NA	NA	NA	NA
	CpG/CD40L	CD19^{+}IL-10^{+}	7	6.90	2.30	0.87	5.25	2.27	0.86	0.1331	0.1091	NA
		CD19^{+}CD5^{+}IL-10^{+}	7	6.25	2.45	0.93	4.63	2.39	0.90	0.1932	0.1091	NA
		CD19^{+}CD5^{hi}IL-10^{+}	7	5.22	2.76	1.04	3.66	2.74	1.03	0.1613	0.2303	NA
		CD19^{+}CD27^{+}IL-10^{+}	7	6.08	2.30	0.87	4.48	2.29	0.87	0.1331	0.1091	NA
		CD19^{+}CD24^{hi}CD38^{hi}IL-10^{+}	7	6.63	2.26	0.86	5.01	2.30	0.87	**0.0460**	0.3152	NA
		CD19^{+}CD1d^{hi}CD5^{+}IL-10^{+}	7	5.94	3.18	1.20	4.29	3.16	1.20	0.5360	**0.0394**	NA
		CD19^{+}CD25^{+}CD71^{hi}CD73^{lo}	7	9.11	5.17	1.95	NA	NA	NA	0.2698	0.8333	NA
GPA OS	Unstimulated	CD19^{+}IL-10^{+}	11	1.60	0.08	0.03	NA	NA	NA	NA	NA	NA
		CD19^{+}CD5^{+}IL-10^{+}	11	1.74	0.13	0.04	NA	NA	NA	NA	NA	NA

		$CD19^+CD5^{hi}IL\text{-}10^+$	11	1.68	0.11	0.03	NA	NA	NA	NA	NA	NA
		$CD19^+CD27^+IL\text{-}10^+$	11	1.64	0.10	0.03	NA	NA	NA	NA	NA	NA
		$CD19^+CD24^{hi}CD38^{hi}IL\text{-}10^+$	10	1.71	0.11	0.03	NA	NA	NA	NA	NA	NA
		$CD19^+CD1d^{hi}CD5^+IL\text{-}10^+$	11	2.17	1.39	0.44	NA	NA	NA	NA	NA	NA
	CpG/CD40L	$CD19^+IL\text{-}10^+$	11	3.27	1.21	0.37	1.71	1.17	0.35	**<0.0001**	**0.0017**	**0.0001**
		$CD19^+CD5^+IL\text{-}10^+$	11	3.50	1.03	0.31	1.77	1.06	0.32	**<0.0001**	**0.0017**	**0.0012**
		$CD19^+CD5^{hi}IL\text{-}10^+$	11	3.53	1.09	0.33	1.85	1.13	0.34	**0.0018**	**0.0215**	0.1509
		$CD19^+CD27^+IL\text{-}10^+$	11	4.69	2.49	0.75	3.12	2.46	0.74	**0.0249**	0.2110	0.3738
		$CD19^+CD24^{hi}CD38^{hi}IL\text{-}10^+$	10	4.91	1.45	0.43	3.20	1.43	0.43	**0.0157**	**0.0067**	0.0566
		$CD19^+CD1d^{hi}CD5^+IL\text{-}10^+$	11	3.60	1.54	0.45	1.82	1.60	0.51	**0.0421**	**0.0114**	0.1280
		$CD19^+CD25^+CD71^{hi}CD73^{lo}$	9	3.80	2.64	0.88	NA	NA	NA	**0.0464**	0.3451	**0.0164**
GP-SCIT IS	Unstimulated	$CD19^+IL\text{-}10^+$	4	1.90	0.05	0.03	NA	NA	NA	NA	NA	NA
		$CD19^+CD5^+IL\text{-}10^+$	4	1.88	0.05	0.02	NA	NA	NA	NA	NA	NA
		$CD19^+CD5^{hi}IL\text{-}10^+$	4	2.05	0.25	0.12	NA	NA	NA	NA	NA	NA
		$CD19^+CD27^+IL\text{-}10^+$	4	1.89	0.11	0.06	NA	NA	NA	NA	NA	NA
		$CD19^+CD24^{hi}CD38^{hi}IL\text{-}10^+$	4	1.73	0.07	0.04	NA	NA	NA	NA	NA	NA
		$CD19^+CD1d^{hi}CD5^+IL\text{-}10^+$	4	3.14	1.79	0.90	NA	NA	NA	NA	NA	NA
	CpG/CD40L	$CD19^+IL\text{-}10^+$	4	5.34	0.90	0.45	3.43	0.94	0.47	**0.0360**	NA	NA
		$CD19^+CD5^+IL\text{-}10^+$	4	4.15	1.83	0.91	2.27	1.82	0.91	**0.0140**	NA	NA
		$CD19^+CD5^{hi}IL\text{-}10^+$	4	3.25	1.67	0.83	1.51	1.39	0.69	**0.0140**	NA	NA
		$CD19^+CD27^+IL\text{-}10^+$	4	4.05	1.87	0.94	2.16	1.80	0.90	**0.0080**	NA	NA
		$CD19^+CD24^{hi}CD38^{hi}IL\text{-}10^+$	4	5.72	0.84	0.42	3.99	0.78	0.39	**0.0080**	NA	NA
		$CD19^+CD1d^{hi}CD5^+IL\text{-}10^+$	4	3.28	1.17	0.59	0.87	1.05	0.53	0.1007	NA	NA
		$CD19^+CD25^+CD71^{hi}CD73^{lo}$	3	11.4	5.18	2.99	NA	NA	NA	0.1119	NA	NA
GP-SCIT OS	Unstimulated	$CD19^+IL\text{-}10^+$	12	1.83	0.08	0.02	NA	NA	NA	NA	NA	NA
		$CD19^+CD5^+IL\text{-}10^+$	12	1.84	0.07	0.02	NA	NA	NA	NA	NA	NA
		$CD19^+CD5^{hi}IL\text{-}10^+$	12	1.83	0.11	0.03	NA	NA	NA	NA	NA	NA
		$CD19^+CD27^+IL\text{-}10^+$	12	1.85	0.10	0.03	NA	NA	NA	NA	NA	NA
		$CD19^+CD24^{hi}CD38^{hi}IL\text{-}10^+$	12	1.79	0.10	0.03	NA	NA	NA	NA	NA	NA
		$CD19^+CD1d^{hi}CD5^+IL\text{-}10^+$	8	2.08	0.73	0.26	NA	NA	NA	NA	NA	NA
	CpG/CD40L	$CD19^+IL\text{-}10^+$	12	7.03	3.11	0.90	5.20	3.11	0.90	0.0691	NA	0.5989
		$CD19^+CD5^+IL\text{-}10^+$	12	6.03	1.93	0.56	4.19	1.88	0.54	**0.0252**	NA	0.1330
		$CD19^+CD5^{hi}IL\text{-}10^+$	12	5.36	1.73	0.50	3.53	1.72	0.50	0.1749	NA	**0.0401**
		$CD19^+CD27^+IL\text{-}10^+$	12	6.77	3.10	0.90	4.91	3.15	0.91	0.3144	NA	0.1033
		$CD19^+CD24^{hi}CD38^{hi}IL\text{-}10^+$	12	7.23	2.03	0.59	5.44	1.99	0.57	0.2302	NA	0.1632
		$CD19^+CD1d^{hi}CD5^+IL\text{-}10^+$	8	6.38	2.18	0.77	4.30	2.20	0.78	0.8785	NA	**0.0162**
		$CD19^+CD25^+CD71^{hi}CD73^{lo}$	12	7.44	8.14	2.35	NA	NA	NA	0.5208	NA	0.2330

Bolded values represent significant ***P*** values. Mann Whitney Test

5.2.2 Evaluation of the effect of SCIT-treatment on TIM-1$^+$ B cells and TIM-1$^+$IL-10$^+$ Breg cell frequencies in GPA

Potential immunomodulatory effect of SCIT-treatment on TIM-1$^+$ B cells and dual positive Tim-1$^+$IL-10$^+$ Breg cell frequencies were evaluated by multi-parametric flow cytometry to aid insight into potential AIT mechanisms of action. No clear modulation between CD19$^+$TIM-1$^+$ B cells were observed between NAC, GPA or SCIT-treated subjects (Figure 5.2.2.1, A and Table 5.2.2.1). Moreover, no aberrations in Tim-1$^+$IL-10$^+$ Breg frequencies were observed inside or outside the GP season in NAC, GPA or SCIT-treated patients in any B cell subset (all subsets, $P > 0.05$, Figure 5.2.2.1, B-D).

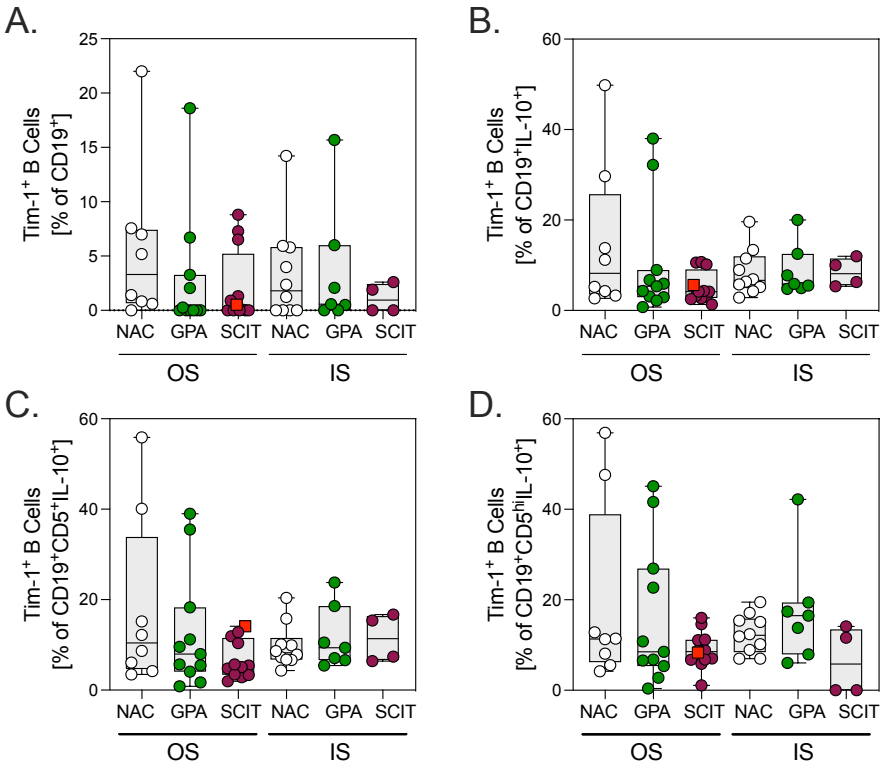


Figure 5.2.2.1 TIM-1$^+$ B Cells and TIM-1$^+$IL-10$^+$ Breg cell frequencies in NAC, GPA and GP-SCIT treated patients.

Flow cytometry data demonstrating expression of **A)** TIM-1$^+$CD19$^+$, **B)** TIM-1$^+$IL-10$^+$CD19$^+$, **C)** TIM-1$^+$IL-10$^+$CD19$^+$CD5$^+$ and **D)** TIM-1$^+$IL-10$^+$CD19$^+$CD5^{hi} B cell subsets. Red square represents n=1 SCIT-treated patient who had withdrawn from treatment. Data representative of n=18 NAC [IS, n=10, OS, n=8] n=18 GPA [IS, n=7, OS, n=11], and n=16 SCIT [IS, n=4, OS, n=12], and presented as mean ± SEM. NAC, non-atopic controls; GPA, grass pollen allergic; SCIT, subcutaneous immunotherapy; IS, in season; OS, out season.

Table 5.2.2.1 TIM-1$^+$ B Cells and TIM-1$^+$IL-10$^+$ B cell frequencies in NAC, GPA and GP-SCIT treated patients.

Atopic Status	Culture Conditions	B Cell Subset	Delta				*P* value vs NAC	*P* value vs GPA	*P* value IS v OS
			n	mean	SD	SEM			
NAC IS	CpG/CD40L	CD19$^+$Tim-1$^+$	10	3.35	4.49	1.42	NA	NA	NA
		CD19$^+$Tim-1$^+$IL-10$^+$	10	8.48	5.08	1.61	NA	NA	NA
		CD19$^+$CD5$^+$Tim-1$^+$IL-10$^+$	10	9.77	4.82	1.52	NA	NA	NA
		CD19$^+$CD5^{hi}Tim-1$^+$IL-10$^+$	10	7.86	5.72	1.81	NA	NA	NA
NAC OS	CpG/CD40L	CD19$^+$Tim-1$^+$	8	5.57	7.28	2.58	NA	NA	0.4023
		CD19$^+$Tim-1$^+$IL-10$^+$	8	15.00	16.65	5.89	NA	NA	0.8968
		CD19$^+$CD5$^+$Tim-1$^+$IL-10$^+$	8	18.23	19.26	6.81	NA	NA	0.8286
		CD19$^+$CD5^{hi}Tim-1$^+$IL-10$^+$	8	19.73	20.44	7.23	NA	NA	0.1011
GPA IS	CpG/CD40L	CD19$^+$Tim-1$^+$	7	3.55	5.76	2.28	0.9432	NA	NA
		CD19$^+$Tim-1$^+$IL-10$^+$	7	8.77	5.64	2.13	>0.9999	NA	NA
		CD19$^+$CD5$^+$Tim-1$^+$IL-10$^+$	7	11.62	6.93	2.62	0.8125	NA	NA
		CD19$^+$CD5^{hi}Tim-1$^+$IL-10$^+$	7	17.61	11.91	4.50	**0.0330**	NA	NA
GPA OS	CpG/CD40L	CD19$^+$Tim-1$^+$	11	2.81	5.65	1.70	0.0994	NA	0.4496
		CD19$^+$Tim-1$^+$IL-10$^+$	11	10.04	12.66	3.82	0.4920	NA	0.4252
		CD19$^+$CD5$^+$Tim-1$^+$IL-10$^+$	11	12.66	13.09	3.95	0.4421	NA	0.6590
		CD19$^+$CD5^{hi}Tim-1$^+$IL-10$^+$	11	16.13	15.67	4.73	0.4920	NA	0.5360
SCIT IS	CpG/CD40L	CD19$^+$Tim-1$^+$	4	1.23	1.33	0.67	0.5015	0.6030	NA
		CD19$^+$Tim-1$^+$IL-10$^+$	4	8.42	3.12	1.56	0.8392	0.7879	NA
		CD19$^+$CD5$^+$Tim-1$^+$IL-10$^+$	4	11.47	5.33	2.66	0.8392	>0.9999	NA
		CD19$^+$CD5^{hi}Tim-1$^+$IL-10$^+$	4	6.43	7.49	3.74	0.6124	0.1030	NA
SCIT OS	CpG/CD40L	CD19$^+$Tim-1$^+$	12	2.12	3.33	0.96	0.1351	0.7732	0.9538
		CD19$^+$Tim-1$^+$IL-10$^+$	12	6.82	4.27	1.23	0.0825	0.6186	0.1033
		CD19$^+$CD5$^+$Tim-1$^+$IL-10$^+$	12	8.86	4.00	1.16	0.1153	0.4491	0.0582
		CD19$^+$CD5^{hi}Tim-1$^+$IL-10$^+$	12	5.21	3.37	0.97	0.3431	0.8452	0.6654

Bolded values represent significant ***P*** values. Mann Whitney Test.

5.2.3 GP-SCIT treatment significantly induces serum grass pollen-specific IgG_4 levels compared to GPA and NAC

ImmunoCAP quantification of serum TG-sIgE, TG-sIgG_4 and tIgE levels were evaluated to alllow a secondary insight on B cell modulation during SCIT. During and outside of the GP season, TG-sIgE was significantly enhanced in GPA and SCIT-treated subjects compared to NAC (all, $P < 0.05$; Figure 5.2.3.1, A and Table 5.2.3.1). However, no clear differences in TG-sIgE serum levels were observed between GPA and SCIT-treated patients. tIgE levels were also significantly enhanced in GPA and SCIT-treated subjects compared to NAC (all, $P < 0.05$) and were enhanced outside of the GP season (Figure 5.2.3.1, B). Moreover, tIgE appeared increased in GPA compared to SCIT-treated patients, although no significance was reached. TG-sIgG_4 was significantly enhanced in SCIT-treated patients compared to NAC and GPA irrespective of GP seasonality (all, $P < 0.05$; Figure 5.2.3.1, C). Outside of the GP season, TG-sIgG_4 serum levels were also significantly enhanced in GPA samples compared to NAC ($P = 0.0373$). Although no clear correlation was observed between TG-sIgE and TG-sIgG_4 levels, there was significant strong correlation between TG-sIgE and tIgE level in SCIT-treated subjects ($P = 0.0061$) and GPA ($P = 0.0303$; Figure 5.2.3.1, D-E). Of note however, the highest TG-sIgG_4 levels in both SCIT and GPA were associated with the lowest TG-sIgE levels, meaning a trend may have become apparent with increased sample size. Interestingly, there was also a trend of positive correlation between tIgE and TG-sIgG_4 levels in both SCIT-treated subjects and GPA (Figure 5.2.3.1, F).

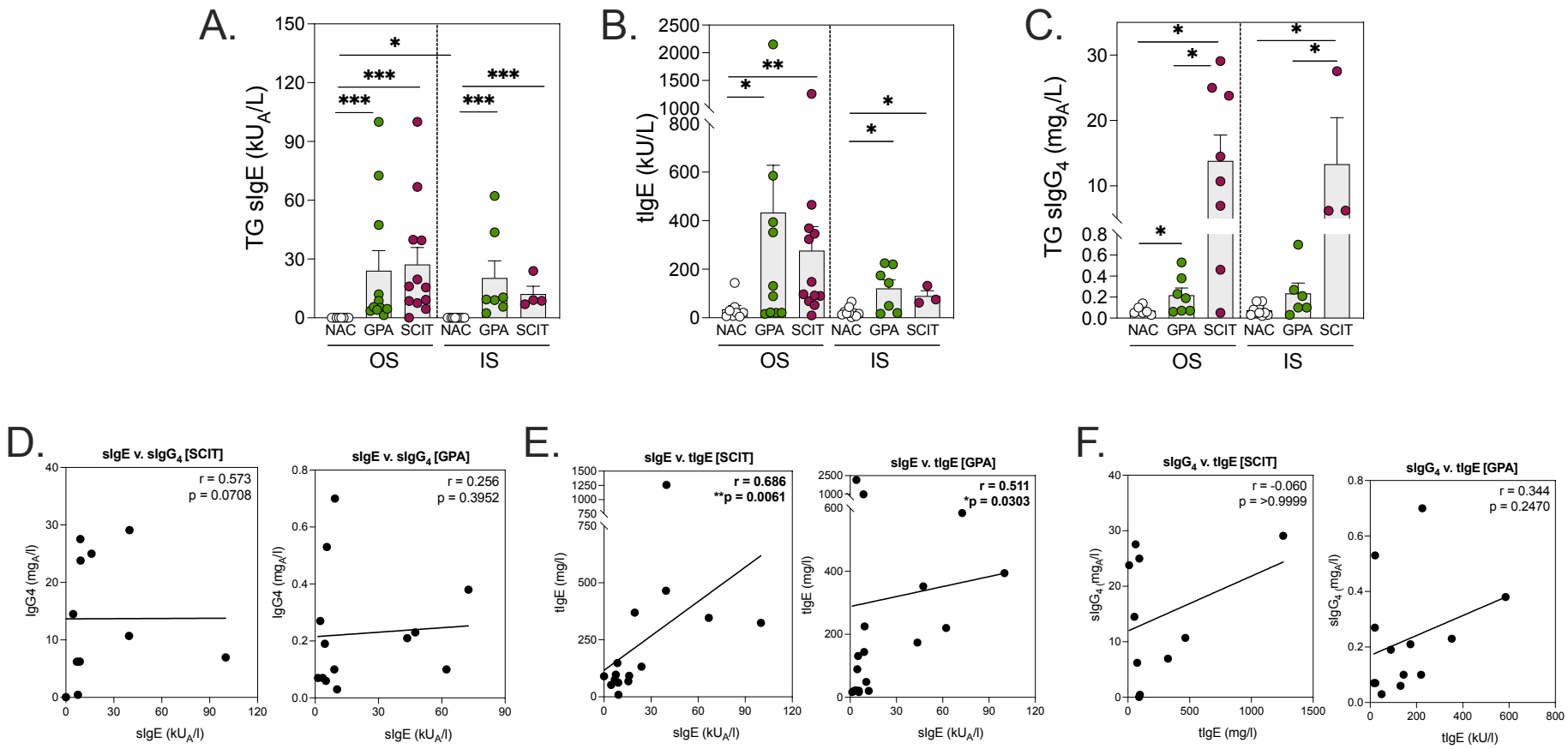


Figure 5.2.3.1 Systemic GP-sIgG$_4$ levels were significantly enhanced in SCIT treated subjects compared to GPA

ImmunoCAP assessment of serum **A)** TG-sIgE, **B)** tIgE and **C)** TG-sIgG$_4$ levels. Correlation between **D)** TG sIgE and sIgG$_4$, **E)** TG sIgE and tIgE$_4$ and **E)** TG sIgG$_4$ and tIgE$_4$. Data representative of NAC [IS, n=10; OS, n=6], GPA [IS, n=7; OS, n=11] and SCIT [IS, n=3; OS, n=12] and presented as mean ±SEM. **A-C**, Mann Whitney Test. **A-F**, Spearman Correlation. * $P < 0.05$, ** $P < 0.01$, *** $P < 0.001$. NAC, non-atopic control; GPA, grass pollen allergic; SCIT, subcutaneous immunotherapy; IS, in season; OS, out season; TG, timothy grass.

Table 5.2.3.1 Systemic GP-sIgG$_4$ levels were significantly enhanced in SCIT treated subjects compared to GPA

Antibody	Atopic Status	Raw				*P* value vs NAC	*P* value vs GPA	*P* value IS v OS
		n	mean	SD	SEM			
sIgG$_4$	NAC IS	10	0.08	0.03	0.02	NA	NA	NA
	NAC OS	6	0.07	0.04	0.02	NA	NA	0.8475
	GPA IS	6	0.24	0.24	0.10	0.0867	NA	NA
	GPA OS	7	0.22	0.18	0.07	**0.0373**	NA	0.9219
	SCIT IS	3	13.3	12.3	7.11	**0.0070**	**0.0238**	NA
	SCIT OS	8	13.8	11.2	4.00	**0.0080**	**0.0193**	0.9212
sIgE	NAC IS	10	0.0	0.0	0.00	NA	NA	NA
	NAC OS	8	0.0	0.0	0.0	NA	NA	**0.0158**
	GPA IS	7	20.4	23.0	8.7	**0.0001**	NA	NA
	GPA OS	11	24.1	33.9	10.2	**<0.0001**	NA	0.5962
	SCIT IS	4	12.1	7.9	4.0	**0.0010**	0.6485	NA
	SCIT OS	12	27.3	29.9	8.62	**<0.0001**	0.3552	0.5209
tIgE	NAC IS	10	23.0	19.0	5.99	NA	NA	NA
	NAC OS	8	34.8	46.1	16.3	NA	NA	0.7145
	GPA IS	7	121	91.5	34.6	**0.0185**	NA	NA
	GPA OS	11	433	646	195	**0.0328**	NA	0.4789
	SCIT IS	3	89.7	37.2	21.5	**0.0140**	0.8333	NA
	SCIT OS	12	277	343	99.1	**0.0022**	>0.9999	0.3648

Bolded values represent significant ***P*** values. Mann Whitney Test

5.2.4 Unbiased machine learning algorithms reveal GP-SCIT upregulates TIM-1 and IL-10 expression on B cell subsets compared to GPA

Flow cytometry data was interrogated further utilising the unbiased mathematical machine learning algorithm tools, viSNE and FlowSOM, to distinguish rare subsets of IL-10$^+$ Breg cells that may be modulated during GP-SCIT treatment. viSNE analysis of CD19$^+$ B cells revealed two IL-10$^+$ islands which were aberrated in GPA compared to NAC and SCIT-treated patients outside of the GP season, corroborating traditional flow cytometry findings (Figure 5.2.4.1, black islands). viSNE map also revealed two TIM-1$^+$ islands which co-localised with IL-10$^+$ islands which were highest in expression in SCIT-treated patients during the GP season and NAC outside of the season. FlowSOM revealed four distinct B cell MC that were modulated during SCIT-treatment, MC 9, MC 15, MC 24, and MC 27 (Figure 5.2.4.2 A). Heatmap analysis phenotyped MC 9, MC 15, MC 24 and MC 27 as CD1d$^+$CD5^{hi}CD27$^+$CD71$^+$, CD1d^{hi}CD5^{hi}CD25$^+$CD27$^+$CD38$^+$CD71^{hi}CD73$^+$, CD1d$^+$CD5^{hi}CD25$^+$CD27^{hi}CD38^{hi}CD71$^+$CD73$^+$ and CD1d$^+$CD38^{hi}CD71$^+$CD73^{lo} B cells, respectively (Figure 5.2.4.2, B). MC 9 represented TIM-1$^+$IL-10^{lo} B cells, MC 15 represented IL-10$^+$ B cells, and MC 24 represented TIM-1$^+$IL-10$^+$ B cells. MC 27 did not express either TIM-1$^+$ or IL-10$^+$, however represented a B cell subset that was clearly targeted through SCIT-treatment. Population abundance of MC 9 (TIM-1$^+$IL-10^{lo} B cells) was significantly reduced in IS SCIT-treated patients compared to GPA (P = 0.0242) and NAC (P = 0.0360) and enhanced in GPA IS samples compared to GPA OS samples (P = 0.0346; Figure 5.2.4.2, C). However, MC 9 IL-10 expression was significantly enhanced in SCIT-treated patients compared to GPA (IS, P = 0.0167; OS, P = 0.0088) and NAC (IS, P = 0.0140; OS, P = 0.0055), with similar trends observed in MC 9 TIM-1 expression (Figure 5.2.4.2, D-E). MC 15 (IL-10$^+$ B cells) IL-10 expression and population abundance correlated strongly with flow cytometry data, revealing significantly increased frequencies in NAC compared to GPA (P = 0.0328) which were partially restored in SCIT-treated subjects outside of the GP season (Figure 5.2.4.2, F-G). MC 15 population abundance was also significantly enhanced in GPA following natural allergen

exposure during the GP season (P = 0.0154). Although no variations in population abundance was observed, MC 24 (TIM-1^{+}IL-10^{+} B cells) TIM-1 expression was greatly enhanced in SCIT-treatment patients compared to NAC (IS, P = 0.0140; OS, P = 0.0320) and OS GPA (P = < 0.0001; Figure 5.2.4.2, H-I). Moreover, TIM-1 expression was greatly enhanced outside of the GP season in NAC compared to GPA (P = 0.0002) and significantly reduced in GPA compared to during the GP season (P = < 0.0001). Interestingly however, contrary to previous findings, MC 24 IL-10 expression was significantly enhanced in GPA outside of the GP season compared to SCIT-treated patients (P = 0.0173) and during the GP season (P = 0.0202; Figure 5.2.4.2, J). Population abundance of MC27 (TIM-1^{-}IL-10^{-}) was significantly enhanced outside of GP season in GPA compared to NAC (P = 0.0328) and IS GPA patients (P = 0.0342; Figure 5.2.4.2, K). Although MC 27 TIM-1 was not highly expressed within the heatmap generated from NAC, this distinct B cell MC gained substantial expression of TIM-1 following SCIT-treatment which was greatly enhanced compared to GPA (P = < 0.0001) and NAC (P = 0.0003) outside of the GP season, and NAC during the GP season (P = 0.0121; Figure 5.2.4.2, L).

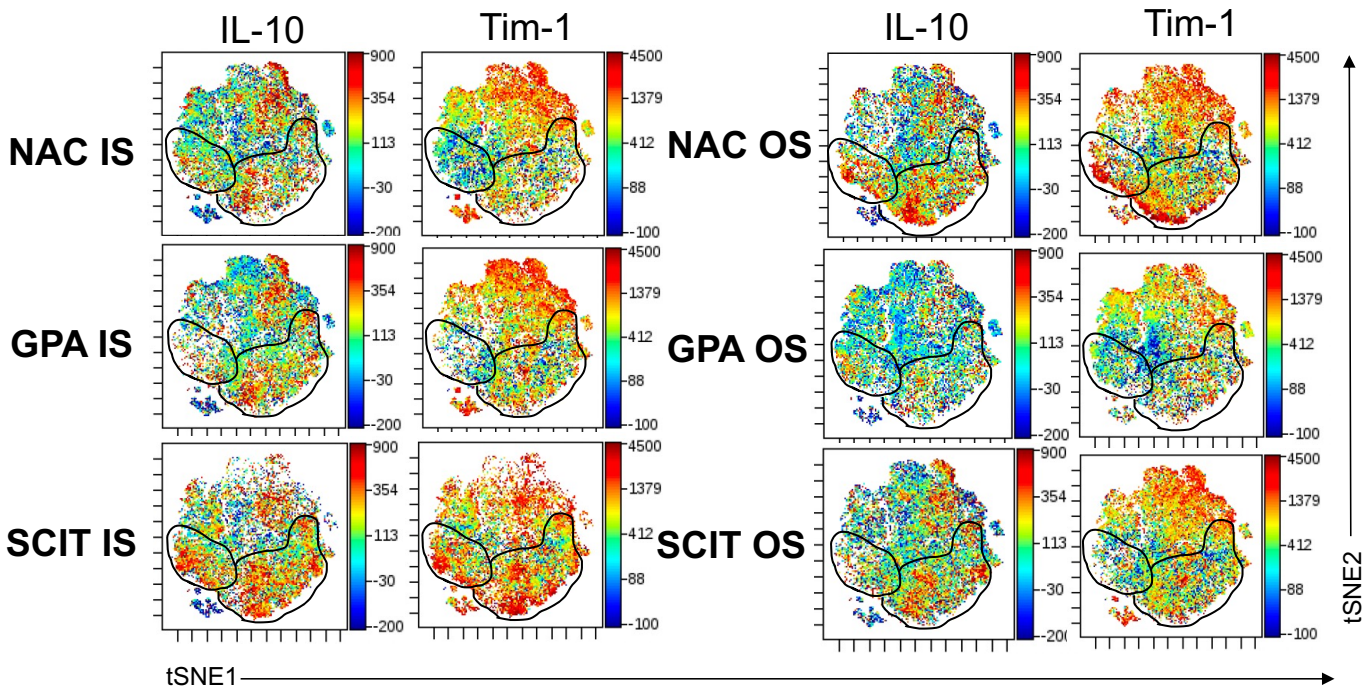


Figure 5.2.4.1 viSNE analysis reveals distinct IL-10$^+$ and IL-10$^+$Tim-1$^+$ Breg subsets dysregulated in GPA are restored during SCIT-treatment.

viSNE map of CD19$^+$ B cells, whereby black islands reveal IL-10$^+$ and Tim-1$^+$ positive islands. viSNE data representative of n=4 concatenated FCS files per condition. NAC, non-atopic control; GPA, grass pollen allergic; SCIT, subcutaneous therapy; IS, in season; OS, out season.

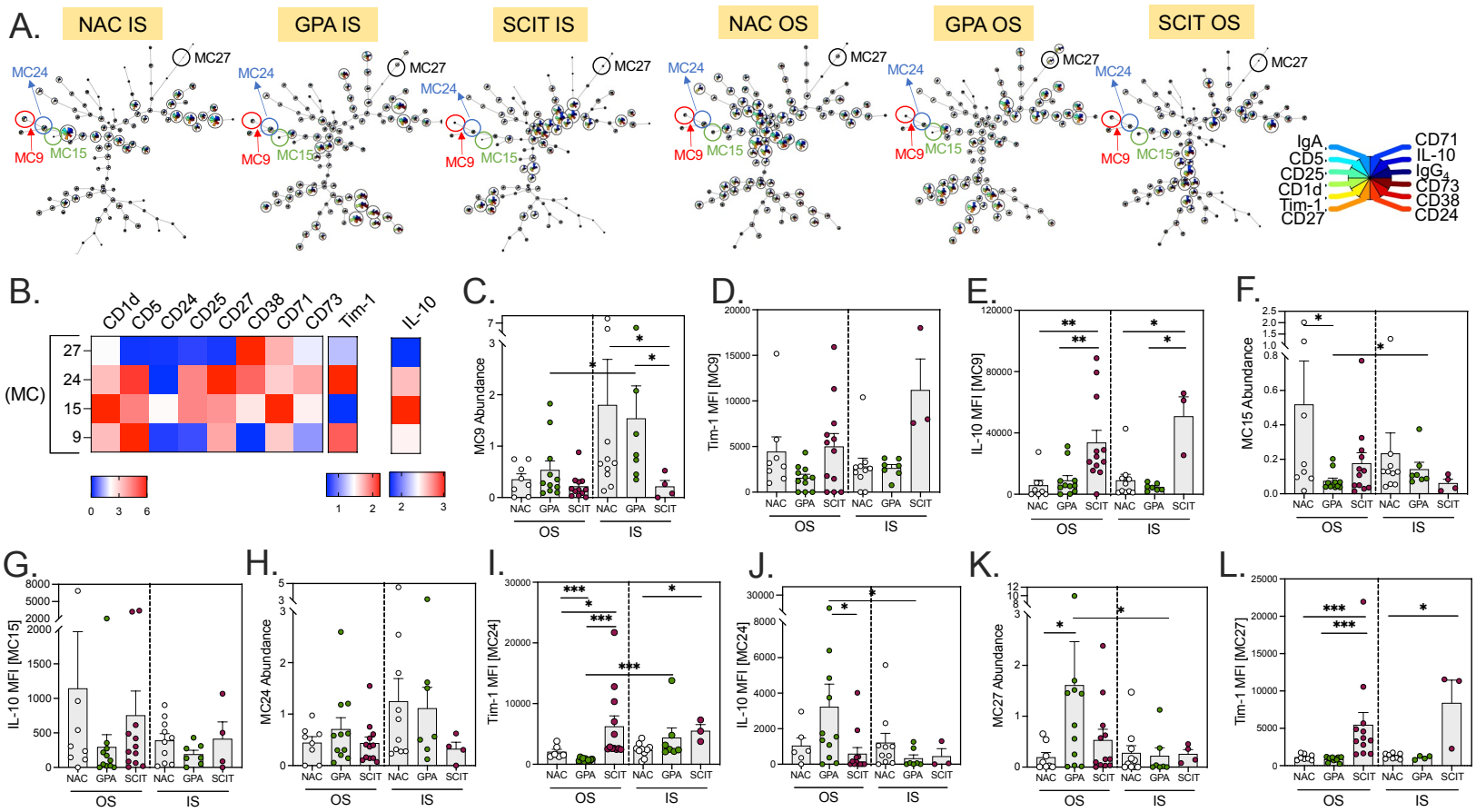


Figure 5.2.4.2 FlowSOM analysis reveals IL-10^{+} and Tim-1^{+} CD19^{+} B cells are enhanced following SCIT-treatment.

A) FlowSOM star plots in IS/OS NAC, GPA and SCIT samples with differentially expressed MC highlighted: MC 9, 15, 24, 27. **B)** Heatmap of n=3 samples concatenated OS NAC samples. Quantification of **C)** MC 9 population abundance, **D)** MC 9 Tim-1 MFI, **E)** MC 9 IL-10 MFI, **F)** MC15 population abundance, **G)** MC15 IL-10 MFI, **H)** MC 24 population abundance, **I)** MC 24 Tim-1 MFI, **J)** MC 24 IL-10 MFI, **K)** MC27 population abundance and **L)** MC27 Tim-1 MFI. Data representative of n=10 NAC IS, n=7 NAC OS, n=7 GPA IS, n=11 GPA OS, n=4 SCIT and n=12 SCIT. **P*<0.05, ***P*<0.01, ****P*<0.001, Mann Whitney Test. NAC, non-atopic control; GPA, grass pollen allergic; SCIT, subcutaneous therapy; IS, in season; OS, out season.

5.2.5 Correlation between IL-10$^+$ Breg Cells, Serum Antibody Levels, Symptom Severity and Treatment Length

To determine associations between SCIT-treated IL-10$^+$ Breg cell frequencies, symptom severity, treatment length and serum antibody levels, correlation analysis was performed. Memory CD27$^+$IL-10$^+$ Breg cells demonstrated a weak positive correlation with increased length of SCIT-treatment, although no trends were observed in any other IL-10$^+$ Breg subset (Figure 5.2.5.1, A). Overall CD19$^+$, memory CD27$^+$ and transitional CD24^{hi}CD38^{hi} IL-10$^+$ Breg cells were negatively correlated with serum GP-sIgE and tIgE levels, although no significance was reached (Figure 5.2.5.1, B-C). No clear correlation between serum GP-sIgG$_4$ levels and IL-10$^+$ Breg cells were observed (Figure 5.2.5.1, D). GP-SCIT CD1d^{hi}IL-10$^+$ Breg cells demonstrated a positive trend with increased GE2 scores, although no clear trend was observed in any other IL-10$^+$ Breg subset (Figure 5.2.5.2, A). Although no trend was observed between any IL-10$^+$ Breg cell subset and TNSS, CD1d^{hi}IL-10$^+$ Breg cells were significantly correlated with VAS (P = 0.0123), with similar positive trends observed in activated CD5^{hi} IL-10$^+$ Breg cellular subsets (Figure 5.2.5.2, B-C). No clear trends between SCIT-length and clinical symptom severity assessed by VAS, TNSS or GE2 were observed (Figure 5.2.5.2, D). GP-sIgE levels were weakly, but positively, correlated with VAS scores, but not GE2 or TNSS (Figure 5.2.5.3, A). Conversely, both tIgE and GP-sIgG$_4$ levels demonstrated a clear positive trend with GE2, and a negative trend with VAS and TNSS (Figure 5.2.5.3, B). Interestingly, length of SCIT treatment was negatively correlated with GP-sIgE and tIgE levels, but positively correlated with an increase in GP-sIgG$_4$.

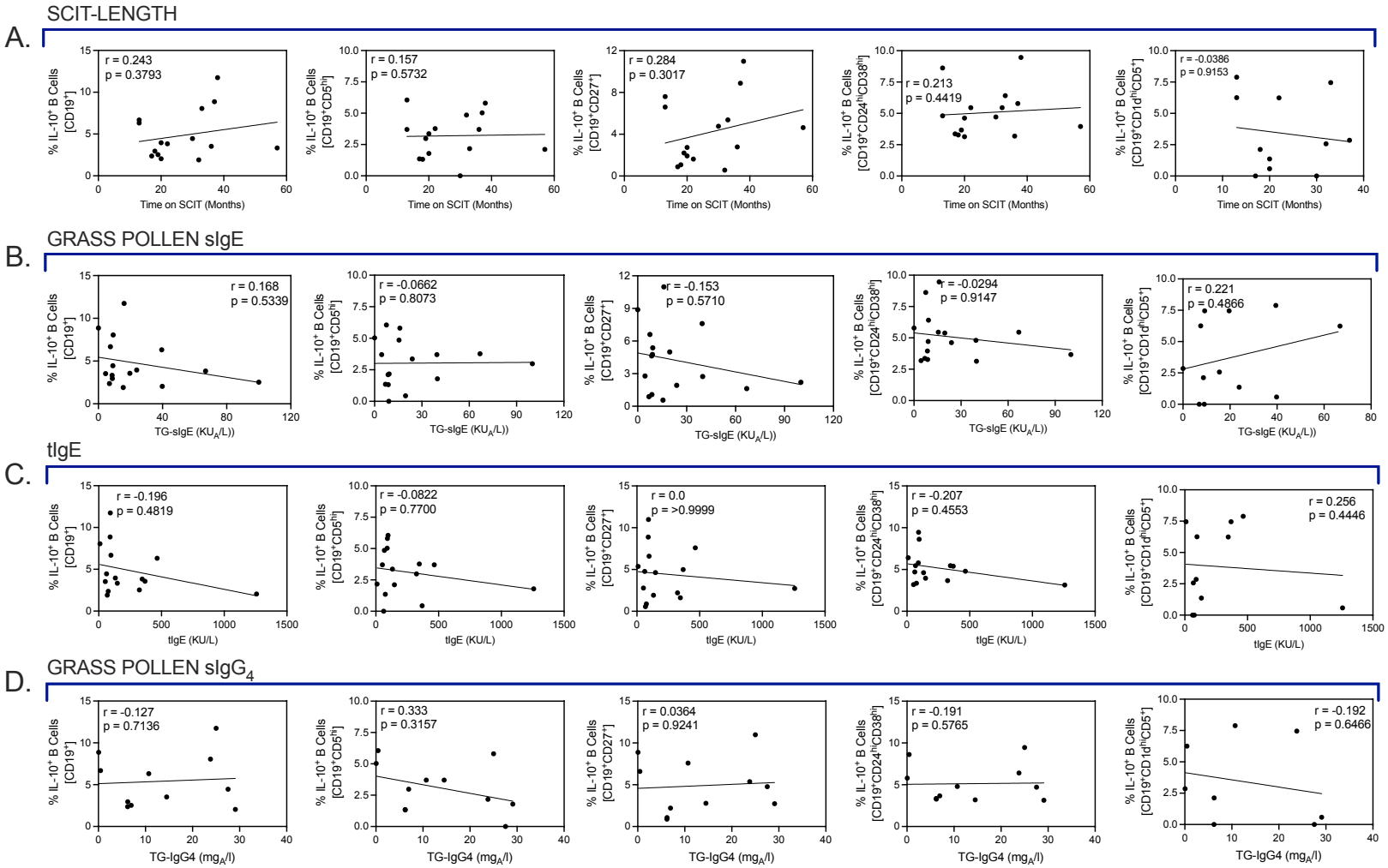


Figure 5.2.5.1 Correlation between SCIT IL-10$^+$ B cell subsets and serum TG-sIgE, TG-sIgG$_4$ and tIgE levels

Correlation between IL-10$^+$ Breg cell subsets and **A)** SCIT-treatment length, **B)** TG-sIgE, **C)** tIgE and **D)** TG-sIgG$_4$. Data is representative of n=16 SCIT-treated patients. *P* value, Spearman Correlation test. TG, timothy grass pollen; sIgE, specific IgE; tIgE, total IgE; sIgG$_4$, specific IgG$_4$

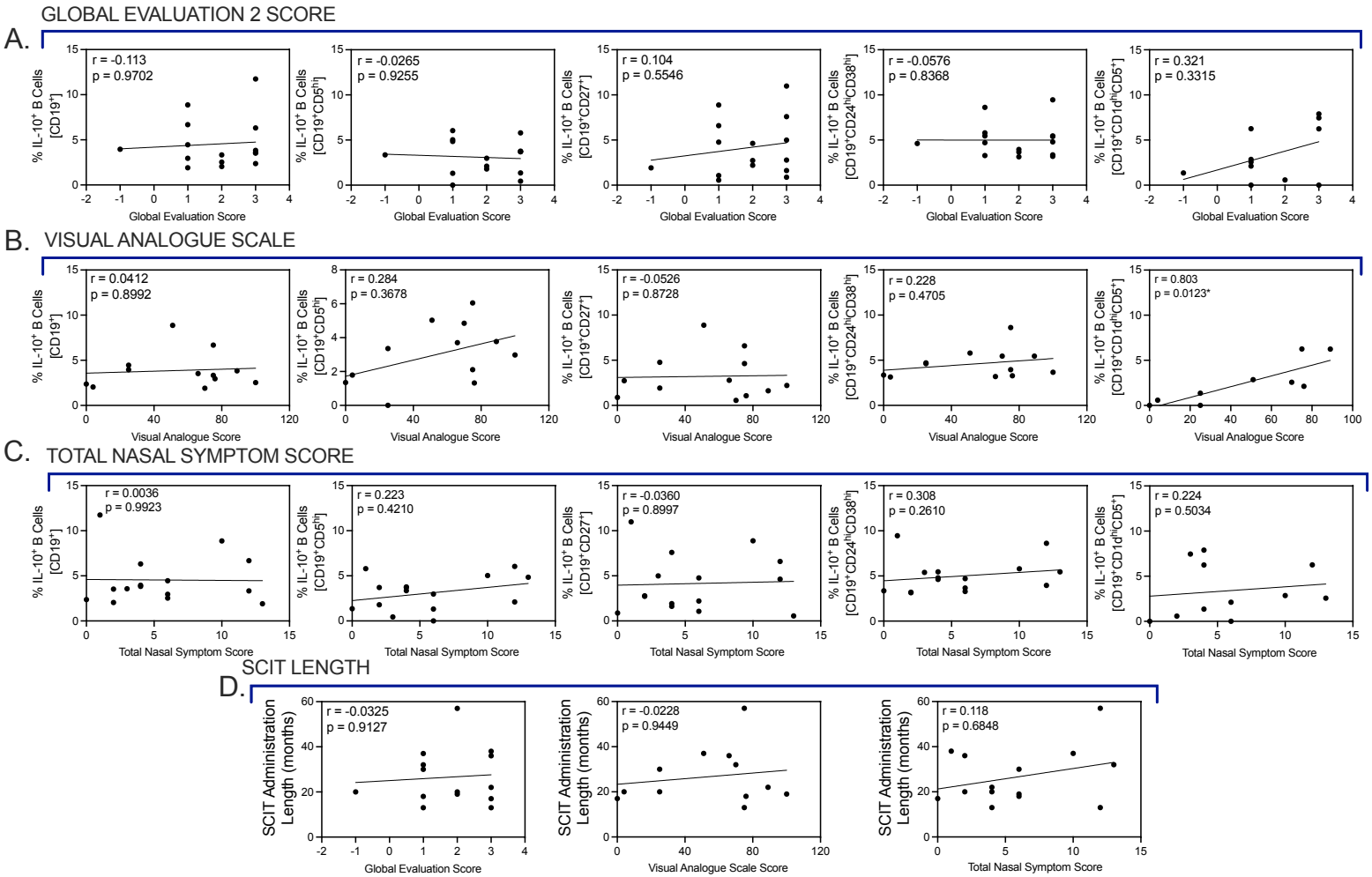


Figure 5.2.5.2 Correlation between SCIT IL-10$^+$ B cell subsets, clinical symptom severity and treatment length

Correlation between IL-10$^+$ Breg subsets and **A)** GE2, **B)** VAS, and **C)** TNSS, and **D)** SCIT-treatment and GE2, VAS, and TNSS. Data is representative of n=16 patients. *P < 0.05, P value, Spearman Correlation test; GE2, global evaluation; VAS, visual analogue scale; TNSS, total nasal symptom score.

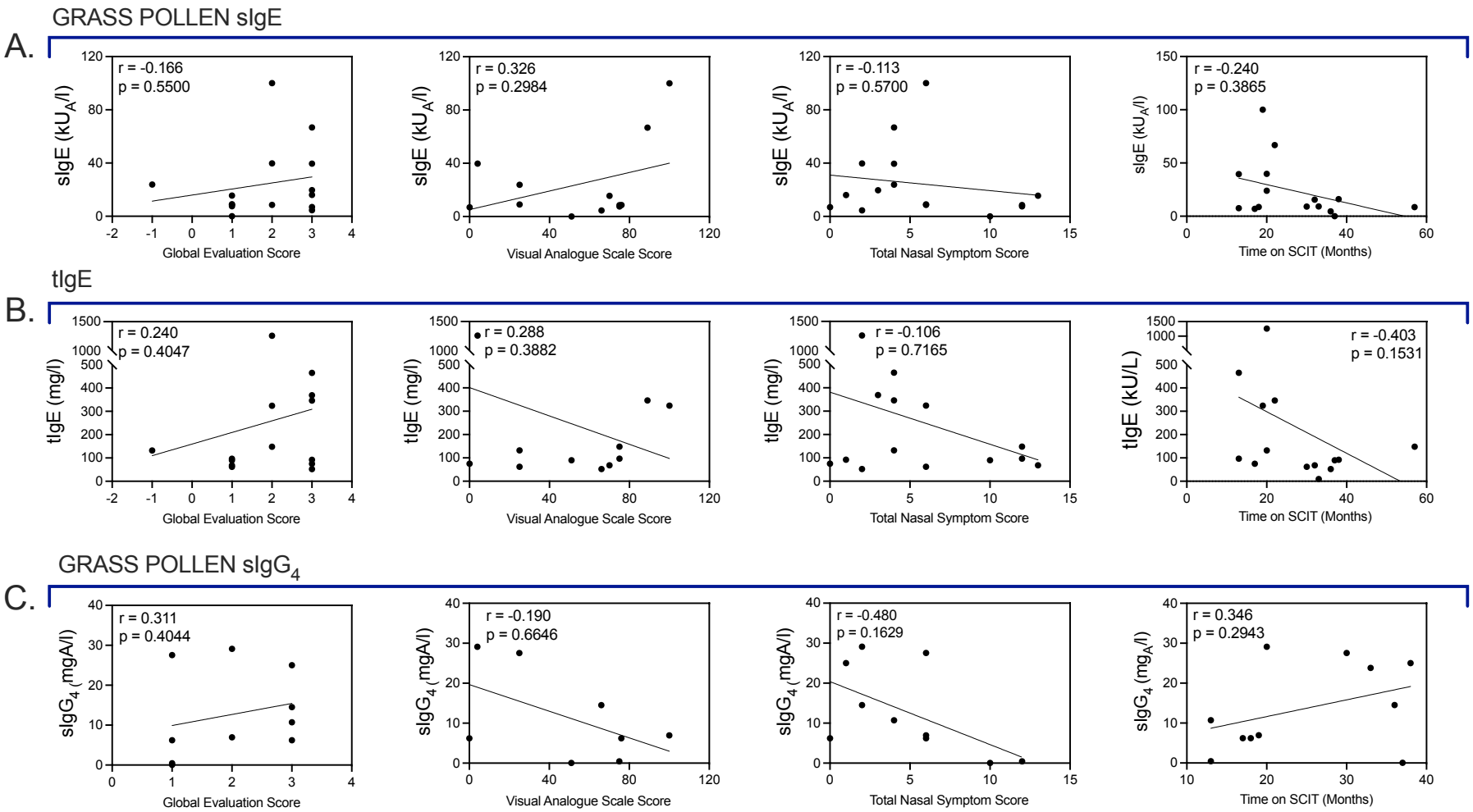


Figure 5.2.5.3 Correlation between systemic TG-sIgE, TG-sIgG$_4$ and tIgE levels, clinical symptom severity and treatment length

Correlation between global evaluation evaluation 2, visual analogue scale scores and total nasal symptom clinical symptom scores and SCIT-treatment length and **A)** TG-sIgE, **B)** tIgE and, **C)** TG-sIgG$_4$ Data is representative of n=16 patients. *P* value, Spearman Correlation test. sIgE, specific IgE; tIgE, total IgE; sIgG$_4$, specific IgG$_4$; TG, timothy grass.

5.3 Summary

In this chapter, it was demonstrated that GP-SCIT significantly restores SAR IL-10^+ Breg cell frequencies outside of the GP season to similar levels observed in healthy controls, in corroboration with previous clinical studies (202). Moreover, IL-10^+ Breg cells were enhanced in SAR following natural exposure to allergen during the GP season. Serological analysis revealed serum TG-sIgG_4 levels were substantially increased in SCIT-treated patients compared to GPA and NAC, irrespective of the seasonality, and positively correlated with increased length of SCIT administration, confirming AIT-mediated induction of IgG_4. However, no clear modulation of either GP-sIgE or tIgE by AIT was observed, although SCIT-treatment length was negatively correlated with serum TG-sIgE and tIgE levels. Although traditional flow cytometry biaxial analysis demonstrated no aberration in TIM-1 expression on B cell subsets following SCIT treatment, unbiased machine learning algorithms were able to delineate rare distinct IL-10^+ and dual positive IL-10^+TIM-1^+ Breg subsets which were significantly enhanced during SCIT-treatment, demonstrating for the first time the ability of AIT to modulate TIM-1^+ B cells. GP-SCIT IL-10^+ Breg cell subset frequencies did not correlate with SCIT length, GP-sIgG_4, GP-sIgE or tIgE levels. However, CD1$d^{hi}$$CD5^+$ IL-10^+ Breg cell frequencies were correlated with increased VAS and GE2 clinical symptom score values. In summary, GP-SCIT treatment significantly restores IL-10^+ Breg frequencies in GPA and induces TIM-1^+ B cell induction. Moreover, GP-SCIT enhances serum allergen-sIgG_4 levels and drives suppression of serum TG-sIgE and tIgE levels with increased treatment length.

CHAPTER 6. NOVEL APPROACHES OF ALLERGEN IMMUNOTHERAPY, TARGETING IL-10^{+} BREG CELLS TO INDUCE TOLERANCE

6.1 Introduction

AIT possess the ability to induce long term clinical tolerance to administered allergen following three years treatment. However, AIT treatment is associated with various challenges, such as patient unresponsiveness, lack of prognostic and predictive biomarker of treatment efficacy and patient compliance for the extended treatment periods required for clinical tolerance establishment. Thus, efforts to develop novel AIT treatments with greater immunogenicity and shorter treatment regimens are warranted. To enhance AIT immunogenicity, novel allergen-carrier systems, such as VLP and eBP, alongside depot adjuvants such as MCT and MPL-A, have been preliminarily investigated. For example, a preclinical murine study of VLP chemically coupled to the major cat allergen, *Fel d* 1, demonstrated robust induction of allergen-sIgG and protection against anaphylaxis following *Fel d* 1 challenge (374). Similar enhancements of IgG responses in mice were observed following AIT treatment with VLP-expressing either *Der p* 1 and *Ara h* 2, in addition to systemic and local protection against anaphylaxis (375-377). Additionally, VLP-expressing *Fel d* 1 and *Ara h* 2 possessed reduced capability to induce mast cell activation compared to soluble *Fel d* 1, suggesting reduced allergenicity through mitigating IgE-mediated effector cell activation (375, 378). However, the ability of allergenic-expressing VLP to modulate the B cell compartment remains to be confirmed. A recent exploratory study reported that *in vivo* naturally assembled plant-derived eBP fused to the major HDM allergenic component, *Der p* 2, demonstrated powerful induction of IgG responses, suggesting the ability of eBP to modulate B cell responses (174). Moreover, plant-derived eBP demonstrated limited potential to induce basophil degranulation despite expressing many copies of allergen which may have induced cross-linking of IgE. Preclinical

studies exploring plant-derived eBP fused to either *Fel d* 1 or *Ara h* 2 also demonstrated ability to upregulate DC activation markers CD83 and CD86 and cytokine production compared to soluble allergens, as well as enhancing T_H1 and Treg cell frequencies (379, 380). However, investigations of eBP modulation of the B cell compartment remain to be confirmed. Finally, to combat challenges observed with patient compliance, clinical studies investigating the clinical efficacy of shorter-term and extended AIT regimes are required to determine whether alternative dosage schedules or use of adjuvants can reduce the time required to restore tolerant immune cells, such as IL-10^+ Breg cells.

6.1.1 Hypothesis and Aims

6.1.1.1 Hypotheses

1. Novel allergen carrier systems, such as eBP or VLP, can generate IL-10^+ Breg cell responses in allergic individuals.
2. Short-term AIT PQ Grass 27600 SU (GP allergoid adjuvanted with MPL-A and MCT) induces IgG, IgG_4 and $IgA_1/_2$ levels in serum and nasal fluid alongside the induction of IL-10^+ B cells in GPA.

6.1.1.2 Aims

4. To assess the ability of novel *Fel d* 1 eBP to amplify IL-10^+ B cell responses in CA subjects and NAC.
5. To determine the ability of VLP-Peanut, adjuvanted with MCT, to generate IL-10^+ B cell responses in PA subjects.
6. To assess the effects of extended or conventional PQ Grass 27600 SU on IgA_1, IgA_2, IgG and IgG_4 immunoglobulin responses in serum and nasal fluid and peripheral blood IL-10^+ B cell responses during a RDBPC study in GPA.

6.2 Results

6.2.1 Exploratory *ex vivo* study of the immunomodulatory potential of plant-derived *Fel d* 1 eBP to generate IL-10^{+} Breg cells in CA

A novel exploratory *ex vivo* study to evaluate the immunogenicity of plant-derived eBP expressing the major cat allergen, *Fel d* 1, to generate IL-10^{+} Breg cells was conducted in collaboration with the Amsterdam University Medical Centre and ANGANY Inc.. Within this preclinical study, biosynthetic allergen lipid eBP derived from *Nicotiana benthamiana plants*, which expressed *Fel d* 1 upon their surface, hereafter referred to as *Fel d* 1 eBP, were investigated (Figure 6.2.1.1). To assess the immunogenicity properties of *Fel d* 1 eBP, NAC and CA were stimulated with increasing concentrations of plant-derived natural purified *Fel d* 1 (hereafter referred to as natural *Fel d* 1) and *Fel d* 1 eBP and the frequency of IL-10^{+} Breg cells was assessed through multi-parametric flow cytometry. Whole bloods were collected from *n*=5 NAC and *n*=7 CA at the Royal Brompton hospital as per inclusion and exclusion criteria (detailed in section 2.2), with all study and associated laboratory research complying with both GCP and GLP guidelines (Table 6.2.1.1). Following whole blood processing to PBMCs, all laboratory operators involved within the study remained blinded to the compounds investigated until data was locked following study completion.

Table 6.2.1.1 Patient Demographics of subjects enrolled for IL-10^{+} Breg culture atopic stimulation experiments with plant-derived *Fel d 1* eBP and natural purified *Fel d* 1.

Characteristic	Non-Atopic (n=5)	Cat Allergic (n=7)
Gender, M:F	1:4	2:5
Age (y), range	25-47	22-58
Cat Dander SPT (mm), mean ± SD	0.0 ± 0.0	8.9 ± 2.4^{++}
tIgE (kU_A/L), mean ± SD	28 ± 27	157 ± 96^{++}
Cat Dander specific IgE (kU_A/L), mean ± SD	0.0 ± 0.0	3.2 ± 2.8^{++}
VAS, mean ± SD	0.0 ± 0.0	49.8 ± 22.5*,$^{++}$

*n=1 VAS not recorded. +, denotates significance between non-atopic and cat allergic. ** P < 0.01, Mann Whitney Test. VAS, Visual Analogue Score; tIgE, total IgE; SPT, skin prick test; SD, standard deviation.

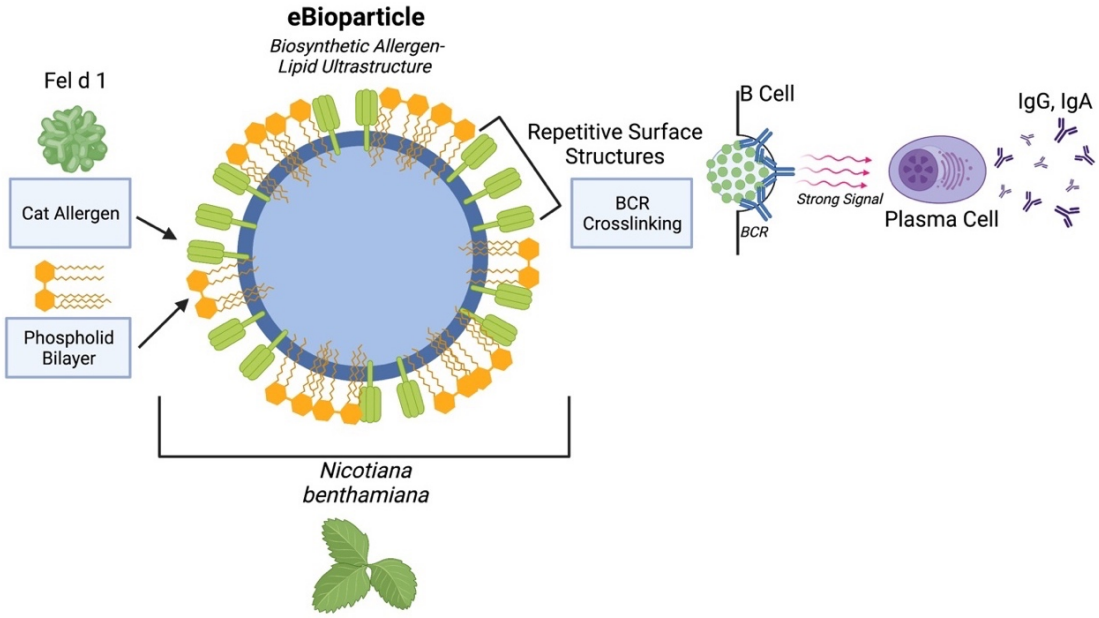


Figure 6.2.1.1 Biosynthetic Allergen eBioparticle expressing *Fel d* 1 upon its lipid ultrastructure.

An eBioparticle expressing the major cat allergen *Fel d* 1 on its surface was produced in the *Nicotiana benthamiana* plant. The eBioparticle was generated to express a phospholipid bilayer. Repetitive surface structures allow BCR cross linking, inducing a strong signal leading to induction of sustained B cell responses through IgA^+ and IgG^+ plasma cell differentiation. eBiopartIce, enveloped bioparticle.

To assess the capability of *Fel d* 1 eBP to generate IL-10^+ Breg cells, isolated PBMCs from NAC and GPA were cultured alongside *Fel d* 1 eBP (0.1μg/mL, 0.3μg/mL, 1μg/mL) and natural *Fel d* 1 (0.1μg/mL, 0.3μg/mL, 1μg/mL) for 72 hours before multi-parametric flow cytometry assessment of IL-10^+ Breg cell subsets. CA demonstrated increased IL-10^+ B cell subset frequencies following natural *Fel d* 1 or *Fel d* 1 eBP compared to NAC (Figure 6.2.1.2 and Table 6.2.1.2). Although plant derived *Fel d* 1-eBP increased the frequency of all IL-10^+ B cell subsets in NAC compared to natural *Fel d* 1, enhancement was minimal, and no significance was found ($P > 0.05$). *Fel d* 1-eBP generated increased frequencies of all IL-10^+ B cell subsets compared to natural *Fel d* 1 in CA, with a peak response at 1μg/mL, significant in the induction of $CD5^+$IL-10^+ Breg cells ($P = 0.0312$). In CA, *Fel d* 1 eBP generated a higher dose response induction of all IL-10^+ Breg cells compared to either NAC or natural *Fel d* 1, confirming eBP immunogenicity in IL-10^+ Breg cell generation.

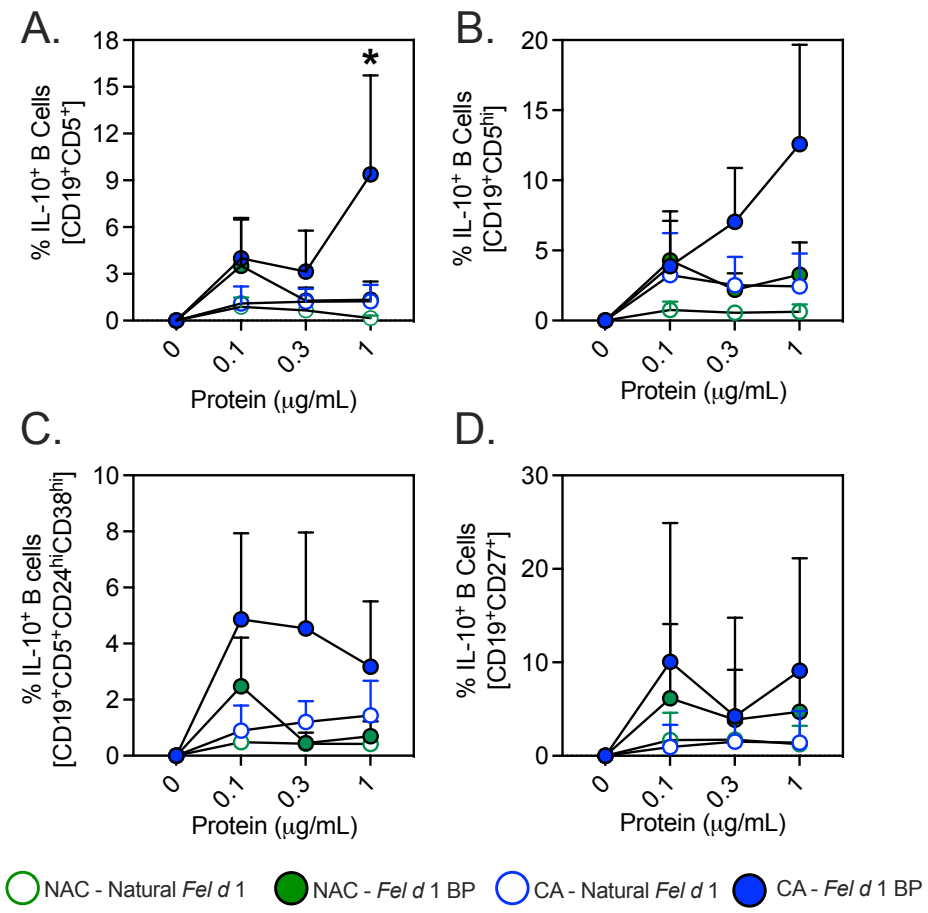


Figure 6.2.1.2 Plant-derived *Fel d* 1 eBP generate enhanced IL-10^{+} B cell frequencies in CA individuals compared to natural *Fel d* 1.

Effect of increasing concentrations of natural *Fel d* 1 and *Fel d* 1 BP on: **A)** IL-10^{+}CD19^{+}CD5^{+}, **B)** IL-10^{+}CD19^{+}CD5^{hi}, **C)** IL-10^{+}CD19^{+}CD5^{+}CD24^{hi}CD38^{hi} and **D)** IL-10^{+}CD19^{+}CD27^{+} cells. Data is representative of n=5 NAC and n=7 CA and presented as mean ± SEM. *P < 0.05, Mann-Whitney Test for between group comparison and Wilcoxon for in group comparison. *, dictates significance between *Fel d* 1 eBP and natural *Fel d* 1. NAC; non atopic control; CA, cat allergic; BP, bioparticle.

Table 6.2.1.2 IL-10$^+$ Breg Cell Subset Expression in CA and NAC following stimulation with *Fel d* 1 eBP or natural *Fel d* 1.

Compound	Concentration (μg/mL)	B Cell Subset	NAC Delta US				CA Delta US				*P* value vs. NAC[1]	*P* value NAC eBP v. natural *Fel d* 1[2]	*P* value CA eBP v. natural *Fel d* 1[2]
			n	mean	SD	SEM	n	mean	SD	SEM			
Fel d 1 eBP	0.1	$CD19^+CD5^+IL\text{-}10^+$	5	3.51	6.65	2.97	7	4.00	6.84	2.59	>0.9999	NA	NA
		$CD19^+CD5^{hi}IL\text{-}10^+$	5	4.28	7.83	3.50	7	3.88	8.57	3.24	0.5758	NA	NA
		$CD19^+CD27^+IL\text{-}10^+$	5	6.16	7.95	3.55	7	10.0	14.9	5.61	>0.9999	NA	NA
		$CD19^+CD24^{hi}CD38^{hi}IL\text{-}10^+$	5	2.47	3.88	1.74	7	4.86	8.13	3.07	0.9747	NA	NA
	0.3	$CD19^+CD5^+IL\text{-}10^+$	5	1.27	1.87	0.84	7	3.15	6.95	2.63	>0.9999	NA	NA
		$CD19^+CD5^{hi}IL\text{-}10^+$	5	2.20	2.63	1.18	7	7.04	10.2	3.84	0.3990	NA	NA
		$CD19^+CD27^+IL\text{-}10^+$	5	3.87	5.32	2.38	7	4.22	10.5	3.99	>0.9999	NA	NA
		$CD19^+CD24^{hi}CD38^{hi}IL\text{-}10^+$	5	0.45	0.84	0.38	7	4.53	9.08	3.43	0.5758	NA	NA
	1	$CD19^+CD5^+IL\text{-}10^+$	5	1.34	2.61	1.17	7	9.38	16.8	6.35	0.1566	NA	NA
		$CD19^+CD5^{hi}IL\text{-}10^+$	5	3.27	5.13	2.30	7	12.6	18.8	7.09	0.4924	NA	NA
		$CD19^+CD27^+IL\text{-}10^+$	5	4.70	4.37	1.95	7	9.10	12.0	4.55	>0.9999	NA	NA
		$CD19^+CD24^{hi}CD38^{hi}IL\text{-}10^+$	5	0.69	1.19	0.53	7	3.17	6.16	2.33	0.7475	NA	NA
Natural *Fel d* 1	0.1	$CD19^+CD5^+IL\text{-}10^+$	5	0.88	1.33	0.60	7	1.10	2.90	1.10	0.0720	0.6250	0.2500
		$CD19^+CD5^{hi}IL\text{-}10^+$	5	0.76	1.31	0.59	7	3.25	7.92	2.99	0.9293	0.2500	0.5000
		$CD19^+CD27^+IL\text{-}10^+$	5	1.68	2.92	1.31	7	0.94	2.37	0.89	0.4078	0.2500	0.1250
		$CD19^+CD24^{hi}CD38^{hi}IL\text{-}10^+$	5	0.49	0.77	0.34	7	0.89	2.37	0.89	0.2222	0.5000	0.2500
	0.3	$CD19^+CD5^+IL\text{-}10^+$	5	0.66	0.92	0.41	7	1.22	2.18	0.83	0.8422	0.5000	0.6250
		$CD19^+CD5^{hi}IL\text{-}10^+$	5	0.56	0.96	0.43	7	2.52	5.35	2.02	0.6591	0.2500	0.1562
		$CD19^+CD27^+IL\text{-}10^+$	5	1.73	1.77	0.79	7	1.52	3.03	1.14	0.5833	0.5000	0.6250
		$CD19^+CD24^{hi}CD38^{hi}IL\text{-}10^+$	5	0.42	0.52	0.23	7	1.21	1.96	0.74	>0.9999	>0.9999	0.4375
	1	$CD19^+CD5^+IL\text{-}10^+$	5	0.16	0.36	0.16	7	1.24	2.81	1.06	0.3990	0.5000	**0.0312**
		$CD19^+CD5^{hi}IL\text{-}10^+$	5	0.62	1.19	0.53	7	2.44	6.19	2.34	>0.9999	0.2500	0.0625
		$CD19^+CD27^+IL\text{-}10^+$	5	1.25	1.97	0.88	7	1.41	3.39	1.28	0.8586	0.1250	0.0625
		$CD19^+CD24^{hi}CD38^{hi}IL\text{-}10^+$	5	0.42	0.61	0.27	7	1.43	3.28	1.24	>0.9999	0.6250	0.1250

Bolded Values Represent significant ***P*** Values. [1]Mann Whitney Test, [2]Wilcoxon paired signed-rank Test. eBP, enveloped Bioparticle; CA, cat allergic; NAC, non-atopic control; US, unstimulated.

6.2.2 Exploratory *ex vivo* study to evaluate the immunogenicity of VLP Peanut, with and without MCT, to generate IL-10^{+} Breg cells from PA

A novel exploratory *ex vivo* study to evaluate the ability of VLP expressing peanut to induce IL-10^{+} Breg cells was conducted in collaboration with Allergy Therapeutics (UK) Ltd. Within this study, the VLP compounds investigated were derived from cucumber mosaic viruses which expressed tetanus toxin epitopes ($CuMV_{TT}$-VLP), which were genetically fused with *Ara h* 2 upon their surface, hereafter referred to as VLP Peanut (Figure 6.2.2.1). To assess the immunogenicity properties of the depot adjuvant MCT and whether this impacts the hypo-allergenicity of VLP Peanut, VLP Peanut was also investigated in combination with MCT, hereafter referred to as VLP Peanut + MCT. In addition to VLP Peanut, with or without MCT, recombinant *Ara h* 2 (*Ara h* 2) and whole peanut extract (WPE) were investigated as controls. Prior to study commencement, VLP Peanut was diluted to a 'working' concentration 10 times higher than the desired final concentration of *Ara h* 2 to accommodate for the 10.57% incorporation rate of *Ara h* 2 into the VLP, thus ensuring the final concentration of *Ara h* 2 fused to VLP Peanut was comparable to the control *Ara h* 2 (i.e., 1 µg of VLP Peanut = 0.157 µg of Ara h 2). To generate VLP Peanut + MCT, compounds were mixed at a 1:1 ratio at 4 °C for 48 hours prior to experimental set-up to allow for a final concentration of 2% MCT. Whole bloods were collected from n=6 PA children (aged between 6-18 years) who had provided informed and optional additional blood donation consent as part of the ongoing BOPI-2 study at ICL and was approved by the NHS Human Research Authority (reference 19/LO/0406), complying with GCP and GLP guidelines (Table 6.2.2.1). Criteria for peanut allergen sensitivity was confirmed as described in section 2.2, with all subjects also undertaking a double-blind placebo-controlled food challenge to confirm allergy to ≤1.44g peanut protein at baseline. Following whole blood processing to PBMCs, all laboratory operators involved within the study remained blinded to the compounds investigated until data was locked following study completion.

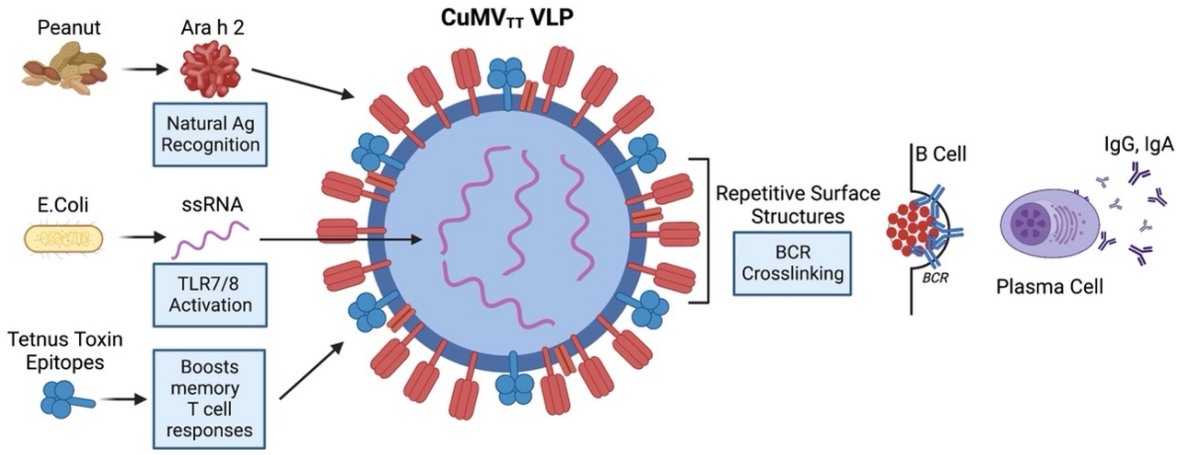


Figure 6.2.2.1 VLP derived from cucumber mosaic virus including tetanus toxin epitopes (CuMV$_{TT}$) genetically fused with *Ara h* 2 for peanut allergy treatment

CuMV-derived VLPs were genetically fused to the major peanut allergy *Ara h* 2, expressed on the exterior surface allowing for natural antigen recognition. Repetitive surface structures allow for BCR cross linking, inducing a strong signal leading to induction of sustained B cell responses through IgA$^+$ and IgG$^+$ plasma cell differentiation. CuMV contain ssRNA derived from E. Coli, able to stimulate TLR7/8 to further enhance B cell activation, and a tetanus toxin ($_{TT}$) derived peptide, which is recognised by previously activated memory T cells. ssRNA, single strand RNA; TLR, toll-like receptor; VLP, virus like particle; BCR, B cell receptor.

Table 6.2.2.1 Patient Demographics of subjects recruited for an exploratory *ex vivo* study to evaluate the reactogenic/hypo-allergic properties of VLP Peanut

Characteristic	PA Children (6-18 years; n=6)
Gender, M:F	6:0
Age (y), range	10 (8:12)
Peanut SPT (mm), mean ± SD	10.33 ± 3.70
tIgE (kU$_A$/L), mean ± SD	1125 ± 761.80
Ara h 1 specific IgE (kU$_A$/L),	58.88 ± 40.50
Ara h 2 specific IgE (kU$_A$/L),	80.75 ± 23.55
Ara h 3 specific IgE (kU$_A$/L),	29.53 ± 29.79
Ara h 8 specific IgE (kU$_A$/L),	0.70 ± 1.21
Ara h 9 specific IgE (kU$_A$/L),	0.81 ± 1.12
Anaphylaxis after food challenge	3/6
Tetanus Vaccination	6/6

SPT, skin prick test; sIgE, specific immunoglobulin E; tIgE, total IgE. VLP, virus-like particle; MCT, microcrystalline tyrosine; WPE, whole peanut extract.

To assess the capability of VLP Peanut to modulate IL-10^{+} Breg cells, PBMCs were stimulated with VLP Peanut (0μg/mL, 1μg/mL, 3μg/mL, 10μg/mL), VLP Peanut+MCT (0μg/mL, 1μg/mL, 3μg/mL, 10μg/mL, *Ara h* 2 (0μg/mL, 1μg/mL, 3μg/mL, 10μg/mL) or WPE (0μg/mL, 1μg/mL, 3μg/mL, 10μg/mL) for 72 hours before multi-parametric flow cytometry assessment. In response to increasing concentrations of *Ara h* 2 and WPE, minimal induction of activated CD5^{+}, CD5^{hi} and transitional CD5^{+}CD24^{hi}CD38^{hi} IL-10^{+} Breg cells was observed (Figure 6.2.2.2, A-E and Table 6.2.2.2). However, *Ara h* 2 and WPE both stimulated a dose-dependent induction of CD27^{+} IL-10^{+} Breg cells (Figure 6.2.2.2, E). VLP Peanut significantly induced CD5^{+}, CD5^{hi} and CD5^{+}CD24^{hi}CD38^{hi} IL-10^{+} Breg cells in a dose-dependent manner, with a peak response observed at 1μg/mL. in CD5^{+} (P = 0.0312), CD5^{hi} (P = 0.0312) and CD5^{+}CD24^{hi}CD38^{hi} IL-10^{+} Breg cells (P = 0.0625). Addition of MCT to VLP Peanut enhanced its immunogenicity to induce IL-10^{+} Breg cells at 10μg/mL in CD5^{+}, CD5^{hi} and CD24^{hi}CD38^{hi} IL-10^{+} Breg cells, although a statistical significance was not reached (P > 0.05). To validate flow cytometry findings, unbiased machine learning clustering algorithms, viSNE and FlowSOM, were performed. Analysis of parameter channels through viSNE algorithm revealed three distinct islands of CD19^{+} B cells that were high in IL-10 expression (Figure 6.2.2.3, A; black arrows and islands). viSNE analysis revealed that all three islands of IL-10^{+} Breg cells were enhanced following VLP Peanut and VLP Peanut + MCT treatment compared to *Ara h* 2 or WPE. FlowSOM analysis to deeper interrogate viSNE data identified four distinct MC of IL-10^{+} Breg cells that were differentially targeted by VLP Peanut, with or without MCT, compared to *Ara h* 2 and WPE, MC 5, MC 7, MC 16, and MC 17 (Figure 6.2.2.3, B). Heatmap analyses were able to phenotype each MC: MC5 (CD5^{+}CD24^{hi}CD27^{+}CD38^{hi}), MC7 (CD5^{hi}CD24^{lo}CD27^{-}CD38^{hi}), MC16 (CD38^{+}) and MC17 (CD5^{+}CD24^{+}CD38^{hi}; Figure 6.2.2.3, C). Quantification of the population abundances of each MC further supported flow cytometry findings through confirming VLP Peanut, with or without MCT, demonstrates a higher capacity to induce MC 5, MC 7 and MC 16 compared to *Ara h* 2 or WPE (Figure 6.2.2.3, D). Interestingly, only MC 17 was induced by VLP Peanut+MCT at 10μg/mL.

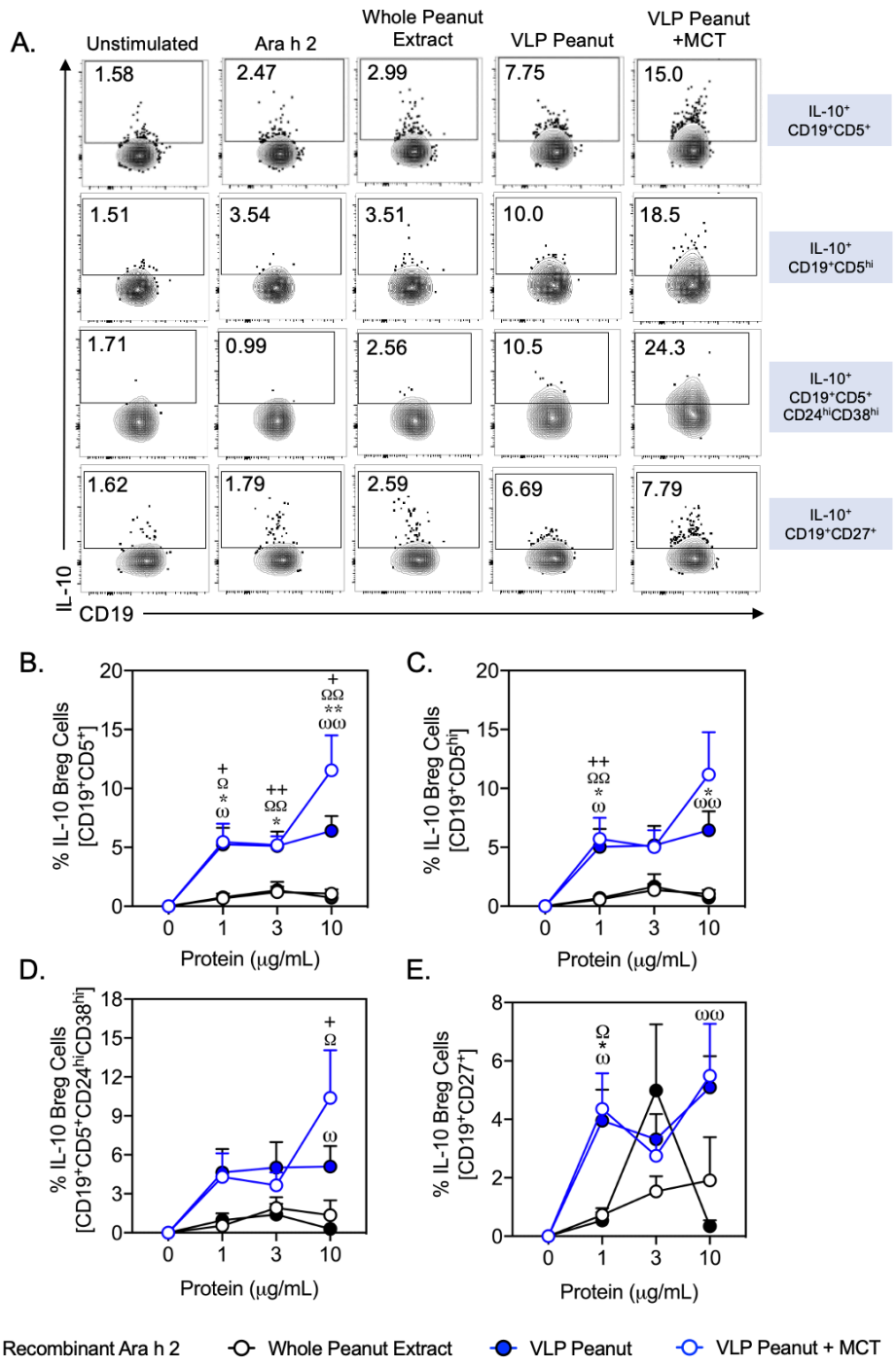


Figure 6.2.2.2 VLP Peanut significantly induces IL-10$^+$ B cells compared to *Ara h* 2 and WPE.

A) Representative flow cytometry plots demonstrating the proportion of IL-10$^+$ B cell subsets in response to 10 mg/mL of *Ara h* 2, WPE, VLP Peanut or VLP Peanut + MCT. Effect of increasing concentrations of *Ara h* 2, WPE, VLP Peanut or VLP Peanut + MCT on: **B)** IL-10$^+$CD5$^+$, **C)** IL-10$^+$CD5^{hi}, **D)** IL-10$^+$CD5$^+$CD24^{hi}CD38^{hi} and **E)** IL-10$^+$CD27$^+$ cells. Data is representative of n=6 PA and presented as mean ± SEM. * $P < 0.05$, ** $P < 0.01$, Mann-Whitney Test for between group comparison and Wilcoxon signed-pairs rank test for within group comparisons. ^{w}, * denotes significance between VLP Peanut and *Ara h* 2 or WPE, respectively. Ω, + denotes significance between VLP Peanut + MCT and *Ara h* 2 or WPE, respectively. WPE, whole peanut extract; VLP, virus-like particle; MCT, microcrystalline tyrosine; PA, peanut allergic.

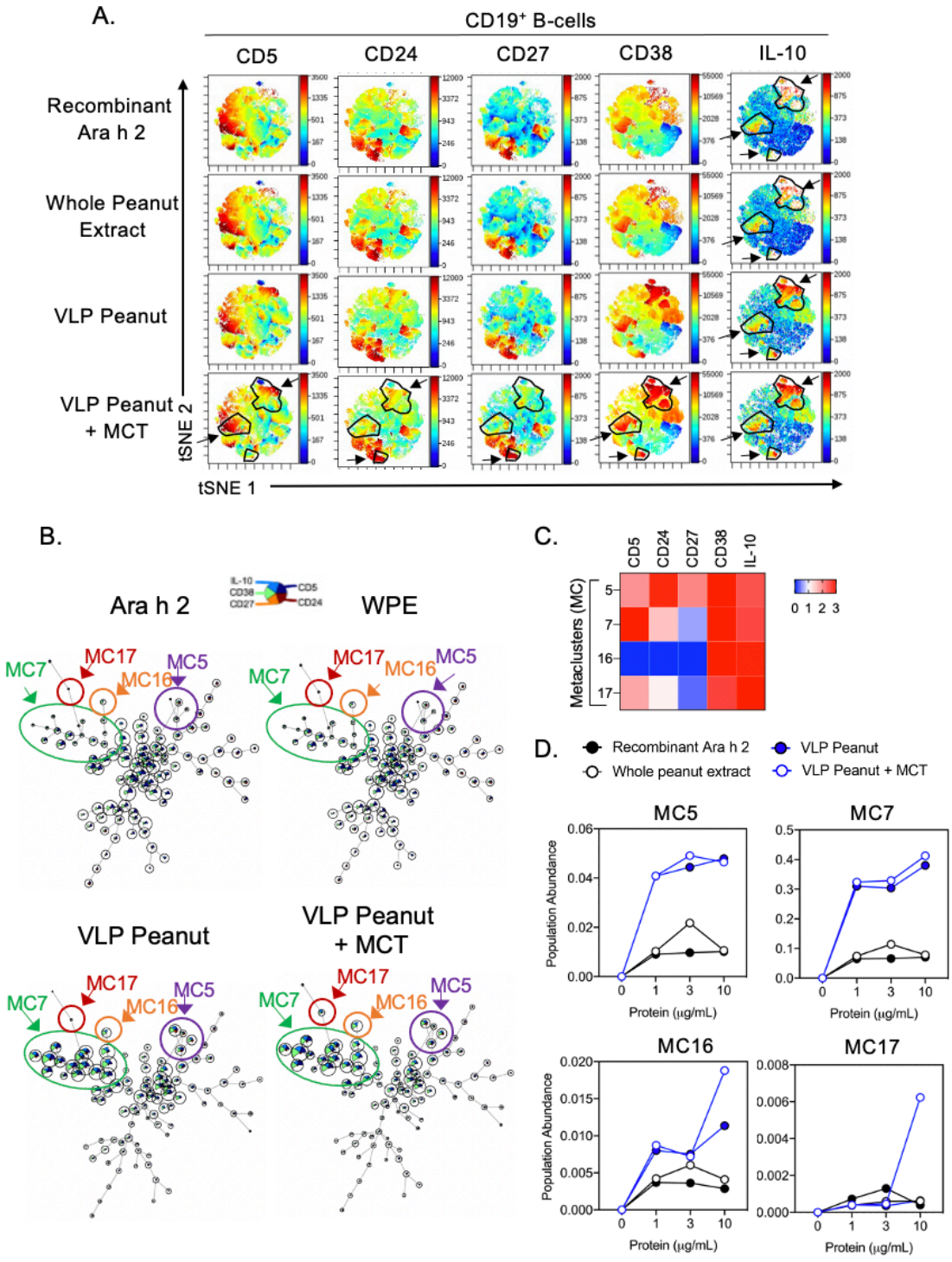


Figure 6.2.2.3 Unbiased clustering analysis reveals VLP Peanut targets four specific metaclusters corresponding to IL-10⁺ B cells.

A) viSNE (concatenated n=6 dataset) to illustrate the effect of *Ara h* 2, WPE, VLP Peanut and VLP Peanut + MCT at 10 mg/mL. Islands of cells corresponding to IL-10⁺ B cell populations are highlighted with black arrows. **B)** FlowSOM star plot analysis illustrate 4 MC are differentially expressed in response to *Ara h* 2, WPE, VLP Peanut and VLP Peanut + MCT. **C)** Heatmap representing the MC phenotype of B cells. **D)** Population abundance demonstrating the effects of varying concentrations of *Ara h* 2, WPE, VLP Peanut and VLP Peanut + MCT on MC 5, MC 7, MC 16, and MC 17. WPE, whole peanut extract; VLP, virus-like particle; MCT, microcrystalline tyrosine; MC, metacluster

Table 6.2.2.2 IL-10$^+$ Breg Cell Subset Expression Following stimulation with VLP Peanut, with and without MCT, *Ara h* 2 and WPE.

Compound	Concentration (μg/mL)	B Cell Subset	Delta Unstimulated				*P* value vs. respective 0μg/mL [0][1]	*P* value vs. VLP Peanut[2]	*P* value vs. VLP Peanut + MCT[2]	*P* value vs. *Ara h* 2[2]
			n	mean	SD	SEM				
VLP Peanut	1	$CD19^+CD5^+IL\text{-}10^+$	6	5.25	3.43	1.40	**0.0312**	NA	NA	NA
		$CD19^+CD5^{hi}IL\text{-}10^+$	6	5.03	3.73	1.52	**0.0312**	NA	NA	NA
		$CD19^+CD27^+IL\text{-}10^+$	6	3.96	2.60	1.06	**0.0312**	NA	NA	NA
		$CD19^+CD24^{hi}CD38^{hi}IL\text{-}10^+$	6	4.64	4.42	1.80	0.0625	NA	NA	NA
	3	$CD19^+CD5^+IL\text{-}10^+$	6	5.12	2.99	1.22	**0.0312**	NA	NA	NA
		$CD19^+CD5^{hi}IL\text{-}10^+$	6	5.16	4.03	1.64	**0.0312**	NA	NA	NA
		$CD19^+CD27^+IL\text{-}10^+$	6	3.32	2.12	0.86	**0.0312**	NA	NA	NA
		$CD19^+CD24^{hi}CD38^{hi}IL\text{-}10^+$	6	5.03	4.77	1.95	0.1250	NA	NA	NA
	10	$CD19^+CD5^+IL\text{-}10^+$	6	6.40	3.07	1.25	**0.0312**	NA	NA	NA
		$CD19^+CD5^{hi}IL\text{-}10^+$	6	6.45	3.93	1.60	**0.0312**	NA	NA	NA
		$CD19^+CD27^+IL\text{-}10^+$	6	5.10	2.62	1.07	**0.0312**	NA	NA	NA
		$CD19^+CD24^{hi}CD38^{hi}IL\text{-}10^+$	6	5.11	3.84	1.57	0.0625	NA	NA	NA
VLP Peanut + MCT	1	$CD19^+CD5^+IL\text{-}10^+$	6	5.46	3.80	1.55	**0.0312**	0.9372	NA	NA
		$CD19^+CD5^{hi}IL\text{-}10^+$	6	5.70	4.42	1.80	**0.0312**	0.8182	NA	NA
		$CD19^+CD27^+IL\text{-}10^+$	6	4.36	2.98	1.22	**0.0312**	0.8182	NA	NA
		$CD19^+CD24^{hi}CD38^{hi}IL\text{-}10^+$	6	4.30	4.47	1.82	0.0625	0.9134	NA	NA
	3	$CD19^+CD5^+IL\text{-}10^+$	6	5.19	1.83	0.75	**0.0312**	0.6991	NA	NA
		$CD19^+CD5^{hi}IL\text{-}10^+$	6	5.02	3.48	1.42	0.0625	>0.9999	NA	NA
		$CD19^+CD27^+IL\text{-}10^+$	6	2.75	1.63	0.66	**0.0312**	0.5887	NA	NA
		$CD19^+CD24^{hi}CD38^{hi}IL\text{-}10^+$	6	3.65	2.44	1.00	0.0625	0.9394	NA	NA
	10	$CD19^+CD5^+IL\text{-}10^+$	6	11.5	7.28	2.97	**0.0312**	0.2403	NA	NA
		$CD19^+CD5^{hi}IL\text{-}10^+$	6	11.2	8.80	3.59	0.1250	0.3701	NA	NA
		$CD19^+CD27^+IL\text{-}10^+$	6	5.49	4.36	1.78	0.0625	0.6234	NA	NA
		$CD19^+CD24^{hi}CD38^{hi}IL\text{-}10^+$	6	10.4	8.98	3.67	0.0625	0.3290	NA	NA
Ara h 2	1	$CD19^+CD5^+IL\text{-}10^+$	6	0.76	1.1	0.44	0.2500	**0.0238**	**0.0238**	NA
		$CD19^+CD5^{hi}IL\text{-}10^+$	6	0.69	0.89	0.36	0.2500	**0.0238**	**0.0087**	NA
		$CD19^+CD27^+IL\text{-}10^+$	6	0.54	0.69	0.28	0.1250	**0.0152**	**0.0260**	NA
		$CD19^+CD24^{hi}CD38^{hi}IL\text{-}10^+$	6	0.96	1.29	0.53	0.1250	0.2338	0.3074	NA
	3	$CD19^+CD5^+IL\text{-}10^+$	6	1.36	1.74	0.71	0.0625	**0.0260**	**0.0087**	NA
		$CD19^+CD5^{hi}IL\text{-}10^+$	6	1.65	2.59	1.06	0.1250	0.1255	0.0909	NA
		$CD19^+CD27^+IL\text{-}10^+$	6	4.99	5.55	2.26	**0.0312**	0.9740	0.9372	NA
		$CD19^+CD24^{hi}CD38^{hi}IL\text{-}10^+$	6	1.40	2.03	0.83	0.1250	0.3550	0.1775	NA
	10	$CD19^+CD5^+IL\text{-}10^+$	6	0.72	0.86	0.35	0.2500	**0.0022**	**0.0087**	NA
		$CD19^+CD5^{hi}IL\text{-}10^+$	6	0.72	0.78	0.32	0.1250	**0.0043**	0.2078	NA
		$CD19^+CD27^+IL\text{-}10^+$	6	0.34	0.49	0.20	0.1250	**0.0043**	0.1775	NA
		$CD19^+CD24^{hi}CD38^{hi}IL\text{-}10^+$	6	0.30	0.72	0.30	>0.9999	**0.0152**	**0.0281**	NA
WPE	1	$CD19^+CD5^+IL\text{-}10^+$	6	0.68	0.99	0.40	0.1250	**0.0260**	**0.0260**	>0.9999
		$CD19^+CD5^{hi}IL\text{-}10^+$	6	0.58	0.65	0.27	0.2500	**0.0152**	**0.0022**	>0.9999
		$CD19^+CD27^+IL\text{-}10^+$	6	0.73	0.57	0.23	0.0625	**0.0260**	0.0714	0.8463
		$CD19^+CD24^{hi}CD38^{hi}IL\text{-}10^+$	6	0.54	0.84	0.35	0.5000	0.0584	0.0801	0.3723
	3	$CD19^+CD5^+IL\text{-}10^+$	6	1.20	1.15	0.47	0.0625	**0.0411**	**0.0043**	0.8593
		$CD19^+CD5^{hi}IL\text{-}10^+$	6	1.36	1.30	0.53	0.0625	0.1320	0.0974	0.8139
		$CD19^+CD27^+IL\text{-}10^+$	6	1.53	1.28	0.52.9	**0.0312**	0.1320	0.2403	0.9740
		$CD19^+CD24^{hi}CD38^{hi}IL\text{-}10^+$	6	1.91	2.04	0.83	0.1250	0.2749	0.2338	0.7965
	10	$CD19^+CD5^+IL\text{-}10^+$	6	1.06	0.91	0.37	0.1250	**0.0022**	**0.0152**	0.5671
		$CD19^+CD5^{hi}IL\text{-}10^+$	6	1.04	0.84	0.34	0.1250	**0.0260**	0.2078	0.5628
		$CD19^+CD27^+IL\text{-}10^+$	6	1.91	3.62	1.48	0.0625	0.1320	0.4177	0.4827
		$CD19^+CD24^{hi}CD38^{hi}IL\text{-}10^+$	6	1.35	2.82	1.15	0.2500	0.1017	0.0433	0.4242

Bolded Values Represent significant ***P*** Values. [1]Wilcoxon paired signed-rank Test, [2]Mann Whitney Test.

6.2.3 RDBPC exploratory study of short-course PQ Grass 27600 SU AIT for the treatment of seasonal allergic rhinoconjuctivitis

In an exploratory RDBPC pilot phase III study, PQ Grass 27600 SU (a GP allergoid adjuvanted with MPL-A and MCT) was assessed to determine whether a short-course of SCIT-treatment can modulate B cell and antibody responses in GPA (NCT04687059; EudraCT number: 2020-000408-13) (381). This novel multi-centre study was run in collaboration with Allergy Therapeutics and involved enrolment of n=119 GPA across 14 investigator sites within Germany and the United States of America. Inclusion criteria included positive SPT for GP (≥3mm), elevated GP-sIgE and clinical history of moderate-severe SAR symptoms, with exclusion criteria including prior history of any allergen AIT. An initial dose regimen study performed by Allergy Therapeutics using cumulative dosages of PQGrass ranging from 5100 SU to 35600 SU demonstrated the 27500U dosage was to be taken forward for further development (EudraCT number 2017-000333-31). GPA were randomised to one of 4 treatment groups in a 2:2:1:1 ratio: PQ Grass 27500U conventional regimes (shorter-term), PQ Grass 27500U extended regimes (cumulative doses over a longer-time period), or placebo with or without MCT. For placebo treatment, GPA subjects received ten injections of either placebo only or placebo containing MCT. For conventional and extended PQGrass AIT treatment arms, GPA received six active injections of PQ Grass compromising up an up-dosing phase (900, 2700 and 6000 SU) followed by a maintenance phase (6000, 6000 and 6000 SU). The up-dosing regimen in both AIT arms consisted of 3 weekly injections, with the conventional treatment arm then administered maintenance dosages weekly whereas the extended treatment arm was administered maintenance dosages monthly. During the study, participants provided nasal fluid and whole blood samples at baseline (Visit 1), visit 12 (~2 weeks before commencement of the GP season) and visit 15 (10 weeks post GP season; Figure 6.2.3.1, A-B). PBMCs were isolated from whole blood at study sites and cryopreserved prior to sample shipments. Samples were shipped to the ITG laboratories at Imperial College London for assessment of changes in serum GP-sIgG, -sIgA1 and -sIgA2 levels and nasal

fluid GP-sIgG and -sIgG$_4$ compared to baseline through ELISA and ImunoCAP assessment. Additionally, the frequency of IL-10$^+$ Breg cells in PBMC samples was quantified through multi-parametric flow cytometry. For clarity, as part of the large clinical study, I contributed towards nasal fluid extraction, ELISA optimisation and final ELISA experiments alongside other ITG laboratory team members. I did not perform ImmunoCAP experiments myself, however, was involved in internal data discussion. I was however solely responsible for conducting the IL-10$^+$ Breg culture experiments on isolated PBMC samples. All laboratory staff were blinded to patient group allocation until all experimental analyses had been completed and data was locked.

To assess IL-10$^+$ Breg cell frequencies, cryopreserved PBMCs were defrosted and counted using a hemocytometer prior to culture set-up. Unfortunately, cell counts determined at sample defrosting were very low with many samples being unable to be utilised in culture systems due to insufficient availability of cells. In line with initial concerns over sample viability, most samples that were cultured were not viable (<20%) and could not be analysed for B cell activation. Thus, I was unable to conclude whether PQ Grass could generate IL-10$^+$ Breg cells and the analysis of IL-10$^+$ B cells was concluded during the study to result in a non-experiment.

ImmunoCAP and ELISA analysis was performed to assess GP specific IgG and IgG$_4$ levels in nasal fluid and GP specific IgG, IgA1 and IgA2 levels within serum samples, to supplement current knowledge of potential AIT biomarkers and mechanisms and provide indirect insight into B cell modulation following AIT. Before ELISA experiments on valuable study samples could be performed, ELISA conditions were first optimised for IgA1, IgA2 and IgG assessment (see Section 2.12.2). Both nasal and serum GP-specific IgG levels were significantly increased following conventional and extended PQ Grass treatment and enhanced further following the GP season (P < 0.001, Figure 6.2.3.1, C-D and Table 6.2.3.1). MCT demonstrated a small immunogenic effect on IgG levels within placebo treated samples, however, levels were not

further increased during the GP season as was observed in placebo without MCT. Nasal fluid levels of GP-specific IgG_4 were increased following conventional and extended PQ Grass AIT and significantly enhanced following the GP season ($P < 0.05$, Figure 6.2.3.1, E). On the other hand, placebo, with and without MCT, drove a downward trend in nasal GP-specific IgG_4 which returned to baseline levels following the GP season. Although both administration regimes of PQ Grass induced significant serum IgA1 and IgA2 antibody levels following treatment administration (both, $P < 0.001$), levels were not maintained during the GP season (Figure 6.2.3.1, F-G). However, serum IgA1 and IgA2 antibody levels remained significantly higher than baseline compared (both, $P < 0.001$). Interestingly, placebo, with or without MCT demonstrated an increase in IgA2 during the GP season but not IgA1, which levels remained at baseline following placebo with MCT treatment and decreased following treatment with placebo only. No difference in any antibody levels was observed following treatment with either extended or conventional AIT ($P > 0.05$).

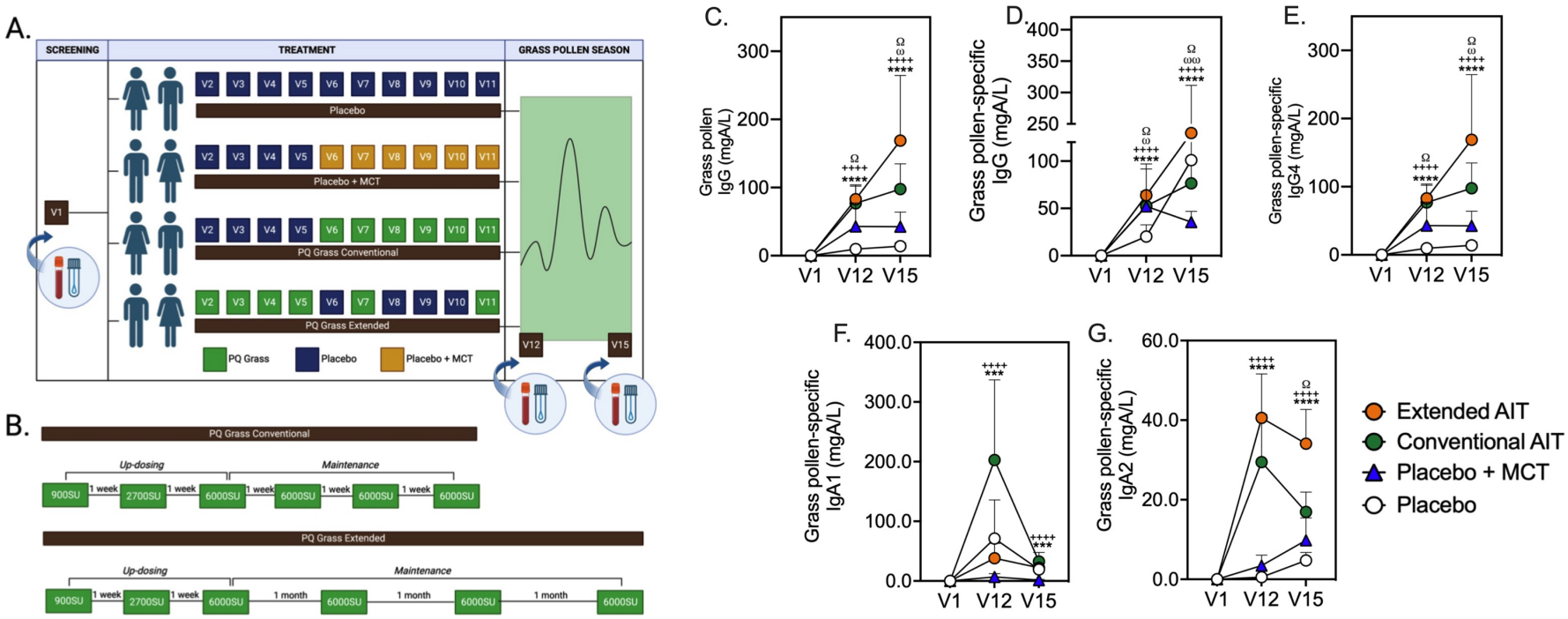


Figure 6.2.3.1 PQGrass 27600 SU Phase III study design and evaluation of GP sIgG, sIgG$_4$, sIgA1 and sIgA2 levels in NF and serum.

A) Treatment options included; 1) 10x injections of placebo, 2) 4x injections of placebo followed by 6x injections of placebo containing MCT, 3) 4x injections of placebo followed by 6x injections of PQ Grass (conventional regime), 4) 4x injections of PQ Grass, followed by 1 injection of placebo, 1x injection of PQ Grass, followed by 3x injections of placebo and 1x final injection of PQ Grass (extended). NF and whole blood samples were collected at V1, V12 and V15. Visit schedule; V2-4, 6-8 days apart; V4-5, 27-29 days apart; V5-6, 20-22 days apart; V6-11, 6-8 days apart. V12 occurs ~2 weeks before commencement of the GP season. V15 occurs 10 weeks after the start of the GP season. **B)** Conventional and extended PQ Grass arms received maintenance dosages weekly, or monthly, respectively. Levels of GP sIgG was measured in: **C)** serum and **D)** NF using ELISA. **C)** Level of GP sIgG$_4$ was measured in NF using ImmunoCAP. Levels of serum GP **(E)** sIgA1 and **(F)** **s**IgA2 were also measured using ELISA. Data are quantified as changes from V1 and are presented as mean ±SEM. Wilcoxon signed rank test, **P* < 0.05, ***P* < 0.01 and ****P* < 0.001. *, +, w, Ω denotes statistical significance at V12 and V15 compared to V1 in conventional AIT, extended AIT, Placebo+MCT and Placebo without MCT, respectively. Conventional AIT, n=23; extended AIT, n=25; placebo + MCT, n=13; placebo without MCT, n=12. AIT, allergen immunotherapy; MCT, microcrystalline tyrosine; V, visit; NF, nasal fluid.

Table 6.2.3.1 ELISA and ImmunoCAP analysis of grass pollen specific IgG, IgG_4, IgA1 and IgA2 levels in nasal fluid and serum

Location	Target	Treatment	Visit	n	mean	SD	SEM	*P* value vs. V1[1]	*P* value vs. V12[1]	*P* value vs. Placebo + MCT[2]	*P* value Conventional. vs Extended AIT[2]
Serum	IgG	Conventional AIT	V1	23	0	0	0	NA	NA	>0.9999	>0.9999
			V12	21	76.85	115.3	25.15	**<0.0001**	NA	0.0725	0.7060
			V15	23	97.64	178.5	37.22	**<0.0001**	0.4473	0.4992	0.2673
		Extended AIT	V1	26	0	0	0	NA	NA	>0.9999	NA
			V12	26	82.86	107.4	21.06	**<0.0001**	NA	**0.0398**	NA
			V15	26	168.8	487.4	95.58	**<0.0001**	0.9441	0.2237	NA
		Placebo + MCT	V1	9	0	0	0	NA	NA	NA	NA
			V12	9	55.22	149.9	49.96	0.0625	NA	NA	NA
			V15	9	58.82	89.61	29.87	**0.0156**	0.5781	NA	NA
		Placebo without MCT	V1	12	0	0	0	NA	NA	NA	NA
			V12	12	9.751	18.17	5.246	**0.0312**	NA	NA	NA
			V15	11	13.94	16.24	4.896	**0.0156**	0.3125	NA	NA
	IgA_1	Conventional AIT	V1	23	0	0	0	NA	NA	>0.9999	>0.9999
			V12	23	202.7	643.9	134.3	**0.0002**	NA	**0.0449**	0.5973
			V15	23	32.57	73.31	15.29	**0.0005**	0.0946	**0.0095**	0.7958
		Extended AIT	V1	26	0	0	0	NA	NA	>0.9999	NA
			V12	26	38.10	126.2	24.75	**<0.0001**	NA	0.0617	NA
			V15	26	22.25	43.36	8.504	**<0.0001**	0.6112	**0.0025**	NA
		Placebo + MCT	V1	13	0	0	0	NA	NA	NA	NA
			V12	13	6.835	19.50	5.408	0.2500	NA	NA	NA
			V15	13	1.379	4.973	1.379	>0.9999	0.5000	NA	NA
		Placebo without MCT	V1	12	0	0	0	NA	NA	NA	NA
			V12	12	71.15	223.7	64.59	0.0625	NA	NA	NA
			V15	12	19.28	35.98	10.39	0.0625	0.8438	NA	NA
	IgA_2	Conventional AIT	V1	23	0	0	0	NA	NA	>0.9999	>0.9999
			V12	23	29.45	57.37	11.96	**<0.0001**	NA	**0.0015**	0.3519
			V15	23	16.93	23.87	4.976	**<0.0001**	0.5459	0.1150	0.0972
		Extended AIT	V1	26	0	0	0	NA	NA	>0.9999	NA
			V12	26	40.57	56.32	11.05	**<0.0001**	NA	**0.0007**	NA
			V15	26	34.09	43.77	8.583	**<0.0001**	0.5937	**0.0108**	NA
		Placebo + MCT	V1	13	0	0	0	NA	NA	NA	NA
			V12	13	3.442	9.418	2.612	0.2500	NA	NA	NA
			V15	13	9.788	20.37	5.649	0.1250	0.4375	NA	NA
		Placebo without MCT	V1	12	0	0	0	NA	NA	NA	NA
			V12	12	0.5258	1.692	0.488	0.2500	NA	NA	NA
			V15	12	4.723	7.000	2.021	**0.0156***	**0.0469**	NA	NA
Nasal Fluid	sIgG	Conventional AIT	V1	23	0	0	0	NA	NA	>0.9999	>0.9999
			V12	23	52.58	73.59	15.34	**<0.0001**	NA	0.0517	0.6071
			V15	23	76.49	123.7	25.8	**<0.0001**	0.8649	0.9932	0.7632

	Extended AIT	V1	24	0	0	0	NA	NA	>0.9999	NA
		V12	24	63.83	136.1	27.78	**<0.0001**	NA	0.1081	NA
		V15	23	182.6	617.6	128.8	**<0.0001**	0.5446	>0.9999	NA
	Placebo + MCT	V1	13	0	0	0	NA	NA	NA	NA
		V12	13	52.14	161.6	44.83	**0.0156**	NA	NA	NA
		V15	12	35.55	38.92	11.23	**0.0039**	0.3008	NA	NA
	Placebo without MCT	V1	12	0	0	0	NA	NA	NA	NA
		V12	12	20.17	43.14	12.45	**0.0312**	NA	NA	NA
		V15	12	101.0	180.6	52.14	**0.0312**	0.1641	NA	NA
$sIgG_4$	Conventional AIT	V1	19	0	0	0	NA	NA	>0.9999	>0.9999
		V12	18	11.30	20.49	4.829	**0.0391**	NA	0.0679	0.8722
		V15	17	47.65	107.6	26.09	**0.0156**	0.4062	0.2146	0.8465
	Extended AIT	V1	21	0	0	0	NA	NA	>0.9999	NA
		V12	18	21.30	74.74	17.62	0.1875	NA	0.0815	NA
		V15	20	69.00	187.4	41.90	**0.0186**	0.2637	0.3086	NA
	Placebo + MCT	V1	10	0	0	0	NA	NA	NA	NA
		V12	10	-10.67	23.77	7.516	0.2500	NA	NA	NA
		V15	9	0.3704	22.39	7.463	>0.9999	0.2500	NA	NA
	Placebo without MCT	V1	10	0	0	0	NA	NA	NA	NA
		V12	10	-22.00	37.88	11.98	0.0938	NA	NA	NA
		V15	9	-2.593	84.98	28.33	>0.9999	0.6250	NA	NA

Bolded Values Represent significant ***P*** Values. [1]Wilcoxon paired signed-rank Test, [2]Mann Whitney Test

6.3 Summary

In this chapter, during an exploratory *ex vivo* preclinical study, plant-derived *Fel d* 1 eBP was demonstrated to possess immunogenicity properties through the significant induction of IL-10^+ Breg cellular subsets compared to natural purified *Fel d* 1 in CA AR subjects, in a dose-dependent manner. Moreover, another exploratory *ex vivo* preclinical study investigating a VLP genetically fused to *Ara h* 2, with and without the depot adjuvant MCT, demonstrated ability to generate a dose-dependent increase in IL-10^+ Breg cellular subsets in children with peanut allergy. IL-10^+ Breg cellular subsets were significantly enhanced compared to *Ara h* 2 and WPE, confirmed by computational mathematical algorithms, demonstrating the immunogenicity of the VLP as an allergen carrier system. Moreover, FlowSOM clustering revealed a distinct IL-10^+ Breg MC that was selectively targeted by MCT. Thus, these results demonstrate the significant immunogenicity of VLP Peanut, and highlight the added benefit of MCT for stimulation of IL-10^+ Breg responses in peanut allergic children. Although the ability of PQGrass 27600 SU SCIT treatment to induce IL-10^+ Breg cells could not be assessed during a Phase III RDBPC clinical trial, both conventional and short-term treatment regimens of PQGrass SCIT 27600 SU SCIT significantly induced GP-sIgG in the nasal fluid and serum, and IgG_4 in nasal fluid compared to baseline. Moreover, short-term PQGrass 27600 SU SCIT was able to significantly induce serum levels of GP-sIgA1 and sIgA2 compared to baseline and placebo. Collectively, these three studies demonstrate the ability of novel approaches of AIT, through BP-allergen carrier systems, and short-term treatment regimens, to induce IL-10^+ Breg cells which may be important for establishment of tolerance to administered allergen.

CHAPTER 7. IL-10$^+$ B CELLS SUPPRESS ALLERGEN-STIMULATED T_H2/T_H2A CELLS AND PROMOTE IL-10$^+$ iTREG CELLULAR RESPONSES IN SAR

7.1 Introduction

Through expression of a plethora of suppressive molecules, such as IL-10, Breg cells have demonstrated ability to constrain a multitude of inflammatory environments (221, 222, 343). One proposed mechanism through which IL-10$^+$ Breg cells mediate tolerance is through modulating T cell responses, namely constraining pro-inflammatory T cell subsets in parallel to promoting Treg subsets, such as IL-10$^+$ iTreg cells (343, 344). SAR disease pathophysiology in response to GP allergen has been well correlated with increased frequency and functionality of T_H2 and allergen-specific T_H2A cells, secreting enhanced quantities of type 2 associated cytokines, such as IL-5, and IL-13 (48). Moreover, studies have demonstrated SAR patients possess attenuated IL-10$^+$ iTreg cell subsets compared to healthy controls, which may contribute towards loss of tolerance to allergen (382). As studies, including data presented in Chapter 4 and Chapters 5 of this thesis, have demonstrated SAR patients present with significant dearth of IL-10$^+$ Breg frequencies, it can be postulated that excessive T_H2 and T_H2A cell functionality is in part due to loss of downregulation by IL-10$^+$ Bregs (349). Moreover, it can be hypothesized that loss of IL-10$^+$ Breg cell subsets in SAR contributes towards dearth in iTreg cell frequencies. Therefore, further studies directly investigating whether IL-10$^+$ Breg cells modulate T_H2/T_H2A and iTreg cell subset frequencies, proliferation, and cytokine production, and through which mode of action this suppression is mediated, are warranted to gain clarity on the impact of dysregulation of IL-10$^+$ Breg frequencies in SAR.

7.1.1 Hypothesis and Aims

7.1.1.1 Hypothesis

1. SAR demonstrate increased T_H2/T_H2A cells and decreased IL-10^+ Breg and IL-10^+ iTreg cell frequencies compared to NAC in response to *Phl p*.

2. rIL-10 suppresses T_H2/T_H2A cell proliferation and associated cytokine production in SAR.

3. IL-10^+ B cells suppress T_H2/T_H2A cell proliferation in parallel to inducing IL-10^+ iTreg cells and anti-inflammatory cytokine production.

4. IL-10^+ B cells suppress T_H2/T_H2A cells and induce IL-10^+ iTreg cells in an IL-10 dependent manner.

7.1.1.2 Aims

1. To characterise αCD3/CD28 stimulated T_H2/T_H2A cells and associated levels of IL-5, and IL-13 in NAC peripheral blood.

2. To evaluate *Phl p* stimulated T_H2/T_H2A, IL-10^+ iTreg and IL-10^+ Breg cells in NAC and SAR.

3. To assess the ability of rIL-10 to suppress *Phl p* activated T_H2/T_H2A and IL-10^+ iTreg cells and IL-5 and IL-10 protein expression.

5. To determine the ability of enriched IL-10^+ B cells to modulate T_H2/T_H2A and IL-10^+ iTreg cell responses to *Phl p* stimulation, and whether this modulation relies on IL-10 or IL-35 mechanisms.

7.2 Results

7.2.1 Characterisation of T_H2, T_H2A and iTreg cells in human peripheral blood

To evaluate the functional properties of IL-10^+ Breg cells on T cells, namely T_H2, T_H2A and IL-10^+ iTreg cells, T cells were investigated in the context of both polyclonal and allergen-stimulation. PBMCs were obtained from *n*=22 GPA and *n*=21 NAC recruited from the Royal Brompton hospital as per inclusion criteria described in section 2.2 (Table 7.2.1.1). To characterise T_H2, T_H2A and iTreg cells from viable, singlet lymphocytes in human peripheral blood (Figure 7.2.2.1, A-C), $CD4^+$ T_H cells were classified based on positive expression of CD4, with proliferating cells differentiated by negative CellTrace Violet staining (Figure 7.2.2.1, D-E). $CD4^+$ T cells were differentiated into T_H2 cells through $CD27^-CRT_H2^+$ expression or T_H2A cells through $CD27^-CD49d^+CD161^+CRT_H2^+$ marker expression, with level of proliferation assessed through CellTrace staining (Figure 7.2.1.1, F-I). $CD4^+$ T_H cells were phenotyped as iTreg cells based upon $CD25^+CD127^-$IL-10^+ staining, with the frequency of proliferating IL-10^+ iTreg also determined through CellTrace staining (Figure 7.2.1.1, J-K).

Table 7.2.1.1 Patient Demographics and clinical characteristics of NAC and GPA subjects enrolled for T cell experiments.

Characteristic	Non-Atopic (n=21)	GP Allergic (n=22)
Gender, M:F	8:13	13:9
Age (years), range	45.9 ±12.5	38.7 ± 9.6
Allergen-specific sIgE (kU_A/L), mean ± SD	0.0 ± 0.0*	30.4 ± 32.9*,$^{+++}$
Allergen-specific SPT (mm^2) ± SD	0.0 ± 0.0	9.5 ± 3.1^{+++}
tIgE (kU_A/L), mean ± SD	13.9 ±12.7*	309.5 ±301.4*,$^{+++}$
Visual Analogue Score	0.0 ± 0.0	77.9 ± 8.1^{+++}

*sIgE and tIgE for n=2 NAC and n=4 GPA not available. +, denotes significance between NAC and GP allergic. *** $P < 0.001$, Mann Whitney Test. SPT, skin prick test; sIgE,specific immunoglobulin E; tIgE, total IgE; GP, grass pollen.

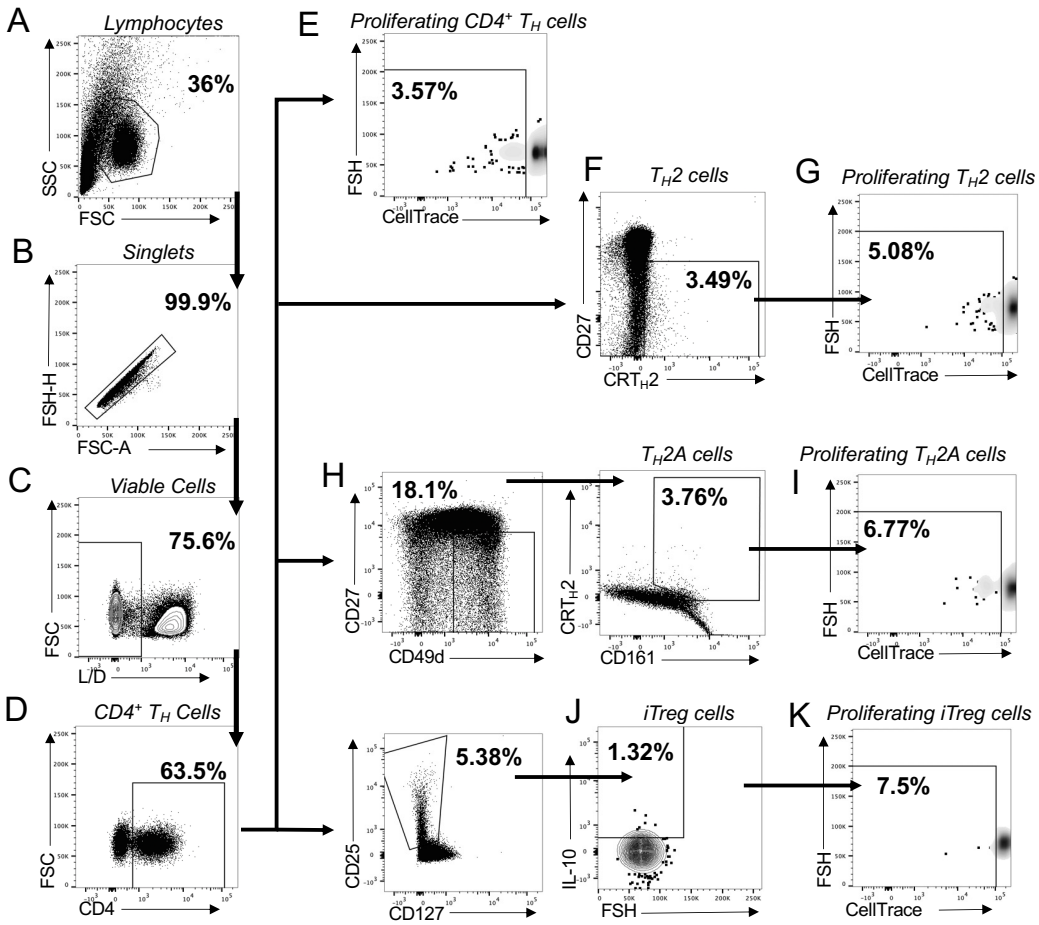


Figure 7.2.1.1 Flow cytometry gating strategy to investigate T_H2, T_H2A and iTreg cells subsets in human peripheral blood.

A) Lymphocytes were phenotyped from PBMCs before **B)** doublet exclusion and **C)** viable cells identification. **D)** $CD4^+$ T_H cells were then categorised. **E)** Proliferating $CD4^+$ T_H cells were differentiated based on CellTrace Violet staining. **F)** T_H2 cells were gated based on $CD27^-CRT_H2^+$ expression, **G)** with proliferating T_H2 cells then evaluated. **H)** T_H2A cells were differentiated based on $CD27^-CD49d^+CD161^+CRT_H2^+$ marker expression, **I)** with proliferating T_H2A cells then evaluated. **J)** iTreg cells were phenotyped upon $CD25^+CD127^-IL\text{-}10^+$ staining, and **K)** frequency of iTreg proliferation. FSC-A, forward scatter-area; FSC-H, forward scatter-height, SSC-A, side scatter area; L/D, Live Dead viability stain.

To charachterise T_H2 and T_H2A cells, NAC PBMCs were stimulated with αCD3 and αCD28 (1μg/mL and 2μg/mL, respectively) to allow for polyclonal stimulation of T cell receptors and evaluated by multi-parametric flow cytometry. Kinetic analysis revealed αCD3/αCD28 stimulation induced significant proliferation of T_H2 and T_H2A cells in a time-dependent manner, with a peak proliferative response following 4 days of stimulation in $CD4^+$ T_H, (*P* = 0.0444), T_H2 (*P* = 0.0047) and T_H2A (*P* = 0.0198; Figure 7.2.1.2, A-E and Table 7.2.1.2). ELISA analysis revealed IL-5 and IL-13 protein levels in cell culture supernature also increased in a time-dependent manner, with both significantly enhanced in αCD3/αCD28 stimulated samples compared to respective unstimulated controls after 6 days in culture (IL-5, *P* = 0.0312; IL-13, *P* = 0.0312; Figure 7.2.1.2, G-H and Table 7.2.1.3).

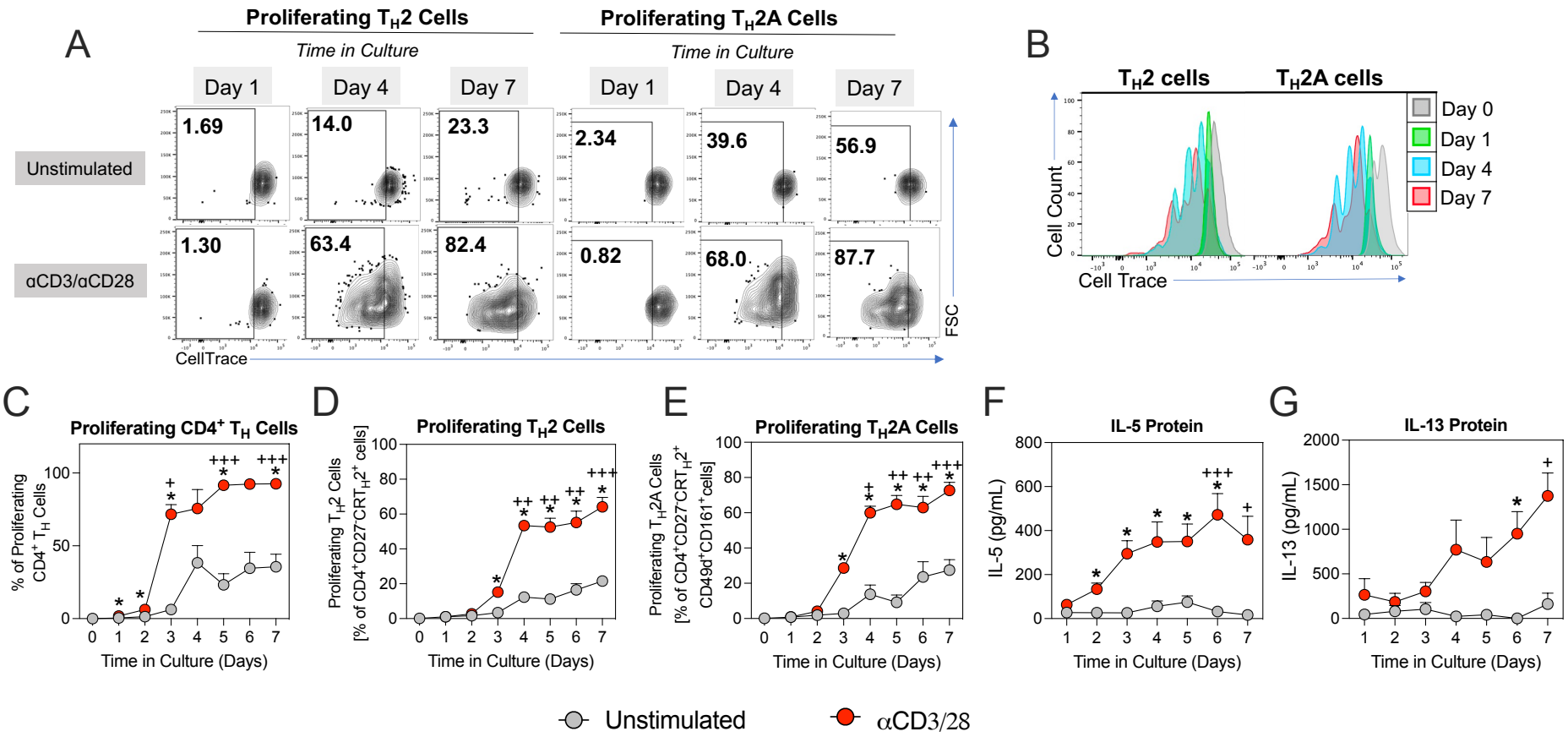


Figure 7.2.1.2 Polyclonal Stimulation induces proliferating T_H2 and T_H2A cells in a time-dependent manner.

Representative flow cytometry plots demonstrating proliferating T_H2 and T_H2A cells in response to αCD3/CD28 stimulation; **A)** contour plots and **B)** histograms. Flow cytometry data demonstrating proliferating **C)** $CD4^+$ T_H, **D)** T_H2 and **E)** T_H2A cells. ELISA data demonstrating **C)** IL-4, **D)** IL-5 and **E)** IL-13 protein levels in culture supernatant. Data representative of n=6 NAC [**C)** D5, n=6; **F)** n=3], and presented as SEM. *, denotes differences between unstimulated and αCD3/CD28 samples at each time-point (Wilcoxon signed-pairs rank test). +, denotes differences compared to D0 within αCD3/CD28 samples (Friedman Test with Dunn's multiple comparisons). *$P < 0.05$, **$P < 0.0.1$, ***$P < 0.001$.

Table 7.2.1.2 Polyclonal Stimulation induces T_H2 and T_H2A in a time-dependent manner

Culture Time (days)	Culture Conditions	B/T Cell Subset	Raw				*P* value[1] v. US	*P* value[2] v. D1
			n	mean	SD	SEM		
0	Unstimulated	$CD4^+$	6	0.04	0.03	0.01	NA	NA
		$CD4^+CD27^+CRT_H2^+$	6	0.15	0.14	0.06	NA	NA
		$CD4^+CD27^+CRT_H2^+CD49d^+CD161^+$	6	0.11	0.18	0.07	NA	NA
1	Unstimulated	$CD4^+$	6	0.47	0.54	0.22	NA	NA
		$CD4^+CD27^+CRT_H2^+$	6	1.03	0.86	0.35	NA	NA
		$CD4^+CD27^+CRT_H2^+CD49d^+CD161^+$	6	0.78	0.95	0.39	NA	NA
	αCD3/αCD28	$CD4^+$	6	1.83	2.00	0.82	**0.0312**	>0.9999
		$CD4^+CD27^+CRT_H2^+$	6	1.09	1.05	0.43	0.8438	>0.9999
		$CD4^+CD27^+CRT_H2^+CD49d^+CD161^+$	6	0.85	1.01	0.41	>0.9999	>0.9999
2	Unstimulated	$CD4^+$	6	1.40	1.73	0.71	NA	NA
		$CD4^+CD27^+CRT_H2^+$	6	1.62	1.46	0.60	NA	NA
		$CD4^+CD27^+CRT_H2^+CD49d^+CD161^+$	6	1.94	2.59	1.06	NA	NA
	αCD3/αCD28	$CD4^+$	6	6.28	6.38	2.61	**0.0312**	>0.9999
		$CD4^+CD27^+CRT_H2^+$	6	2.73	2.12	0.87	0.0938	>0.9999
		$CD4^+CD27^+CRT_H2^+CD49d^+CD161^+$	6	4.14	4.17	1.70	0.0625	>0.9999
3	Unstimulated	$CD4^+$	6	6.23	7.06	2.88	NA	NA
		$CD4^+CD27^+CRT_H2^+$	6	3.44	2.57	1.05	NA	NA
		$CD4^+CD27^+CRT_H2^+CD49d^+CD161^+$	6	2.93	3.37	1.37	NA	NA
	αCD3/αCD28	$CD4^+$	6	71.7	16.0	6.54	**0.0312**	0.2335
		$CD4^+CD27^+CRT_H2^+$	6	15.2	2.28	0.93	**0.0312**	0.8957
		$CD4^+CD27^+CRT_H2^+CD49d^+CD161^+$	6	28.7	7.34	3.00	**0.0312**	>0.9999
4	Unstimulated	$CD4^+$	6	38.4	28.8	11.7	NA	NA
		$CD4^+CD27^+CRT_H2^+$	6	12.3	6.22	2.54	NA	NA
		$CD4^+CD27^+CRT_H2^+CD49d^+CD161^+$	6	13.8	12.9	5.28	NA	NA
	αCD3/αCD28	$CD4^+$	6	75.6	32.0	13.1	0.3125	**0.0444**
		$CD4^+CD27^+CRT_H2^+$	6	53.4	7.11	2.90	**0.0312**	**0.0047**
		$CD4^+CD27^+CRT_H2^+CD49d^+CD161^+$	6	60.0	8.99	3.67	**0.0312**	**0.0198**
5	Unstimulated	$CD4^+$	6	23.32	18.6	7.59	NA	NA
		$CD4^+CD27^+CRT_H2^+$	6	11.2	7.29	2.98	NA	NA
		$CD4^+CD27^+CRT_H2^+CD49d^+CD161^+$	6	9.21	10.1	4.14	NA	NA
	αCD3/αCD28	$CD4^+$	6	91.6	3.31	1.35	**0.0312**	**0.0007**
		$CD4^+CD27^+CRT_H2^+$	6	52.5	12.5	5.11	**0.0312**	**0.0051**
		$CD4^+CD27^+CRT_H2^+CD49d^+CD161^+$	6	64.8	12.2	4.97	**0.0312**	**0.0044**
6	Unstimulated	$CD4^+$	5	34.6	24.6	11.0	NA	NA
		$CD4^+CD27^+CRT_H2^+$	6	16.5	8.63	3.52	NA	NA
		$CD4^+CD27^+CRT_H2^+CD49d^+CD161^+$	6	23.6	21.2	8.65	NA	NA
	αCD3/αCD28	$CD4^+$	5	92.4	2.4	1.07	0.0625	NA
		$CD4^+CD27^+CRT_H2^+$	6	55.2	16.0	6.52	**0.0312**	**0.0023**
		$CD4^+CD27^+CRT_H2^+CD49d^+CD161^+$	6	63.0	15.5	6.32	**0.0312**	**0.0041**
7	Unstimulated	$CD4^+$	6	35.6	21.2	8.67	NA	NA
		$CD4^+CD27^+CRT_H2^+$	6	21.5	3.86	1.58	NA	NA
		$CD4^+CD27^+CRT_H2^+CD49d^+CD161^+$	6	27.5	14.4	5.86	NA	NA
	αCD3/αCD28	$CD4^+$	6	92.6	1.95	0.80	**0.0312**	**<0.0001**
		$CD4^+CD27^+CRT_H2^+$	6	64.2	13.3	5.42	**0.0312**	**0.0001**
		$CD4^+CD27^+CRT_H2^+CD49d^+CD161^+$	6	72.7	11.3	4.61	**0.0312**	**0.0003**

Bolded Values Represent Significant *P* Values. 1) Wilcoxon-signed pairs rank test, 2) Friedman Test with Dunn's Multiple Comparisons

Table 7.2.1.3 Polyclonal stimulation induces IL-5 and IL-13 production from PBMCs in a time-dependent manner

Culture Time (days)	Culture Conditions	ELISA Protein	Raw				*P* value[1] v. Unstimulated	*P* value[2] v. D1
			n	mean	SD	SEM		
1	Unstimulated	IL-5	6	27.2	25.1	10.3	NA	NA
		IL-13	6	45.3	74.8	30.6	NA	NA
	αCD3/αCD28	IL-5	6	63.2	23.9	9.77	0.0938	NA
		IL-13	6	265	446	182	0.2500	NA
2	Unstimulated	IL-5	6	26.6	22.9	9.34	NA	NA
		IL-13	6	79.8	159	7.16	NA	NA
	αCD3/αCD28	IL-5	6	134	68.0	27.8	**0.0312**	>0.9999
		IL-13	6	186	237	96.6	0.5000	>0.9999
3	Unstimulated	IL-5	6	26.0	32.7	13.3	NA	NA
		IL-13	6	104	185	75.4	NA	NA
	αCD3/αCD28	IL-5	6	295	143	58.6	**0.0312**	0.9454
		IL-13	6	304	244	99.5	0.0625	>0.9999
4	Unstimulated	IL-5	6	55.8	60.3	24.6	NA	NA
		IL-13	6	22.3	54.7	22.3	NA	NA
	αCD3/αCD28	IL-5	6	348	224	91.3	**0.0312**	0.1581
		IL-13	6	772	813	332	0.0625	>0.9999
5	Unstimulated	IL-5	6	75.1	69.1	28.3	NA	NA
		IL-13	6	42.3	83.6	34.1	NA	NA
	CD3/αCD28	IL-5	6	350	194	79.3	**0.0312**	0.1581
		IL-13	6	534	671	274	0.0625	>0.9999
6	Unstimulated	IL-5	6	32.1	22.4	9.14	NA	NA
		IL-13	6	0.48	1.18	0.48	NA	NA
	αCD3/αCD28	IL-5	6	472	235	95.9	**0.0312**	**0.0002**
		IL-13	6	951	606	248	**0.0312**	0.4478
7	Unstimulated	IL-5	6	16.6	19.2	7.86	NA	NA
		IL-13	6	161	301	123	NA	NA
	αCD3/αCD28	IL-5	6	359	261	106	0.0625	**0.0175**
		IL-13	6	1375	630	257	0.0625	**0.0400**

Bolded Values Represent Significant *P* Values. 1) Wilcoxon-signed pairs rank test, 2) Friedman Test with Dunn's Multiple Comparisons.

To assess whether the major GP allergen *Phl p* induces T_H2, T_H2A and IL-10^+ iTreg cells, NAC and GPA PBMCs were stimulated with of *Phl p* (0.1μg/mL, 0.3μg/mL, 1μg/mL, 3μg/mL and 10μg/mL) and assessed by multi-parametric flow cytometry. *Phl p* stimulated T cell proliferation in a dose-dependent manner in both GPA and NAC, significant at 1μg/mL in $CD4^+$ T_H, (P = 0.0156), T_H2 (P = 0.0312), T_H2A (P = 0.0156) and IL-10^+ iTreg (P = 0.0312) cells (Figure 7.2.1.3, A-D and Table 7.2.1.4). Moreover, GPA demonstrated a trend of increased $CD4^+$ T_H, T_H2A and IL-10^+ iTreg proliferation in response to 3μg/mL *Phl p* compared to NAC (all, P = 0.0156). Stimulation with 1μg/mL *Phl p* generated significantly enhanced frequencies of $CD4^+$ T_H (P = 0.0467) and T_H2A (P = 0.0495) in GPA compared to NAC. The frequency and proliferation of IL-10^+ iTreg cells also increased in a *Phl p* dose-dependent manner in both NAC and GPA, significant at 0.1μg/mL (P = 0.0312), 1μg/mL (P = 0.0156) and 3μg/mL (P = 0.0156; Figure 7.2.1.3, E-F). In contrast, IL-10^+ Breg cells frequencies were increased in NAC compared to GPA in response to *Phl p* stimulation and were induced in a dose-dependent manner in both subject groups, with a peak increase observed at 1μg/mL Phlp (both, P = 0.0312; Figure 7.2.1.3, G-H). Strikingly, IL-10 production also increased in line with increasing *Phl p* concentration and was significantly enhanced in NAC compared to GPA at 1μg/mL (P = 0.0082), 3μg/mL (P = 0.0023) and 10μg/mL (P = 0.0140) *Phl p* (Figure 7.2.1.3, I).

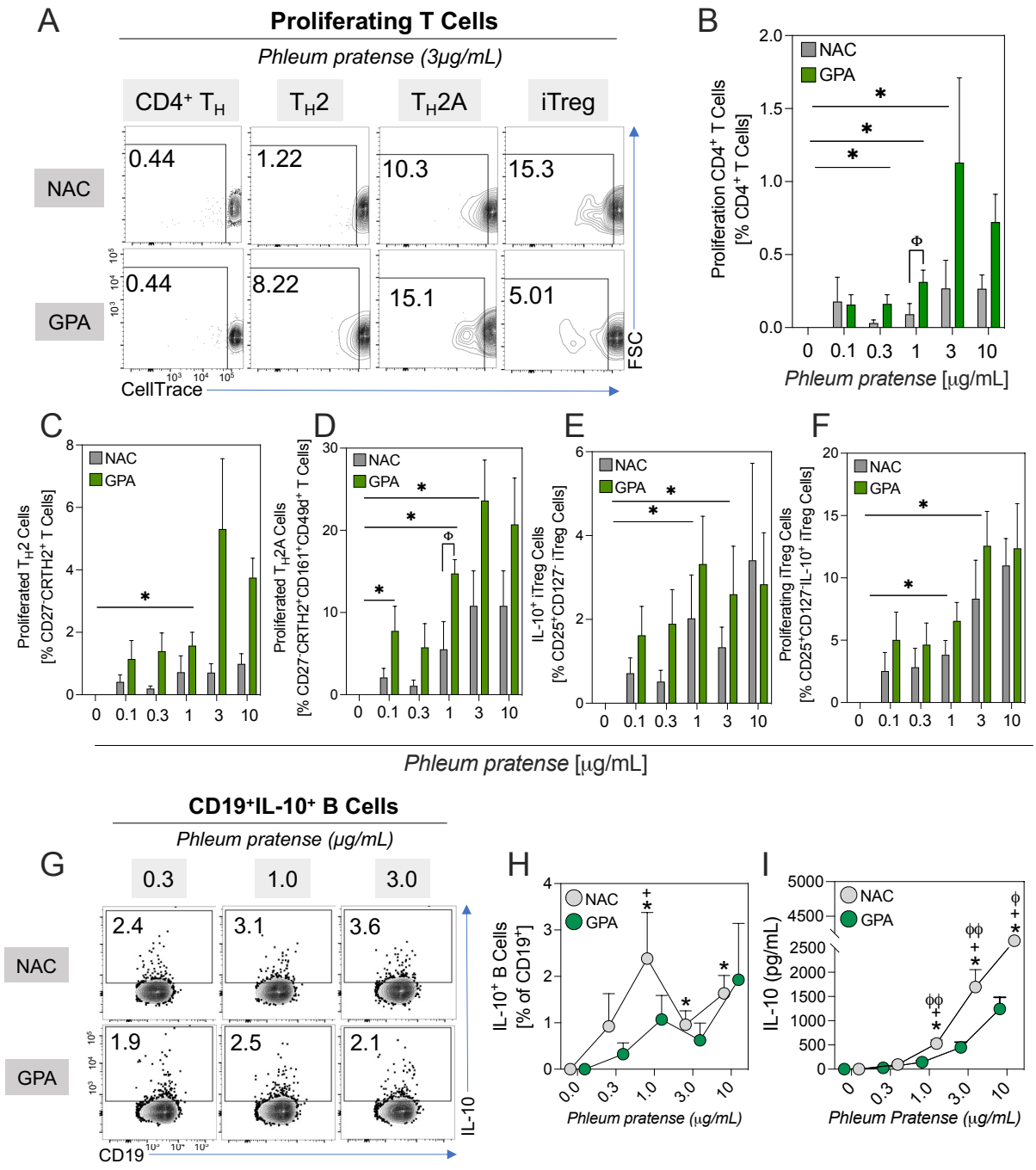


Figure 7.2.1.3 *Phl p* induces IL-10⁺ Breg cells, CD4⁺ T cells, T_H2, T_H2A and iTreg Subsets in NAC and GPA.

A) Representative plots demonstrating proliferating CD4⁺ T_H cells, T_H2, T_H2A and iTreg cells in response to *Phl p* stimulation. Flow cytometry plots demonstrating proliferating **B)** CD4⁺ T cells **C)** T_H2 cells and **D)** T_H2A cells, and **E)** IL-10⁺ iTreg cells and **F)** proliferating IL-10⁺ iTreg cells in response to *Phl p* stimulation. **G)** Representative flow cytometry plots demonstrating IL-10⁺ Breg cells in response to *Phl p* stimulation. **H)** Flow cytometry data demonstrating IL-10⁺ Breg cells and **I)** ELISA data of IL-10 protein levels in cell culture supernatant. Data representative of NAC, *n*=6 and GPA, *n*=7, and presented as mean ± SEM. ⁺, denotes NAC; *, detonates GPA, significance compared to respective 0µg/mL, as determined by Wilcoxon signed-pairs rank test. ϕ denotes difference between NAC and GPA, Mann Whitney U test, **P* < 0.05, ***P* < 0.01. NAC, non-atopic control; GPA, grass pollen allergic.

Table 7.2.1.4 *Phl p* induces IL-10$^+$ Breg cells and proliferating CD4$^+$ T cells, T_H2, T_H2A and iTreg subsets in NAC and GPA samples.

Cell Type	Atopic Status	Phlp Conc. (μg/mL)	B/T Cell Subset	Raw				Delta (Unstimulated)			*P* value NAC vs GPA[1]	*P* value vs 0[2]
				n	mean	SD	SEM	mean	SD	SEM		
B Cell	**NAC**	0	CD19$^+$IL-10$^+$	6	1.78	0.10	0.04	NA	NA	NA	NA	NA
		0.3	CD19$^+$IL-10$^+$	6	3.05	2.22	0.91	1.02	1.69	0.69	NA	0.0625
		1.0	CD19$^+$IL-10$^+$	6	4.17	2.34	0.95	2.38	2.43	0.99	NA	**0.0312**
		3.0	CD19$^+$IL-10$^+$	6	2.75	0.68	0.28	0.96	0.74	0.30	NA	**0.0312**
		10.0	CD19$^+$IL-10$^+$	6	3.54	0.87	0.36	1.63	0.94	0.39	NA	**0.0312**
	GPA	0	CD19$^+$IL-10$^+$	7	1.77	0.06	0.02	NA	NA	NA	NA	NA
		0.3	CD19$^+$IL-10$^+$	7	1.54	1.10	0.42	0.32	0.64	0.24	0.2191	0.2500
		1.0	CD19$^+$IL-10$^+$	7	2.61	1.65	0.62	1.21	1.29	0.49	0.2343	**0.0312**
		3.0	CD19$^+$IL-10$^+$	7	2.11	1.28	0.52	0.46	0.91	0.37	0.1277	0.2500
		10.0	CD19$^+$IL-10$^+$	7	3.51	2.88	1.29	2.41	2.88	1.44	>0.9999	0.2500
T Cell (Cell Trace$^-$)	**NAC**	0	CD4$^+$	6	0.33	0.25	0.10	NA	NA	NA	NA	NA
			CD4$^+$CD27$^+$CRT$_H$2$^+$	6	1.46	1.15	0.47	NA	NA	NA	NA	NA
			CD4$^+$CD27$^+$CRT$_H$2$^+$CD49d$^+$CD161$^+$	6	1.61	0.96	0.39	NA	NA	NA	NA	NA
			CD4$^+$CD25$^+$CD127$^+$IL-10$^+$	6	9.32	7.49	3.06	NA	NA	NA	NA	NA
		0.1	CD4$^+$	6	0.44	0.44	0.18	0.18	0.41	0.17	NA	0.5000
			CD4$^+$CD27$^+$CRT$_H$2$^+$	6	1.66	1.09	0.44	0.42	0.55	0.22	NA	0.1250
			CD4$^+$CD27$^+$CRT$_H$2$^+$CD49d$^+$CD161$^+$	6	2.46	2.76	1.13	2.10	2.71	1.11	NA	0.0625
			CD4$^+$CD25$^+$CD127$^+$IL-10$^+$	6	11.01	7.86	3.21	2.53	3.64	1.49	NA	0.2500
		0.3	CD4$^+$	6	0.28	0.15	0.06	0.03	0.05	0.02	NA	0.2500
			CD4$^+$CD27$^+$CRT$_H$2$^+$	6	1.17	0.25	0.10	0.19	0.21	0.09	NA	0.1250
			CD4$^+$CD27$^+$CRT$_H$2$^+$CD49d$^+$CD161$^+$	6	1.96	2.15	0.88	1.07	1.72	0.70	NA	0.5000
			CD4$^+$CD25$^+$CD127$^+$IL-10$^+$	6	10.74	9.56	3.90	2.83	3.75	1.53	NA	0.1250
		1.0	CD4$^+$	6	0.36	0.19	0.08	0.09	0.16	0.07	NA	0.2500
			CD4$^+$CD27$^+$CRT$_H$2$^+$	6	1.68	1.73	0.71	0.72	1.29	0.53	NA	0.1818
			CD4$^+$CD27$^+$CRT$_H$2$^+$CD49d$^+$CD161$^+$	6	6.89	8.56	3.49	5.52	8.22	3.36	NA	0.1250
			CD4$^+$CD25$^+$CD127$^+$IL-10$^+$	6	11.65	7.60	3.10	3.83	2.81	1.15	NA	0.0625
		3.0	CD4$^+$	6	0.53	0.47	0.19	0.27	0.47	0.09	NA	0.1250
			CD4$^+$CD27$^+$CRT$_H$2$^+$	6	1.84	0.87	0.35	0.71	0.70	0.29	NA	0.1250
			CD4$^+$CD27$^+$CRT$_H$2$^+$CD49d$^+$CD161$^+$	6	12.16	10.40	4.25	10.8	10.4	4.26	NA	0.1250
			CD4$^+$CD25$^+$CD127$^+$IL-10$^+$	6	17.55	3.56	1.45	8.33	7.58	3.09	NA	0.0625
		10.0	CD4$^+$	3	0.49	0.12	0.07	0.27	0.16	0.09	NA	0.2500
			CD4$^+$CD27$^+$CRT$_H$2$^+$	3	2.11	0.97	0.56	0.99	0.57	0.33	NA	0.2500
			CD4$^+$CD27$^+$CRT$_H$2$^+$CD49d$^+$CD161$^+$	3	12.49	6.69	3.87	10.8	7.38	4.26	NA	0.2500
			CD4$^+$CD25$^+$CD127$^+$IL-10$^+$	3	15.87	3.52	2.03	11.0	3.75	2.17	NA	0.2500
	GPA	0	CD4$^+$	7	0.19	0.22	0.08	NA	NA	NA	NA	NA
			CD4$^+$CD27$^+$CRT$_H$2$^+$	7	1.83	1.00	0.38	NA	NA	NA	NA	NA
			CD4$^+$CD27$^+$CRT$_H$2$^+$CD49d$^+$CD161$^+$	7	7.88	17.35	6.65	NA	NA	NA	NA	NA
			CD4$^+$CD25$^+$CD127$^+$IL-10$^+$	7	4.41	6.85	2.59	NA	NA	NA	NA	NA
		0.1	CD4$^+$	7	0.33	0.16	0.06	0.16	0.18	0.07	0.4983	0.1250

			$CD4^+CD27^+CRT_H2^+$	7	2.77	1.52	0.58	1.14	1.57	0.59	0.9417	0.1250
			$CD4^+CD27^+CRT_H2^+CD49d^+CD161^+$	7	13.84	11.71	4.43	7.76	7.94	3.00	0.2471	**0.0312**
			$CD4^+CD25^+CD127^+IL\text{-}10^+$	7	8.74	6.94	2.62	5.03	5.89	2.23	0.4289	0.1250
		0.3	$CD4^+$	7	0.35	0.17	0.06	0.16	0.16	0.06	0.0641	**0.0312**
			$CD4^+CD27^+CRT_H2^+$	7	3.08	1.73	0.66	1.39	1.54	0.58	0.0915	0.0625
			$CD4^+CD27^+CRT_H2^+CD49d^+CD161^+$	7	12.84	15.33	5.79	5.76	7.64	2.89	0.2022	0.0625
			$CD4^+CD25^+CD127^+IL\text{-}10^+$	7	8.38	5.03	1.90	4.64	4.60	1.74	0.6020	0.0625
		1.0	$CD4^+$	7	0.51	0.39	0.15	0.31	0.21	0.08	**0.0467**	**0.0156**
			$CD4^+CD27^+CRT_H2^+$	7	3.36	1.58	0.60	1.57	1.14	0.43	0.1480	**0.0312**
			$CD4^+CD27^+CRT_H2^+CD49d^+CD161^+$	7	22.62	18.26	6.90	14.7	4.43	1.68	**0.0495**	**0.0156**
			$CD4^+CD25^+CD127^+IL\text{-}10^+$	7	10.92	8.77	3.32	6.55	3.93	1.48	0.1445	**0.0312**
		3.0	$CD4^+$	7	1.32	1.74	0.66	1.13	1.54	0.58	0.0501	**0.0156**
			$CD4^+CD27^+CRT_H2^+$	7	7.03	6.69	2.53	5.31	5.96	2.25	0.1305	0.0625
			$CD4^+CD27^+CRT_H2^+CD49d^+CD161^+$	7	31.50	19.17	7.24	23.6	13.0	4.92	0.4697	**0.0156**
			$CD4^+CD25^+CD127^+IL\text{-}10^+$	7	16.98	11.46	4.33	12.6	7.32	2.77	0.7308	**0.0156**
		10.0	$CD4^+$	4	0.95	0.53	0.27	0.72	0.38	0.19	0.2000	0.1250
			$CD4^+CD27^+CRT_H2^+$	4	5.34	2.22	1.11	3.75	1.25	0.06	0.0571	0.1250
			$CD4^+CD27^+CRT_H2^+CD49d^+CD161^+$	4	33.55	22.78	11.39	20.7	11.3	5.64	0.4000	0.1250
			$CD4^+CD25^+CD127^+IL\text{-}10^+$	4	18.15	14.51	7.26	12.4	7.17	3.58	0.8571	0.1250
$IL\text{-}10^+$	**NAC**	0	$CD4^+CD25^+CD127^+$	6	2.04	0.61	0.25	NA	NA	NA	NA	NA
		0.1	$CD4^+CD25^+CD127^+$	6	2.73	1.15	0.47	0.72	0.90	0.37	NA	0.1250
Treg Cell		0.3	$CD4^+CD25^+CD127^+$	6	2.13	0.98	0.40	0.52	0.66	0.27	NA	0.2500
		1.0	$CD4^+CD25^+CD127^+$	6	3.77	2.83	1.15	2.03	2.54	1.04	NA	0.1250
		3.0	$CD4^+CD25^+CD127^+$	6	3.22	1.90	0.77	1.34	1.18	0.48	NA	0.1250
		10.0	$CD4^+CD25^+CD127^+$	6	5.17	4.39	2.54	3.41	4.01	2.32	NA	0.2500
	GPA	0	$CD4^+CD25^+CD127^+$	7	1.73	0.12	0.04	NA	NA	NA	NA	NA
		0.1	$CD4^+CD25^+CD127^+$	7	3.18	2.10	0.79	1.62	1.82	0.69	0.3840	**0.0312**
		0.3	$CD4^+CD25^+CD127^+$	7	3.37	2.51	0.95	1.90	2.15	0.81	0.2191	0.0625
		1.0	$CD4^+CD25^+CD127^+$	7	5.05	3,05	1,15	3.32	3.02	1.14	0.3456	**0.0156**
		3.0	$CD4^+CD25^+CD127^+$	7	4.33	3.09	1.15	2.60	3.03	1.15	0.3456	**0.0156**
		10.0	$CD4^+CD25^+CD127^+$	7	4.56	2.59	1.30	2.84	2.46	1.23	>0.9999	0.1250

Bolded Values Represent ***P*** Significant Values. [1]Mann Whitney Test, [2]Wilcoxon signed-pairs test. NAC, Non-Atopic Control; Grass Pollen Allergic, GPA.

7.2.2 *Phl p* stimulated T_H2 and T_H2A cell proliferation and cytokine production are suppressed by IL-10

To assess the ability of IL-10 to modulate *Phl p* activation of T_H2, T_H2A and IL-10^+ iTreg cell proliferation and IL-4, IL-13, IL-35 and IL-10 cytokine production, GPA PBMCs were stimulated with 1μg/mL *Phl p*, 50ng/mL rIL-10 and 1μg/mL αIL-10 and assessed by multi-parametric flow cytometry. The unbiased computational algorithm, viSNE, revealed a distinct $CD4^+$ T_H cell cluster which co-localised with $CD27^-CD49d^+CD161^+CRT_H2^+IL\text{-}4^+IL\text{-}13^+$ parameter channels, and thus could be phenotyped as T_H2/T_H2A cells (Figure 7.2.2.1, A, black islands). Addition of IL-10 alongside *Phl p* significantly suppressed frequencies of proliferating $CD4^+$ T_H (78% reduction, $P = 0.0156$), T_H2 (70% reduction, $P = 0.0156$) and T_H2A (60% decrease, $P = 0.0156$) cells compared to *Phl p* stimulation alone (Figure 7.2.2.1, B-E and Table 7.2.2.1). The effect of IL-10 was confirmed through addition of αIL-10 to culture systems, driving an enhancement of proliferating $CD4^+$ T_H (41% increase, $P = 0.0469$), T_H2 (30% increase, $P = 0.0469$) and T_H2A (37% increase, $P = 0.0156$) cells. However, IL-10 also suppressed proliferating IL-10^+ iTreg cells (68% decrease, $P = 0.0156$), partially ameliorated by αIL-10 treatment (61% increase, $P = 0.0156$; Figure 7.2.2.1, F). Despite attenuating frequencies of IL-$10^+CD25^+CD127^+$ iTreg cells, IL-10 treatment enhanced IL-35 production from $CD25^+CD127^+$ iTreg cells (Figure 7.2.2.1, G-H). ELISA analysis of cell culture supernatant revealed IL-5 protein levels were significantly reduced following treatment with IL-10 (90% decrease, $P = 0.0156$), reversed through addition of αIL-10 (38% decrease, $P = 0.0312$; Figure 7.2.2.1, I).

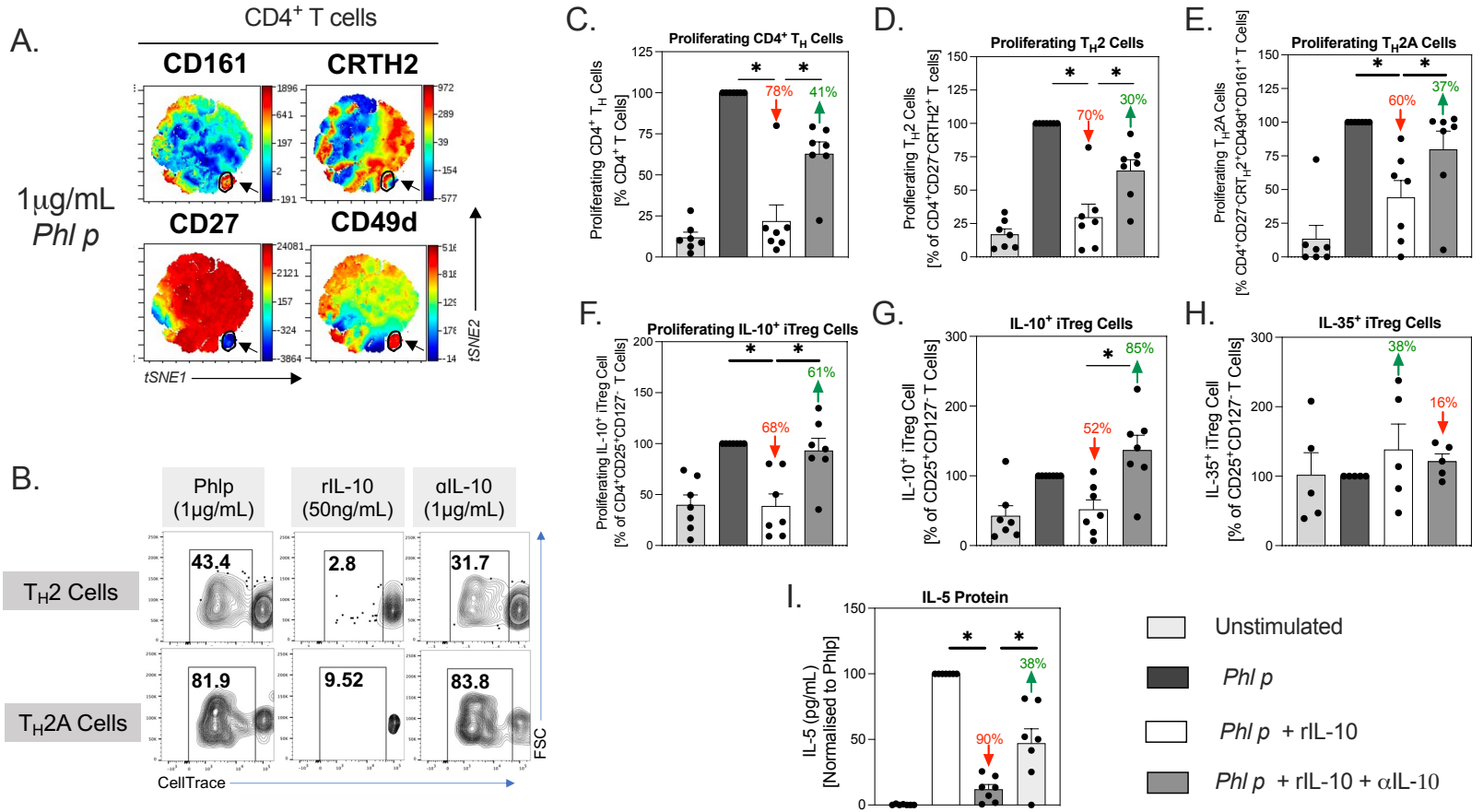


Figure 7.2.2.1 IL-10 significantly suppresses T_H2 and T_H2A cell subset proliferation.

A) viSNE map of $CD4^+$ T cells demonstrating a distinct cellular island positive for CD161, CRT_H2, CD27 and CD161 expression, indicated by black island and arrows. **B)** Representative flow cytometry plots demonstrating T_H2/T_H2A cell proliferation in response to *Phl p*, rIL-10 or αIL-10+rIL-10. Effect of rIL-10 on allergen-stimulated proliferating **C)** $CD4^+$ T cells, **D)** T_H2 **E)** T_H2A and **F)** $IL\text{-}10^+$ iTreg cells, and **G)** $IL\text{-}10^+$ and **H)** $IL\text{-}35^+$ iTreg cell frequencies. ELISA data demonstrating **I)** IL-5, protein in cell culture supernatant. Data representative of GPA, n=7 [N.B. **H)** n=5] and presented as mean ± SEM of percentage change from *Phl p* stimulation alone, with red and green numbers and arrows indicating decreases and increases, respectively. $*P < 0.05$, Wilcoxon-paired rank test. rIL-10, recombinant IL-10; αIL-10, anti-IL-10; *Phl p*, *Phleum pratense*.

Table 7.2.2.1 Recombinant IL-10 suppresses *PhI p*-activated $CD4^+$ T cells, T_H2 and T_H2A cell proliferation

Culture Conditions	Flow Cytometry - B/T Cell Subset	Raw				Normalised to Phlp			*P* value v. Phlp	*P* value v. rIL-10 50ng/ml
		n	mean	SD	SEM	mean	SD	SEM		
Unstimulated	$CD4^+$CellTrace$^-$	7	0.46	0.40	0.15	NA	NA	NA	NA	NA
	$CD4^+CD27^+CRT_H2^+$CellTrace$^-$	7	3.48	1.65	0.63	NA	NA	NA	NA	NA
	$CD4^+CD27^+CRT_H2^+CD49d^+CD161^+$CellTrace$^-$	7	8.76	17.1	6.46	NA	NA	NA	NA	NA
	$CD4^+CD25^-CD127^+$IL-10$^+$	7	3.39	3.88	1.47	NA	NA	NA	NA	NA
	$CD4^+CD25^-CD127^+$IL-35$^+$	5	3.78	0.52	0.23	NA	NA	NA	NA	NA
	$CD4^+CD25^-CD127^+$IL-10$^+$CellTrace$^-$	7	27.3	22.2	8.38	NA	NA	NA	NA	NA
1μg/mL (Phlp)	$CD4^+$CellTrace$^-$	7	6.52	9.26	3.50	100	0	0	NA	NA
	$CD4^+CD27^+CRT_H2^+$CellTrace$^-$	7	29.7	23.7	8.95	100	0	0	NA	NA
	$CD4^+CD27^+CRT_H2^+CD49d^+CD161^+$CellTrace$^-$	7	68.2	20.0	7.54	100	0	0	NA	NA
	$CD4^+CD25^-CD127^+$IL-10$^+$	7	8.56	4.11	1.55	100	0	0	NA	NA
	$CD4^+CD25^-CD127^+$IL-35$^+$	5	5.14	2.81	1.26	100	0	0	NA	NA
	$CD4^+CD25^-CD127^+$IL-10$^+$CellTrace$^-$	7	67.7	27.8	10.5	100	0	0	NA	NA
50ng/mL rIL-10	$CD4^+$CellTrace$^-$	7	0.77	0.86	0.32	21.9	26.1	9.86	**0.0156**	NA
	$CD4^+CD27^+CRT_H2^+$CellTrace$^-$	7	7.20	7.60	2.87	29.8	25.7	9.73	**0.0156**	NA
	$CD4^+CD27^+CRT_H2^+CD49d^+CD161^+$CellTrace$^-$	7	31.0	26.4	9.98	44.3	32.9	12.4	**0.0156**	NA
	$CD4^+CD25^-CD127^+$IL-10$^+$	7	4.62	4.86	1.84	51.9	36.0	13.6	0.0625	NA
	$CD4^+CD25^-CD127^+$IL-35$^+$	5	6.10	4.30	1.92	138	82.4	36.8	0.6250	NA
	$CD4^+CD25^-CD127^+$IL-10$^+$CellTrace$^-$	7	30.3	31.3	11.8	38.8	31.4	11.9	**0.0156**	NA
1μg/mL αIL-10	$CD4^+$CellTrace$^-$	7	4.19	5.75	2.17	62.9	19.1	7.23	NA	**0.0469**
	$CD4^+CD27^+CRT_H2^+$CellTrace$^-$	7	22.0	23.1	8.75	64.7	21.4	8.11	NA	**0.0469**
	$CD4^+CD27^+CRT_H2^+CD49d^+CD161^+$CellTrace$^-$	7	58.7	33.8	12.8	79.8	35.9	12.4	NA	**0.0156**
	$CD4^+CD25^-CD127^+$IL-10$^+$	7	11.8	7.26	2.75	137	56.4	21.3	NA	**0.0312**
	$CD4^+CD25^-CD127^+$IL-35$^+$	5	6.09	3.26	1.46	122	23.8	10.7	NA	0.8125
	$CD4^+CD25^-CD127^+$IL-10$^+$CellTrace$^-$	7	58.7	26.6	10.1	93.3	31.4	11.9	NA	**0.0156**
IL-5 Protein - ELISA										
	Unstimulated	7	0.73	1.78	0.67	NA	NA	NA	NA	NA
	αCD3/αCD28	7	233	291	110	100	0	0	NA	NA
	50ng/mL rIL-10	7	40.6	80.9	30.6	12.0	9.61	3.63	**0.0156**	NA
	1μg/mLαIL-10	7	127	152	57.6	47.2	28.9	10.9	NA	**0.0312**

Bolded Values Represent Significant ***P*** Values. Wilcoxon-signed pairs rank test.

7.2.3 T cell co-culture system with CpG and CD40L stimulated 'primed' B cells

Following confirmation of IL-10 elicited suppression of $CD4^+$ T cell subsets, the functional ability of IL-10^+ Breg cells to modulate T_H2/T_H2A cell responses to polyclonal or *Phl p* stimulation was explored within co-culture systems. The initial approach taken for co-culture analysis was to utilise enriched B cells that had been pre-cultured in TCM alone (unprimed) or stimulated with CpG/CD40L (1μg/mL/2.5μg/mL, respectively; primed) for three days prior to being co-cultured alongside polyclonally stimulated isolated autologous $CD4^+$ T cells at increasing ratios of T:B cells (1:1, 2:1, 4:1, 8:1, 16:1, 32:1, 64:1) for 4 days. Surprisingly, flow cytometry analysis revealed primed B cells elicited a ratio-dependent proinflammatory effect on $CD4^+$ T_H and T_H2 cell proliferation compared to unprimed B cells and αCD3/αCD28 stimulation alone (Appendix Figure 13.1.1.5, A-E). To evaluate whether primed B cells maintained stimulatory effects on T cells with increased co-culture duration, culture systems were investigated at days 4, 7 and 10, however, no clear relationship could be established (Appendix Figure 13.1.1.5, F-G). Next, to determine whether these proinflammatory trends were also observed with allergen-stimulated T cells, unprimed and primed B cells were co-cultured at a 1:1 ratio alongside autologous PBMCs in the presence of 1μg/mL *Phl p*. Similarly, primed B cells induced greater $CD4^+$ T_H, T_H2 and IL-10^+ iTreg cell proliferation compared to unprimed B cells and *Phl p* stimulation alone in a time-dependent manner (Appendix Figure 13.1.1.5, H-J). To investigate whether primed B cells were driving proinflammatory effects through soluble mechanisms, culture supernatant from unprimed and primed enriched B cells was added to autologous PBMCs. Like previous observations, primed B cell culture supernatant induced greater $CD4^+$ T_H cell, T_H2 ($P = 0.0312$), T_H2A proliferation ($P = 0.0312$) and IL-10^+ iTreg cell frequencies ($P = 0.0312$) compared to *Phl p* stimulation alone in a dose-dependent manner (Appendix Figure 13.1.1.6 and Appendix Table 13.1.1.1).

7.2.4 T cell co-culture system with enriched IL-10$^+$ Breg cells

Following observations that CpG/CD40L primed B cell co-culture systems were potentially causing a pan-activation of both effector and suppressor B cells which was skewing ability to assess suppressive B cells, a new experimental approach was developed to enrich IL-10$^+$ Breg cells within the suppressive sample population. To perform this, enriched B cells which had been cultured for 3 days alongside CpG/CD40L were labelled with an anti-IL-10 PE microbead, allowing the tagging of IL-10$^+$ secretory Breg cells. Labelled B cells were then separated into either labelled (IL-10$^+$) Breg cells or unlabeled (IL-10$^-$) B cell populations and cultured alongside autologous PBMCs at a 1:1 ratio in the presence of 1μg/mL *Phl p* for 6 days and evaluated by multi-parametric flow cytometry. Compared to IL-10$^-$ B cells, other than two outliers, enriched IL-10$^+$ Breg cells suppressed proliferation of CD4$^+$ T_H (36% reduction, P = 0.1055) and T_H2A (40% reduction, P = 0.0547) cells in response to *Phl p* stimulation, although no clear trends were observed in T_H2 cells (P = 0. 8457; Figure 7.2.4.1 A-D and Table 7.2.4.1). Upon investigating Treg cell fractions, the majority of IL-10$^+$ Breg cell co-cultures demonstrated increased IL-10$^+$ iTreg cell frequencies (47% increase, P = 0.4316) and proliferation (72% increase, P = 0.9102) compared to IL-10$^-$ B cell co-cultures in response to *Phl p* stimulation (Figure 7.2.4.1, E, J).

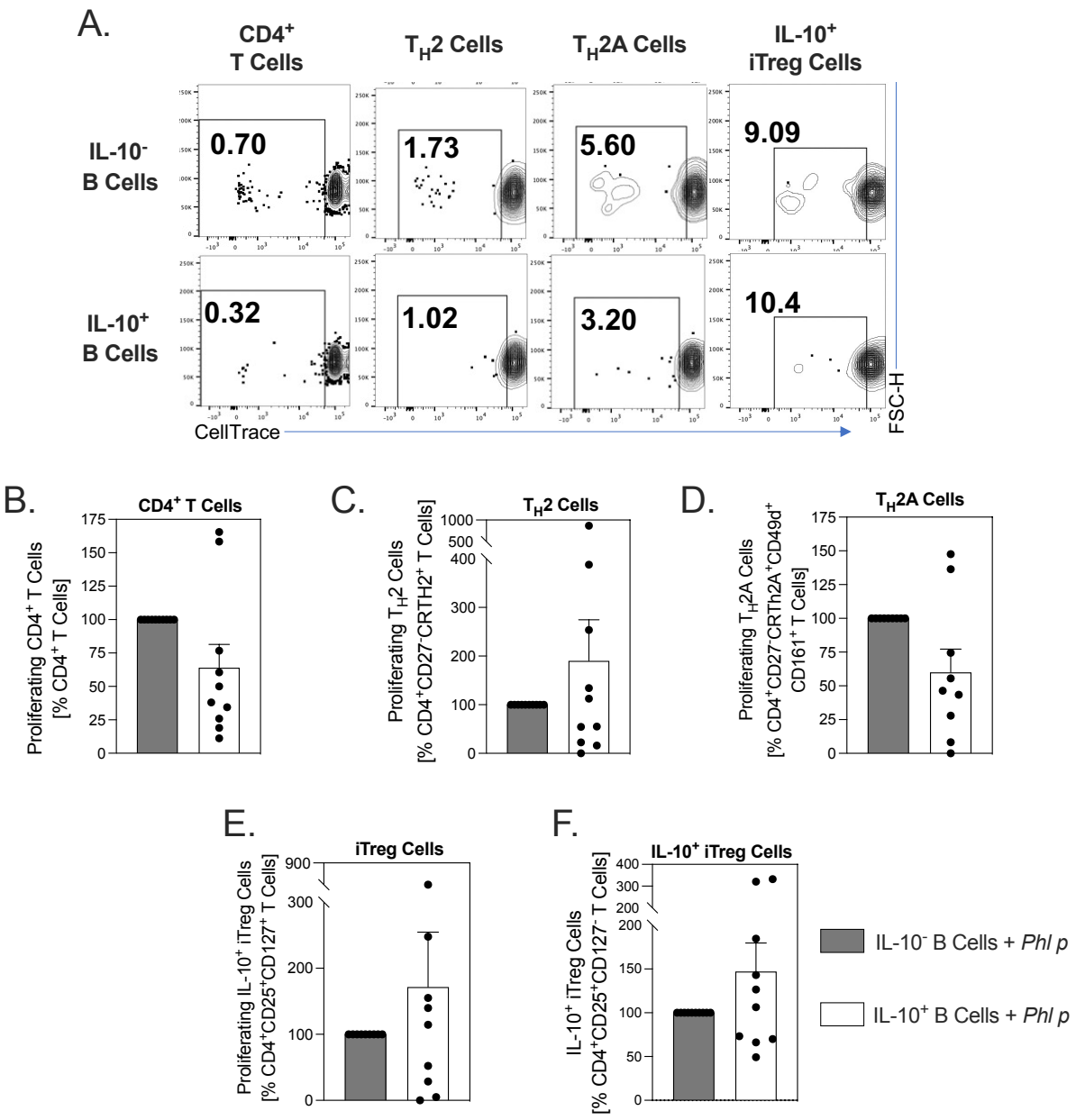


Figure 7.2.4.1 IL-10$^+$ Breg cells demonstrate trends of suppressing CD4$^+$ and T$_H$2A cell proliferation compared to IL-10$^-$ B cells.

A) Representative flow cytometry plots demonstrating CD4$^+$ T$_H$, T$_H$2, T$_H$2A and IL-10$^+$ iTreg cell proliferation in response to IL-10$^-$ or IL-10$^+$ B cells. Flow cytometry data demonstrating proliferating **B)** CD4$^+$ T$_H$, **C)** T$_H$2, **D)** T$_H$2A and **E)** iTreg cells, and frequencies of **F)** IL-10$^+$ iTreg cells. Data representative of GPA, n=10 [N.B. **D** and **E)** n=9; **J**] and presented as mean ± SEM following percentage change from to IL-10$^+$ B cell cultures. Wilcoxon signed-pairs rank rest. *Phl p*, *Phleum pratense*.

To decipher whether the mechanism through which IL-10$^+$ Breg cells were exerting their effects on T cells was in part mediated by IL-10 or IL-35, 1μg/mL αIL-10 or 10μg/mL αIL-35 was added alongside IL-10$^+$ Breg cell and autologous PBMC *Phl p* stimulated co-cultures and evaluated by multi-parametric flow cytometry. Neutralising IL-10 enhanced CD4$^+$ T (73% increase, P = 0.2188) and T_H2A (155% increase, P = 0.1250) cell proliferation, with no clear trend on T_H2 cells compared to IL-10$^+$ Breg cell treatment alone (Figure 7.2.4.2, A-C, and Table 7.2.4.2). Although neutralisation of IL-35 partly ameliorated IL-10$^+$ B cell suppression of CD4$^+$ T cell proliferation (55% increase, P = 0.2188), no clear trends were observed in either T_H2 or T_H2A cells. Interestingly however, a clear reduction of IL-10$^+$ iTreg cell frequencies was observed following IL-10 (28% decrease, P = 0.0938) and IL-35 (14% decrease, P = 0.5625) neutralisation (Figure 7.2.4.2, E). Conversely however, IL-10$^+$ iTreg cell proliferation was enhanced following amelioration of IL-35 (129% increase, P = 0.3125; Figure 7.2.4.2, D).

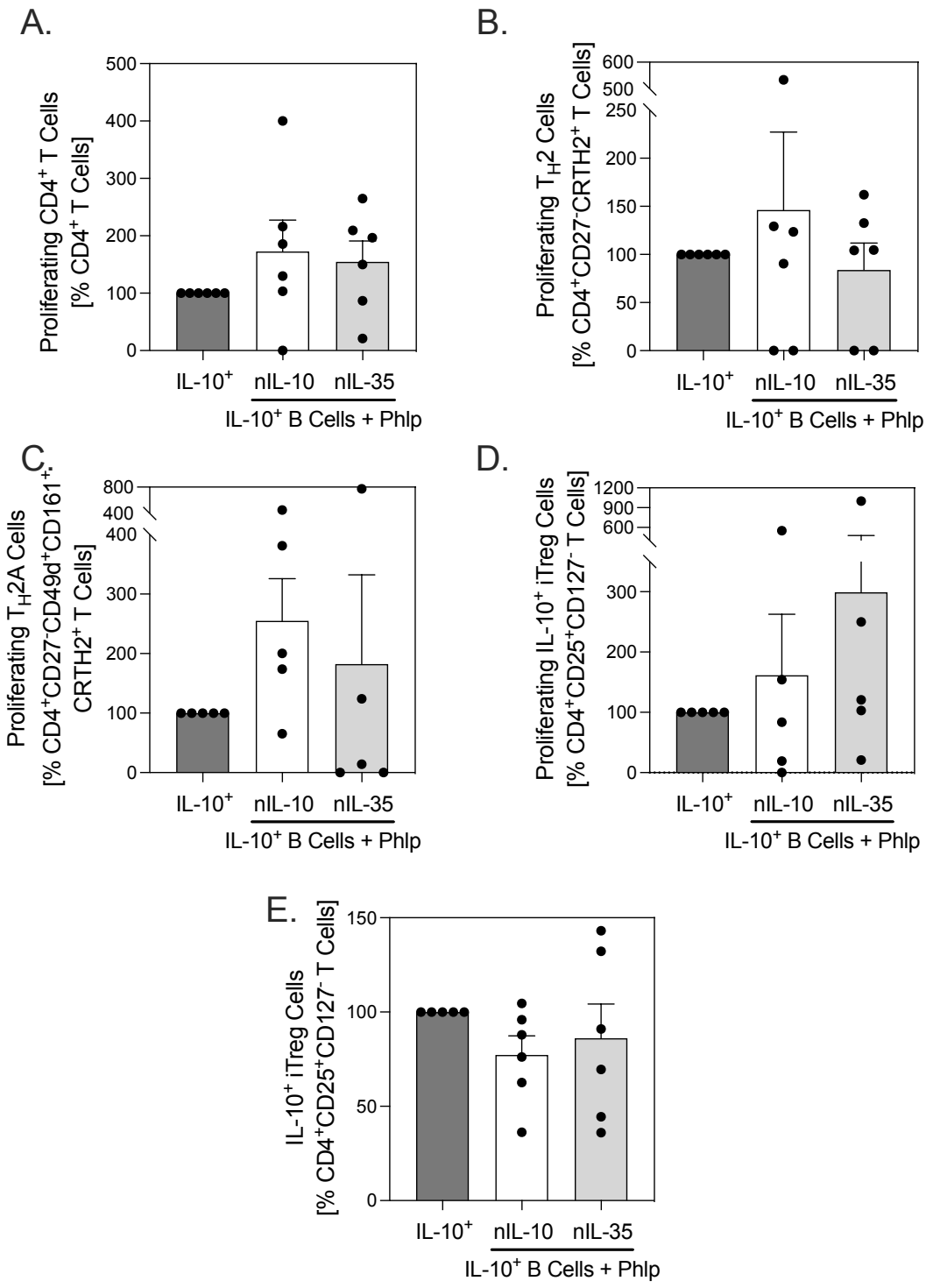


Figure 7.2.4.2 Neutralisation of IL-10 reduces IL-10$^+$ B cell suppressive capacity on T_H2A cell proliferation.

Flow cytometry data demonstrating **A)** CD4$^+$ T_H, **B)** T_H2, **C)** T_H2A and **D)** IL-10$^+$ iTreg cell proliferation, and **E)** IL-10+ iTreg cell freuqncies, in response to Phlp stimulation in the presence of IL-10$^+$ B cells alone or alongside IL-10$^+$ B cells and αIL-10 or αIL-35. Data representative of GPA, n= 6 [N.B. **C,** n=5**; D)** αIL-10, n=5] and presented as mean ± SEM, as percentage change from IL-10$^+$ B cells. Wilcoxon signed-pairs rank rest. αIL-10/IL-35, anti-IL-10/IL-35; *Phl p*, *Phleum pratense*

Table 7.2.4.1 Enriched IL-10$^+$ Breg cells and IL-10$^-$ B cells effects on *PhI p*-stimulated T_H2/T_H2A and iTreg cell subsets.

Culture Conditions	B/T Cell Subset	Raw				Delta Normalised to PhIp			Normalised to IL-10$^-$ B cells			*P* value v. IL-10 B Cells
		n	mean	SD	SEM	mean	SD	SEM	SEM	SD	SEM	
IL-10$^-$ B Cells	CD4$^+$CellTrace$^-$	10	1.74	1.90	0.60	1.47	1.86	0.59	100	0	0	NA
	CD4$^+$CD27$^+$CRT$_H$2$^+$CellTrace$^-$	10	4.65	3.91	1.24	3.49	3.34	1.06	100	0	0	NA
	CD4$^+$CD27$^+$CRT$_H$2$^+$CD49d$^+$CD161$^+$CellTrace$^-$	9	11.5	11.0	3.67	10.8	10.7	3.58	100	0	0	NA
	CD4$^+$CD25$^-$CD127$^+$IL-10$^+$	8	3.23	1.42	0.50	NA	NA	NA	100	0	0	NA
	CD4$^+$CD25$^-$CD127$^+$IL-10$^+$CellTrace$^-$	8	19.2	18.4	6.49	NA	NA	NA	100	0	0	NA
IL-10$^+$ B Cells	CD4$^+$CellTrace$^-$	10	0.84	0.53	0.17	0.57	0.48	0.15	64.0	55.2	17.4	0.1055
	CD4$^+$CD27$^+$CRT$_H$2$^+$CellTrace$^-$	10	4.48	4.56	1.44	3.33	4.00	1.26	190	267	84.4	0.8457
	CD4$^+$CD27$^+$CRT$_H$2$^+$CD49d$^+$CD161$^+$CellTrace$^-$	9	5.05	4.34	1.45	4.33	3.93	1.31	60.0	51.8	17.3	0.0547
	CD4$^+$CD25$^-$CD127$^+$IL-10$^+$	8	3.52	2.20	0.78	NA	NA	NA	147	103	33	0.4316
	CD4$^+$CD25$^-$CD127$^+$IL-10$^+$CellTrace$^-$	8	18.4	20.4	7.20	NA	NA	NA	172	250	83.2	0.9102

Bolded Values Represent ***P*** Significant Values. Wilcoxon-signed pairs rank test.

Table 7.2.4.2 IL-10$^+$ B cells partly mediate suppression of PhIp-stimulated T cell proliferation through IL-10 and IL-35.

Culture Conditions	B/T Cell Subset	Raw				Delta US [Data Above] Normalised to PhIp			Normalised to IL-10$^+$ B cells			*P* value v. IL-10$^+$ B Cells
		n	mean	SD	SEM	mean	SD	SEM	SEM	SD	SEM	
IL-10$^+$ B Cells	CD4$^+$CellTrace$^-$	6	0.69	0.41	0.17	0.36	0.26	0.11	100	0	0	NA
	CD4$^+$CD27$^+$CRT$_H$2$^+$CellTrace$^-$	6	1.96	1.39	0.57	1.11	1.49	0.61	100	0	0	NA
	CD4$^+$CD27$^+$CRT$_H$2$^+$CD49d$^+$CD161$^+$CellTrace$^-$	5	2.40	1.40	0.63	2.02	1.18	0.53	100	0	0	NA
	CD4$^+$CD25$^-$CD127$^+$IL-10$^+$	6	3.88	2.38	0.97	NA	NA	NA	100	0	0	NA
	CD4$^+$CD25$^-$CD127$^+$IL-10$^+$CellTrace$^-$	5	11.6	7.66	3.43	NA	NA	NA	100	0	0	NA
IL-10$^+$ B Cells	CD4$^+$CellTrace$^-$	6	0.79	0.19	0.08	0.48	0.33	0.133	173	134	54.8	0.2188
	CD4$^+$CD27$^+$CRT$_H$2$^+$CellTrace$^-$	6	3.12	2.14	0.87	2.26	2.26	0.92	146	199	81.1	0.9375
	CD4$^+$CD27$^+$CRT$_H$2$^+$CD49d$^+$CD161$^+$CellTrace$^-$	5	6.48	4.99	2.23	6.10	4.74	2.12	255	159	71.0	0.1250
	CD4$^+$CD25$^-$CD127$^+$IL-10$^+$	6	2.72	1.15	0.47	NA	NA	NA	77.2	24.9	10.2	0.0938
	CD4$^+$CD25$^-$CD127$^+$IL-10$^+$CellTrace$^-$	5	10.1	7.78	3.48	NA	NA	NA	162	226	101	>0.9999
IL-10$^+$ B Cells	CD4$^+$CellTrace$^-$	6	0.89	0.56	0.23	0.57	0.63	0.26	155	88.7	36.2	0.2188
	CD4$^+$CD27$^+$CRT$_H$2$^+$CellTrace$^-$	6	2.50	1.82	0.74	1.68	1.83	0.75	83.9	68.4	27.9	0.9375
	CD4$^+$CD27$^+$CRT$_H$2$^+$CD49d$^+$CD161$^+$CellTrace$^-$	5	4.65	8.17	3.66	4.27	7.94	3.55	183	335	150	0.7500
	CD4$^+$CD25$^-$CD127$^+$IL-10$^+$	6	3.19	1.79	0.73	NA	NA	NA	86.1	44.5	18.2	0.5625
	CD4$^+$CD25$^-$CD127$^+$IL-10$^+$CellTrace$^-$	5	20.4	19.5	8.70	NA	NA	NA	299	400	179	0.3125

Bolded Values Represent ***P*** Significant Values. Wilcoxon-signed pairs rank test.

7.3 Summary

In this chapter, I confirmed T_H2 and T_H2A cell subsets are present in human peripheral blood and demonstrate peak proliferative responses and IL-5 and IL-13 production following 4 days of polyclonal TCR stimulation with αCD3 and αCD28. Moreover, I confirmed that native *Phl p* allergen stimulation generated a dose-dependent increase in proliferating $CD4^+$ T, T_H2 and T_H2A subsets in GPA which were significantly enhanced following exposure to 1μg/mL *Phl p* compared to NAC, highlighting their T cell reactivity to allergen extract. Unbiased mathematical algorithms confirmed presence of a distinct $CD161^+CD27^-CD49d^+CRT_H2^+$ T_H2A subset following 1μg/mL *Phl p* stimulation. IL-10 significantly suppressed $CD4^+$, T_H2 and T_H2A cellular proliferation, confirmed through additive treatment with neutralising IL-10, which ameliorated suppression. Similarly, IL-10 suppressed cellular production of IL-5 protein. However, although IL-10 suppressed $IL\text{-}10^+$ iTreg cells frequencies and proliferative capacity, $IL\text{-}35^+$ iTreg cell subsets were enhanced upon exposure to IL-10. Cell co-culture systems utilising CpG and CD40L 'primed' Breg cells demonstrated a clear pro-inflammatory effect on autologous enriched $CD4^+$ T cell subset proliferation. However, T:B co-culture systems utilising enriched $IL\text{-}10^+$ Breg cells and autologous PBMCs attenuated proliferation of allergen-activated $CD4^+$ and T_H2A cellular subsets compared to enriched $IL\text{-}10^-$ B cells. Culture alongside $IL\text{-}10^+$ Breg cells also enhanced frequencies of $IL\text{-}10^+$ iTreg cells compared to $IL\text{-}10^-$ B cells. Finally, this chapter demonstrated neutralisation of IL-10 within $IL\text{-}10^+$ Breg:T cell co-culture systems partially reversed $IL\text{-}10^+$ Breg cell mediated suppression of $CD4^+$ and T_H2A proliferation, and reduced frequencies of $IL\text{-}10^+$ iTreg cells. Collectively, this chapter confirmed that $IL\text{-}10^+$ Breg cells can exert suppression of GP activated $CD4^+$ and T_H2A proliferation in SAR and enhance $IL\text{-}10^+$ iTreg cellular frequencies, which is in part mediated through IL-10.

CHAPTER 8. DISCUSSION

8.1 Heterogenous IL-10$^+$ Breg cell populations in human peripheral blood are expanded by CpG and CD40L stimulation

In Chapter 3, it was confirmed that IL-10$^+$ Breg cells are present in human peripheral blood and have capacity to produce IL-10 in response to CpG and CD40L stimulation. IL-10$^+$ Breg cells were comparably enriched from activated CD5$^+$, memory CD27$^+$ and transitional CD24^{hi}CD38^{hi} B cell subsets, with unbiased t-*SNE* clustering analysis of B cell surface markers confirming peripheral IL-10$^+$ Breg cell phenotypes are highly heterogenous (383). These data support the concept that B cells throughout the development and maturation process possess the ability to acquire immunoregulatory phenotypes and produce IL-10 in response to local environmental cues, as opposed to residing within a clear Breg phenotype. CD40L stimulation induced significant, but marginal, increases in IL-10$^+$ Breg subset frequencies, consistent with numerous studies reporting singular CD40L stimulation at a range of concentrations can expand relatively small frequencies of IL-10$^+$ Breg cells (263, 384, 385). Although a clear signaling pathway derived from CD40L stimulation to IL-10 secretion remains enigmatic, studies have reported a clear link between transgenic over-expression of CD40L and enhanced IL-10$^+$ Breg populations in murine models. Moreover, recent exploratory studies demonstrated CD40L-expressing irradiated cell lines induced *ex vivo* expansion of IL-10$^+$ Breg cells that lost propensity to secrete IL-10 upon cessation of CD40L stimulation, reverting to an effector B cell phenotype (246). IL-10$^+$ Breg subset activation and subsequent IL-10 protein production occurred in a CpG concentration dose-dependent manner, optimum at 1μg/mL and 3μg/mL CpG, confirmed utilising unbiased machine clustering algorithms and consistent with concentrations published previously (253, 263). The molecular mechanism of TLR signaling-mediated activation of IL-10 expression in B cells has been associated with MyD88, ERK1/2, P38, DOCK8, c-MAF and STAT3 signalling pathways, leading to enhanced IL-10 transcription

(345, 386-388). Therefore, localisation and expression of IL-10 in certain B cell subsets, and not others, may be due to the extent of their capability to activate these signalling pathways, although this hypothesis was not explored within the scope of this thesis. In addition to B cells, TLR9 signalling can drive IL-10 signalling in numerous other cell types, including T_R1, DC and macrophages (389-391). The physiological relevance of CpG stimulation within AD models can be understood following observations that DOCK8-$CD4^+$ T cell deficient mice possessing diminished responses to TLR9 signalling exhibited reduced functional IL-10^+ Breg cells which were associated with enhanced inflammatory cell infiltration in murine models of asthma (345, 392). Moreover, a recent study studying the role of CpG as an adjuvant during AIT also demonstrated its ability to suppress airway inflammation and induce type-1 DC when provided to mice alongside HDM extract (245). Building on this, the importance of CpG and CD40L stimulation in tolerance induction can also be understood by observations that injection with CpG and CD40L induced IL-10^+ Breg cells and suppressed inflammation within murine models of experimental periodontitis (393). Combined CpG and CD40L stimulation significantly expanded IL-10^+ Breg subsets following 72 hours stimulation, confirmed by unbiased machine learning algorithms and in agreement with similar accounts across the literature (226). IL-10^+ Breg subsets secreted the highest amount of IL-10 after 72 hours of repeated CpG and CD40L stimulation, consistent with recent observations by Shankar *et al.* that expanded IL-10^+ Breg cell populations can be maintained in culture with media replenishment (246). Although not within the scope of this project, previous studies investigating *IL-10* gene expression kinetics in IL-10^+ Breg cells following CD40L and CpG stimulation demonstrated a maximal induction at 24-48 hours, which is consistent with the observed increase in protein production at 72 hours (226, 393). Thereby, these findings corroborate numerous previous studies evidencing that CpG sequences are a major stimulus for IL-10^+ Breg cell activation, which can be expanded further following $CD4^+$ T cell cognate signals mediated through CD40L (263, 384).

In Chapter 3, it was also demonstrated that CpG and CD40L stimulation drives greater than 20-fold increase of PD-L1 expression on the surface of B cells, and marginal increases in PD-1 expression, in-line with previous reports (275, 383, 384). PD-L1 and PD-1 expression were clearly upregulated on IL-10^{+} Breg cells, supporting previous studies demonstrating significant upregulation of PD-L1 mRNA within cell-sorted IL-10^{+} Breg cells compared to IL-10^{-} B cells (253). Although the functionality of PD-L1^{+} Breg cells were not investigated in this thesis, previous studies have demonstrated their ability to suppress cytotoxic T cells, through TGF-β section, and T_{FH} cells (230, 394-397). Thereby, PD-L1^{+} Breg cells may play important regulatory roles during allergic inflammation through skewing T_H2/T_H2A and IL-4^{+} T_{FH} cell responses, thus inhibiting promotion of allergenic IgE^{+} Breg cells. Interestingly, studies utilising unbiased clustering approaches identified PD-L1^{+} Breg clusters that are TGF-β^{+} but IL-10^{-}, suggesting that PD-L1^{+} Breg may also work in an IL-10-independent manner (398). Therefore, these data contribute towards a building body of evidence that PD-L1 expression is associated with IL-10^{+} Breg cells and can also drive IL-10-independent Breg suppression, warranting further exploration. CpG and CD40L stimulation also induced significant upregulation of CD80 and CD86 expression on B cell surfaces, in-line with previous studies (246, 275, 384). However, in contrast to genome-wide transcriptional studies which demonstrated highest expression of CD80 on CD27^{lo} B cells, this study reported CD80 expression was particularly enhanced within memory CD27^{+} B cells, which may be important for post-GC B cell cognate interactions with local resident CD4^{+} T cells (399). Recent microarray studies have demonstrated that *cd80* gene expression was greater than 6-fold upregulation on IL-10^{+} compared to IL-10^{-} B cells (400). Although in this thesis CD86, but not CD80, was significantly upregulated on activated CD5$^{+/hi}$IL-10^{+} Breg cells compared to IL-10^{-} Breg cells, the discrepancies between studies may be due to investigating protein, compared to gene expression. These results suggest that upregulation of CD86, but not CD80, may be important for IL-10^{+} Breg-cell functionality, such as by enhancing cognate interactions with T cells which may increase T cell susceptibility to Breg modulation, although further research is

needed to confirm this relationship. TIM-1 expression was significantly upregulated on activated $CD5^{+/hi}$ and transitional $CD24^{hi}CD38^{hi}$ Breg cells following CpG and CD40L stimulation, in agreement with numerous other studies (246). Suppressive functionality of TIM-1^+ Breg cells has been previously demonstrated following observations that FACS-sorted CD40L-induced TIM-1^+ B cells exerted greater suppression of stimulated $CD4^+$ T_H cells compared to TIM-1^- B cells, and were able to prolong skin graft survival in humanised mouse models of human skin transplantation (246). Although some studies have proposed that TIM-1 is a unique marker for identification of the Breg phenotype, in this study TIM-1 expression was not significantly upregulated on memory $CD27^+$ or transitional $CD24^{hi}CD38^{hi}$ IL-10^+ Breg cells. Thus, although murine studies have reported that the TIM-1 signaling pathway acts as a master regulator of STAT-3 mediated IL-10 activation, these data suggest its expression is not required for Breg expression of IL-10, and thus contradicts the theory that TIM-1 is a defining Breg phenotypic marker (300-302). Furthermore, TIM-1 is also expressed on various T cell subsets, such as $CD4^+$ T cells, and has been described as playing central role in regulating T_H2 cellular responses, also highlighting that TIM-1 is not an appropriate Breg specific marker (401, 402). Thereby, further work to delineate the functionality of TIM-1^+ Breg cells, such as their regulation of IL-10 secretion or potential IL-10-independent mediated suppressive roles, are required. CpG and CD40L stimulation significantly upregulated both IL-35 and TGF-β1 expression from all investigated B cell subsets, confirming previous studies demonstrating their secretion from B cells (229, 230, 383, 403, 404). Traditional biaxial flow cytometry analysis revealed neither IL-35 or TGF-β1 was significantly associated with IL-10 expression, indicating their expression from both IL-10^+ Breg cells and IL-10^- B cells. Thus, these results support the concept that Breg-mediated suppression can occur in an IL-10-independent manner through secretion of other anti-inflammatory cytokines. None-the-less, studies have reported that similar molecular signalling pathways, involving the IRF4/IRF8 axis and STAT3 activation, underlie IL-10, TGF-β1 and IL-35 transcriptional programmes and may maximise their secretory capacity from Breg cells (295, 405, 406). Unbiased t-*SNE* clustering

interrogation of flow-cytometry data revealed the presence of a triple positive IL-35^{+}TGF-β1^{+}IL-10^{+} Breg subset, which was significantly upregulated following CpG and CD40L stimulation, confirmed through another mathematical unbiased approach, SPADE. To my knowledge, this is the first demonstration of distinct IL-35^{+}TGF-β1^{+}IL-10^{+} Breg subsets which are expanded through CpG and CD40L stimulation. viSNE map analysis also revealed CpG and CD40L induced Ebi3 subunit expression within islands of B cells which were IL-12p35^{-}. Ebi3 is known to form heterodimers with IL-27p28 to form IL-27, and thus it can be postulated that CpG and CD40L stimulation also induces an IL-27^{+} Breg population (407). Very few studies to date have reported the existence of IL-27^{+} Breg subsets, evidenced to play important immunosuppressant roles during neuroinflammation, uveitis, and promote tumorigenesis of solid tumours through enhancing Treg frequencies (408-410). Like IL-10 and IL-35, IL-27 is upregulated following TLR and CD40L stimulation and requires IRF8 expression for secretion from Breg cells (410). Collectively, these observations warrant further investigations of the relationships between suppressive cytokines secreted from Breg cells, including IL-27, and their potential dysregulation in states of hyperinflammation, such as AD.

8.2 IL-10^{+} and TIM-1^{+} Breg cells are significantly dysregulated in SAR and PAR

Despite IL-10^{+} Breg cell attenuation during AR being well-documented, no studies have yet directly explored Breg dysregulation between SAR and PAR in a large cross-sectional study. Therefore, following characterisation of heterogenic IL-10^{+} Breg cell subsets in human peripheral blood in Chapter 3, next this thesis enumerated IL-10^{+} Breg cell subsets in NAC, SAR, and PAR to decipher potential dysregulation which may contribute towards loss of tolerance to allergen. Chapter 4 confirmed there is a clear dysregulation in distinct IL-10^{+} Breg cell frequencies and IL-10 production propensity in response to CpG and CD40L stimulation between NAC and AR patients, in agreement with previous studies and confirmed through

unbiased machine learning algorithms (349, 411). IL-10^{+} Breg subset cell surface expression remained for-most part consistent across NAC, SAR, and PAR, demonstrating the stability of IL-10^{+} Breg cell phenotypes across both healthy controls and allergenic groups. Although the presence of human peripheral CD1d^{hi}CD5^{+}IL-10^{+} Breg cells were confirmed, frequencies were not dysregulated in SAR or PAR patients compared to NAC, conflicting with data demonstrating their significant aberration during AD, such as hypersensitivity reactions, allergic asthma, and AR (252, 340, 347, 349, 412, 413). Moreover, IL-10^{+}CD25^{+}CD71^{hi}CD73^{lo} Breg cell frequencies were not aberrated between SAR, PAR and NAC, although IL-10^{+} Breg cells were associated with enhanced CD25 and CD71 expression and reduced CD73 expression compared to IL-10^{-} B cells, supporting previous observations by Van de Veen and colleagues (200, 253). IL-10^{+}CD25^{+}CD71^{hi}CD73^{lo} Breg cell frequency dysregulation has not yet been explored in PAR and SAR, however, their importance in allergen tolerance has been demonstrated during venom AIT models (200). Therefore, it can be suggested that although CD25, CD71 and CD73 expression is significantly altered on IL-10^{+} Breg cells compared to IL-10^{-} B cells, this Breg cell subset may not contribute towards AD pathogenesis, although may still be targeted by AIT. Surprisingly, IL-10^{+} Breg cell frequencies positively correlated with clinical symptom severity in SAR, but not PAR patients, potentially due to shorter seasonal exposure to allergen causing increases in SAR clinical symptoms, but also briefly enhancing IL-10^{+} Breg frequencies, which aren't observed following constant perennial allergen exposure. Supporting this theory, as observed in Chapter 5, and demonstrated by Shamji and colleagues, both IL-10^{+} Breg frequencies and VAS scores are enhanced during the GP season (202). IL-10^{+} Breg frequencies were also correlated with SPT in all AR groups. However, these findings are conflicting to the hypothesis that dysregulation in IL-10^{+} Breg cells contribute towards increased disease severity, and further investigations are needed to confirm these observations. Finally, correlation analysis confirmed IL-10^{+} Breg cell dysregulation was due to atopic status, irrespective of polysensitization, and not age or gender. In Chapter 3, CpG and CD40L also demonstrated capacity to induce B cell TIM-1 expression. Thus, enumeration of TIM-1^{+} B cells and IL-10^{+}TIM-1^{+} Breg cells was performed

to decipher potential novel dysregulation underlying SAR, PAR and NAC. Distinct subsets of TIM-1$^+$ B cells and dual positive IL-10$^+$TIM-1$^+$ Breg cells were enhanced in HDMA compared to SAR, and NAC, with unbiased machine learning algorithms identifying a further IL-10$^+$TIM-1$^+$ Breg cell subset that was significantly enhanced in frequency in CA compared to SAR and NAC. To my knowledge, these results presented in Chapter 4 are the first quantification of TIM-1$^+$ Breg cells in human SAR and PAR patients and support the body of evidence that dysregulation of TIM-1 expression on B cells may contribute towards allergic inflammation, although the exact role that TIM-1 exerts, and why it is differentially expressed between SAR and PAR, remains to be determined. It can be suggested that chronic low-dose allergen during exposure to perennial allergens, such as HDM and cat allergen, induces consistent expression of TIM-1 on B cell surfaces, allowing more frequent crosstalk and regulation with effector T cell subsets to modulate cellular responses during allergic inflammation. The role of TIM-1 in AD remains uncertain, with conflicting studies describing TIM-1 as both a driver and suppressor of T_H2-allergic inflammation (246) (364) (302) (365) (414). Therefore, although it is speculated that PAR demonstrate enhanced TIM-1 expression, and thus greater ability to interact with T cells compared to SAR, it is not clear within this study and from the current literature whether this may aid to suppress or promote allergic inflammation. Interestingly, computational algorithms revealed CA demonstrated substantial increased frequency of another B cell subset compared to other allergenic groups and NAC, which did not express either TIM-1 or IL-10. Although the B cell markers investigated within this study were not able to discriminate the phenotype of this B cell subset, further B cell markers should be included in future studies to decipher this novel B cell compartment, which may be induced distinctly through cat, but not HDM or GP allergens. Collectively, these results highlight dysregulation of IL-10$^+$ Breg cells in AR patients, albeit seasonal or perennial, and suggest increased TIM-1$^+$ Breg subsets in PAR results may play key roles in allergic inflammation. Moreover, these results demonstrate, for the first-time, potential aberrations in Breg compartments driven by seasonal and perennial exposure to allergen.

Although the relationship between IgG_4 and IL-10^+ Breg cells is often postulated, there is a scarcity of reports throughout the literature investigating whether IL-10^+ Breg cells are responsible for secreting this immunosuppressive antibody. For example, patients with IgG_4-related disease, underscored by excessive IgG_4 serum levels and IgG_4^+ plasmablasts, demonstrated elevated IL-10 serum levels compared to healthy controls, although this was not directly linked to an increase in IL-10^+ Breg cells (318). In line with these observations, numerous clinical studies have demonstrated AIT drives expansion of peripheral IL-10^+ Breg cell frequencies in parallel to induction of allergen $sIgG_4$ levels, indicating a relationship (83, 198, 199).These insights indicated the need for deeper immunophenotyping studies directly investigating IgG_4 expression on Breg cells, leading van de Veen and colleagues to perform small-scale PCR experiments on FACS-sorted IL-10^+ B cells, demonstrating significant increases in IgG_4 mRNA expression compared to IL-10^- B cells (253). In Chapter 4, these initial observations were confirmed during a large study through the demonstration that IgG_4 antibody expression was significantly enhanced on $CD19^+$IL-10^+ Breg cells compared to $CD19^+$IL-10^- B cells in all subject groups. Interestingly, IgG_4 was enhanced on memory $CD27^+$IL-10^+ Breg cells in NAC to a much larger extent than in SAR and PAR subjects, suggesting an impairment in ability of memory $CD19^+CD27^+$IL-10^+ Breg cell to express IgG_4 in AR patients. Although traditional biaxial flow cytometry analysis was unable to identify dysregulation in dual positive IgG_4^+IL-10^+ Breg cell subset frequencies between NAC and AR patients, *tSNE*-based clustering approaches revealed a memory $CD27^+$ IL-$10^{lo}$$IgG4^+$ Breg cell subset which was attenuated in abundance, IL-10 and IgG_4 expression in HDMA and CA compared to GPA. Therefore, these results confirm in a large cross-study that IL-10^+ Breg cells are associated with significant expression of IgG_4 and may be specifically reduced in PAR compared to SAR patients. The relationship between IgA and IL-10^+ Breg cells remains enigmatic, with conflicting reports throughout the literature. For example, although AIT studies have reported expansion of peripheral IL-10^+ Breg cell frequencies in parallel to induction of

IgA levels, studies in IgA nephropathy patients have demonstrated IgA serum levels to negatively correlate with peripheral IL-10$^+$ Breg frequencies (415). However, recent studies have described IgA$^+$ Breg subsets characterised by positive IL-10 expression, which functionally suppress inflammation in murine contact hypersensitivity models and neuroinflammation (256, 313). Therefore, further studies are required to unpick this discrepancy and to determine whether IgA is associated with IL-10$^+$ secretion from Breg cells. Within Chapter 4, no clear relationship between IgA expression and CD19$^+$IL-10$^+$ Bregs were observed. However, AR patients demonstrated significant reductions in IgA expression on the surface of memory CD27$^+$IL-10$^+$ Bregs compared to CD27$^+$IL-10$^-$ B cells, which was not observed in NAC, suggesting memory IL-10$^+$ Breg cells in AR patients possess reduced ability to produce IgA compared to NAC. These observations are in-line with previous accounts demonstrating that murine models with IL-10-overexpressing B cells were associated with significant decreases in IgA expression (276). No aberration between IgA$^+$IL-10$^+$ Breg frequencies in NAC and AR were determined, confirmed through unbiased machine learning algorithms. Interestingly, memory IL-10$^+$IgA$^+$ and IL-10$^+$IgG$_4^+$ Breg cells were positively correlated, but demonstrated no correlation with allergen sIgE levels, suggesting that CSR promotion of IgA and IgG$_4$ C regions may occur through similar mechanisms or in relation to one another.

8.2.1 IL-10$^+$IL-35$^+$TGF-β^+ Breg cells are dysregulated in SAR patients compared to NAC

Following confirmation that IL-10$^+$ Breg cell subsets were dysregulated in SAR, deeper analysis of their aberration compared to NAC was performed. SAR IL-10$^+$ Breg cell subsets demonstrated reduced capacity to respond to singular CpG stimulation compared to NAC, as well as generating lower dose-response curves following exposure to increasing concentrations of CpG in combination with CD40L, confirming reduced capacity to respond to both innate and T-cell-mediated activation (202, 349). Neither CD80 or CD86 expression on

B cells or IL-10$^+$ Breg cells was altered in GPA compared to NAC, suggesting no dysregulation in the ability of GPA B cells to interact with T cells following stimulation. Although not explored within this thesis, it is important to consider that antigen-specific stimulation may have enhanced GPA B cells ability to upregulate cognate molecules, understood through allergy model studies whereby significant upregulation of CD80 expression on splenic B cells in mice with nut allergy, and CD86 expression on asthmatic patients, was observed following allergen exposure compared to relative healthy controls have been demonstrated (416) (417). Although IL-35 has been well documented to be produced by B cells and studies have demonstrated that IL-35 levels are reduced in allergic asthmatic and AR patients, no studies yet have directly investigated IL-35$^+$ Breg cells in SAR (149, 229, 230, 352, 353). For the first time, IL-35$^+$ and dual positive IL-10$^+$IL-35$^+$ Breg cells were demonstrated to be significantly reduced in SAR compared to NAC, confirmed by unbiased mathematical algorithms. Previous studies have demonstrated IL-35 to play important inhibitory roles during allergic inflammation, able to suppress IgE production from B cells and stimulate iT$_R$35 cells (418). Thereby, the observed dearth of IL-35$^+$ Breg cells in GPA compared to healthy controls may contribute to suboptimal allergic inflammation control, potentially representing another pathway towards disease pathogenesis. Although traditional flow-cytometry analysis did not reveal any difference in TGF-β expression in SAR B cells compared to NAC, *tSNE*-clustering revealed distinct TGF-β^+ B cell subsets which were differentially expressed in SAR. Moreover, supporting observations in Chapter 3, TGF-β^+ B cells subsets which were downregulated in SAR co-expressed IL-10 and IL-35, representing the novel triple positive IL-35$^+$TGF-β1$^+$IL-10$^+$ Breg cellular subset, which were reduced in abundance, IL-12p35 and IL-10 expression in SAR compared to NAC. Although these observations support similar studies revealing that local mucosal TGF-β^+ Breg cells are decreased in ovalbumin-challenged mice, serum TGF-β^+ levels are reduced in AR patients and TGF-β^+ Breg cell frequencies are reduced in milk-allergic patients compared to healthy controls, these findings are the first time that TGF-β^+ Breg cells have been demonstrated to be reduced in SAR compared to NAC (356, 419, 420).

As previous studies have highlighted that TGF-β1 employs important regulatory roles during AD through induction of Treg cells and inhibition of eosinophil cell infiltrate, the observed decrease in TGF-β1$^+$ Breg cells in GPA can be postulated to contribute towards AR disease progression (360). As previously described, Ebi3 can form dimers with IL-27p38 to form IL-27. Interestingly, B cell islands that were Ebi3$^+$, but IL-12p35$^-$, were also decreased in GPA compared to NAC, suggesting GPA may also possess aberrated IL-27$^+$ Breg cells.

8.3 SCIT restores IL-10$^+$ Breg cell frequencies in SAR to similar levels observed in NAC outside the pollen season

Following confirmation in Chapter 4 that IL-10$^+$ Breg subsets are dysregulated in SAR, next this thesis aimed to assess the ability of GP-SCIT to restore IL-10$^+$ Breg cell frequencies and IL-10 propensity. Outside of the GP season, GP-SCIT significantly enhanced IL-10$^+$ Breg cell frequencies in GPA to similar levels observed in NAC, confirmed by unbiased clustering algorithms. IL-10$^+$ Breg cell frequencies were enhanced in GPA during the GP season, potentially due to antigen-specific activation and subsequent expansion following natural exposure to sensitising allergen. Interestingly, CD25$^+$CD71^{hi}CD73^{lo} and CD1d^{hi}CD5$^+$ IL-10$^+$ Breg subsets were significantly downregulated outside of the GP season but enhanced during the GP season compared to NAC, suggesting that these IL-10$^+$ Breg subsets in SAR may be particularly sensitive to allergen-specific activation. Supporting this theory, allergen-stimulation during venom AIT has demonstrated substantial ability to enhance CD25$^+$CD71^{hi}CD73^{lo} B cell cellular frequencies (200). Moreover, despite the small sample size, computational algorithms revealed a distinct CD1d^{hi}CD5$^+$IL-10$^+$ Breg subset which was significantly enhanced in GP-SCIT-treated subjects, both inside and outside of the GP season, compared to SAR and NAC. However, contrasting with these findings, Shamji *et al.* directly demonstrated maintained attenuation of CD1d^{hi}CD5$^+$ IL-10$^+$ Breg cells compared to NAC during the GP season (202). Although increased frequencies of CD1d^{hi}CD5$^+$IL-10$^+$ Breg cells

were positively correlated with improvement in clinical symptom severity as measured by GE2, adding weight that this is one of the predominant IL-10^{+} Breg subsets modulated by GP-SCIT, CD1d^{hi}CD5^{+}IL-10^{+} Breg cell subsets also significantly correlated with increased clinical symptom burden, as measured by VAS, in GP-SCIT. Although the reason for this discrepancy is not clear, it can be postulated that although these patients perceived an improvement in their clinical AR symptoms (i.e., provided a GE2 value of +1-+3), their VAS scores, although reduced, remained relatively high (i.e., reduced from 90 to 75). Thereby, although not available as part of this cross-sectional study, in future studies it would be beneficial to collect and compare VAS scores to those before treatment. These findings corroborate a similar study performed by Zissler *et al.* in which expansion of IL-10^{+}CD1d^{hi}CD5^{+} Breg cells following 3 years of GP-AIT positively correlated with treatment responders (199). Collectively, these findings confirm the immunomodulatory ability of SCIT to generate IL-10^{+} Breg cells during AIT and highlight the potential role IL-10^{+} Breg cells may plan in AIT mechanism. Moreover, GP-SCIT may target IL-10-producing Breg cells within distinct B cell compartments as opposed to all Breg cells, and further research to understand the sensitivity of distinct IL-10^{+} Breg immunophenotypes to allergen-specific activation may identify IL-10^{+} Breg cells that are most susceptible to modulation by AIT, and thus may represent treatment biomarkers. Within Chapter 5, the ability of GP-SCIT to modify TIM-1 expression on B cells was also assessed, with clustering analysis revealing two CD1d^{hi}CD5^{+}TIM-1^{+} Breg cell subsets that were enhanced in TIM-1 expression in GP-SCIT-treated patients compared to both NAC and SAR. These findings are the first quantification of TIM-1^{+} B cells following GP-SCIT treatment and highlight the ability of GP-SCIT to upregulate TIM-1 expression on B cells, particularly on CD1d^{hi}CD5^{+} B cells. As TIM-1 is an important regulator of T cell activation, it can be postulated that this AIT-mediated increase in TIM-1 expression on IL-10^{+} Breg cells provides greater ability of Breg cells to regulate T cellular responses, such as through suppression of pro-allergenic T_H2 cells and promotion of Treg cell subsets. Finally, *tSNE*-clustering analysis revealed a distinct B cell subset that was negative for both IL-10 and TIM-1 expression that was significantly enhanced in patients receiving GP-SCIT. Although the suppressive

phenotype of this Breg cell could not be determined within this experimental panel, it could be postulated that these $CD38^{hi}CD71^{+}$ Breg cells are associated with other immunosuppressive mediators, such as IL-35 or PD-L1 expression.

Chapter 5 also assessed the effect of GP-SCIT on humoral responses through enumerating serum levels of GP-sIgE, GP-sIgG_4 and tIgE. Although levels were not significantly reduced compared to SAR, GP-SCIT treatment mediated time-dependent reductions of GP-sIgE and tIgE levels, indicating that treatment was driving isotype class switch in B cells away from IgE. which may contribute towards reduction of allergic inflammation through attenuating IgE-mediated effector cell activation (96, 198, 199). However, neither sIgE nor tIgE serum levels were associated with reduction of clinical symptom severity, which is conflicting with similar AIT studies in HDM-SCIT patients whereby attenuation of sIgE and tIgE was associated with positive treatment response (214). Therefore, these studies do not support the reliability of allergen-sIgE or tIgE as AIT efficacy biomarkers. In contrast, serum GP-sIgG_4 levels were substantially enhanced in GP-SCIT treated subjects compared to GPA, and positively correlated with length of SCIT treatment, supporting previous observations in AIT clinical studies (96, 199). However, allergen TG-sIgG_4 serum levels did not demonstrate clear correlation with any investigated IL-10^{+} Breg subset, meaning no suggestion could be drawn as to whether IL-10^{+} Breg subsets were responsible for production of enhanced levels of systemic IgG_4. Despite being substantially increased by SCIT treatment, IgG_4 levels were not correlated with clinical symptom severity, in agreement with observations reported during HDM-AIT studies (214). However, these observations conflict with other AIT studies demonstrating that both serum and salivary glands HDM allergen-sIgG_4 levels were closely related to AIT efficacy in AR and asthmatic children (421).Therefore, the current discrepancies in IgG_4 correlation with AIT efficacy data, both within this thesis and across AIT trials, currently does not support the suitability of allergen-sIgG_4 as a SCIT efficacy biomarker. Collectively, these findings evidence that length of GP-SCIT treatment is associated with increased GP-

$sIgG_4$ in parallel to reduction of GP-sIgE and tIgE levels, supporting the notion that AIT modulates humoral responses to instate tolerance to the causative allergen.

8.4 Novel AIT Approaches modulate IL-10$^+$ Breg cell subsets and enhance levels of protective local and systemic antibodies

Following confirmation in Chapter 5 that conventional approaches of AIT were able to significantly enhance frequencies of IL-10$^+$ Breg cells, next, the ability of alternative AIT approaches, such as utilising BP as novel allergen-carrier systems and shorter regimens of AIT, to induce IL-10$^+$ Breg cells was assessed.

8.4.1 *Fel d 1* expressing-eBP stimulates greater frequencies of IL-10$^+$ Breg cell subsets compared to *Fel d 1* alone

In Chapter 6, an exploratory preclinical study deciphering the ability of *in vivo* plant assembled eBP expressing multivalent high-density *Fel d 1* allergen to induce IL-10$^+$ Breg cells subsets in cat-sensitised AR patients was conducted. eBP-expressing *Fel d 1* stimulated enhanced frequencies of IL-10$^+$ Breg cells in CA compared to NAC, confirming CA patient B cell reactivity, and thus sensitivity, to the major cat allergen component. Immunogenicity of eBP-expressing *Fel d 1* was confirmed through its ability to generate greater frequencies of IL-10$^+$ Breg cell subsets compared to *Fel d 1* stimulation alone. Biosynthetic eBP express repetitive high-density allergen structures on their 3D phospholipid bilayer exterior, postulated to stimulate strong BCR signalling through enhanced allergen-crosslinking. In line with this theory, sustained IgG responses were observed during previous preclinical studies of *Der p 1*-expressing eBP, although direct modulation any B cell compartment was not confirmed (174)n. This thesis evidences, for the first time, the immunogenicity of allergen-expressing eBP to modulate B cell compartments through induction of tolerance-mediating IL-10$^+$ Breg

cells. As IL-10$^+$ Breg cells have been associated with IgG responses, both in published accounts and in Chapter 4 of this thesis, it can be postulated that expansion of IgG antibody levels following *Der p 1*-expressing eBP stimulation may be due to eBP-mediated expansion of IgG$^+$IL-10$^+$ Breg cell frequencies (253). Collectively these results, in combination with supporting evidence in the literature, support the use of eBP as a novel immunomodulatory therapeutic for the treatment of AD, such as AR.

8.4.2 VLP-Peanut, with and without MCT, is competent at generating IL-10$^+$ Breg cells in children with peanut allergy.

In Chapter 6 the ability of another BP, a multimeric CuMV$_{TT}$-VLP genetically fused to *Ara h 2*, was preclinically assessed for its ability to generate IL-10$^+$ Breg cell frequencies in PA children. For the first time, allergen-expressing VLP was demonstrated to significantly increase frequencies of heterogenous IL-10$^+$ Breg cell subsets compared to recombinant allergen treatment alone in allergic individuals, demonstrating the strong immunogenicity capacity of VLP, confirmed by unbiased *tSNE*-clustering algorithms. These findings support similar preclinical studies in which VLP-expressing the allergenic components *Ara h 2*, *Fel d 1* and *Der p 1* demonstrate immunomodulatory potential through robust and sustained induction of IgG responses, although direct investigations of VLP modulation on B cell compartment were not conducted (374-376). CuMV$_{TT}$-VLP are postulated to possess substantial ability to modulate B cell responses through *E. coli*-derived single-strand RNA, a potent TLR 7/8 agonist, and strong BCR cross-linking. Therefore, as IL-10$^+$ Breg cells have been previously associated with IgG responses, it can be postulated that TLR7/8-mediated activation of Breg cells, alongside strong BCR signalling from allergen recognition, activated IL-10$^+$ Breg cell subsets, inducing CSR towards IgG isotypes, and thus VLP-mediated expansion of IgG$^+$IL-10$^+$ Breg cell frequencies. Interestingly, in addition to enhancing the immunogenicity of VLP, MCT targeted a distinct IL-10$^+$ Breg cell subset phenotyped as CD5$^+$CD38^{hi}. MCT is a biodegradable depot adjuvant which has demonstrated ability to polarise T$_H$1 responses in

addition to boosting IgG responses following malaria-expressing $CuMV_{TT}$-VLP stimulation and within murine models of *Fel- d 1* AIT (422-424). Therefore, MCT-specific induction of specific IL-10^+ Breg cell subsets unpicks a novel potential mechanism of actions of adjuvant-driven IgG increases during AIT. Collectively, these results contribute towards a growing body of evidence demonstrating the immunogenicity of VLP allergen-carrier systems and highlights their potential usage for AIT.

8.4.3 PQGrass 27600 SU AIT induces local and systemic levels of grass pollen $sIgG_4$, $sIgA_1$ and $sIgA_2$ blocking antibodies

Although it is well established that long-term AIT approaches are efficacious and associated with cellular and humoral compartment modulations, shorter-term AIT treatment regimens are under investigation due to their potential to be less-time consuming and associated with fewer adverse effects. In Chapter 6, the ability of short-term administration of PQGrass to induce IL-10^+ Breg cells in parallel to local and systemic IgA and IgG levels was assessed during an exploratory RDBPC pilot phase III study. Although effects of PQGrass AIT on IL-10^+ Breg cell subset frequencies could not be determined due to issues with sample viability, induction of local and systemic IgA and IgG antibody levels indirectly confirmed ability of PQGrass to modulate B cell responses, supporting previous accounts (83). Short-term PQGrass AIT, whereby maintenance doses were administered weekly, demonstrated ability to significantly enhance both systemic and local IgG and IgG_4 levels and systemic IgA_1 and IgA_2 levels, to comparable levels observed with conventional monthly maintenance doses. Interestingly, despite treatment cessation IgG and IgG_4 levels were enhanced further during the GP season, potentially due to continued exposure to allergen through natural exposure. However, effects of PQGrass-modulation of IgA_1 and IgA_2 were not sustained through natural exposure to allergen, becoming reduced following treatment cessation. As previous studies, including in this thesis, have demonstrated IgG_4, but not IgA, antibody expression is enhanced within IL-10^+ Breg cells, it can be inferred that seasonal expansion of IL-10^+ Breg cells,are responsible

for maintaining levels of IgG_4, but not IgA, explaining its dearth (253). Collectively, these results confirm the ability of shorter-term PQGrass administration to induce similar levels of IgA and IgG antibodies compared to conventional PQGrass AIT treatment regimens and supports its use a less-time consuming AIT approach that maintains clinical efficacy.

8.5 IL-10$^+$ Breg cells suppress T_H2/T_H2A cellular responses through attenuating proliferative capacity

Following confirmation of SAR IL-10$^+$ Breg cell dysregulation in Chapters 4 and Chapter 5, this thesis assessed the effect this dearth may have during allergic inflammation through assessing the functionality of IL-10$^+$ Breg cells in modulating T_H2/T_H2A and iTreg cellular responses. To initially perform immunophenotyping of T cell subsets, cells were stimulated with αCD3 and αCD28, allowing strong polyclonal activation of the $\alpha\beta$-TCR complex by partially mimicking APC stimulation, resulting in an extensive proliferative response in previously characterised T_H2 ($CRT_H2^+CD27^-$) and T_H2A ($CRT_H2^+CD27^-CD161^+CD49d^+$) cell subsets, confirming their presence in human peripheral blood (125, 425). TCR-activation and proliferative responses of T_H2 and T_H2A cells occurred in a time-dependent manner, peaking in all subsets at 4 days stimulation, in-line with results in previous kinetic studies (426). Analysis of cell culture supernatant revealed IL-5 and IL-13, signature T2 inflammatory cytokines, were also induced in a time-dependent manner following αCD3/αCD28 stimulation, supporting previous evidence in the literature outlining their production from T_H2 and T_H2A cells (427-429). Additionally, stimulation with native *Phl p* generated a dose-dependent increase in proliferating allergen-specificT_H2 and T_H2A subsets, confirming the ability of allergen to activate T cells, in line with reports from similar preclinical exploratory studies (152, 430). Moreover, pro-allergenic T_H2A cell proliferative responses were significantly enhanced following exposure to 1μg/mL *Phl p* compared to NAC, confirming their allergic status by highlighting their enhanced T cell reactivity to allergen extract. However, no aberration in the

frequency or proliferative capacity of IL-10$^+$ iTreg cells was observed in SAR compared to NAC in response to allergen, indicating iTreg compartment dysregulation is not a factor in AR disease pathogenesis. Supporting this theory, no aberration was observed in frequencies of CD4$^+$CD25$^+$ Treg cells in milk tolerant and allergic individuals, or between healthy controls and birch-pollen allergic subjects (431, 432). However, previous studies have demonstrated a clear reduction in *foxp3* gene expression in patients with allergy and asthma compared to healthy controls, as well as attenuated regulatory functionality (382, 433, 434). Thus, although the consensus within the field remains that SAR possess reduced IL-10$^+$ iTreg cells compared to NAC, contributing towards the loss of peripheral tolerance to allergen, no clear conclusion could be drawn from the dataset in this study. In contrast, native allergen stimulation generated a small, but significant, dose-dependent induction of IL-10$^+$ Breg cells which was enhanced in NAC compared to GPA, at similar frequencies observed in previous studies (152). Thereby, these findings support the notion that in response to allergen, SAR possess impaired ability to generate IL-10$^+$ Breg cells. Although IL-10 protein levels in Breg culture supernatant did not correlate with IL-10$^+$ Breg frequencies, it can be theorised that the dose-dependent induction of IL-10 protein is a result of *Phl p* activation of other IL-10 producing cells, such as monocytes, T cells, and DC, although additional experiments to confirm this theory are required.

Following confirmation native *Phl p* extract activates T_H2, T_H2A and IL-10$^+$ iTreg cells, the ability of IL-10, the most well characterised immunosuppressant molecule produced by Breg cells, to modulate allergen-activated T cell responses was evaluated. IL-10 significantly prevented *Phl p* activation of both pro-allergenic T_H2 and T_H2A cell subsets, confirming its strong immunosuppressant properties (221, 261). Interestingly IL-5 protein levels in culture supernatant were also significantly attenuated by IL-10, indicating IL-10 also constrained activation of pro-inflammatory IL-5$^+$ CD4$^+$ T cells. Surprisingly, IL-10 also suppressed allergen-activated IL-10$^+$ iTreg cells, conflicting with accounts from previous studies whereby IL-10 induces Treg subset frequencies (265). Although these data suggest that IL-10 is not able to

induce allergen-specific iTreg cell subsets, it can be suggested that the chosen concentration of IL-10 was too potent to induce IL-10^{+} iTreg cells, causing pan-suppression of all T cell subsets. Moreover, it is also possible that heterogenic Treg subsets may respond differently to levels of IL-10. In line with this theory, IL-10 expanded IL-35^{+} iTreg cells in over half of the investigated patients, and therefore it can be speculated that different iTreg subsets respond to higher concentrations of IL-10 to assist with constraining inflammation. Therefore, it would be beneficial to perform IL-10 dose-dependent responses investigating numerous Treg subsets to confirm which are more susceptible to induction through various doses of IL-10.

Initial co-culture approaches utilising CpG and CD40L primed B cells failed to demonstrate suppressive effects on either polyclonal or allergen-activated T cell proliferation, instead enhancing T-cell activation. Moreover, allergen activated T_H2/T_H2A cell proliferation was enhanced following culture within supernatant collected from primed B cell cultures, implying that B cell mediated activation of T cells occurred through soluble mechanisms. These findings contrast with similar studies whereby CD40L-primed B cells constrained polyclonal T cell activation at T:B ratios of 1:1 or 1:2 following 5 days co-culture, demonstrating greater than 30% proliferative T cell suppression (246, 435). Therefore, it was theorised that, in addition to IL-10^{+} Breg cells, CpG and CD40L stimulation activated proinflammatory B cell subsets which secreted soluble pro-inflammatory mediators, such as IL-6, which were enhancing both polyclonal and allergen-driven T cell activation. As such, it was concluded that CpG and CD40L primed B cell cultures were not suitable for distinguishing the activity of IL-10^{+} Breg cells within this thesis. Instead, T:B co-culture systems utilsing IL-10^{+} Breg and IL-10^{-} B cells, which had been selectively enriched through magnetic column separation, were performed. IL-10^{+} Breg cells constrained allergen-driven CD4^{+} proliferative responses compared to IL-10^{-} B cell cultures, confirming previous studies utilsiing FACS-sorted CD25^{+}CD71^{lo}CD73^{hi} B cells, demonstrated to be enhanced in IL-10 expression and suppressed greater than 40% proliferating allergen-stimulated CD4^{+} T cells in response to allergen stimulation (253).

Interestingly, although no clear modulation of T_H2 cells was observed, exposure to IL-10^+ Breg cells attenuated T_H2A cell proliferation in response to allergen, compared to IL-10^- B cells. To my knowledge, this is the first demonstration of the ability of IL-10^+ Breg cells to suppress GP-driven T_H2A cellular responses compared to IL-10^- B cells. As SAR demonstrate reduced Breg cellular subsets compared to healthy controls, these findings imply that this results in lack of IL-10^+ Breg cell-mediated regulation of allergen-activated T_H2A cells, thereby failing to attenuate the excessive T_H2A responses responsible for allergic inflammation. IL-10^+ Breg cell-mediated regulation of T_H2A cells was confirmed to be mediated in part through IL-10, but not IL-35, which demonstrated no clear modulation to T_H2/T_H2A cell proliferative capacity upon neutralization. Although these results imply that B cell derived IL-35 does not suppress T cell responses, as IL-35 is not exclusively co-expressed with IL-10, as demonstrated in chapter 1, IL-35^+ Breg cells may have been selected against during the IL-10^+ Breg cell enrichment process, impeding ability to assess these cells accurately within this co-culture model. Although IL-10^+ Breg cells did not modulate allergen-stimulated IL-10^+ iTreg frequencies or proliferative capacity compared to IL-10^- B cells, removal of IL-10 from the culture system clearly suppressed frequencies of ITregs, indicating the importance of IL-10 in maintaining allergen specific iTreg cell responses. Although neutralisation of IL-10 and IL-35 demonstrated no modulation on iTreg cell proliferation, this effect may be due to the reduced iTreg populations following nIL-10 and nIL-35 treatment.

8.6 IL-10^+ Breg cells are dysregulated in AR, restored by AIT and suppress allergen-specific T_H2A cellular responses

This study hypothesised that Breg cells are dysregulated in patients with AR, restored during AIT and modulate allergen activated T_H2A and Treg responses. To test these overall hypotheses, this study was performed in several sections. Firstly, in Chapter 3 robust culture models utilising CpG ODN and CD40L stimuli to investigate IL-10^+ Breg cells in human

peripheral blood were optimised, successfully establishing reproducible experimental protocols for use throughout the rest of the study. In Chapter 3, efforts were also made to characterise additional Breg cells induced through *ex vivo* CpG ODN and CD40L stimulation to identify novel Breg cell markers that could be investigated during the SAR/PAR and SCIT cross-sectional studies in Chapter 4 and Chapter 5, respectively. As such, during Chapter 3 it was noted that TIM-1, IL-35 and TGFβ1 were associated with IL-10$^+$ Breg cells and were taken forward for analysis in AR patients in Chapter 4. Within Chapter 4, for the first time, a blinded cross-sectional study demonstrated that SAR and PAR patients possessed dysregulated IL-10$^+$ Breg cells compared to NAC, including investigation of TIM-1$^+$, IgA$^+$ and IgG$_4^+$ IL-10$^+$ Breg cells. To build upon findings in Chapter 3 that IL-10$^+$ Breg cells are associated with TGFβ1 and IL-35 expression, a sub-study confirmed, for the first time, that IL-35$^+$ and TGFβ1$^+$ Breg cells are dysregulated in SAR patients compared to NAC. Following confirmation in Chapter 4 that IL-10$^+$ Breg cells are dysregulated in SAR, Chapter 5 next investigated the ability of SCIT to restore IL-10$^+$ Breg cells. As TIM-1$^+$ Breg cells were observed to be significantly upregulated in PAR in Chapter 4, potentially due to chronic allergen exposure, TIM-1$^+$ Breg cells were also selected for investigation during the SCIT cross-sectional study in Chapter 5. In addition to driving upregulation of TIM-1$^+$ Breg cells, Chapter 5 demonstrated that AIT increases serum allergen-specific IgG$_4$. Following confirmation that traditional AIT approaches can induce IL-10$^+$ Breg cells, Chapter 6 evaluated the ability of novel allergen carrier systems, such as eBP or VLP, to generate IL-10$^+$ Breg cell responses in allergic individuals during preclinical exploratory studies. Although issues with sample viability prevented ability to validate observations in Chapter 4 that IL-10$^+$ Breg cells are associated with IgG, but not IgA during a prospective AIT clinical study, the ability of short-term administration of PQ Grass 27600 SU AIT to induce IgG and IgA subclasses was demonstrated, supporting findings in Chapter 5. Finally, Chapter 6 allowed insight into the effects that the dearth of IL-10$^+$ Breg cells may have in AR through demonstrating that IL-10$^+$ Breg cells are able to suppress allergen-specific T_H2A cells in parallel to inducing iTreg cells, in an IL-10 manner. These

functional observations suggest that the dysregulation of IL-10^{+} Breg cells observed in AR patients in Chapter 4 may contribute towards a loss of IL-10^{+} Breg cell-mediated regulation of allergen-specific T_H2A cells and induction of iTreg cells, resulting in inappropriate allergic immune responses to allergen. Moreover, restoration of these IL-10^{+} Breg cells during AIT, as observed in Chapters 5 and 6, may contribute towards skewing towards a tolerogenic T cellular response to allergen. Therefore, the sections of this thesis complement one another to confirm the hypothesis that Breg cells are dysregulated in patients with AR, restored during AIT and modulate allergen driven T_H2A and Treg responses.

CHAPTER 9. SUMMARY AND CONCLUDING REMARKS

The data presented in this thesis confirmed IL-10$^+$ Breg cells reside within heterogenous B cell compartments in peripheral human blood and can be expanded through CpG and CD40L stimulation in a dose and time-dependent manner, confirmed by computational unbiased analysis. In addition to IL-10, Breg cells can also express PD-L1, PD-1, TIM-1, IL-35, TGF-β, CD80 and CD86, highlighting the diverse and pleiotropic mechanisms Breg cells may utilise to constrain inflammation. Moreover, a distinct triple positive IL-10$^+$IL-35$^+$TGF-β$^+$ Breg subset was identified through unbiased *tSNE*-clustering algorithms. Expression of CD86 and TIM-1 were significantly associated with IL-10 expression from Breg cells, inferring their involvement in IL-10 signaling pathways.

A blinded cross-sectional study of IL-10$^+$ Breg cells in NAC, SAR and PAR demonstrated attenuation of IL-10$^+$ Breg frequencies and IL-10 provision underly sensitisation to both seasonal and perennial allergens, confirmed by computational algorithms. In all groups, IL-10$^+$ Breg cells were associated with significant expression of IgG_4, but not IgA, compared to IL-10$^-$ B cells. For the first time, distinct subsets of dual positive IL-10$^+$TIM-1$^+$ Breg cells were revealed to be dysregulated between SAR and PAR patients, suggesting distinct allergens elicit differential effects on TIM-1 expression on Breg cells. Moreover, for the first time, memory CD27$^+$IL-35$^+$ B cells and IL-10$^+$IL-35$^+$TGF-β$^+$ Breg cells were demonstrated to be significantly reduced in SAR compared to NAC, highlighting the potential implication of IL-35$^+$ Breg cell subsets in the pathophysiology of SAR disease.

Another blinded cross-sectional study of GP-SCIT confirmed its ability to significantly restore IL-10$^+$ Breg cells outside of the GP season in SAR to similar levels observed in NAC.

Computational analysis revealed SCIT to be particularly efficient at boosting both frequencies and IL-10 expression from $CD1d^{hi}CD5^{+}IL\text{-}10^{+}$ Breg cells. For the first time, SCIT was demonstrated to significantly enhance TIM-1 expression on the surface of both $IL\text{-}10^{-}$ B cells and $IL\text{-}10^{+}$ Breg cells, highlighting its potential immunomodulatory role during AIT. Finally, it was confirmed that GP-SCIT significantly enhanced serum levels of IgG_4 which correlated with increased length of SCIT administration.

In addition to conventional AIT approaches, the ability of alternative approaches of AIT to elicit modulations to the B cell compartment was confirmed. For the first time, during two preclinical studies, the immunogenicity of allergen-expressing eBP and VLP to modulate B cell responses was confirmed through demonstration of their ability to enhance $IL\text{-}10^{+}$ Breg frequencies. Therefore, highlighting their potential therapeutic potential for the treatment of AR, which is underscored by dysregulation of $IL\text{-}10^{+}$ Breg cells. Moreover, during a RDBPC Phase III trial, the ability of short-term treatment regimens of PQGrass was demonstrated to enhance local and systemic IgA and IgG levels. Thus, administration of short-term AIT able to maintain significant immunomodulatory treatment may reduce lengthy treatment regimens, thereby improving patient compliance.

The presence of allergen specific T_H2 and T_H2A cells in human peripheral blood was confirmed, demonstrating greater proliferative responses in response to native *Phl p* allergen stimulation in SAR compared to NAC. IL-10 significantly suppressed T_H2 and T_H2A cellular proliferation and IL-5 protein production, in addition to exerting differential effects on $IL\text{-}10^{+}$ and $IL\text{-}35^{+}$ allergen-specific iTreg cellular subsets. $IL\text{-}10^{+}$ Breg cells attenuated proliferation of allergen-activated T_H2A cells, which was partly mediated through IL-10. Moreover, IL-10 demonstrated importance in maintaining allergen-specific $IL\text{-}10^{+}$ iTreg frequencies.

In conclusion, the studies described in this thesis performed deep immunophenotyping of IL-10^+ Breg cells, exploring additional B cell suppressive molecular mechanisms, leading to the identification of a novel triple positive IL-10^+IL-35^+TGF-β^+ Breg subset. SAR and PAR patients demonstrate significant dearth of heterogenous IL-10^+ Breg cell frequencies and IL-10 provision compared to NAC, with TIM-1 expression on B cells being aberrantly expressed between SAR and PAR, highlighting differential disease pathways which may underly perennial and seasonal allergy. Conventional GP SCIT effectively enhanced IL-10^+ Breg cells, TIM-1^+ B cells and serum GP-IgG_4 levels, providing evidence of AIT mechanism of action. Moreover, alternative AIT approaches, such as BP and short-term treatment regimens, demonstrated ability to generate IL-10^+ Breg cells, highlighting their potential therapeutic benefit for effective AD modification. Finally, IL-10^+ Breg cells suppressed allergen-activated T_H2A proliferation, highlighting their ability to suppress allergic inflammation.

Although it has been previously established that IL-10^+ Breg cells are dysregulated in AR patients (202, 349), this study contributes towards knowledge by evidencing for the first time that SAR and PAR patients possess dysregulated frequencies of TIM-1^+ B cells and IL-10^+TIM-1^+ Breg cells compared to one another, highlighting differential immune signatures may underscore seasonal and perennial allergies. Interestingly, for the first time TIM-1^+ B cells and IL-10^+TIM-1^+ Breg cells were also observed to be modulated during SCIT AIT, potentially identifying a novel mechanism through which AIT may modulate allergic inflammation. However, this theory could not be investigated further during this thesis due to time constraints. Although IL-10^+ Breg cell dysregulation has been described in GPA and HDM, this study presents the first observation that CA AR patients possess dysregulated AR compared to NAC. Previous studies have demonstrated that IL-10^+ Breg cells can express IL-35, and that IL-35 demonstrates immunoregulatory activity during AR, although no studies to date have investigated IL-35^+ and IL-35^+IL-10^+ Breg cells in SAR (149, 229, 230, 418). This study, for the first time demonstrates that IL-35^+ Breg cells are significantly attenuated in SAR

compared to NAC, adding new insights into regulatory cell dysregulation that may contribute towards loss of tolerance to allergen. Moreover, although one small scale study on 4 subjects by van der Veen *et al.* demonstrated that IgG4 mRNA was enhanced in IL-10^+ Breg cells compared to IL-10^- B cells, this study validates these findings for the first time in a large cross-sectional study (253). For the first time, during two preclinical studies, the immunogenicity of allergen-expressing eBP and VLP to modulate B cell responses was confirmed through demonstration of their ability to enhance IL-10^+ Breg frequencies, highlighting their potential therapeutic potential for the treatment of AR. Additionally, although an initial Phase 3 study demonstrated that the 27600 SU dosage of PQGrass reduced clinical symptoms by 39.5%, the mechanisms underlying this clinical observation had not been investigated (381). This study therefore contributes towards knowledge by demonstrating that PQGrass 27600 SU was capable of inducing subclasses of igA and IgG_4, which may contribute towards the previously reported clinical benefit. Finally, utilizing co-culture models of enriched IL-10^+ Breg cells, this thesis demonstrated for the first time that GPA patient IL-10^+ Breg cells possess functional ability to suppress proliferation of GP specific T_H2A cells, insinuating that their observed dearth in AR patients may contribute towards excessive T_H2A cellular responses to allergen.

CHAPTER 10. STUDY LIMITATIONS

Although the cross-sectional study in Chapter 5 demonstrates the ability of GP-SCIT to restore IL-10$^+$ Breg cells in GPA outside of the GP season, it was not possible to draw any conclusive observations regarding SCIT-modulation of IL-10$^+$ or TIM-1$^+$ Breg cells during the GP season due to the limited number of IS SCIT samples collected, which was only confirmed following sample unblinding. Moreover, another limitation of this cross-sectional SCIT study was the absence of numerous time-points able to demonstrate a time-course induction of Breg cells throughout treatment, as would have been observed during a prospective study, which unfortunately could not be performed within the time-constraints of this thesis. Although efforts were made to perform this analysis as part of the Phase III PQGrass exploratory clinical study in Chapter 6, issues with sample viability were detrimental to sample analysis accuracy, meaning it could not be included in this thesis. Although co-culture assays were performed utilising isolated IL-10$^+$ Breg cells, the proportions of IL-10$^+$ Breg cells in peripheral blood, even following expansion with *ex vivo* stimulus, remain small. Due to this low frequency, it was not possible to investigate varying ratios of enriched IL-10$^+$ Breg cells and autologous PBMCs, meaning a concentration dependent effect of IL-10$^+$ Breg cell-mediated suppression of T cells could not be observed. Equally, the low proportions of IL-10$^+$ Breg cells available for co-culture assays meant additional suppressive molecules identified in Chapter 3 to be associated with IL-10$^+$ Breg cells, PD-L1, PD-1, TIM-1, IL-35, and TGF-β, could not be investigated for their ability to exert suppressive functions on T cells. Although the use of flow cytometry to investigate cellular subsets provides a robust and accurate analytical method, limitations are faced through the limited number of filters, and thus antibodies, which can be investigated at one time during a flow-cytometry panel design. Within these studies for example, it would have been beneficial to investigate previously described pro-inflammatory cytokine production, namely IL-6 and TNF-α, from B cells in parallel to IL-10 production following CpG and CD40L stimulation (436). Although these studies could not be performed within the time-constraints

of this thesis, these findings would have allowed confirmation of the observed pro-inflammatory effect of effector T cells following co-culture systems with primed B cells. Moreover, within this study it was not possible to investigate FOXP3$^+$ Treg cells due to being unable to perform both nuclear and intracellular cell staining within the same panel, limiting the ability to investigate IL-10$^+$ Breg modulation of nTreg subsets in parallel to iTreg cells. Unfortunately, although allergen was observed to marginally induce frequencies of IL-10$^+$ Breg cells in Chapter 7, no direct investigations of allergen-specific IL-10$^+$ Breg cells were performed as part of this thesis. Discrepancy of antigen-specific B cells can be achieved through staining with tetramers conjugated to a fluorochrome as assessed through flow cytometry. Specifically, to investigate antigen-specific Breg cells, utilisiation of dCODE Klickmer technology to identify these cells, as previously utilised in SARS-CoV-2 studies, was considered as part of experimental design during this project, but unfortunately could not be feasibly completed within the timeframe of this project due to unexpected complications faced upon generation of a GP-specific klickmer (437). Finally, although this thesis uncovered new relationships between IL-10 secretion and other molecules, studies were focused on IL-10$^+$ Breg cells and investigated previously reported B cell suppressive molecules. Thereby, this study was limited in its ability to identify novel Breg-associated molecules aberrated during allergic inflammation pathophysiology or restored following AIT approaches.

CHAPTER 11. FUTURE STUDIES

Although stimulation utilsing CpG and CD40L was demonstrated to induce suppressive cytokine production from B cells, studies investigating whether CpG and CD40L also induces pro-inflammatory cytokines from B cells should also be performed to determine whether Breg cells completely switch to IL-10 production, reduce pro-inflammatory cytokine production, or simply gain capability to produce IL-10 alongside pro-inflammatory cytokines. In Chapter 3, following postulation that B cells expressing Ebi3, but not IL-12p35, may represent IL-27$^+$ Breg cells, this theory should be confirmed through addition of IL-12p28 to the flow cytometry panel design, followed by investigations of their aberration in AR patients. Additional novel suppressive soluble molecules could also be identified utilising proteomics and transcriptomics on enriched IL-10$^+$ Breg and IL-10$^-$ B cells to identify potential novel proteins for investigation. Moreover, qPCR analysis utilising pre-designed TaqMan assays at numerous time-points could be used to investigate *Il10, p35* and *Ebi3*, *ighg1, igha1* and *p28* gene expression to allow investigations of the kinetics of IL-10, IL-27, IL-35, IgA_1 and IgG_1 expression.

This study reported IL-10$^+$ Breg dysregulation in AR patients which could be partially restored outside of the GP season in SAR following conventional SCIT in a proof-of-concept cross sectional study. Firstly, recruitment of additional IS GP-SCIT donors should be undertaken to increase sample size, allowing determination of the effects of SCIT on IL-10$^+$ Breg cells during the pollen season. Although IL-10 was utilised as a functional phenotypic marker of the Breg state, various studies have demonstrated that Breg-mediated functionality is not exclusive to IL-10, and that other suppressive markers can be present in the absence of IL-10 provision. Thereby, an important additional study would be to investigate the ability of SCIT to modulate additional Breg cell subsets, such as IL-35$^+$ and TGF-β^+ Breg cells. Moreover, the importance

of the observed TIM-1$^+$ B cell subset during AIT should be evaluated, for example, through co-culture models to determine their effects on T cell modulation which may contribute towards tolerance instatement to allergen. In addition to IL-10$^+$ Breg cells, AIT has been associated in with induction of IL-10$^+$ Treg cells. However, the relative importance that IL-10-producing Breg cells and IL-10$^+$ Treg cells play compared to each other in terms of level of level of IL-10 production and potency of immunosuppressive activities during AIT remains to be elucidated.

In Chapter 4, IgG_4 expression was demonstrated to be significantly associated with IL-10$^+$ Breg cells. Although it was postulated that the increase of IL-10$^+$ Breg cells correlated with the increase of serum IgG_4 during the cross-sectional study, direct investigations of IgG_4^+IL-10$^+$ Breg cells were not performed. Therefore, it is of utmost importance to investigate IgG_4^+IL-10$^+$ Breg cells during a prospective AIT study with multiple mechanistic time-points to confirm this relationship. Bioinformatic analysis of single cell data can identify sIgG_4 B-cells, allowing interrogation of heavy and light chain rearrangement to assess specificity to allergenic proteins and antibody evolution. For example, detection of antigen-specific B-cells, with dCODE® Klickmer technology (ImmuDex), containing an incorporated DNA barcode can be utilised for multi-omics analysis to characterise BCR sequences, chromatin accessibility landscapes and transcriptomic profiles at a single-cell resolution. Thus, utilising dCODE® Klickmers can allow for assessment of antigen-specific B-cell frequency and BCR repertoires in NAC, allergic individuals, and AIT-treated patients. Although not within the scope of this project, it would be interesting to also conduct further studies to affirm whether additional Breg suppressive markers, such as IL-35, PD-L1 and TGF-β1, are more defining of the ability of B cells to produce IgG_4 or IgA than IL-10.

CHAPTER 12. BIBLIOGRAPHY

1. Shin YH, Hwang J, Kwon R, Lee SW, Kim MS, Collaborators GBDAD, et al. Global, regional, and national burden of allergic disorders and their risk factors in 204 countries and territories, from 1990 to 2019: A systematic analysis for the Global Burden of Disease Study 2019. Allergy. 2023;78(8):2232-54.

2. Gupta R, Sheikh A, Strachan DP, Anderson HR. Burden of allergic disease in the UK: secondary analyses of national databases. Clin Exp Allergy. 2004;34(4):520-6.

3. Li J, Zhang Y, Zhang L. Discovering susceptibility genes for allergic rhinitis and allergy using a genome-wide association study strategy. Curr Opin Allergy Clin Immunol. 2015;15(1):33-40.

4. Deckers J, Lambrecht BN, Hammad H. How a farming environment protects from atopy. Curr Opin Immunol. 2019;60:163-9.

5. Eller E, Roll S, Chen CM, Herbarth O, Wichmann HE, von Berg A, et al. Meta-analysis of determinants for pet ownership in 12 European birth cohorts on asthma and allergies: a GA2LEN initiative. Allergy. 2008;63(11):1491-8.

6. Sroka-Tomaszewska J, Trzeciak M. Molecular Mechanisms of Atopic Dermatitis Pathogenesis. Int J Mol Sci. 2021;22(8).

7. Sinyor B, Concepcion Perez L. Pathophysiology Of Asthma. StatPearls. Treasure Island (FL)2024.

8. Yu W, Freeland DMH, Nadeau KC. Food allergy: immune mechanisms, diagnosis and immunotherapy. Nat Rev Immunol. 2016;16(12):751-65.

9. Akhouri S, House SA. Allergic Rhinitis. StatPearls. Treasure Island (FL)2024.

10. Cibella F, Ferrante G, Cuttitta G, Bucchieri S, Melis MR, La Grutta S, et al. The burden of rhinitis and rhinoconjunctivitis in adolescents. Allergy Asthma Immunol Res. 2015;7(1):44-50.

11. Siroux V, Boudier A, Nadif R, Lupinek C, Valenta R, Bousquet J. Association between asthma, rhinitis, and conjunctivitis multimorbidities with molecular IgE sensitization in adults. Allergy. 2019;74(4):824-7.

12. Brozek JL, Bousquet J, Agache I, Agarwal A, Bachert C, Bosnic-Anticevich S, et al. Allergic Rhinitis and its Impact on Asthma (ARIA) guidelines-2016 revision. J Allergy Clin Immunol. 2017;140(4):950-8.

13. Eifan AO, Durham SR. Pathogenesis of rhinitis. Clin Exp Allergy. 2016;46(9):1139-51.

14. Savoure M, Bousquet J, Jaakkola JJK, Jaakkola MS, Jacquemin B, Nadif R. Worldwide prevalence of rhinitis in adults: A review of definitions and temporal evolution. Clin Transl Allergy. 2022;12(3):e12130.

15. Greisner WA, 3rd, Settipane RJ, Settipane GA. Natural history of hay fever: a 23-year follow-up of college students. Allergy Asthma Proc. 1998;19(5):271-5.

16. Asher MI, Montefort S, Bjorksten B, Lai CK, Strachan DP, Weiland SK, et al. Worldwide time trends in the prevalence of symptoms of asthma, allergic rhinoconjunctivitis, and eczema in childhood: ISAAC Phases One and Three repeat multicountry cross-sectional surveys. Lancet. 2006;368(9537):733-43.

17. Chung SJ, Kim BK, Oh JH, Shim JS, Chang YS, Cho SH, et al. Novel tobacco products including electronic cigarette and heated tobacco products increase risk of allergic rhinitis and asthma in adolescents: Analysis of Korean youth survey. Allergy. 2020;75(7):1640-8.

18. Venter C, Meyer RW, Nwaru BI, Roduit C, Untersmayr E, Adel-Patient K, et al. EAACI position paper: Influence of dietary fatty acids on asthma, food allergy, and atopic dermatitis. Allergy. 2019;74(8):1429-44.

19. Zhou J, Luo F, Han Y, Lou H, Tang X, Zhang L. Obesity/overweight and risk of allergic rhinitis: A meta-analysis of observational studies. Allergy. 2020;75(5):1272-5.

20. Asher MI, Stewart AW, Mallol J, Montefort S, Lai CK, Ait-Khaled N, et al. Which population level environmental factors are associated with asthma, rhinoconjunctivitis and eczema? Review of the ecological analyses of ISAAC Phase One. Respir Res. 2010;11(1):8.

21. Vandenplas O, Vinnikov D, Blanc PD, Agache I, Bachert C, Bewick M, et al. Impact of Rhinitis on Work Productivity: A Systematic Review. J Allergy Clin Immunol Pract. 2018;6(4):1274-86 e9.

22. Zuberbier T, Lotvall J, Simoens S, Subramanian SV, Church MK. Economic burden of inadequate management of allergic diseases in the European Union: a GA(2) LEN review. Allergy. 2014;69(10):1275-9.

23. Colas C, Brosa M, Anton E, Montoro J, Navarro A, Dordal MT, et al. Estimate of the total costs of allergic rhinitis in specialized care based on real-world data: the FERIN Study. Allergy. 2017;72(6):959-66.

24. Walker S, Khan-Wasti S, Fletcher M, Cullinan P, Harris J, Sheikh A. Seasonal allergic rhinitis is associated with a detrimental effect on examination performance in United Kingdom teenagers: case-control study. J Allergy Clin Immunol. 2007;120(2):381-7.

25. Dass K, Petrusan AJ, Beaumont J, Zee P, Lai JS, Fishbein A. Assessment of sleep disturbance in children with allergic rhinitis. Ann Allergy Asthma Immunol. 2017;118(4):505-6.

26. Devillier P, Bousquet J, Salvator H, Naline E, Grassin-Delyle S, de Beaumont O. In allergic rhinitis, work, classroom and activity impairments are weakly related to other outcome measures. Clin Exp Allergy. 2016;46(11):1456-64.

27. Adams-Groom B, Selby K, Derrett S, Frisk CA, Pashley CH, Satchwell J, et al. Pollen season trends as markers of climate change impact: Betula, Quercus and Poaceae. Sci Total Environ. 2022;831:154882.

28. Frisk CA, Adams-Groom B, Smith M. Isolating the species element in grass pollen allergy: A review. Sci Total Environ. 2023;883:163661.

29. Huang HJ, Sarzsinszky E, Vrtala S. House dust mite allergy: The importance of house dust mite allergens for diagnosis and immunotherapy. Mol Immunol. 2023;158:54-67.

30. Nadeem A, Al-Harbi NO, Ahmad SF, Ibrahim KE, Alotaibi MR, Siddiqui N, et al. Protease activated receptor-2 mediated upregulation of IL-17 receptor signaling on airway epithelial cells is responsible for neutrophilic infiltration during acute exposure of house dust mite allergens in mice. Chem Biol Interact. 2019;304:52-60.

31. Gronlund H, Saarne T, Gafvelin G, van Hage M. The major cat allergen, Fel d 1, in diagnosis and therapy. Int Arch Allergy Immunol. 2010;151(4):265-74.

32. Niesler A, Scigala G, Ludzen-Izbinska B. Cat (Fel d 1) and dog (Can f 1) allergen levels in cars, dwellings and schools. Aerobiologia (Bologna). 2016;32(3):571-80.

33. Wise SK, Damask C, Roland LT, Ebert C, Levy JM, Lin S, et al. International consensus statement on allergy and rhinology: Allergic rhinitis - 2023. Int Forum Allergy Rhinol. 2023;13(4):293-859.

34. Wheatley LM, Togias A. Clinical practice. Allergic rhinitis. N Engl J Med. 2015;372(5):456-63.

35. Agache I, Palmer E, Sanver D, Kirtland M, Shamji MH. Molecular allergology approach to allergic asthma. Mol Aspects Med. 2022;85:101027.

36. Saleem R, Keymer C, Patel D, Egner W, Rowbottom AW. UK NEQAS survey of allergen component testing across the United Kingdom and other European countries. Clin Exp Immunol. 2017;188(3):387-93.

37. Steering Committee A, Review Panel M. A WAO - ARIA - GA(2)LEN consensus document on molecular-based allergy diagnosis (PAMD@): Update 2020. World Allergy Organ J. 2020;13(2):100091.

38. Alpan O, Wasserman RL, Kim T, Darter A, Shah A, Jones D, et al. Towards an FDA-cleared basophil activation test. Front Allergy. 2022;3:1009437.

39. Bahri R, Bulfone-Paus S. Mast Cell Activation Test (MAT). Methods Mol Biol. 2020;2163:227-38.

40. Corren J, Ziegler SF. TSLP: from allergy to cancer. Nat Immunol. 2019;20(12):1603-9.

41. Zhang R, Zhang L, Li P, Pang K, Liu H, Tian L. Epithelial Barrier in the Nasal Mucosa, Related Risk Factors and Diseases. Int Arch Allergy Immunol. 2023;184(5):481-501.

42. Jakwerth CA, Ordovas-Montanes J, Blank S, Schmidt-Weber CB, Zissler UM. Role of Respiratory Epithelial Cells in Allergic Diseases. Cells. 2022;11(9).

43. Halim TY, Steer CA, Matha L, Gold MJ, Martinez-Gonzalez I, McNagny KM, et al. Group 2 innate lymphoid cells are critical for the initiation of adaptive T helper 2 cell-mediated allergic lung inflammation. Immunity. 2014;40(3):425-35.

44. Toki S, Goleniewska K, Zhang J, Zhou W, Newcomb DC, Zhou B, et al. TSLP and IL-33 reciprocally promote each other's lung protein expression and ILC2 receptor expression to enhance innate type-2 airway inflammation. Allergy. 2020;75(7):1606-17.

45. Humeniuk P, Dubiela P, Hoffmann-Sommergruber K. Dendritic Cells and Their Role in Allergy: Uptake, Proteolytic Processing and Presentation of Allergens. Int J Mol Sci. 2017;18(7).

46. Takano K, Kojima T, Go M, Murata M, Ichimiya S, Himi T, et al. HLA-DR- and CD11c-positive dendritic cells penetrate beyond well-developed epithelial tight junctions in human nasal mucosa of allergic rhinitis. J Histochem Cytochem. 2005;53(5):611-9.

47. Peng YQ, Qin ZL, Fang SB, Xu ZB, Zhang HY, Chen D, et al. Effects of myeloid and plasmacytoid dendritic cells on ILC2s in patients with allergic rhinitis. J Allergy Clin Immunol. 2020;145(3):855-67 e8.

48. Nakayama T, Hirahara K, Onodera A, Endo Y, Hosokawa H, Shinoda K, et al. Th2 Cells in Health and Disease. Annu Rev Immunol. 2017;35:53-84.

49. Palomares O, Akdis M, Martin-Fontecha M, Akdis CA. Mechanisms of immune regulation in allergic diseases: the role of regulatory T and B cells. Immunol Rev. 2017;278(1):219-36.

50. Varricchi G, Harker J, Borriello F, Marone G, Durham SR, Shamji MH. T follicular helper (Tfh) cells in normal immune responses and in allergic disorders. Allergy. 2016;71(8):1086-94.

51. Shamji MH, Bellido V, Scadding GW, Layhadi JA, Cheung DK, Calderon MA, et al. Effector cell signature in peripheral blood following nasal allergen challenge in grass pollen allergic individuals. Allergy. 2015;70(2):171-9.

52. Scadding GW, Eifan A, Penagos M, Dumitru A, Switzer A, McMahon O, et al. Local and systemic effects of cat allergen nasal provocation. Clin Exp Allergy. 2015;45(3):613-23.

53. Sarin S, Undem B, Sanico A, Togias A. The role of the nervous system in rhinitis. J Allergy Clin Immunol. 2006;118(5):999-1016.

54. Naclerio R. Clinical manifestations of the release of histamine and other inflammatory mediators. J Allergy Clin Immunol. 1999;103(3 Pt 2):S382-5.

55. Gould HJ, Takhar P, Harries HE, Durham SR, Corrigan CJ. Germinal-centre reactions in allergic inflammation. Trends Immunol. 2006;27(10):446-52.

56. Kraft S, Kinet JP. New developments in FcepsilonRI regulation, function and inhibition. Nat Rev Immunol. 2007;7(5):365-78.

57. Horiguchi S, Okamoto Y, Chazono H, Sakurai D, Kobayashi K. Expression of membrane-bound CD23 in nasal mucosal B cells from patients with perennial allergic rhinitis. Ann Allergy Asthma Immunol. 2005;94(2):286-91.

58. Yao Y, Wang N, Chen CL, Pan L, Wang ZC, Yunis J, et al. CD23 expression on switched memory B cells bridges T-B cell interaction in allergic rhinitis. Allergy. 2020;75(10):2599-612.

59. Dykewicz MS, Wallace DV, Amrol DJ, Baroody FM, Bernstein JA, Craig TJ, et al. Rhinitis 2020: A practice parameter update. J Allergy Clin Immunol. 2020;146(4):721-67.

60. Yanez A, Rodrigo GJ. Intranasal corticosteroids versus topical H1 receptor antagonists for the treatment of allergic rhinitis: a systematic review with meta-analysis. Ann Allergy Asthma Immunol. 2002;89(5):479-84.

61. Wilson AM, Orr LC, Sims EJ, Lipworth BJ. Effects of monotherapy with intra-nasal corticosteroid or combined oral histamine and leukotriene receptor antagonists in seasonal allergic rhinitis. Clin Exp Allergy. 2001;31(1):61-8.

62. Chen H, Zhang L, Lou H, Wang Y, Cao F, Wang C. A Randomized Trial of Comparing a Combination of Montelukast and Budesonide With Budesonide in Allergic Rhinitis. Laryngoscope. 2021;131(4):E1054-E61.

63. Shamji MH, Palmer E, Layhadi JA, Moraes TJ, Eiwegger T. Biological treatment in allergic disease. Allergy. 2021;76(9):2934-7.

64. Casale TB, Condemi J, LaForce C, Nayak A, Rowe M, Watrous M, et al. Effect of omalizumab on symptoms of seasonal allergic rhinitis: a randomized controlled trial. JAMA. 2001;286(23):2956-67.

65. Zhang Y, Xi L, Gao Y, Huang Y, Cao F, Xiong W, et al. Omalizumab is effective in the preseasonal treatment of seasonal allergic rhinitis. Clin Transl Allergy. 2022;12(1):e12094.

66. Jonstam K, Swanson BN, Mannent LP, Cardell LO, Tian N, Wang Y, et al. Dupilumab reduces local type 2 pro-inflammatory biomarkers in chronic rhinosinusitis with nasal polyposis. Allergy. 2019;74(4):743-52.

67. Busse WW, Maspero JF, Lu Y, Corren J, Hanania NA, Chipps BE, et al. Efficacy of dupilumab on clinical outcomes in patients with asthma and perennial allergic rhinitis. Ann Allergy Asthma Immunol. 2020;125(5):565-76 e1.

68. Noon L. Prophylactic inoculation against hay fever (historical document). Ann Allergy. 1955;13(6):713-6; passim.

69. Freeman J. Further observations on the treatment of hay fever by hypodermic inoculations of pollen vaccine. Historical document. Ann Allergy. 1960;18:427-34.

70. Buters J, Prank M, Sofiev M, Pusch G, Albertini R, Annesi-Maesano I, et al. Variation of the group 5 grass pollen allergen content of airborne pollen in relation to geographic location and time in season. J Allergy Clin Immunol. 2015;136(1):87-95 e6.

71. Jin JJ, Li JT, Klimek L, Pfaar O. Sublingual Immunotherapy Dosing Regimens: What Is Ideal? J Allergy Clin Immunol Pract. 2017;5(1):1-10.

72. Jung S, Estrella N, Pfaffl MW, Hartmann S, Handelshauser E, Menzel A. Grass pollen production and group V allergen content of agriculturally relevant species and cultivars. PLoS One. 2018;13(3):e0193958.

73. Norman PS, Lichtenstein LM. Comparisons of alum-precipitated and unprecipitated aqueous ragweed pollen extracts in the treatment of hay fever. J Allergy Clin Immunol. 1978;61(6):384-9.

74. Scadding GW, Calderon MA, Shamji MH, Eifan AO, Penagos M, Dumitru F, et al. Effect of 2 Years of Treatment With Sublingual Grass Pollen Immunotherapy on Nasal Response to Allergen Challenge at 3 Years Among Patients With Moderate to Severe Seasonal Allergic Rhinitis: The GRASS Randomized Clinical Trial. JAMA. 2017;317(6):615-25.

75. Borg M, Lokke A, Hilberg O. Compliance in subcutaneous and sublingual allergen immunotherapy: A nationwide study. Respir Med. 2020;170:106039.

76. Nurmatov U, Dhami S, Arasi S, Roberts G, Pfaar O, Muraro A, et al. Allergen immunotherapy for allergic rhinoconjunctivitis: a systematic overview of systematic reviews. Clin Transl Allergy. 2017;7:24.

77. Dhami S, Kakourou A, Asamoah F, Agache I, Lau S, Jutel M, et al. Allergen immunotherapy for allergic asthma: A systematic review and meta-analysis. Allergy. 2017;72(12):1825-48.

78. Yonekura S, Gotoh M, Kaneko S, Maekawa Y, Okubo K, Okamoto Y. Disease-Modifying Effect of Japanese Cedar Pollen Sublingual Immunotherapy Tablets. J Allergy Clin Immunol Pract. 2021;9(11):4103-16 e14.

79. Durham SR, Emminger W, Kapp A, de Monchy JG, Rak S, Scadding GK, et al. SQ-standardized sublingual grass immunotherapy: confirmation of disease modification 2 years after 3 years of treatment in a randomized trial. J Allergy Clin Immunol. 2012;129(3):717-25 e5.

80. Didier A, Malling HJ, Worm M, Horak F, Sussman GL. Prolonged efficacy of the 300IR 5-grass pollen tablet up to 2 years after treatment cessation, as measured by a recommended daily combined score. Clin Transl Allergy. 2015;5:12.

81. Valovirta E, Petersen TH, Piotrowska T, Laursen MK, Andersen JS, Sorensen HF, et al. Results from the 5-year SQ grass sublingual immunotherapy tablet asthma prevention (GAP) trial in children with grass pollen allergy. J Allergy Clin Immunol. 2018;141(2):529-38 e13.

82. Bozek A, Bogacz-Piaseczynska A, Miodonska M, Sadowska D. Long-term benefit after allergen immunotherapy to HDM in elderly patients with allergic rhinitis. Postepy Dermatol Alergol. 2023;40(5):688-92.

83. Scadding GW, Shamji MH, Jacobson MR, Lee DI, Wilson D, Lima MT, et al. Sublingual grass pollen immunotherapy is associated with increases in sublingual Foxp3-expressing cells and elevated allergen-specific immunoglobulin G4, immunoglobulin A and serum inhibitory activity for immunoglobulin E-facilitated allergen binding to B cells. Clin Exp Allergy. 2010;40(4):598-606.

84. Fritzsching B, Contoli M, Porsbjerg C, Buchs S, Larsen JR, Elliott L, et al. Long-term real-world effectiveness of allergy immunotherapy in patients with allergic rhinitis and asthma: Results from the REACT study, a retrospective cohort study. Lancet Reg Health Eur. 2022;13:100275.

85. Durham SR. The allergen specificity of allergen immunotherapy-doubt no more. Allergy. 2019;74(11):2054-6.

86. Frankland AW, Augustin R. Prophylaxis of summer hay-fever and asthma: a controlled trial comparing crude grass-pollen extracts with the isolated main protein component. Lancet. 1954;266(6821):1055-7.

87. Norman PS, Ohman JL, Jr., Long AA, Creticos PS, Gefter MA, Shaked Z, et al. Treatment of cat allergy with T-cell reactive peptides. Am J Respir Crit Care Med. 1996;154(6 Pt 1):1623-8.

88. Passalacqua G, Albano M, Fregonese L, Riccio A, Pronzato C, Mela GS, et al. Randomised controlled trial of local allergoid immunotherapy on allergic inflammation in mite-induced rhinoconjunctivitis. Lancet. 1998;351(9103):629-32.

89. Durham SR, Walker SM, Varga EM, Jacobson MR, O'Brien F, Noble W, et al. Long-term clinical efficacy of grass-pollen immunotherapy. N Engl J Med. 1999;341(7):468-75.

90. Jacobsen L, Niggemann B, Dreborg S, Ferdousi HA, Halken S, Host A, et al. Specific immunotherapy has long-term preventive effect of seasonal and perennial asthma: 10-year follow-up on the PAT study. Allergy. 2007;62(8):943-8.

91. Senti G, Prinz Vavricka BM, Erdmann I, Diaz MI, Markus R, McCormack SJ, et al. Intralymphatic allergen administration renders specific immunotherapy faster and safer: a randomized controlled trial. Proc Natl Acad Sci U S A. 2008;105(46):17908-12.

92. Senti G, Graf N, Haug S, Ruedi N, von Moos S, Sonderegger T, et al. Epicutaneous allergen administration as a novel method of allergen-specific immunotherapy. J Allergy Clin Immunol. 2009;124(5):997-1002.

93. DuBuske LM, Frew AJ, Horak F, Keith PK, Corrigan CJ, Aberer W, et al. Ultrashort-specific immunotherapy successfully treats seasonal allergic rhinoconjunctivitis to grass pollen. Allergy Asthma Proc. 2011;32(3):239-47.

94. Niederberger V, Neubauer A, Gevaert P, Zidarn M, Worm M, Aberer W, et al. Safety and efficacy of immunotherapy with the recombinant B-cell epitope-based grass pollen vaccine BM32. J Allergy Clin Immunol. 2018;142(2):497-509 e9.

95. Orengo JM, Radin AR, Kamat V, Badithe A, Ben LH, Bennett BL, et al. Treating cat allergy with monoclonal IgG antibodies that bind allergen and prevent IgE engagement. Nat Commun. 2018;9(1):1421.

96. Shamji MH, Larson D, Eifan A, Scadding GW, Qin T, Lawson K, et al. Differential induction of allergen-specific IgA responses following timothy grass subcutaneous and sublingual immunotherapy. J Allergy Clin Immunol. 2021;148(4):1061-71 e11.

97. Lieberman JA, Gupta RS, Knibb RC, Haselkorn T, Tilles S, Mack DP, et al. The global burden of illness of peanut allergy: A comprehensive literature review. Allergy. 2021;76(5):1367-84.

98. Sicherer SH, Sampson HA. Food allergy: A review and update on epidemiology, pathogenesis, diagnosis, prevention, and management. J Allergy Clin Immunol. 2018;141(1):41-58.

99. Shreffler WG, Beyer K, Chu TH, Burks AW, Sampson HA. Microarray immunoassay: association of clinical history, in vitro IgE function, and heterogeneity of allergenic peanut epitopes. J Allergy Clin Immunol. 2004;113(4):776-82.

100. Kukkonen AK, Pelkonen AS, Makinen-Kiljunen S, Voutilainen H, Makela MJ. Ara h 2 and Ara 6 are the best predictors of severe peanut allergy: a double-blind placebo-controlled study. Allergy. 2015;70(10):1239-45.

101. Dyer AA, Rivkina V, Perumal D, Smeltzer BM, Smith BM, Gupta RS. Epidemiology of childhood peanut allergy. Allergy Asthma Proc. 2015;36(1):58-64.

102. Pajno GB, Fernandez-Rivas M, Arasi S, Roberts G, Akdis CA, Alvaro-Lozano M, et al. EAACI Guidelines on allergen immunotherapy: IgE-mediated food allergy. Allergy. 2018;73(4):799-815.

103. Chu DK, Wood RA, French S, Fiocchi A, Jordana M, Waserman S, et al. Oral immunotherapy for peanut allergy (PACE): a systematic review and meta-analysis of efficacy and safety. Lancet. 2019;393(10187):2222-32.

104. Jones SM, Kim EH, Nadeau KC, Nowak-Wegrzyn A, Wood RA, Sampson HA, et al. Efficacy and safety of oral immunotherapy in children aged 1-3 years with peanut allergy

(the Immune Tolerance Network IMPACT trial): a randomised placebo-controlled study. Lancet. 2022;399(10322):359-71.

105. Koppelman SJ, Peillon A, Agbotounou W, Sampson HA, Martin L. Epicutaneous immunotherapy for peanut allergy modifies IgG(4) responses to major peanut allergens. J Allergy Clin Immunol. 2019;143(3):1218-21 e4.

106. Soller L, Abrams EM, Carr S, Kapur S, Rex GA, Leo S, et al. First Real-World Safety Analysis of Preschool Peanut Oral Immunotherapy. J Allergy Clin Immunol Pract. 2019;7(8):2759-67 e5.

107. J OBH, Beyer K, Abbas A, Fernandez-Rivas M, Turner PJ, Blumchen K, et al. Efficacy and safety of oral immunotherapy with AR101 in European children with a peanut allergy (ARTEMIS): a multicentre, double-blind, randomised, placebo-controlled phase 3 trial. Lancet Child Adolesc Health. 2020;4(10):728-39.

108. Bird JA, Spergel JM, Jones SM, Rachid R, Assa'ad AH, Wang J, et al. Efficacy and Safety of AR101 in Oral Immunotherapy for Peanut Allergy: Results of ARC001, a Randomized, Double-Blind, Placebo-Controlled Phase 2 Clinical Trial. J Allergy Clin Immunol Pract. 2018;6(2):476-85 e3.

109. Chinthrajah RS, Purington N, Andorf S, Long A, O'Laughlin KL, Lyu SC, et al. Sustained outcomes in oral immunotherapy for peanut allergy (POISED study): a large, randomised, double-blind, placebo-controlled, phase 2 study. Lancet. 2019;394(10207):1437-49.

110. Altman MC, Segnitz RM, Larson D, Jayavelu ND, Smith MT, Patel S, et al. Nasal and blood transcriptomic pathways underpinning the clinical response to grass pollen immunotherapy. J Allergy Clin Immunol. 2023;152(5):1247-60.

111. Woehlk C, Ramu S, Sverrild A, Nieto-Fontarigo JJ, Vazquez-Mera S, Cerps S, et al. Allergen Immunotherapy Enhances Airway Epithelial Antiviral Immunity in Patients with Allergic Asthma (VITAL Study): A Double-Blind Randomized Controlled Trial. Am J Respir Crit Care Med. 2023;207(9):1161-70.

112. Durham SR, Ying S, Varney VA, Jacobson MR, Sudderick RM, Mackay IS, et al. Grass pollen immunotherapy inhibits allergen-induced infiltration of CD4+ T lymphocytes

and eosinophils in the nasal mucosa and increases the number of cells expressing messenger RNA for interferon-gamma. J Allergy Clin Immunol. 1996;97(6):1356-65.

113. Hamid QA, Schotman E, Jacobson MR, Walker SM, Durham SR. Increases in IL-12 messenger RNA+ cells accompany inhibition of allergen-induced late skin responses after successful grass pollen immunotherapy. J Allergy Clin Immunol. 1997;99(2):254-60.

114. Shamji MH, Layhadi JA, Scadding GW, Cheung DKM, Calderon MA, Turka LA, et al. Basophil expression of diamine oxidase: a novel biomarker of allergen immunotherapy response. J Allergy Clin Immunol. 2015;135(4):913-21 e9.

115. Plewako H, Wosinska K, Arvidsson M, Bjorkander J, Skov PS, Hakansson L, et al. Basophil interleukin 4 and interleukin 13 production is suppressed during the early phase of rush immunotherapy. Int Arch Allergy Immunol. 2006;141(4):346-53.

116. Zimmer A, Bouley J, Le Mignon M, Pliquet E, Horiot S, Turfkruyer M, et al. A regulatory dendritic cell signature correlates with the clinical efficacy of allergen-specific sublingual immunotherapy. J Allergy Clin Immunol. 2012;129(4):1020-30.

117. Gueguen C, Bouley J, Moussu H, Luce S, Duchateau M, Chamot-Rooke J, et al. Changes in markers associated with dendritic cells driving the differentiation of either TH2 cells or regulatory T cells correlate with clinical benefit during allergen immunotherapy. J Allergy Clin Immunol. 2016;137(2):545-58.

118. Angelini F, Pacciani V, Corrente S, Silenzi R, Di Pede A, Polito A, et al. Dendritic cells modification during sublingual immunotherapy in children with allergic symptoms to house dust mites. World J Pediatr. 2011;7(1):24-30.

119. Haczku A, Takeda K, Redai I, Hamelmann E, Cieslewicz G, Joetham A, et al. Anti-CD86 (B7.2) treatment abolishes allergic airway hyperresponsiveness in mice. Am J Respir Crit Care Med. 1999;159(5 Pt 1):1638-43.

120. Lombardi V, Beuraud C, Neukirch C, Moussu H, Morizur L, Horiot S, et al. Circulating innate lymphoid cells are differentially regulated in allergic and nonallergic subjects. J Allergy Clin Immunol. 2016;138(1):305-8.

121. Eljaszewicz A, Ruchti F, Radzikowska U, Globinska A, Boonpiyathad T, Gschwend A, et al. Trained immunity and tolerance in innate lymphoid cells, monocytes, and dendritic cells during allergen-specific immunotherapy. J Allergy Clin Immunol. 2021;147(5):1865-77.

122. Lao-Araya M, Steveling E, Scadding GW, Durham SR, Shamji MH. Seasonal increases in peripheral innate lymphoid type 2 cells are inhibited by subcutaneous grass pollen immunotherapy. J Allergy Clin Immunol. 2014;134(5):1193-5 e4.

123. Golebski K, Layhadi JA, Sahiner U, Steveling-Klein EH, Lenormand MM, Li RCY, et al. Induction of IL-10-producing type 2 innate lymphoid cells by allergen immunotherapy is associated with clinical response. Immunity. 2021;54(2):291-307 e7.

124. Iinuma T, Okamoto Y, Morimoto Y, Arai T, Sakurai T, Yonekura S, et al. Pathogenicity of memory Th2 cells is linked to stage of allergic rhinitis. Allergy. 2018;73(2):479-89.

125. Wambre E, Bajzik V, DeLong JH, O'Brien K, Nguyen QA, Speake C, et al. A phenotypically and functionally distinct human T(H)2 cell subpopulation is associated with allergic disorders. Sci Transl Med. 2017;9(401).

126. Calise J, Garabatos N, Bajzik V, Farrington M, Robinson D, Jeong D, et al. Optimal human pathogenic T(H)2 cell effector function requires local epithelial cytokine signaling. J Allergy Clin Immunol. 2021;148(3):867-75 e4.

127. Renand A, Shamji MH, Harris KM, Qin T, Wambre E, Scadding GW, et al. Synchronous immune alterations mirror clinical response during allergen immunotherapy. J Allergy Clin Immunol. 2018;141(5):1750-60 e1.

128. Luce S, Batard T, Bordas-Le Floch V, Le Gall M, Mascarell L. Decrease in CD38(+) TH2A cell frequencies following immunotherapy with house dust mite tablet correlates with humoral responses. Clin Exp Allergy. 2021;51(8):1057-68.

129. Scadding GW, Eifan AO, Lao-Araya M, Penagos M, Poon SY, Steveling E, et al. Effect of grass pollen immunotherapy on clinical and local immune response to nasal allergen challenge. Allergy. 2015;70(6):689-96.

130. Reithofer M, Boell SL, Kitzmueller C, Horak F, Bohle B, Jahn-Schmid B. T-cell subset changes during the first year of pre-seasonal allergoid allergen-specific immunotherapy. Heliyon. 2023;9(11):e21878.

131. Starchenka S, Oluwayi K, Heath M, Armfield O, Shamji M, Layhadi J, et al. Peripheral blood mononuclear cell transcriptome profile in a clinical trial with subcutaneous, grass pollen allergoid immunotherapy. Clin Exp Allergy. 2024;54(2):130-42.

132. Guerra F, Carracedo J, Solana-Lara R, Sanchez-Guijo P, Ramirez R. TH2 lymphocytes from atopic patients treated with immunotherapy undergo rapid apoptosis after culture with specific allergens. J Allergy Clin Immunol. 2001;107(4):647-53.

133. Wambre E, DeLong JH, James EA, LaFond RE, Robinson D, Kwok WW. Differentiation stage determines pathologic and protective allergen-specific CD4+ T-cell outcomes during specific immunotherapy. J Allergy Clin Immunol. 2012;129(2):544-51, 51 e1-7.

134. Bohle B, Kinaciyan T, Gerstmayr M, Radakovics A, Jahn-Schmid B, Ebner C. Sublingual immunotherapy induces IL-10-producing T regulatory cells, allergen-specific T-cell tolerance, and immune deviation. J Allergy Clin Immunol. 2007;120(3):707-13.

135. Mobs C, Slotosch C, Loffler H, Jakob T, Hertl M, Pfutzner W. Birch pollen immunotherapy leads to differential induction of regulatory T cells and delayed helper T cell immune deviation. J Immunol. 2010;184(4):2194-203.

136. Ebner C, Siemann U, Bohle B, Willheim M, Wiedermann U, Schenk S, et al. Immunological changes during specific immunotherapy of grass pollen allergy: reduced lymphoproliferative responses to allergen and shift from TH2 to TH1 in T-cell clones specific for Phl p 1, a major grass pollen allergen. Clin Exp Allergy. 1997;27(9):1007-15.

137. Ciepiela O, Zawadzka-Krajewska A, Kotula I, van Overveld F, Kulus M, Demkow U. Sublingual Immunotherapy for Asthma: Affects T-Cells but Does not Impact Basophil Activation. Pediatr Allergy Immunol Pulmonol. 2014;27(1):17-23.

138. Scholz J, Kuhrau J, Heinrich F, Heinz GA, Hutloff A, Worm M, et al. Vitamin A controls the allergic response through T follicular helper cell as well as plasmablast differentiation. Allergy. 2021;76(4):1109-22.

139. Zhang B, Liu E, Gertie JA, Joseph J, Xu L, Pinker EY, et al. Divergent T follicular helper cell requirement for IgA and IgE production to peanut during allergic sensitization. Sci Immunol. 2020;5(47).

140. Haynes NM, Allen CD, Lesley R, Ansel KM, Killeen N, Cyster JG. Role of CXCR5 and CCR7 in follicular Th cell positioning and appearance of a programmed cell death gene-1high germinal center-associated subpopulation. J Immunol. 2007;179(8):5099-108.

141. Sharif H, Acharya S, Dhondalay GKR, Varricchi G, Krasner-Macleod S, Laisuan W, et al. Altered chromatin landscape in circulating T follicular helper and regulatory cells following grass pollen subcutaneous and sublingual immunotherapy. J Allergy Clin Immunol. 2021;147(2):663-76.

142. Yao Y, Chen CL, Wang N, Wang ZC, Ma J, Zhu RF, et al. Correlation of allergen-specific T follicular helper cell counts with specific IgE levels and efficacy of allergen immunotherapy. J Allergy Clin Immunol. 2018;142(1):321-4 e10.

143. Clement RL, Daccache J, Mohammed MT, Diallo A, Blazar BR, Kuchroo VK, et al. Follicular regulatory T cells control humoral and allergic immunity by restraining early B cell responses. Nat Immunol. 2019;20(10):1360-71.

144. Schulten V, Tripple V, Seumois G, Qian Y, Scheuermann RH, Fu Z, et al. Allergen-specific immunotherapy modulates the balance of circulating Tfh and Tfr cells. J Allergy Clin Immunol. 2018;141(2):775-7 e6.

145. Yao Y, Wang ZC, Wang N, Zhou PC, Chen CL, Song J, et al. Allergen immunotherapy improves defective follicular regulatory T cells in patients with allergic rhinitis. J Allergy Clin Immunol. 2019;144(1):118-28.

146. Shigehara K, Kamekura R, Ikegami I, Sakamoto H, Yanagi M, Kamiya S, et al. Circulating T follicular helper 2 cells, T follicular regulatory cells and regulatory B cells are effective biomarkers for predicting the response to house dust mite sublingual immunotherapy in patients with allergic respiratory diseases. Front Immunol. 2023;14:1284205.

147. Long Y, Li W, Feng J, Ma Y, Sun Y, Xu L, et al. Follicular helper and follicular regulatory T cell subset imbalance is associated with higher activated B cells and abnormal

autoantibody production in primary anti-phospholipid syndrome patients. Clin Exp Immunol. 2021;206(2):141-52.

148. Radulovic S, Jacobson MR, Durham SR, Nouri-Aria KT. Grass pollen immunotherapy induces Foxp3-expressing CD4+ CD25+ cells in the nasal mucosa. J Allergy Clin Immunol. 2008;121(6):1467-72, 72 e1.

149. Shamji MH, Layhadi JA, Achkova D, Kouser L, Perera-Webb A, Couto-Francisco NC, et al. Role of IL-35 in sublingual allergen immunotherapy. J Allergy Clin Immunol. 2019;143(3):1131-42 e4.

150. Swamy RS, Reshamwala N, Hunter T, Vissamsetti S, Santos CB, Baroody FM, et al. Epigenetic modifications and improved regulatory T-cell function in subjects undergoing dual sublingual immunotherapy. J Allergy Clin Immunol. 2012;130(1):215-24 e7.

151. Terada T, Matsuda M, Inaba M, Hamaguchi J, Takemoto N, Kikuoka Y, et al. Sublingual immunotherapy for 4 years increased the number of Foxp3(+) Treg cells, which correlated with clinical effects. Inflamm Res. 2021;70(5):581-9.

152. Layhadi JA, Moya R, Tan TJ, Lenormand MM, Sharif H, Parkin RV, et al. Single-cell RNA sequencing identifies precise tolerogenic cellular and molecular pathways induced by depigmented-polymerized grass pollen allergen extract. J Allergy Clin Immunol. 2023;151(5):1357-70 e9.

153. Romero-Wolf M, Shin B, Zhou W, Koizumi M, Rothenberg EV, Hosokawa H. Notch2 complements Notch1 to mediate inductive signaling that initiates early T cell development. J Cell Biol. 2020;219(10).

154. Jiao WE, Sun L, Xu S, Deng YQ, Qiao YL, Xi Y, et al. Notch2 suppresses the development of allergic rhinitis by promoting FOXP3 expression and Treg cell differentiation. Life Sci. 2021;284:119922.

155. Zhang Y, Yang Y, Guo J, Cui L, Yang L, Li Y, et al. miR-146a enhances regulatory T-cell differentiation and function in allergic rhinitis by targeting STAT5b. Allergy. 2022;77(2):550-8.

156. Shamji MH, Ljorring C, Francis JN, Calderon MA, Larche M, Kimber I, et al. Functional rather than immunoreactive levels of IgG4 correlate closely with clinical response to grass pollen immunotherapy. Allergy. 2012;67(2):217-26.

157. James LK, Shamji MH, Walker SM, Wilson DR, Wachholz PA, Francis JN, et al. Long-term tolerance after allergen immunotherapy is accompanied by selective persistence of blocking antibodies. J Allergy Clin Immunol. 2011;127(2):509-16 e1-5.

158. van de Veen W, Stanic B, Wirz OF, Jansen K, Globinska A, Akdis M. Role of regulatory B cells in immune tolerance to allergens and beyond. J Allergy Clin Immunol. 2016;138(3):654-65.

159. Layhadi JA, Lalioti A, Palmer E, van Zelm MC, Wambre E, Shamji MH. Mechanisms and Predictive Biomarkers of Allergen Immunotherapy in the Clinic. J Allergy Clin Immunol Pract. 2024;12(1):59-66.

160. Caminati M, Dama AR, Djuric I, Montagni M, Schiappoli M, Ridolo E, et al. Incidence and risk factors for subcutaneous immunotherapy anaphylaxis: the optimization of safety. Expert Rev Clin Immunol. 2015;11(2):233-45.

161. Zylke JW. Epicutaneous Immunotherapy vs Placebo for Peanut Protein Ingestion Among Peanut-Allergic Children. JAMA. 2019;321(10):956.

162. Skaarup SH, Schmid JM, Skjold T, Graumann O, Hoffmann HJ. Intralymphatic immunotherapy improves grass pollen allergic rhinoconjunctivitis: A 3-year randomized placebo-controlled trial. J Allergy Clin Immunol. 2021;147(3):1011-9.

163. Marsh DG, Lichtenstein LM, Campbell DH. Studies on "allergoids" prepared from naturally occurring allergens. I. Assay of allergenicity and antigenicity of formalinized rye group I component. Immunology. 1970;18(5):705-22.

164. Mosges R, Kasche EM, Raskopf E, Singh J, Sohlich L, Astvatsatourov A, et al. A randomized, double-blind, placebo-controlled, dose-finding trial with Lolium perenne peptide immunotherapy. Allergy. 2018;73(4):896-904.

165. Kettner A, DellaCorte G, de Blay F, Jacobsen L, Jutel M, Worm M, et al. Benefit of Bet v 1 contiguous overlapping peptide immunotherapy persists during first follow-up season. J Allergy Clin Immunol. 2018;142(2):678-80 e7.

166. Worm M, Rak S, Samolinski B, Antila J, Hoiby AS, Kruse B, et al. Efficacy and safety of birch pollen allergoid subcutaneous immunotherapy: A 2-year double-blind, placebo-controlled, randomized trial plus 1-year open-label extension. Clin Exp Allergy. 2019;49(4):516-25.

167. De Souza Reboucas J, Esparza I, Ferrer M, Sanz ML, Irache JM, Gamazo C. Nanoparticulate adjuvants and delivery systems for allergen immunotherapy. J Biomed Biotechnol. 2012;2012:474605.

168. Singha S, Shao K, Ellestad KK, Yang Y, Santamaria P. Nanoparticles for Immune Stimulation Against Infection, Cancer, and Autoimmunity. ACS Nano. 2018;12(11):10621-35.

169. Klimek L, Kundig T, Kramer MF, Guethoff S, Jensen-Jarolim E, Schmidt-Weber CB, et al. Virus-like particles (VLP) in prophylaxis and immunotherapy of allergic diseases. Allergo J Int. 2018;27(8):245-55.

170. Anzaghe M, Schulke S, Scheurer S. Virus-Like Particles as Carrier Systems to Enhance Immunomodulation in Allergen Immunotherapy. Curr Allergy Asthma Rep. 2018;18(12):71.

171. Pazos-Castro D, Margain C, Gonzalez-Klein Z, Amores-Borge M, Yuste-Calvo C, Garrido-Arandia M, et al. Suitability of potyviral recombinant virus-like particles bearing a complete food allergen for immunotherapy vaccines. Front Immunol. 2022;13:986823.

172. Klimek L, Willers J, Hammann-Haenni A, Pfaar O, Stocker H, Mueller P, et al. Assessment of clinical efficacy of CYT003-QbG10 in patients with allergic rhinoconjunctivitis: a phase IIb study. Clin Exp Allergy. 2011;41(9):1305-12.

173. Beeh KM, Kanniess F, Wagner F, Schilder C, Naudts I, Hammann-Haenni A, et al. The novel TLR-9 agonist QbG10 shows clinical efficacy in persistent allergic asthma. J Allergy Clin Immunol. 2013;131(3):866-74.

174. Gomord V, Stordeur V, Fitchette AC, Fixman ED, Tropper G, Garnier L, et al. Design, production and immunomodulatory potency of a novel allergen bioparticle. PLoS One. 2020;15(12):e0242867.

175. Wang Y, Liu J, Burrows PD, Wang JY. B Cell Development and Maturation. Adv Exp Med Biol. 2020;1254:1-22.

176. Pieper K, Grimbacher B, Eibel H. B-cell biology and development. J Allergy Clin Immunol. 2013;131(4):959-71.

177. Nemazee D. Mechanisms of central tolerance for B cells. Nat Rev Immunol. 2017;17(5):281-94.

178. Marie-Cardine A, Divay F, Dutot I, Green A, Perdrix A, Boyer O, et al. Transitional B cells in humans: characterization and insight from B lymphocyte reconstitution after hematopoietic stem cell transplantation. Clin Immunol. 2008;127(1):14-25.

179. Cerutti A, Cols M, Puga I. Marginal zone B cells: virtues of innate-like antibody-producing lymphocytes. Nat Rev Immunol. 2013;13(2):118-32.

180. Young C, Brink R. The unique biology of germinal center B cells. Immunity. 2021;54(8):1652-64.

181. Gitlin AD, Mayer CT, Oliveira TY, Shulman Z, Jones MJ, Koren A, et al. HUMORAL IMMUNITY. T cell help controls the speed of the cell cycle in germinal center B cells. Science. 2015;349(6248):643-6.

182. Casamayor-Palleja M, Feuillard J, Ball J, Drew M, MacLennan IC. Centrocytes rapidly adopt a memory B cell phenotype on co-culture with autologous germinal centre T cell-enriched preparations. Int Immunol. 1996;8(5):737-44.

183. Doria-Rose NA, Joyce MG. Strategies to guide the antibody affinity maturation process. Curr Opin Virol. 2015;11:137-47.

184. Shulman Z, Gitlin AD, Weinstein JS, Lainez B, Esplugues E, Flavell RA, et al. Dynamic signaling by T follicular helper cells during germinal center B cell selection. Science. 2014;345(6200):1058-62.

185. Gowthaman U, Chen JS, Zhang B, Flynn WF, Lu Y, Song W, et al. Identification of a T follicular helper cell subset that drives anaphylactic IgE. Science. 2019;365(6456).

186. Lindsly S, Gupta M, Stansbury C, Rajapakse I. Understanding memory B cell selection. J Theor Biol. 2021;531:110905.

187. Ise W, Fujii K, Shiroguchi K, Ito A, Kometani K, Takeda K, et al. T Follicular Helper Cell-Germinal Center B Cell Interaction Strength Regulates Entry into Plasma Cell or Recycling Germinal Center Cell Fate. Immunity. 2018;48(4):702-15 e4.

188. Sensi LG, Piacentini GL, Nobile E, Ghebregzabher M, Brunori R, Zanolla L, et al. Changes in nasal specific IgE to mites after periods of allergen exposure-avoidance: a comparison with serum levels. Clin Exp Allergy. 1994;24(4):377-82.

189. KleinJan A, Vinke JG, Severijnen LW, Fokkens WJ. Local production and detection of (specific) IgE in nasal B-cells and plasma cells of allergic rhinitis patients. Eur Respir J. 2000;15(3):491-7.

190. Smurthwaite L, Durham SR. Local IgE synthesis in allergic rhinitis and asthma. Curr Allergy Asthma Rep. 2002;2(3):231-8.

191. Powe DG, Jagger C, Kleinjan A, Carney AS, Jenkins D, Jones NS. 'Entopy': localized mucosal allergic disease in the absence of systemic responses for atopy. Clin Exp Allergy. 2003;33(10):1374-9.

192. Takhar P, Smurthwaite L, Coker HA, Fear DJ, Banfield GK, Carr VA, et al. Allergen drives class switching to IgE in the nasal mucosa in allergic rhinitis. J Immunol. 2005;174(8):5024-32.

193. Cameron LA, Durham SR, Jacobson MR, Masuyama K, Juliusson S, Gould HJ, et al. Expression of IL-4, Cepsilon RNA, and Iepsilon RNA in the nasal mucosa of patients with seasonal rhinitis: effect of topical corticosteroids. J Allergy Clin Immunol. 1998;101(3):330-6.

194. Ying S, Humbert M, Meng Q, Pfister R, Menz G, Gould HJ, et al. Local expression of epsilon germline gene transcripts and RNA for the epsilon heavy chain of IgE in

the bronchial mucosa in atopic and nonatopic asthma. J Allergy Clin Immunol. 2001;107(4):686-92.

195. Corrado A, Ramonell RP, Woodruff MC, Tipton C, Wise S, Levy J, et al. Extrafollicular IgD+ B cells generate IgE antibody secreting cells in the nasal mucosa. Mucosal Immunol. 2021;14(5):1144-59.

196. Testera-Montes A, Palomares F, Jurado-Escobar R, Fernandez-Santamaria R, Ariza A, Verge J, et al. Sequential class switch recombination to IgE and allergen-induced accumulation of IgE(+) plasmablasts occur in the nasal mucosa of local allergic rhinitis patients. Allergy. 2022;77(9):2712-24.

197. Hoof I, Schulten V, Layhadi JA, Stranzl T, Christensen LH, Herrera de la Mata S, et al. Allergen-specific IgG(+) memory B cells are temporally linked to IgE memory responses. J Allergy Clin Immunol. 2020;146(1):180-91.

198. Boonpiyathad T, van de Veen W, Wirz O, Sokolowska M, Ruckert B, Tan G, et al. Role of Der p 1-specific B cells in immune tolerance during 2 years of house dust mite-specific immunotherapy. J Allergy Clin Immunol. 2019;143(3):1077-86 e10.

199. Zissler UM, Jakwerth CA, Guerth FM, Pechtold L, Aguilar-Pimentel JA, Dietz K, et al. Early IL-10 producing B-cells and coinciding Th/Tr17 shifts during three year grass-pollen AIT. EBioMedicine. 2018;36:475-88.

200. Boonpiyathad T, Meyer N, Moniuszko M, Sokolowska M, Eljaszewicz A, Wirz OF, et al. High-dose bee venom exposure induces similar tolerogenic B-cell responses in allergic patients and healthy beekeepers. Allergy. 2017;72(3):407-15.

201. Zhang YZ, Luo J, Wang ZH, Wang J. Efficacy and safety of sublingual dust mite drops in children with mono- or polysensitized allergic rhinitis. Am J Otolaryngol. 2019;40(5):755-60.

202. Shamji MH, Kappen J, Abubakar-Waziri H, Zhang J, Steveling E, Watchman S, et al. Nasal allergen-neutralizing IgG(4) antibodies block IgE-mediated responses: Novel biomarker of subcutaneous grass pollen immunotherapy. J Allergy Clin Immunol. 2019;143(3):1067-76.

203. Cooke RA, Barnard JH, Hebald S, Stull A. Serological Evidence of Immunity with Coexisting Sensitization in a Type of Human Allergy (Hay Fever). J Exp Med. 1935;62(6):733-50.

204. Nouri-Aria KT, Wachholz PA, Francis JN, Jacobson MR, Walker SM, Wilcock LK, et al. Grass pollen immunotherapy induces mucosal and peripheral IL-10 responses and blocking IgG activity. J Immunol. 2004;172(5):3252-9.

205. Heldner A, Alessandrini F, Russkamp D, Heine S, Schnautz B, Chaker A, et al. Immunological effects of adjuvanted low-dose allergoid allergen-specific immunotherapy in experimental murine house dust mite allergy. Allergy. 2022;77(3):907-19.

206. Heeringa JJ, McKenzie CI, Varese N, Hew M, Bakx A, Aui PM, et al. Induction of IgG(2) and IgG(4) B-cell memory following sublingual immunotherapy for ryegrass pollen allergy. Allergy. 2020;75(5):1121-32.

207. Bordas-Le Floch V, Berjont N, Batard T, Varese N, O'Hehir RE, Canonica WG, et al. Coordinated IgG2 and IgE responses as a marker of allergen immunotherapy efficacy. Allergy. 2022;77(4):1263-73.

208. Berjont N, Floch VVB, O'Hehir RE, Canonica WG, van Zelm MC, Batard T, et al. Early increase in serum specific IgG2 upon allergen immunotherapy with a 300 IR sublingual house dust mite tablet. Allergy. 2023;78(7):2040-3.

209. van der Neut Kolfschoten M, Schuurman J, Losen M, Bleeker WK, Martinez-Martinez P, Vermeulen E, et al. Anti-inflammatory activity of human IgG4 antibodies by dynamic Fab arm exchange. Science. 2007;317(5844):1554-7.

210. Shamji MH, Francis JN, Wurtzen PA, Lund K, Durham SR, Till SJ. Cell-free detection of allergen-IgE cross-linking with immobilized phase CD23: inhibition by blocking antibody responses after immunotherapy. J Allergy Clin Immunol. 2013;132(4):1003-5 e1-4.

211. van de Veen W, Akdis M. Role of IgG(4) in IgE-mediated allergic responses. J Allergy Clin Immunol. 2016;138(5):1434-5.

212. McKenzie CI, Varese N, Aui PM, Reinwald S, Wines BD, Hogarth PM, et al. RNA sequencing of single allergen-specific memory B cells after grass pollen immunotherapy:

Two unique cell fates and CD29 as a biomarker for treatment effect. Allergy. 2023;78(3):822-35.

213. Nikolov G, Todordova Y, Emilova R, Hristova D, Nikolova M, Petrunov B. Allergen-Specific IgE and IgG4 as Biomarkers for Immunologic Changes during Subcutaneous Allergen Immunotherapy. Antibodies (Basel). 2021;10(4).

214. Chen J, Zhou Y, Wang Y, Zheng Y, Lai X, Westermann-Clark E, et al. Specific immunoglobulin E and immunoglobulin G4 toward major allergens of house-dust mite during allergen-specific immunotherapy. Am J Rhinol Allergy. 2017;31(3):156-60.

215. He Y, Liu J, Zhao D, Zhang S, Hao G, Sun Y, et al. The IgE Blocking Activity Induced by Dermatophagoides pteronyssinus Subcutaneous Immunotherapy Does Not Correlate with Specific IgA but with IgG4 in both Serum and Saliva. Int Arch Allergy Immunol. 2021;182(12):1231-44.

216. Pilette C, Nouri-Aria KT, Jacobson MR, Wilcock LK, Detry B, Walker SM, et al. Grass pollen immunotherapy induces an allergen-specific IgA2 antibody response associated with mucosal TGF-beta expression. J Immunol. 2007;178(7):4658-66.

217. Neta R, Salvin SB. Specific suppression of delayed hypersensitivity: the possible presence of a suppressor B cell in the regulation of delayed hypersensitivity. J Immunol. 1974;113(6):1716-25.

218. Katz SI, Parker D, Turk JL. B-cell suppression of delayed hypersensitivity reactions. Nature. 1974;251(5475):550-1.

219. Wolf SD, Dittel BN, Hardardottir F, Janeway CA, Jr. Experimental autoimmune encephalomyelitis induction in genetically B cell-deficient mice. J Exp Med. 1996;184(6):2271-8.

220. O'Garra A, Stapleton G, Dhar V, Pearce M, Schumacher J, Rugo H, et al. Production of cytokines by mouse B cells: B lymphomas and normal B cells produce interleukin 10. Int Immunol. 1990;2(9):821-32.

221. Mizoguchi A, Mizoguchi E, Takedatsu H, Blumberg RS, Bhan AK. Chronic intestinal inflammatory condition generates IL-10-producing regulatory B cell subset characterized by CD1d upregulation. Immunity. 2002;16(2):219-30.

222. Fillatreau S, Sweenie CH, McGeachy MJ, Gray D, Anderton SM. B cells regulate autoimmunity by provision of IL-10. Nat Immunol. 2002;3(10):944-50.

223. Goetz M, Atreya R, Ghalibafian M, Galle PR, Neurath MF. Exacerbation of ulcerative colitis after rituximab salvage therapy. Inflamm Bowel Dis. 2007;13(11):1365-8.

224. Dass S, Vital EM, Emery P. Development of psoriasis after B cell depletion with rituximab. Arthritis Rheum. 2007;56(8):2715-8.

225. Blair PA, Norena LY, Flores-Borja F, Rawlings DJ, Isenberg DA, Ehrenstein MR, et al. CD19(+)CD24(hi)CD38(hi) B cells exhibit regulatory capacity in healthy individuals but are functionally impaired in systemic Lupus Erythematosus patients. Immunity. 2010;32(1):129-40.

226. Iwata Y, Matsushita T, Horikawa M, Dilillo DJ, Yanaba K, Venturi GM, et al. Characterization of a rare IL-10-competent B-cell subset in humans that parallels mouse regulatory B10 cells. Blood. 2011;117(2):530-41.

227. Mizoguchi A, Mizoguchi E, Smith RN, Preffer FI, Bhan AK. Suppressive role of B cells in chronic colitis of T cell receptor alpha mutant mice. J Exp Med. 1997;186(10):1749-56.

228. Evans JG, Chavez-Rueda KA, Eddaoudi A, Meyer-Bahlburg A, Rawlings DJ, Ehrenstein MR, et al. Novel suppressive function of transitional 2 B cells in experimental arthritis. J Immunol. 2007;178(12):7868-78.

229. Wang RX, Yu CR, Dambuza IM, Mahdi RM, Dolinska MB, Sergeev YV, et al. Interleukin-35 induces regulatory B cells that suppress autoimmune disease. Nat Med. 2014;20(6):633-41.

230. Shen P, Roch T, Lampropoulou V, O'Connor RA, Stervbo U, Hilgenberg E, et al. IL-35-producing B cells are critical regulators of immunity during autoimmune and infectious diseases. Nature. 2014;507(7492):366-70.

231. Yoshizaki A, Miyagaki T, DiLillo DJ, Matsushita T, Horikawa M, Kountikov EI, et al. Regulatory B cells control T-cell autoimmunity through IL-21-dependent cognate interactions. Nature. 2012;491(7423):264-8.

232. Matsumoto M, Baba A, Yokota T, Nishikawa H, Ohkawa Y, Kayama H, et al. Interleukin-10-producing plasmablasts exert regulatory function in autoimmune inflammation. Immunity. 2014;41(6):1040-51.

233. Yanaba K, Bouaziz JD, Haas KM, Poe JC, Fujimoto M, Tedder TF. A regulatory B cell subset with a unique CD1dhiCD5+ phenotype controls T cell-dependent inflammatory responses. Immunity. 2008;28(5):639-50.

234. Hua C, Audo R, Yeremenko N, Baeten D, Hahne M, Combe B, et al. A proliferation inducing ligand (APRIL) promotes IL-10 production and regulatory functions of human B cells. J Autoimmun. 2016;73:64-72.

235. Rosser EC, Oleinika K, Tonon S, Doyle R, Bosma A, Carter NA, et al. Regulatory B cells are induced by gut microbiota-driven interleukin-1beta and interleukin-6 production. Nat Med. 2014;20(11):1334-9.

236. Yang M, Sun L, Wang S, Ko KH, Xu H, Zheng BJ, et al. Novel function of B cell-activating factor in the induction of IL-10-producing regulatory B cells. J Immunol. 2010;184(7):3321-5.

237. Zhu J, Xu Y, Zhu C, Zhao J, Meng X, Chen S, et al. IL-33 induces both regulatory B cells and regulatory T cells in dextran sulfate sodium-induced colitis. Int Immunopharmacol. 2017;46:38-47.

238. Sheng JR, Quan S, Soliven B. CD1d(hi)CD5+ B cells expanded by GM-CSF in vivo suppress experimental autoimmune myasthenia gravis. J Immunol. 2014;193(6):2669-77.

239. Peng SL. Signaling in B cells via Toll-like receptors. Curr Opin Immunol. 2005;17(3):230-6.

240. Wagner H. Interactions between bacterial CpG-DNA and TLR9 bridge innate and adaptive immunity. Curr Opin Microbiol. 2002;5(1):62-9.

241. Cain JA, Montibus B, Oakey RJ. Intragenic CpG Islands and Their Impact on Gene Regulation. Front Cell Dev Biol. 2022;10:832348.

242. Shirota H, Klinman DM. Recent progress concerning CpG DNA and its use as a vaccine adjuvant. Expert Rev Vaccines. 2014;13(2):299-312.

243. Campbell JD. Development of the CpG Adjuvant 1018: A Case Study. Methods Mol Biol. 2017;1494:15-27.

244. Chen W, Jiang M, Yu W, Xu Z, Liu X, Jia Q, et al. CpG-Based Nanovaccines for Cancer Immunotherapy. Int J Nanomedicine. 2021;16:5281-99.

245. Zhang A, Mo L, Chen X, Tang P, Liu Y, Zhang W, et al. Direct exposure to CpG and specific antigens mitigate airway allergy through modulating dendritic cell properties. Biomed Pharmacother. 2024;174:116510.

246. Shankar S, Stolp J, Juvet SC, Beckett J, Macklin PS, Issa F, et al. Ex vivo-expanded human CD19(+)TIM-1(+) regulatory B cells suppress immune responses in vivo and are dependent upon the TIM-1/STAT3 axis. Nat Commun. 2022;13(1):3121.

247. Lin W, Cerny D, Chua E, Duan K, Yi JT, Shadan NB, et al. Human regulatory B cells combine phenotypic and genetic hallmarks with a distinct differentiation fate. J Immunol. 2014;193(5):2258-66.

248. Dubois F, Limou S, Chesneau M, Degauque N, Brouard S, Danger R. Transcriptional meta-analysis of regulatory B cells. Eur J Immunol. 2020;50(11):1757-69.

249. Flores-Borja F, Bosma A, Ng D, Reddy V, Ehrenstein MR, Isenberg DA, et al. CD19+CD24hiCD38hi B cells maintain regulatory T cells while limiting TH1 and TH17 differentiation. Sci Transl Med. 2013;5(173):173ra23.

250. Lundy SK, Fox DA. Reduced Fas ligand-expressing splenic CD5+ B lymphocytes in severe collagen-induced arthritis. Arthritis Res Ther. 2009;11(4):R128.

251. Bosma A, Abdel-Gadir A, Isenberg DA, Jury EC, Mauri C. Lipid-antigen presentation by CD1d(+) B cells is essential for the maintenance of invariant natural killer T cells. Immunity. 2012;36(3):477-90.

252. Karim MR, Wang YF. Phenotypic identification of CD19(+)CD5(+)CD1d(+) regulatory B cells that produce interleukin 10 and transforming growth factor beta(1) in human peripheral blood. Arch Med Sci. 2019;15(5):1176-83.

253. van de Veen W, Stanic B, Yaman G, Wawrzyniak M, Sollner S, Akdis DG, et al. IgG4 production is confined to human IL-10-producing regulatory B cells that suppress antigen-specific immune responses. J Allergy Clin Immunol. 2013;131(4):1204-12.

254. Doi T, Kanai T, Mikami Y, Sujino T, Jun L, Ono Y, et al. IgA plasma cells express the negative regulatory co-stimulatory molecule programmed cell death 1 ligand and have a potential tolerogenic role in the intestine. Biochem Biophys Res Commun. 2012;425(4):918-23.

255. Lino AC, Dang VD, Lampropoulou V, Welle A, Joedicke J, Pohar J, et al. LAG-3 Inhibitory Receptor Expression Identifies Immunosuppressive Natural Regulatory Plasma Cells. Immunity. 2018;49(1):120-33 e9.

256. Rojas OL, Probstel AK, Porfilio EA, Wang AA, Charabati M, Sun T, et al. Recirculating Intestinal IgA-Producing Cells Regulate Neuroinflammation via IL-10. Cell. 2019;176(3):610-24 e18.

257. Chesneau M, Mai HL, Danger R, Le Bot S, Nguyen TV, Bernard J, et al. Efficient Expansion of Human Granzyme B-Expressing B Cells with Potent Regulatory Properties. J Immunol. 2020;205(9):2391-401.

258. Wang L, Fu Y, Yu B, Jiang X, Liu H, Liu J, et al. HSP70, a Novel Regulatory Molecule in B Cell-Mediated Suppression of Autoimmune Diseases. J Mol Biol. 2021;433(1):166634.

259. Saraiva M, Vieira P, O'Garra A. Biology and therapeutic potential of interleukin-10. J Exp Med. 2020;217(1).

260. Shouval DS, Ouahed J, Biswas A, Goettel JA, Horwitz BH, Klein C, et al. Interleukin 10 receptor signaling: master regulator of intestinal mucosal homeostasis in mice and humans. Adv Immunol. 2014;122:177-210.

261. Carter NA, Vasconcellos R, Rosser EC, Tulone C, Munoz-Suano A, Kamanaka M, et al. Mice lacking endogenous IL-10-producing regulatory B cells develop exacerbated disease and present with an increased frequency of Th1/Th17 but a decrease in regulatory T cells. J Immunol. 2011;186(10):5569-79.

262. Murai M, Turovskaya O, Kim G, Madan R, Karp CL, Cheroutre H, et al. Interleukin 10 acts on regulatory T cells to maintain expression of the transcription factor Foxp3 and suppressive function in mice with colitis. Nat Immunol. 2009;10(11):1178-84.

263. Banko Z, Pozsgay J, Szili D, Toth M, Gati T, Nagy G, et al. Induction and Differentiation of IL-10-Producing Regulatory B Cells from Healthy Blood Donors and Rheumatoid Arthritis Patients. J Immunol. 2017;198(4):1512-20.

264. Lopez-Abente J, Prieto-Sanchez A, Munoz-Fernandez MA, Correa-Rocha R, Pion M. Human immunodeficiency virus type-1 induces a regulatory B cell-like phenotype in vitro. Cell Mol Immunol. 2018;15(10):917-33.

265. Hsu P, Santner-Nanan B, Hu M, Skarratt K, Lee CH, Stormon M, et al. IL-10 Potentiates Differentiation of Human Induced Regulatory T Cells via STAT3 and Foxo1. J Immunol. 2015;195(8):3665-74.

266. Pereira JA, Lanzar Z, Clark JT, Hart AP, Douglas BB, Shallberg L, et al. PD-1 and CTLA-4 exert additive control of effector regulatory T cells at homeostasis. Front Immunol. 2023;14:997376.

267. Luz-Crawford P, Kurte M, Bravo-Alegria J, Contreras R, Nova-Lamperti E, Tejedor G, et al. Mesenchymal stem cells generate a CD4+CD25+Foxp3+ regulatory T cell population during the differentiation process of Th1 and Th17 cells. Stem Cell Res Ther. 2013;4(3):65.

268. Rousset F, Garcia E, Defrance T, Peronne C, Vezzio N, Hsu DH, et al. Interleukin 10 is a potent growth and differentiation factor for activated human B lymphocytes. Proc Natl Acad Sci U S A. 1992;89(5):1890-3.

269. Itoh K, Hirohata S. The role of IL-10 in human B cell activation, proliferation, and differentiation. J Immunol. 1995;154(9):4341-50.

270. Heine G, Drozdenko G, Grun JR, Chang HD, Radbruch A, Worm M. Autocrine IL-10 promotes human B-cell differentiation into IgM- or IgG-secreting plasmablasts. Eur J Immunol. 2014;44(6):1615-21.

271. Sattler S, Ling GS, Xu D, Hussaarts L, Romaine A, Zhao H, et al. IL-10-producing regulatory B cells induced by IL-33 (Breg(IL-33)) effectively attenuate mucosal inflammatory responses in the gut. J Autoimmun. 2014;50(100):107-22.

272. Bogdan C, Vodovotz Y, Nathan C. Macrophage deactivation by interleukin 10. J Exp Med. 1991;174(6):1549-55.

273. Macatonia SE, Doherty TM, Knight SC, O'Garra A. Differential effect of IL-10 on dendritic cell-induced T cell proliferation and IFN-gamma production. J Immunol. 1993;150(9):3755-65.

274. Ghosh R, Dey R, Sawoo R, Haque W, Bishayi B. Endogenous neutralization of TGF-beta and IL-6 ameliorates septic arthritis by altering RANKL/OPG interaction in lymphocytes. Mol Immunol. 2022;152:183-206.

275. Boldison J, Da Rosa LC, Davies J, Wen L, Wong FS. Dendritic cells license regulatory B cells to produce IL-10 and mediate suppression of antigen-specific CD8 T cells. Cell Mol Immunol. 2020;17(8):843-55.

276. Stanic B, van de Veen W, Wirz OF, Ruckert B, Morita H, Sollner S, et al. IL-10-overexpressing B cells regulate innate and adaptive immune responses. J Allergy Clin Immunol. 2015;135(3):771-80 e8.

277. Kehrl JH, Roberts AB, Wakefield LM, Jakowlew S, Sporn MB, Fauci AS. Transforming growth factor beta is an important immunomodulatory protein for human B lymphocytes. J Immunol. 1986;137(12):3855-60.

278. Bjarnadottir K, Benkhoucha M, Merkler D, Weber MS, Payne NL, Bernard CCA, et al. B cell-derived transforming growth factor-beta1 expression limits the induction phase of autoimmune neuroinflammation. Sci Rep. 2016;6:34594.

279. Ray A, Wang L, Dittel BN. IL-10-independent regulatory B-cell subsets and mechanisms of action. Int Immunol. 2015;27(10):531-6.

280. Nouel A, Pochard P, Simon Q, Segalen I, Le Meur Y, Pers JO, et al. B-Cells induce regulatory T cells through TGF-beta/IDO production in A CTLA-4 dependent manner. J Autoimmun. 2015;59:53-60.

281. Konkel JE, Zhang D, Zanvit P, Chia C, Zangarle-Murray T, Jin W, et al. Transforming Growth Factor-beta Signaling in Regulatory T Cells Controls T Helper-17 Cells and Tissue-Specific Immune Responses. Immunity. 2017;46(4):660-74.

282. Shah S, Qiao L. Resting B cells expand a CD4+CD25+Foxp3+ Treg population via TGF-beta3. Eur J Immunol. 2008;38(9):2488-98.

283. Larmonier N, Marron M, Zeng Y, Cantrell J, Romanoski A, Sepassi M, et al. Tumor-derived CD4(+)CD25(+) regulatory T cell suppression of dendritic cell function involves TGF-beta and IL-10. Cancer Immunol Immunother. 2007;56(1):48-59.

284. Parekh VV, Prasad DV, Banerjee PP, Joshi BN, Kumar A, Mishra GC. B cells activated by lipopolysaccharide, but not by anti-Ig and anti-CD40 antibody, induce anergy in CD8+ T cells: role of TGF-beta 1. J Immunol. 2003;170(12):5897-911.

285. Song J, Chen X, Wang M, Xing Y, Zheng Z, Hu S. Cardiac endothelial cell-derived exosomes induce specific regulatory B cells. Sci Rep. 2014;4:7583.

286. Joly MS, Martin RP, Mitra-Kaushik S, Phillips L, D'Angona A, Richards SM, et al. Transient low-dose methotrexate generates B regulatory cells that mediate antigen-specific tolerance to alglucosidase alfa. J Immunol. 2014;193(8):3947-58.

287. Yang SY, Long J, Huang MX, Luo PY, Bian ZH, Xu YF, et al. Characterization of Organ-Specific Regulatory B Cells Using Single-Cell RNA Sequencing. Front Immunol. 2021;12:711980.

288. Ye C, Yano H, Workman CJ, Vignali DAA. Interleukin-35: Structure, Function and Its Impact on Immune-Related Diseases. J Interferon Cytokine Res. 2021;41(11):391-406.

289. Haller S, Duval A, Migliorini R, Stevanin M, Mack V, Acha-Orbea H. Interleukin-35-Producing CD8alpha(+) Dendritic Cells Acquire a Tolerogenic State and Regulate T Cell Function. Front Immunol. 2017;8:98.

290. Shao Y, Yang WY, Saaoud F, Drummer Ct, Sun Y, Xu K, et al. IL-35 promotes CD4+Foxp3+ Tregs and inhibits atherosclerosis via maintaining CCR5-amplified Treg-suppressive mechanisms. JCI Insight. 2021;6(19).

291. Lee CC, Lin JC, Hwang WL, Kuo YJ, Chen HK, Tai SK, et al. Macrophage-secreted interleukin-35 regulates cancer cell plasticity to facilitate metastatic colonization. Nat Commun. 2018;9(1):3763.

292. Ye Z, Jiang Y, Sun D, Zhong W, Zhao L, Jiang Z. The Plasma Interleukin (IL)-35 Level and Frequency of Circulating IL-35(+) Regulatory B Cells are Decreased in a Cohort of Chinese Patients with New-onset Systemic Lupus Erythematosus. Sci Rep. 2019;9(1):13210.

293. Wang K, Liu J, Li J. IL-35-producing B cells in gastric cancer patients. Medicine (Baltimore). 2018;97(19):e0710.

294. Chen C, Xu H, Peng Y, Luo H, Huang GX, Wu XJ, et al. Elevation in the counts of IL-35-producing B cells infiltrating into lung tissue in mycobacterial infection is associated with the downregulation of Th1/Th17 and upregulation of Foxp3(+)Treg. Sci Rep. 2020;10(1):13212.

295. Yu CR, Choi JK, Uche AN, Egwuagu CE. Production of IL-35 by Bregs is mediated through binding of BATF-IRF-4-IRF-8 complex to il12a and ebi3 promoter elements. J Leukoc Biol. 2018;104(6):1147-57.

296. Kang M, Choi JK, Jittayasothorn Y, Egwuagu CE. Interleukin 35-Producing Exosomes Suppress Neuroinflammation and Autoimmune Uveitis. Front Immunol. 2020;11:1051.

297. Meyers JH, Sabatos CA, Chakravarti S, Kuchroo VK. The TIM gene family regulates autoimmune and allergic diseases. Trends Mol Med. 2005;11(8):362-9.

298. Freeman GJ, Casasnovas JM, Umetsu DT, DeKruyff RH. TIM genes: a family of cell surface phosphatidylserine receptors that regulate innate and adaptive immunity. Immunol Rev. 2010;235(1):172-89.

299. Umetsu SE, Lee WL, McIntire JJ, Downey L, Sanjanwala B, Akbari O, et al. TIM-1 induces T cell activation and inhibits the development of peripheral tolerance. Nat Immunol. 2005;6(5):447-54.

300. Yeung MY, Ding Q, Brooks CR, Xiao S, Workman CJ, Vignali DA, et al. TIM-1 signaling is required for maintenance and induction of regulatory B cells. Am J Transplant. 2015;15(4):942-53.

301. Xiao S, Brooks CR, Zhu C, Wu C, Sweere JM, Petecka S, et al. Defect in regulatory B-cell function and development of systemic autoimmunity in T-cell Ig mucin 1 (Tim-1) mucin domain-mutant mice. Proc Natl Acad Sci U S A. 2012;109(30):12105-10.

302. Ding Q, Yeung M, Camirand G, Zeng Q, Akiba H, Yagita H, et al. Regulatory B cells are identified by expression of TIM-1 and can be induced through TIM-1 ligation to promote tolerance in mice. J Clin Invest. 2011;121(9):3645-56.

303. Ma L, Liu B, Jiang Z, Jiang Y. Reduced numbers of regulatory B cells are negatively correlated with disease activity in patients with new-onset rheumatoid arthritis. Clin Rheumatol. 2014;33(2):187-95.

304. Aravena O, Ferrier A, Menon M, Mauri C, Aguillon JC, Soto L, et al. TIM-1 defines a human regulatory B cell population that is altered in frequency and function in systemic sclerosis patients. Arthritis Res Ther. 2017;19(1):8.

305. Gu XL, He H, Lin L, Luo GX, Wen YF, Xiang DC, et al. Tim-1(+) B cells suppress T cell interferon-gamma production and promote Foxp3 expression, but have impaired regulatory function in coronary artery disease. APMIS. 2017;125(10):872-9.

306. Gutierrez C, Lopez-Abente J, Perez-Fernandez V, Prieto-Sanchez A, Correa-Rocha R, Moreno-Guillen S, et al. Analysis of the dysregulation between regulatory B and T cells (Breg and Treg) in human immunodeficiency virus (HIV)-infected patients. PLoS One. 2019;14(3):e0213744.

307. Ye L, Zhang Q, Cheng Y, Chen X, Wang G, Shi M, et al. Tumor-derived exosomal HMGB1 fosters hepatocellular carcinoma immune evasion by promoting TIM-1(+) regulatory B cell expansion. J Immunother Cancer. 2018;6(1):145.

308. Xiao S, Bod L, Pochet N, Kota SB, Hu D, Madi A, et al. Checkpoint Receptor TIGIT Expressed on Tim-1(+) B Cells Regulates Tissue Inflammation. Cell Rep. 2020;32(2):107892.

309. Zacca ER, Onofrio LI, Acosta CDV, Ferrero PV, Alonso SM, Ramello MC, et al. PD-L1(+) Regulatory B Cells Are Significantly Decreased in Rheumatoid Arthritis Patients and Increase After Successful Treatment. Front Immunol. 2018;9:2241.

310. Kim Y, Kim G, Shin HJ, Hyun JW, Kim SH, Lee E, et al. Restoration of regulatory B cell deficiency following alemtuzumab therapy in patients with relapsing multiple sclerosis. J Neuroinflammation. 2018;15(1):300.

311. Siewe B, Wallace J, Rygielski S, Stapleton JT, Martin J, Deeks SG, et al. Regulatory B cells inhibit cytotoxic T lymphocyte (CTL) activity and elimination of infected CD4 T cells after in vitro reactivation of HIV latent reservoirs. PLoS One. 2014;9(4):e92934.

312. Xiao X, Lao XM, Chen MM, Liu RX, Wei Y, Ouyang FZ, et al. PD-1hi Identifies a Novel Regulatory B-cell Population in Human Hepatoma That Promotes Disease Progression. Cancer Discov. 2016;6(5):546-59.

313. Fehres CM, van Uden NO, Yeremenko NG, Fernandez L, Franco Salinas G, van Duivenvoorde LM, et al. APRIL Induces a Novel Subset of IgA(+) Regulatory B Cells That Suppress Inflammation via Expression of IL-10 and PD-L1. Front Immunol. 2019;10:1368.

314. Greenwald RJ, Freeman GJ, Sharpe AH. The B7 family revisited. Annu Rev Immunol. 2005;23:515-48.

315. Mohib K, Cherukuri A, Zhou Y, Ding Q, Watkins SC, Rothstein DM. Antigen-dependent interactions between regulatory B cells and T cells at the T:B border inhibit subsequent T cell interactions with DCs. Am J Transplant. 2020;20(1):52-63.

316. Zheng Y, Manzotti CN, Liu M, Burke F, Mead KI, Sansom DM. CD86 and CD80 differentially modulate the suppressive function of human regulatory T cells. J Immunol. 2004;172(5):2778-84.

317. Salomon B, Lenschow DJ, Rhee L, Ashourian N, Singh B, Sharpe A, et al. B7/CD28 costimulation is essential for the homeostasis of the CD4+CD25+ immunoregulatory T cells that control autoimmune diabetes. Immunity. 2000;12(4):431-40.

318. Lin W, Jin L, Chen H, Wu Q, Fei Y, Zheng W, et al. B cell subsets and dysfunction of regulatory B cells in IgG4-related diseases and primary Sjogren's syndrome: the similarities and differences. Arthritis Res Ther. 2014;16(3):R118.

319. Wang L, Ray A, Jiang X, Wang JY, Basu S, Liu X, et al. T regulatory cells and B cells cooperate to form a regulatory loop that maintains gut homeostasis and suppresses dextran sulfate sodium-induced colitis. Mucosal Immunol. 2015;8(6):1297-312.

320. Liu R, Lu Z, Gu J, Liu J, Huang E, Liu X, et al. MicroRNAs 15A and 16-1 Activate Signaling Pathways That Mediate Chemotaxis of Immune Regulatory B cells to Colorectal Tumors. Gastroenterology. 2018;154(3):637-51 e7.

321. Zha B, Wang L, Liu X, Liu J, Chen Z, Xu J, et al. Decrease in proportion of CD19+ CD24(hi) CD27+ B cells and impairment of their suppressive function in Graves' disease. PLoS One. 2012;7(11):e49835.

322. Knippenberg S, Peelen E, Smolders J, Thewissen M, Menheere P, Cohen Tervaert JW, et al. Reduction in IL-10 producing B cells (Breg) in multiple sclerosis is accompanied by a reduced naive/memory Breg ratio during a relapse but not in remission. J Neuroimmunol. 2011;239(1-2):80-6.

323. Guo Y, Zhang X, Qin M, Wang X. Changes in peripheral CD19(+)Foxp3(+) and CD19(+)TGFbeta(+) regulatory B cell populations in rheumatoid arthritis patients with interstitial lung disease. J Thorac Dis. 2015;7(3):471-7.

324. Zacca ER, Amezcua Vesely MC, Ferrero PV, Acosta CDV, Ponce NE, Bossio SN, et al. B cells from Patients with Rheumatoid Arthritis Show Conserved CD39-Mediated Regulatory Function and increased CD39 Expression After Positive Response to Therapy. J Mol Biol. 2021;433(1):166687.

325. Crescioli S, Correa I, Karagiannis P, Davies AM, Sutton BJ, Nestle FO, et al. IgG4 Characteristics and Functions in Cancer Immunity. Curr Allergy Asthma Rep. 2016;16(1):7.

326. Li D, Ma Y. B10 cells: Development, phenotype, and function in cancer. Adv Clin Exp Med. 2024.

327. Kim S, Fridlender ZG, Dunn R, Kehry MR, Kapoor V, Blouin A, et al. B-cell depletion using an anti-CD20 antibody augments antitumor immune responses and immunotherapy in nonhematopoetic murine tumor models. J Immunother. 2008;31(5):446-57.

328. Hu HT, Ai X, Lu M, Song Z, Li H. Characterization of intratumoral and circulating IL-10-producing B cells in gastric cancer. Exp Cell Res. 2019;384(2):111652.

329. Pylayeva-Gupta Y, Das S, Handler JS, Hajdu CH, Coffre M, Koralov SB, et al. IL35-Producing B Cells Promote the Development of Pancreatic Neoplasia. Cancer Discov. 2016;6(3):247-55.

330. Horikawa M, Weimer ET, DiLillo DJ, Venturi GM, Spolski R, Leonard WJ, et al. Regulatory B cell (B10 Cell) expansion during Listeria infection governs innate and cellular immune responses in mice. J Immunol. 2013;190(3):1158-68.

331. Kozakiewicz L, Chen Y, Xu J, Wang Y, Dunussi-Joannopoulos K, Ou Q, et al. B cells regulate neutrophilia during Mycobacterium tuberculosis infection and BCG vaccination by modulating the interleukin-17 response. PLoS Pathog. 2013;9(7):e1003472.

332. Zhang M, Zeng G, Yang Q, Zhang J, Zhu X, Chen Q, et al. Anti-tuberculosis treatment enhances the production of IL-22 through reducing the frequencies of regulatory B cell. Tuberculosis (Edinb). 2014;94(3):238-44.

333. Das A, Ellis G, Pallant C, Lopes AR, Khanna P, Peppa D, et al. IL-10-producing regulatory B cells in the pathogenesis of chronic hepatitis B virus infection. J Immunol. 2012;189(8):3925-35.

334. Khan AR, Amu S, Saunders SP, Fallon PG. The generation of regulatory B cells by helminth parasites. Methods Mol Biol. 2014;1190:143-62.

335. Shabir S, Girdlestone J, Briggs D, Kaul B, Smith H, Daga S, et al. Transitional B lymphocytes are associated with protection from kidney allograft rejection: a prospective study. Am J Transplant. 2015;15(5):1384-91.

336. Brosseau C, Danger R, Durand M, Durand E, Foureau A, Lacoste P, et al. Blood CD9(+) B cell, a biomarker of bronchiolitis obliterans syndrome after lung transplantation. Am J Transplant. 2019;19(11):3162-75.

337. Kimura S, Rickert CG, Kojima L, Aburawi M, Tanimine N, Fontan F, et al. Regulatory B cells require antigen recognition for effective allograft tolerance induction. Am J Transplant. 2020;20(4):977-87.

338. Newell KA, Asare A, Kirk AD, Gisler TD, Bourcier K, Suthanthiran M, et al. Identification of a B cell signature associated with renal transplant tolerance in humans. J Clin Invest. 2010;120(6):1836-47.

339. Lal G, Kulkarni N, Nakayama Y, Singh AK, Sethi A, Burrell BE, et al. IL-10 from marginal zone precursor B cells controls the differentiation of Th17, Tfh and Tfr cells in transplantation tolerance. Immunol Lett. 2016;170:52-63.

340. van der Vlugt LE, Labuda LA, Ozir-Fazalalikhan A, Lievers E, Gloudemans AK, Liu KY, et al. Schistosomes induce regulatory features in human and mouse CD1d(hi) B cells: inhibition of allergic inflammation by IL-10 and regulatory T cells. PLoS One. 2012;7(2):e30883.

341. Amu S, Saunders SP, Kronenberg M, Mangan NE, Atzberger A, Fallon PG. Regulatory B cells prevent and reverse allergic airway inflammation via FoxP3-positive T regulatory cells in a murine model. J Allergy Clin Immunol. 2010;125(5):1114-24 e8.

342. Khan AR, Amu S, Saunders SP, Hams E, Blackshields G, Leonard MO, et al. Ligation of TLR7 on CD19(+) CD1d(hi) B cells suppresses allergic lung inflammation via regulatory T cells. Eur J Immunol. 2015;45(6):1842-54.

343. Braza F, Chesne J, Durand M, Dirou S, Brosseau C, Mahay G, et al. A regulatory CD9(+) B-cell subset inhibits HDM-induced allergic airway inflammation. Allergy. 2015;70(11):1421-31.

344. Habener A, Happle C, Grychtol R, Skuljec J, Busse M, Daluge K, et al. Regulatory B cells control airway hyperreactivity and lung remodeling in a murine asthma model. J Allergy Clin Immunol. 2021;147(6):2281-94 e7.

345. Jiang J, Qin T, Zhang L, Liu Q, Wu J, Dai R, et al. IL-21 Rescues the Defect of IL-10-Producing Regulatory B Cells and Improves Allergic Asthma in DOCK8 Deficient Mice. Front Immunol. 2021;12:695596.

346. van der Vlugt LE, Mlejnek E, Ozir-Fazalalikhan A, Janssen Bonas M, Dijksman TR, Labuda LA, et al. CD24(hi)CD27(+) B cells from patients with allergic asthma have impaired regulatory activity in response to lipopolysaccharide. Clin Exp Allergy. 2014;44(4):517-28.

347. Wiest M, Upchurch K, Hasan MM, Cardenas J, Lanier B, Millard M, et al. Phenotypic and functional alterations of regulatory B cell subsets in adult allergic asthma patients. Clin Exp Allergy. 2019;49(9):1214-24.

348. Wirz OF, Globinska A, Ochsner U, van de Veen W, Eller E, Christiansen ES, et al. Comparison of regulatory B cells in asthma and allergic rhinitis. Allergy. 2019;74(4):815-8.

349. Kim AS, Doherty TA, Karta MR, Das S, Baum R, Rosenthal P, et al. Regulatory B cells and T follicular helper cells are reduced in allergic rhinitis. J Allergy Clin Immunol. 2016;138(4):1192-5 e5.

350. Lundy SK, Berlin AA, Martens TF, Lukacs NW. Deficiency of regulatory B cells increases allergic airway inflammation. Inflamm Res. 2005;54(12):514-21.

351. Kim HS, Kim AR, Kim DK, Kim HW, Park YH, Jang GH, et al. Interleukin-10-producing CD5+ B cells inhibit mast cells during immunoglobulin E-mediated allergic responses. Sci Signal. 2015;8(368):ra28.

352. Abushouk A, Alkhalaf H, Aldamegh M, Bin Shigair S, Mahabbat N, Hakami M, et al. IL-35 and IL-37 are negatively correlated with high IgE production among children with asthma in Saudi Arabia. J Asthma. 2022;59(4):655-62.

353. Zeng Q, Zeng Y, Tang Y, Liu W, Sun C. Effect of IL-35 on apoptosis, adhesion, migration, and activation of eosinophils in allergic rhinitis. Pediatr Allergy Immunol. 2022;33(2):e13717.

354. Yoshihara Y, Ishiuji Y, Yoshizaki A, Kurita M, Hayashi M, Ishiji T, et al. IL-10-Producing Regulatory B Cells Are Decreased in Patients with Atopic Dermatitis. J Invest Dermatol. 2019;139(2):475-8.

355. Jiang J, Yan S, Zhou X, Zhou J, Bai X, Tan Q, et al. Crosstalk Between Circulating Follicular T Helper Cells and Regulatory B Cells in Children With Extrinsic Atopic Dermatitis. Front Immunol. 2021;12:785549.

356. Lee JH, Noh J, Noh G, Choi WS, Cho S, Lee SS. Allergen-specific transforming growth factor-beta-producing CD19+CD5+ regulatory B-cell (Br3) responses in human late eczematous allergic reactions to cow's milk. J Interferon Cytokine Res. 2011;31(5):441-9.

357. Noh J, Lee JH, Noh G, Bang SY, Kim HS, Choi WS, et al. Characterisation of allergen-specific responses of IL-10-producing regulatory B cells (Br1) in Cow Milk Allergy. Cell Immunol. 2010;264(2):143-9.

358. Noh J, Noh G, Kim HS, Kim AR, Choi WS. Allergen-specific responses of CD19(+)CD5(+)Foxp3(+) regulatory B cells (Bregs) and CD4(+)Foxp3(+) regulatory T cell (Tregs) in immune tolerance of cow milk allergy of late eczematous reactions. Cell Immunol. 2012;274(1-2):109-14.

359. Liu ZQ, Wu Y, Song JP, Liu X, Liu Z, Zheng PY, et al. Tolerogenic CX3CR1+ B cells suppress food allergy-induced intestinal inflammation in mice. Allergy. 2013;68(10):1241-8.

360. Hong JY, Kim M, Sol IS, Kim KW, Lee CM, Elias JA, et al. Chitotriosidase inhibits allergic asthmatic airways via regulation of TGF-beta expression and Foxp3(+) Treg cells. Allergy. 2018;73(8):1686-99.

361. Voskamp AL, de Jong NW, Jochems SP, Ozir-Fazalalikhan A, van Hengel ORJ, van der Vlugt L, et al. Early expansion of allergen-responsive LAP(+) B regulatory cells in allergic rhinitis but not in allergic asthma subjects during allergen immunotherapy. Allergy. 2024.

362. Sharif H, Singh I, Kouser L, Mosges R, Bonny MA, Karamani A, et al. Immunologic mechanisms of a short-course of Lolium perenne peptide immunotherapy: A

randomized, double-blind, placebo-controlled trial. J Allergy Clin Immunol. 2019;144(3):738-49.

363. Dedobbeleer O, Stockis J, van der Woning B, Coulie PG, Lucas S. Cutting Edge: Active TGF-beta1 Released from GARP/TGF-beta1 Complexes on the Surface of Stimulated Human B Lymphocytes Increases Class-Switch Recombination and Production of IgA. J Immunol. 2017;199(2):391-6.

364. McIntire JJ, Umetsu DT, DeKruyff RH. TIM-1, a novel allergy and asthma susceptibility gene. Springer Semin Immunopathol. 2004;25(3-4):335-48.

365. Sonar SS, Hsu YM, Conrad ML, Majeau GR, Kilic A, Garber E, et al. Antagonism of TIM-1 blocks the development of disease in a humanized mouse model of allergic asthma. J Clin Invest. 2010;120(8):2767-81.

366. Shamji MH, Kappen JH, Akdis M, Jensen-Jarolim E, Knol EF, Kleine-Tebbe J, et al. Biomarkers for monitoring clinical efficacy of allergen immunotherapy for allergic rhinoconjunctivitis and allergic asthma: an EAACI Position Paper. Allergy. 2017;72(8):1156-73.

367. Di Lorenzo G, Mansueto P, Pacor ML, Rizzo M, Castello F, Martinelli N, et al. Evaluation of serum s-IgE/total IgE ratio in predicting clinical response to allergen-specific immunotherapy. J Allergy Clin Immunol. 2009;123(5):1103-10, 10 e1-4.

368. Suarez-Fueyo A, Ramos T, Galan A, Jimeno L, Wurtzen PA, Marin A, et al. Grass tablet sublingual immunotherapy downregulates the TH2 cytokine response followed by regulatory T-cell generation. J Allergy Clin Immunol. 2014;133(1):130-8 e1-2.

369. Xie S, Jiang S, Zhang H, Wang F, Liu Y, She Y, et al. Prediction of sublingual immunotherapy efficacy in allergic rhinitis by serum metabolomics analysis. Int Immunopharmacol. 2021;90:107211.

370. Shi HY, Pan C, Ma TT, Chen YL, Yan WJ, Liu JG, et al. Clinical Efficacy Evaluation of 1-Year Subcutaneous Immunotherapy for Artemisia sieversiana Pollen Allergic Rhinitis by Serum Metabolomics. Front Pharmacol. 2020;11:305.

371. Shamji MH, Wilcock LK, Wachholz PA, Dearman RJ, Kimber I, Wurtzen PA, et al. The IgE-facilitated allergen binding (FAB) assay: validation of a novel flow-cytometric based method for the detection of inhibitory antibody responses. J Immunol Methods. 2006;317(1-2):71-9.

372. Moreno V, Alvarino M, Rodriguez F, Roger A, Pena-Arellano MI, Lleonart R, et al. Randomized dose-response study of subcutaneous immunotherapy with a Dermatophagoides pteronyssinus extract in patients with respiratory allergy. Immunotherapy. 2016;8(3):265-77.

373. Hajdu K, Kapitany A, Dajnoki Z, Soltesz L, Barath S, Hendrik Z, et al. Improvement of clinical and immunological parameters after allergen-specific immunotherapy in atopic dermatitis. J Eur Acad Dermatol Venereol. 2021;35(6):1357-61.

374. Schmitz N, Dietmeier K, Bauer M, Maudrich M, Utzinger S, Muntwiler S, et al. Displaying Fel d1 on virus-like particles prevents reactogenicity despite greatly enhanced immunogenicity: a novel therapy for cat allergy. J Exp Med. 2009;206(9):1941-55.

375. Storni F, Zeltins A, Balke I, Heath MD, Kramer MF, Skinner MA, et al. Vaccine against peanut allergy based on engineered virus-like particles displaying single major peanut allergens. J Allergy Clin Immunol. 2020;145(4):1240-53 e3.

376. Jitthamstaporn S, Sander AF, Jacquet A. Virus-like particles displaying recombinant Der p 1 zymogen to optimize IgG blocking antibody response. Allergy. 2022;77(2):664-7.

377. Sobczak JM, Krenger PS, Storni F, Mohsen MO, Balke I, Resevica G, et al. The next generation virus-like particle platform for the treatment of peanut allergy. Allergy. 2023;78(7):1980-96.

378. Engeroff P, Caviezel F, Storni F, Thoms F, Vogel M, Bachmann MF. Allergens displayed on virus-like particles are highly immunogenic but fail to activate human mast cells. Allergy. 2018;73(2):341-9.

379. Busold S, Aglas L, Menage C, Auger L, Desgagnes R, Faye L, et al. Fel d 1 surface expression on plant-made eBioparticles combines potent immune activation and hypoallergenicity. Allergy. 2022;77(10):3124-6.

380. Castenmiller C, Nagy NA, Kroon PZ, Auger L, Desgagnes R, Martel C, et al. A novel peanut allergy immunotherapy: Plant-based enveloped Ara h 2 Bioparticles activate dendritic cells and polarize T cell responses to Th1. World Allergy Organ J. 2023;16(11):100839.

381. de Kam PJ, Zielen S, Bernstein JA, Berger U, Berger M, Cuevas M, et al. Response to Correspondence to "Short-course subcutaneous treatment with PQ Grass strongly improves symptom and medication scores in grass allergy". Allergy. 2024.

382. Marques CR, Costa RS, Costa GNO, da Silva TM, Teixeira TO, de Andrade EMM, et al. Genetic and epigenetic studies of FOXP3 in asthma and allergy. Asthma Res Pract. 2015;1:10.

383. Hasan MM, Thompson-Snipes L, Klintmalm G, Demetris AJ, O'Leary J, Oh S, et al. CD24(hi)CD38(hi) and CD24(hi)CD27(+) Human Regulatory B Cells Display Common and Distinct Functional Characteristics. J Immunol. 2019;203(8):2110-20.

384. Gallego-Valle J, Perez-Fernandez VA, Correa-Rocha R, Pion M. Generation of Human Breg-Like Phenotype with Regulatory Function In Vitro with Bacteria-Derived Oligodeoxynucleotides. Int J Mol Sci. 2018;19(6).

385. Yang B, Tan X, Xiong X, Wu D, Zhang G, Wang M, et al. Effect of CD40/CD40L signaling on IL-10-producing regulatory B cells in Chinese children with Henoch-Schonlein purpura nephritis. Immunol Res. 2017;65(3):592-604.

386. Liu QB, Zhou RH, Liu CM. TLR9/FCRL3 regulates B cell viability, apoptosis, and antibody and IL-10 production through ERK1/2, p38, and STAT3 signaling pathways. In Vitro Cell Dev Biol Anim. 2022;58(8):702-11.

387. Liu BS, Cao Y, Huizinga TW, Hafler DA, Toes RE. TLR-mediated STAT3 and ERK activation controls IL-10 secretion by human B cells. Eur J Immunol. 2014;44(7):2121-9.

388. Michee-Cospolite M, Boudigou M, Grasseau A, Simon Q, Mignen O, Pers JO, et al. Molecular Mechanisms Driving IL-10- Producing B Cells Functions: STAT3 and c-MAF as Underestimated Central Key Regulators? Front Immunol. 2022;13:818814.

389. Schmitt H, Ulmschneider J, Billmeier U, Vieth M, Scarozza P, Sonnewald S, et al. The TLR9 Agonist Cobitolimod Induces IL10-Producing Wound Healing Macrophages and Regulatory T Cells in Ulcerative Colitis. J Crohns Colitis. 2020;14(4):508-24.

390. Yim LY, Lau CS, Chan VS. Heightened TLR7/9-Induced IL-10 and CXCL13 Production with Dysregulated NF-κB Activation in CD11c(hi)CD11b(+) Dendritic Cells in NZB/W F1 Mice. Int J Mol Sci. 2019;20(18).

391. Hsu K, Chung YM, Endoh Y, Geczy CL. TLR9 ligands induce S100A8 in macrophages via a STAT3-dependent pathway which requires IL-10 and PGE2. PLoS One. 2014;9(8):e103629.

392. Zhao Q, Hu Y, Deng S, Yu P, Chen B, Wang Z, et al. Cytidine-phosphate-guanosine oligodeoxynucleotides in combination with CD40 ligand decrease periodontal inflammation and alveolar bone loss in a TLR9-independent manner. J Appl Oral Sci. 2018;26:e20170451.

393. Yu P, Hu Y, Liu Z, Kawai T, Taubman MA, Li W, et al. Local Induction of B Cell Interleukin-10 Competency Alleviates Inflammation and Bone Loss in Ligature-Induced Experimental Periodontitis in Mice. Infect Immun. 2017;85(1).

394. Schaut RG, Lamb IM, Toepp AJ, Scott B, Mendes-Aguiar CO, Coutinho JF, et al. Regulatory IgDhi B Cells Suppress T Cell Function via IL-10 and PD-L1 during Progressive Visceral Leishmaniasis. J Immunol. 2016;196(10):4100-9.

395. Zhao Y, Shen M, Feng Y, He R, Xu X, Xie Y, et al. Regulatory B cells induced by pancreatic cancer cell-derived interleukin-18 promote immune tolerance via the PD-1/PD-L1 pathway. Oncotarget. 2018;9(19):14803-14.

396. Ray A, Basu S, Williams CB, Salzman NH, Dittel BN. A novel IL-10-independent regulatory role for B cells in suppressing autoimmunity by maintenance of regulatory T cells via GITR ligand. J Immunol. 2012;188(7):3188-98.

397. Khan AR, Hams E, Floudas A, Sparwasser T, Weaver CT, Fallon PG. PD-L1hi B cells are critical regulators of humoral immunity. Nat Commun. 2015;6:5997.

398. Patel AJ, Willsmore ZN, Khan N, Richter A, Naidu B, Drayson MT, et al. Regulatory B cell repertoire defects predispose lung cancer patients to immune-related toxicity following checkpoint blockade. Nat Commun. 2022;13(1):3148.

399. Henn AD, Laski M, Yang H, Welle S, Qiu X, Miao H, et al. Functionally Distinct Subpopulations of CpG-Activated Memory B Cells. Sci Rep. 2012;2:345.

400. Matsushita T, Le Huu D, Kobayashi T, Hamaguchi Y, Hasegawa M, Naka K, et al. A novel splenic B1 regulatory cell subset suppresses allergic disease through phosphatidylinositol 3-kinase-Akt pathway activation. J Allergy Clin Immunol. 2016;138(4):1170-82 e9.

401. de Souza AJ, Oriss TB, O'Malley K J, Ray A, Kane LP. T cell Ig and mucin 1 (TIM-1) is expressed on in vivo-activated T cells and provides a costimulatory signal for T cell activation. Proc Natl Acad Sci U S A. 2005;102(47):17113-8.

402. Curtiss M, Colgan J. The role of the T-cell costimulatory molecule Tim-1 in the immune response. Immunol Res. 2007;39(1-3):52-61.

403. Zheremyan EA, Ustiugova AS, Uvarova AN, Karamushka NM, Stasevich EM, Gogoleva VS, et al. Differentially activated B cells develop regulatory phenotype and show varying immunosuppressive features: a comparative study. Front Immunol. 2023;14:1178445.

404. Dambuza IM, He C, Choi JK, Yu CR, Wang R, Mattapallil MJ, et al. IL-12p35 induces expansion of IL-10 and IL-35-expressing regulatory B cells and ameliorates autoimmune disease. Nat Commun. 2017;8(1):719.

405. Yoshida Y, Yoshimi R, Yoshii H, Kim D, Dey A, Xiong H, et al. The transcription factor IRF8 activates integrin-mediated TGF-beta signaling and promotes neuroinflammation. Immunity. 2014;40(2):187-98.

406. Ibrahim ML, Klement JD, Lu C, Redd PS, Xiao W, Yang D, et al. Myeloid-Derived Suppressor Cells Produce IL-10 to Elicit DNMT3b-Dependent IRF8 Silencing to Promote Colitis-Associated Colon Tumorigenesis. Cell Rep. 2018;25(11):3036-46 e6.

407. Carl JW, Bai XF. IL27: its roles in the induction and inhibition of inflammation. Int J Clin Exp Pathol. 2008;1(2):117-23.

408. Kang M, Yadav MK, Mbanefo EC, Yu CR, Egwuagu CE. IL-27-containing exosomes secreted by innate B-1a cells suppress and ameliorate uveitis. Front Immunol. 2023;14:1071162.

409. Schwartz M, Zhang Y, Rosenblatt JD. B cell regulation of the anti-tumor response and role in carcinogenesis. J Immunother Cancer. 2016;4:40.

410. Choi JK, Yu CR, Bing SJ, Jittayasothorn Y, Mattapallil MJ, Kang M, et al. IL-27-producing B-1a cells suppress neuroinflammation and CNS autoimmune diseases. Proc Natl Acad Sci U S A. 2021;118(47).

411. Sun X, Guo C, Zhao F, Zhu J, Xu Y, Liu ZQ, et al. Vasoactive intestinal peptide stabilizes intestinal immune homeostasis through maintaining interleukin-10 expression in regulatory B cells. Theranostics. 2019;9(10):2800-11.

412. Luo J, Guo H, Liu Z, Peng T, Hu X, Han M, et al. Analysis of Peripheral B Cell Subsets in Patients With Allergic Rhinitis. Allergy Asthma Immunol Res. 2018;10(3):236-43.

413. Wang K, Tao L, Su J, Zhang Y, Zou B, Wang Y, et al. TLR4 supports the expansion of FasL(+)CD5(+)CD1d(hi) regulatory B cells, which decreases in contact hypersensitivity. Mol Immunol. 2017;87:188-99.

414. Barlow JL, Wong SH, Ballantyne SJ, Jolin HE, McKenzie AN. Tim1 and Tim3 are not essential for experimental allergic asthma. Clin Exp Allergy. 2011;41(7):1012-21.

415. Wang YY, Zhang L, Zhao PW, Ma L, Li C, Zou HB, et al. Functional implications of regulatory B cells in human IgA nephropathy. Scand J Immunol. 2014;79(1):51-60.

416. Gonipeta B, Duriancik D, Kim E, Gardner E, Gangur V. Identification of T- and B-Cell Subsets That Expand in the Central and Peripheral Lymphoid Organs during the Establishment of Nut Allergy in an Adjuvant-Free Mouse Model. ISRN Allergy. 2013;2013:509427.

417. Hofer MF, Jirapongsananuruk O, Trumble AE, Leung DY. Upregulation of B7.2, but not B7.1, on B cells from patients with allergic asthma. J Allergy Clin Immunol. 1998;101(1 Pt 1):96-102.

418. Kouzaki H, Arai Y, Nakamura K, Murao T, Tojima I, Shimizu S, et al. Anti-inflammatory roles of interleukin-35 in the pathogenesis of Japanese cedar pollinosis. Asia Pac Allergy. 2021;11(3):e34.

419. Rosas A, Valencia MP, Sanchez M, Bautista M, Rico G, Vega GB. Transforming growth factor beta and platelets in allergic rhinitis and sinusitis. Rev Alerg Mex. 2011;58(2):93-8.

420. Wang M, Gu Z, Yang J, Zhao H, Cao Z. Changes among TGF-beta1(+) Breg cells and helper T cell subsets in a murine model of allergic rhinitis with prolonged OVA challenge. Int Immunopharmacol. 2019;69:347-57.

421. Liu J, Hu M, Tao X, He J, Wang J, Song Z, et al. Salivary IgG4 Levels Contribute to Assessing the Efficacy of Dermatophagoides pteronyssinus Subcutaneous Immunotherapy in Children with Asthma or Allergic Rhinitis. J Clin Med. 2023;12(4).

422. Leuthard DS, Duda A, Freiberger SN, Weiss S, Dommann I, Fenini G, et al. Microcrystalline Tyrosine and Aluminum as Adjuvants in Allergen-Specific Immunotherapy Protect from IgE-Mediated Reactivity in Mouse Models and Act Independently of Inflammasome and TLR Signaling. J Immunol. 2018;200(9):3151-9.

423. Heath MD, Mohsen MO, de Kam PJ, Carreno Velazquez TL, Hewings SJ, Kramer MF, et al. Shaping Modern Vaccines: Adjuvant Systems Using MicroCrystalline Tyrosine (MCT((R))). Front Immunol. 2020;11:594911.

424. Cabral-Miranda G, Heath MD, Mohsen MO, Gomes AC, Engeroff P, Flaxman A, et al. Virus-Like Particle (VLP) Plus Microcrystalline Tyrosine (MCT) Adjuvants Enhance Vaccine Efficacy Improving T and B Cell Immunogenicity and Protection against Plasmodium berghei/vivax. Vaccines (Basel). 2017;5(2).

425. Trickett A, Kwan YL. T cell stimulation and expansion using anti-CD3/CD28 beads. J Immunol Methods. 2003;275(1-2):251-5.

426. Li Y, Kurlander RJ. Comparison of anti-CD3 and anti-CD28-coated beads with soluble anti-CD3 for expanding human T cells: differing impact on CD8 T cell phenotype and responsiveness to restimulation. J Transl Med. 2010;8:104.

427. Coffman RL, Seymour BW, Hudak S, Jackson J, Rennick D. Antibody to interleukin-5 inhibits helminth-induced eosinophilia in mice. Science. 1989;245(4915):308-10.

428. Lee DU, Rao A. Molecular analysis of a locus control region in the T helper 2 cytokine gene cluster: a target for STAT6 but not GATA3. Proc Natl Acad Sci U S A. 2004;101(45):16010-5.

429. Zhu J. T helper 2 (Th2) cell differentiation, type 2 innate lymphoid cell (ILC2) development and regulation of interleukin-4 (IL-4) and IL-13 production. Cytokine. 2015;75(1):14-24.

430. Kahler H, Stuwe H, Cromwell O, Fiebig H. Reactivity of T cells with grass pollen allergen extract and allergoid. Int Arch Allergy Immunol. 1999;120(2):146-57.

431. Karlsson MR, Rugtveit J, Brandtzaeg P. Allergen-responsive CD4+CD25+ regulatory T cells in children who have outgrown cow's milk allergy. J Exp Med. 2004;199(12):1679-88.

432. Bacher P, Heinrich F, Stervbo U, Nienen M, Vahldieck M, Iwert C, et al. Regulatory T Cell Specificity Directs Tolerance versus Allergy against Aeroantigens in Humans. Cell. 2016;167(4):1067-78 e16.

433. Kinoshita T, Baatjes A, Smith SG, Dua B, Watson R, Kawayama T, et al. Natural regulatory T cells in isolated early responders compared with dual responders with allergic asthma. J Allergy Clin Immunol. 2014;133(3):696-703.

434. Lin YL, Shieh CC, Wang JY. The functional insufficiency of human CD4+CD25 high T-regulatory cells in allergic asthma is subjected to TNF-alpha modulation. Allergy. 2008;63(1):67-74.

435. Lemoine S, Morva A, Youinou P, Jamin C. Human T cells induce their own regulation through activation of B cells. J Autoimmun. 2011;36(3-4):228-38.

436. Rieckmann P, Tuscano JM, Kehrl JH. Tumor necrosis factor-alpha (TNF-alpha) and interleukin-6 (IL-6) in B-lymphocyte function. Methods. 1997;11(1):128-32.

437. Scharf L, Axelsson H, Emmanouilidi A, Mathew NR, Sheward DJ, Leach S, et al. Longitudinal single-cell analysis of SARS-CoV-2-reactive B cells uncovers persistence of early-formed, antigen-specific clones. JCI Insight. 2023;8(1).

CHAPTER 13. APPENDIX

13.1.1 Appendix Figures

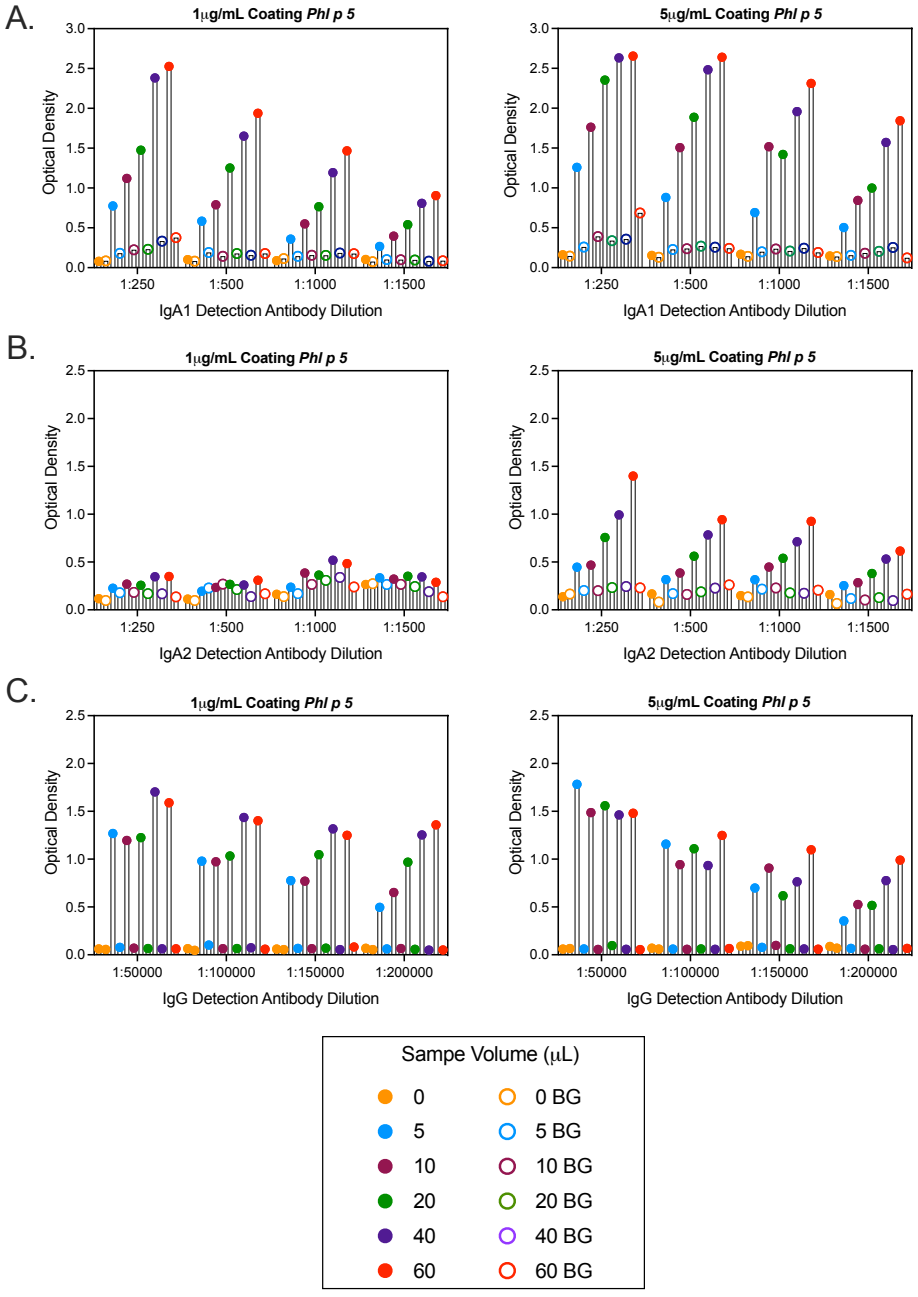


Figure 13.1.1.1 ELISA optimisation for analysis of *Phl p 5* sIgG, sIgA$_1$ and sIgA$_2$ levels in nasal fluid and serum.

ELISA plates coated with 1μg/mL or 5μg/mL *Phl p* 5, increasing detection antibody dilutions and sample volumes for detection of *Phl p* 5 **A)** sIgA$_1$, **B)** sIgA$_2$ and **C) s**IgG by ELISA. Data is representative of n=1 GP-SCIT subject and presented as the average of duplicate wells per condition. BG, background.

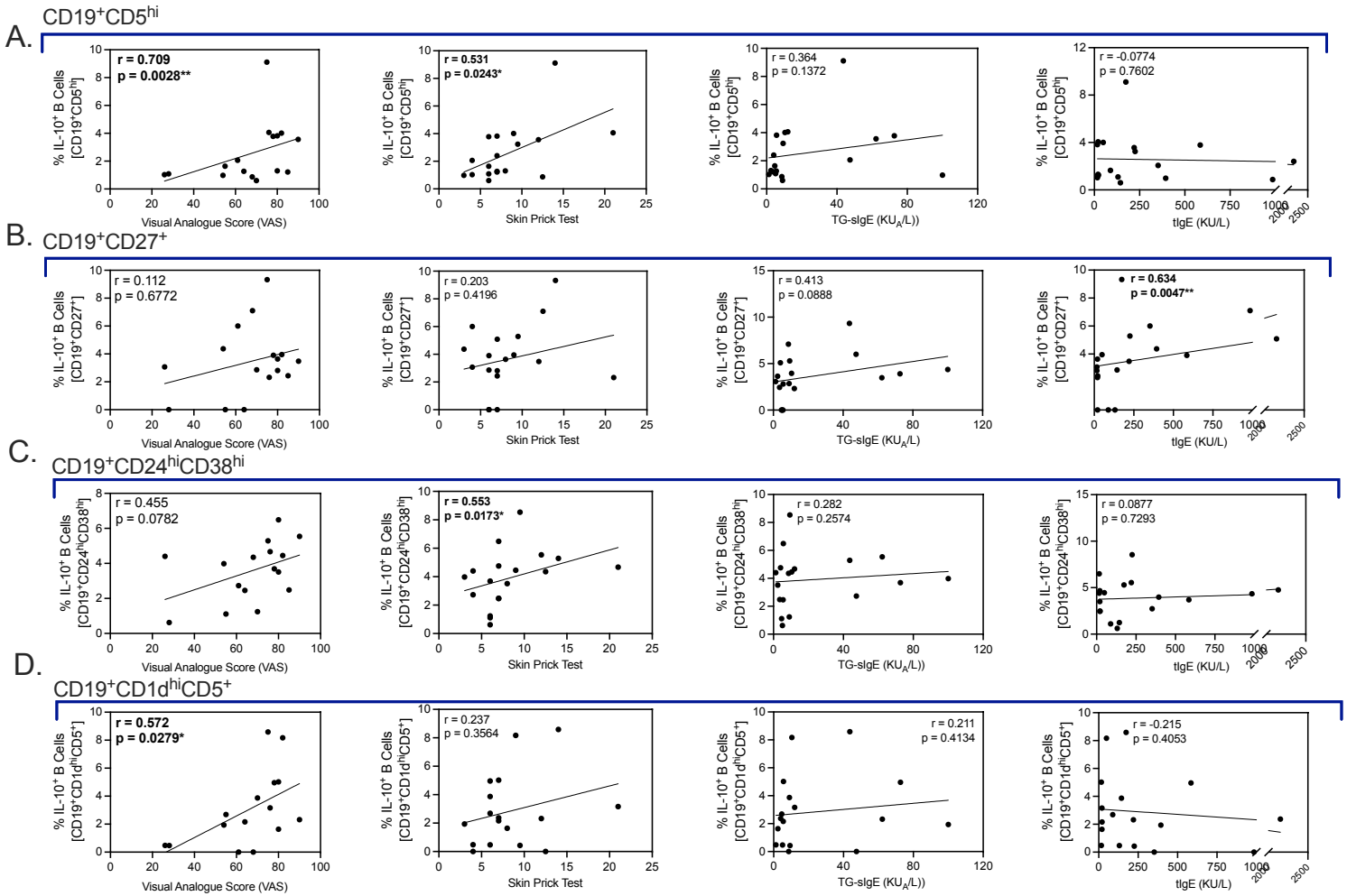


Figure 13.1.1.2 Correlation between IL-10$^+$ Breg cell subsets and GPA SAR patient demographics.

Correlation between **A)** CD5^{hi}IL-10$^+$, **B)** CD27$^+$IL-10$^+$, **C)** CD24^{hi}CD38^{hi}IL-10$^+$ and **D)** CD1d^{hi}CD5$^+$IL-10$^+$ Breg cells and visual analogue scale scores, spin prick test scores, timothy-grass sIgE and tIgE. Spearman Correlation test, *P < 0.05, **P < 0.001. Data representative of GPA, n=18 subjects.

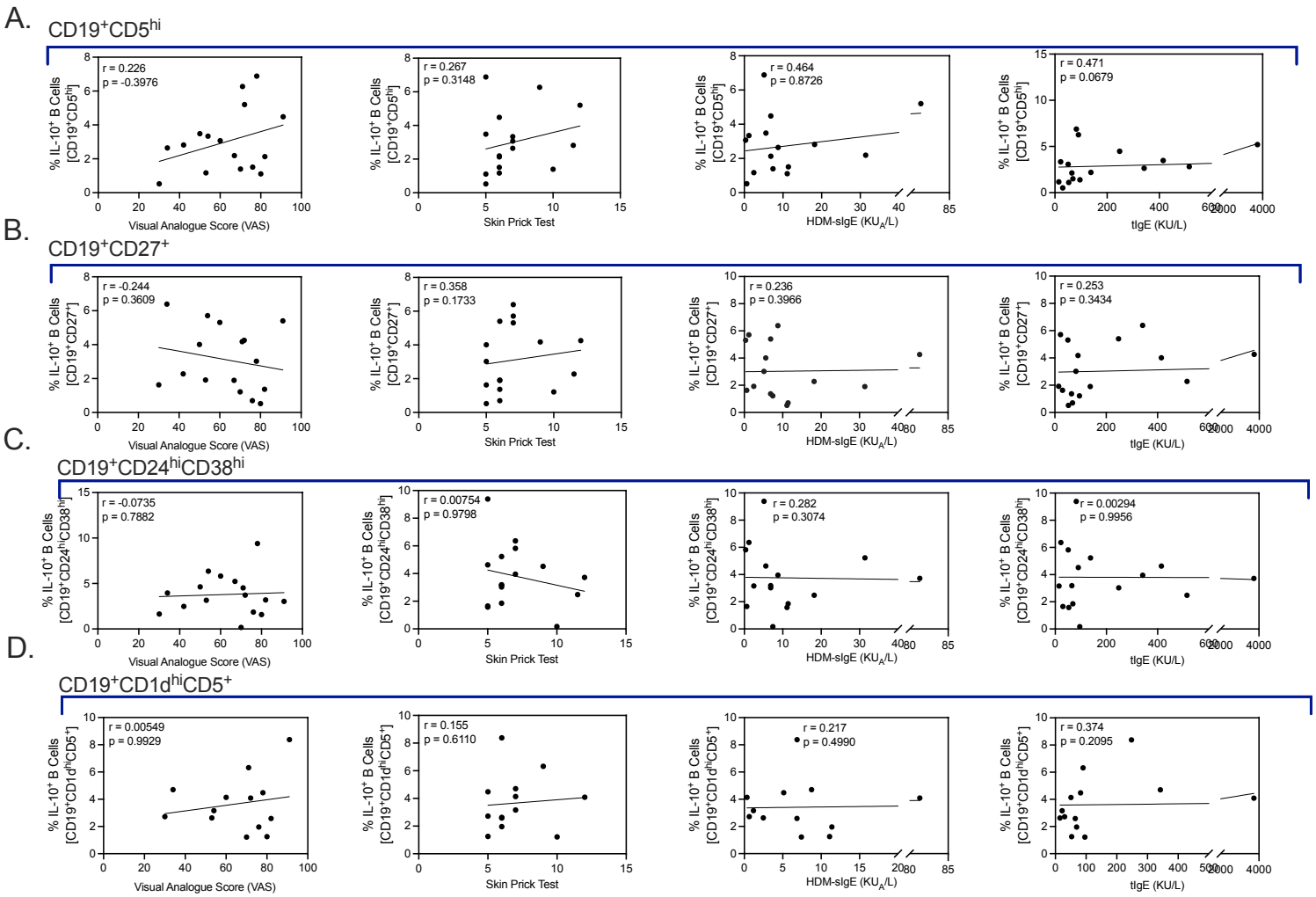


Figure 13.1.1.3 Correlation between IL-10^{+} Breg cell subsets and HDMA PAR patient demographics.

Correlation between **A)** CD5^{hi}IL-10^{+}, **C)** CD27^{+}IL-10^{+}, **C)** CD24^{hi}CD38^{hi}IL-10^{+} and **C)** CD1d^{hi}CD5^{+}IL-10^{+} Breg cells and visual analogue scale scores, spin prick test scores, HDM sIgE and tIgE. Spearman Correlation test. Data representative of HDMA, n=16 subjects.

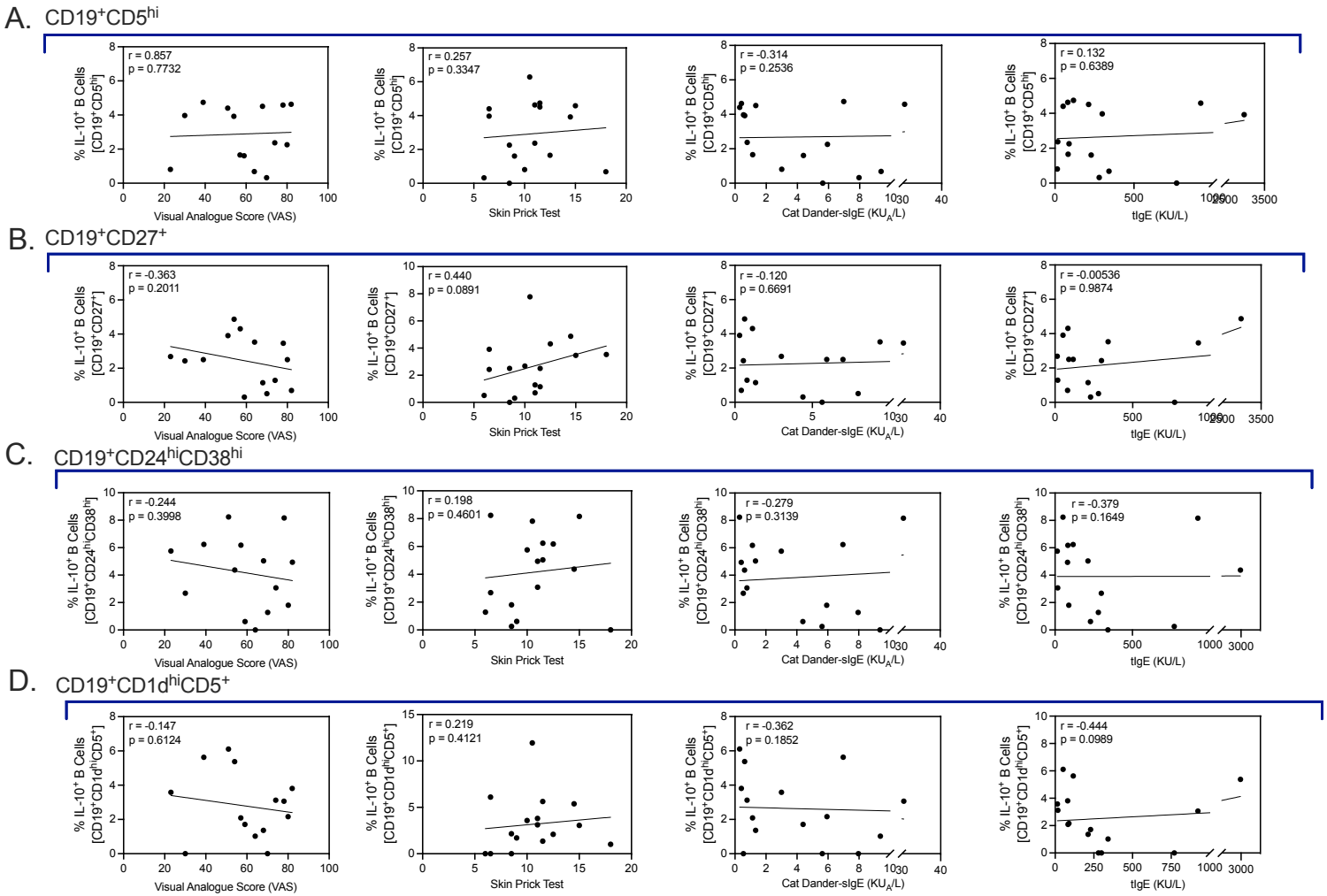


Figure 13.1.1.4 Correlation between IL-10$^+$ Breg cell subsets and CA PAR patient demographics.

Correlation between **A)** CD5^{hi}IL-10$^+$, **C)** CD27$^+$IL-10$^+$, **C)** CD24^{hi}CD38^{hi}IL-10$^+$ and **C)** CD1d^{hi}CD5$^+$IL-10$^+$ Breg cells and visual analogue scale scores, total prick test scores, cat-dander sIgE and tIgE. Spearman Correlation test. Data representative of CA, n=16 subjects.

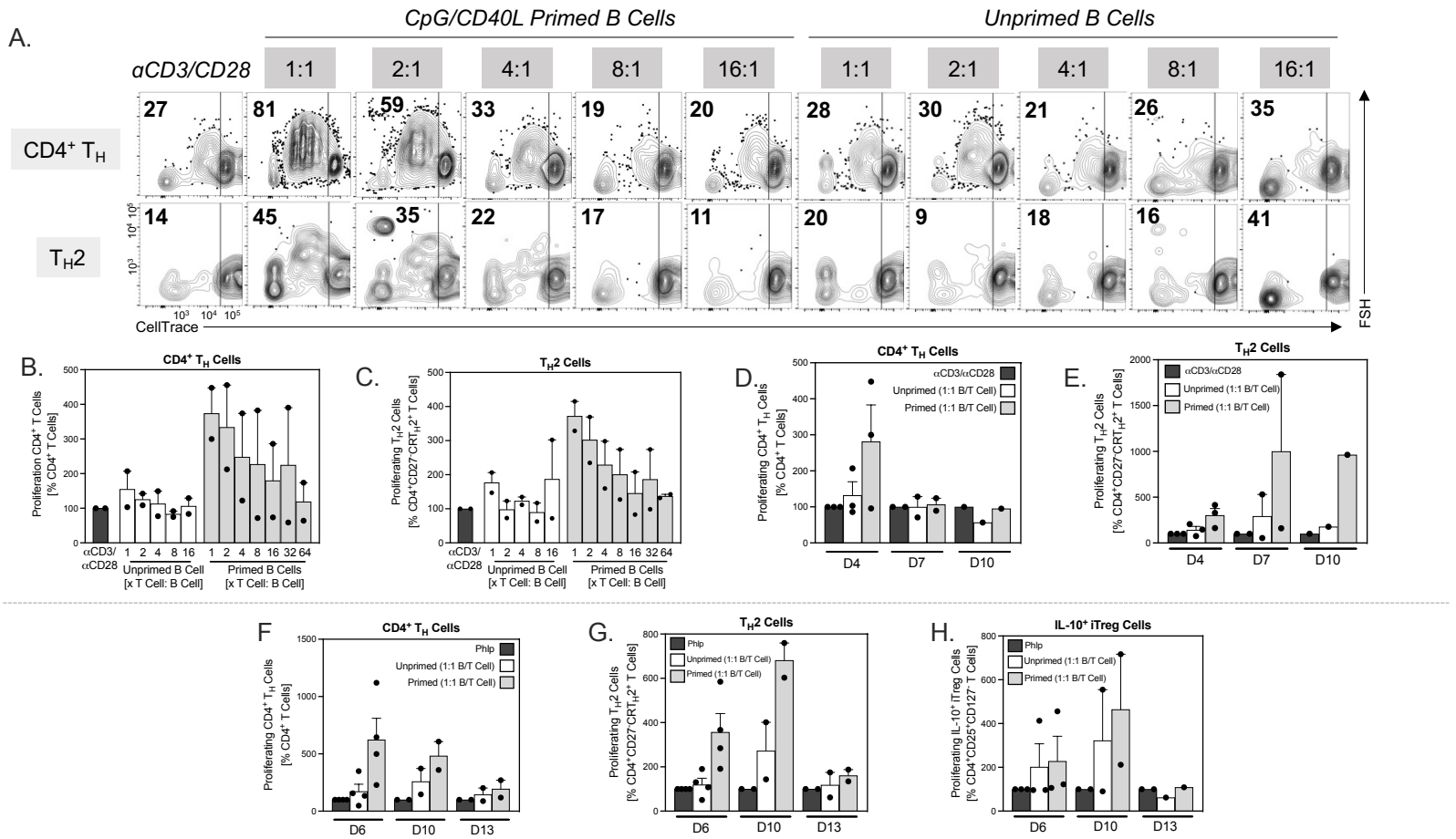


Figure 13.1.1.5 CpG/CD40L primed B cells enhance CD4$^+$ T_H and T_H2 cell proliferation in response to polyclonal and allergen stimulation.

A) Representative flow cytometry plots demonstrating CD4$^+$ T_H and T_H2 cell proliferation in response to αCD3/CD28 stimulation alongside co-culture with CpG/CD40L primed and unprimed B cells. Effect of increasing ratios of CpG/CD40L primed and unprimed B cells on **B)** CD4$^+$ T_H and **C)** T_H2 cells proliferation, and increased culture duration on **F)** CD4$^+$ T_H and **G)** T_H2 cell proliferation. Effect of increasing culture duration of unprimed and primed B/T cell co-cultures on **F)** CD4$^+$ T_H, **G)** T_H2 and **G)** IL-10$^+$ iTreg cell proliferation in response to *Phl p* stimulation. Data representative of GPA, n=2, and presented as mean ± SEM.

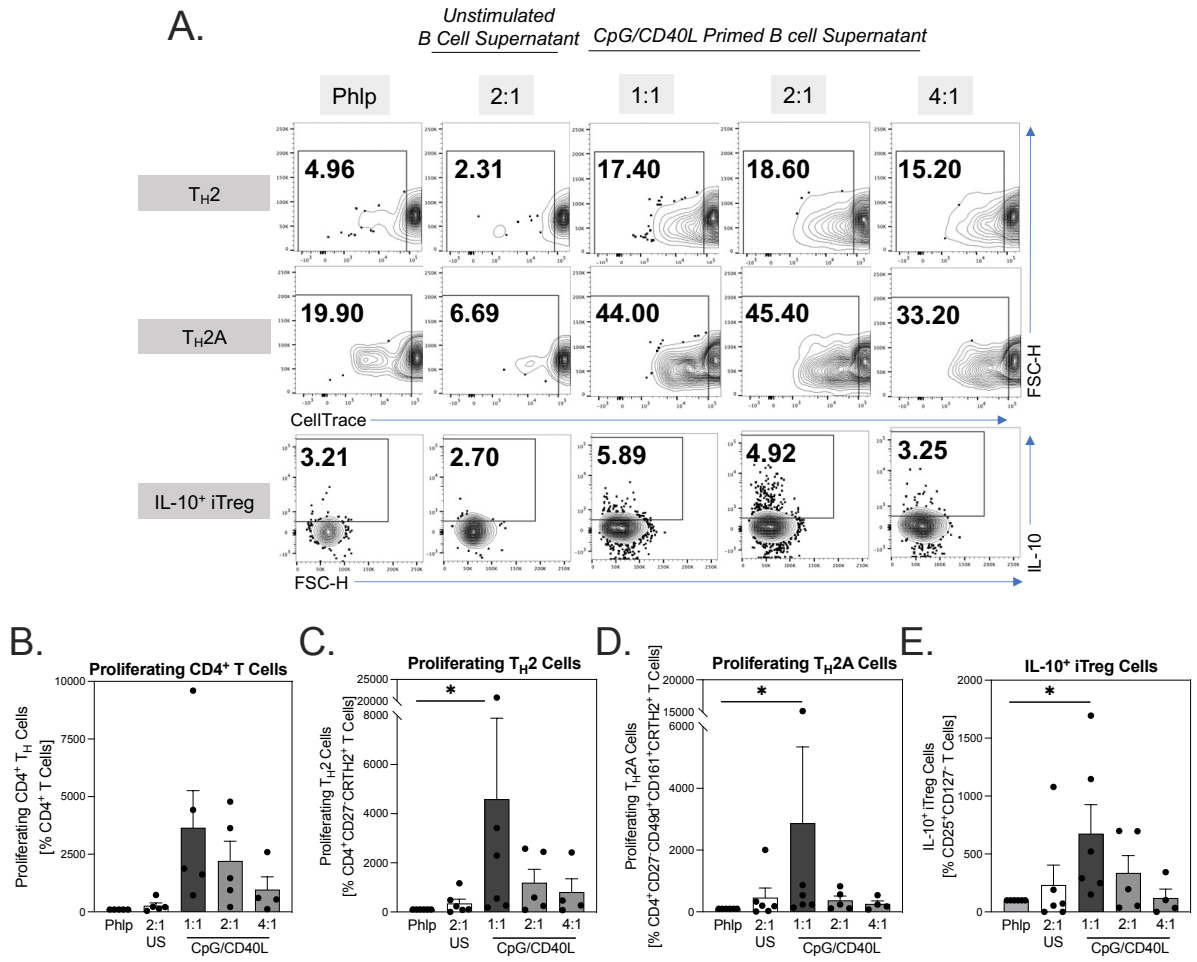


Figure 13.1.1.6 CpG/CD40L primed B cell culture supernatant significantly enhances *Phl p* stimulated T_H2 and T_H2A proliferation and IL-10^+ iTreg cells.

A) Representative flow cytometry plots demonstrating T_H2 and T_H2A proliferation and IL-10^+ iTreg cell frequencies in response to unprimed and primed B cell culture supernatant. Effect of unprimed and primed B cell culture supernatant on **B)** $CD4^+$ T, **C)** T_H2, **D)** T_H2A cell proliferation and **E)** IL-10^+ iTreg cell frequencies. Data representative of GPA, n=6 [N.B. 2:1 primed B cells, n=5; 4:1 primed B cells, n=4], and presented as mean ± SEM. Wilcoxon-signed pairs rank test, **P* < 0.05. US, unstimulated; Phlp, *Phleum pratense*.

Table 13.1.1.1 Primed B cell culture supernatant enhances *PhI* p-stimulated T_H2, T_H2A proliferation and IL-10^+ iTreg cells.

Culture Conditions	B/T Cell Subset	Raw				Normalised to PhIp			*P* value v. PhIp	*P* value v. 1:1 Primed B Cells	*P* value v. 2:1 US B Cells
		n	mean	SD	SEM	mean	SD	SEM			
Unstimulated	$CD4^+CD27^+CRT_H2^+CellTrace^-$	6	2.29	1.07	0.44	NA	NA	NA	NA	NA	NA
	$CD4^+CD27^+CRT_H2^+CD49d^+CD161^+CellTrace^-$	6	4.21	6.00	2.45	NA	NA	NA	NA	NA	NA
	$CD4^+CD25^-CD127^+IL\text{-}10^+CellTrace^-$	6	1.74	0.22	0.09	NA	NA	NA	NA	NA	NA
PhIp	$CD4^+CD27^+CRT_H2^+CellTrace^-$	6	5.11	3.04	1.24	100	0	0	NA	NA	NA
	$CD4^+CD27^+CRT_H2^+CD49d^+CD161^+CellTrace^-$	6	14.9	9.33	3.81	100	0	0	NA	NA	NA
	$CD4^+CD25^-CD127^+IL\text{-}10^+CellTrace^-$	6	2.88	0.81	0.33	100	0	0	NA	NA	NA
2:1	$CD4^+CD27^+CRT_H2^+CellTrace^-$	6	5.75	2.55	1.04	346	435	178	0.3125	NA	NA
Unstimulated	$CD4^+CD27^+CRT_H2^+CD49d^+CD161^+CellTrace^-$	6	18.6	14.4	5.86	460	767	313	0.2188	NA	NA
Supernatant	$CD4^+CD25^-CD127^+IL\text{-}10^+CellTrace^-$	6	3.33	2.89	1.18	233	420	172	0.8125	NA	NA
1:1	$CD4^+CD27^+CRT_H2^+CellTrace^-$	6	27.8	18.5	7.53	4593	8072	3295	**0.0312**	NA	NA
Primed B Cells	$CD4^+CD27^+CRT_H2^+CD49d^+CD161^+CellTrace^-$	6	53.0	19.8	8.10	2871	6052	2471	**0.0312**	NA	NA
Supernatant	$CD4^+CD25^-CD127^+IL\text{-}10^+CellTrace^-$	6	7.93	2.89	1.18	675	615	251	**0.0312**	NA	NA
2:1	$CD4^+CD27^+CRT_H2^+CellTrace^-$	6	19.6	13.0	5.82	1189	1223	547	0.1250	NA	0.1250
Primed B Cells	$CD4^+CD27^+CRT_H2^+CD49d^+CD161^+CellTrace^-$	6	43.4	21.0	9.37	372	315	141	0.0625	NA	0.1250
Supernatant	$CD4^+CD25^-CD127^+IL\text{-}10^+CellTrace^-$	6	4.49	1.85	0.83	336	336	150	0.3125	NA	0.4375
4:1	$CD4^+CD27^+CRT_H2^+CellTrace^-$	6	19.6	13.8	6.91	809	1087	544	0.2500	NA	NA
Primed B Cells	$CD4^+CD27^+CRT_H2^+CD49d^+CD161^+CellTrace^-$	6	40.5	24.2	12.1	256	200	99.9	0.2500	NA	NA
Supernatant	$CD4^+CD25^-CD127^+IL\text{-}10^+CellTrace^-$	6	2.67	1.11	0.55	120	155	77.5	>0.9999	NA	NA

Bolded Values Represent Significant ***P*** Values. Wilcoxon-signed pairs rank test.